Pump Troubleshooting

Volume 1

Technical Report

Pump Troubleshooting

Volume 1

TR-114612-V1

Final Report, April 2000

EPRI Project Manager
M. Pugh

EPRI • 3412 Hillview Avenue, Palo Alto, California 94304 • PO Box 10412, Palo Alto, California 94303 • USA
800.313.3774 • 650.855.2121 • askepri@epri.com • www.epri.com

DISCLAIMER OF WARRANTIES AND LIMITATION OF LIABILITIES

ORGANIZATION(S) THAT PREPARED THIS DOCUMENT

Southern Nuclear Services

ORDERING INFORMATION

Requests for copies of this report should be directed to the EPRI Distribution Center, 207 Coggins Drive, P.O. Box 23205, Pleasant Hill, CA 94523, (800) 313-3774.

CITATIONS

This report was prepared by

Southern Nuclear Services
42 Inverness Center Parkway
Birmingham, AL 35242

Principal Author
W. Gates

Nuclear Maintenance Applications Center (NMAC)
1300 W.T. Harris Blvd.
Charlotte, NC 28262

This report describes research sponsored by EPRI.

The report is a corporate document that should be cited in the literature in the following manner:

Pump Troubleshooting, Volume 1. EPRI, Palo Alto, CA: 1999. TR-114612-V1.

REPORT SUMMARY

Background

Pumps are an integral part of many systems in nuclear power plants. Reliable operation and maintenance of these components are vital to sustained plant operation and availability. The ability to accurately diagnose and troubleshoot pump problems is vital to the maintenance, engineering, and operating staffs of these power plants. Significant research and experience was achieved by the late Dr. Elemer Makay, a world-renowned expert in the field of pump design, operation, and troubleshooting. This work has been collected with the assistance of Will Gates, an understudy of Dr. Makay, and is presented in this Volume 1 of a two-volume report on pump troubleshooting.

Objective

- To capture the knowledge and experience of Dr. Makay
- To provide a vehicle to preserve and share this information with maintenance, engineering, and operations personnel in nuclear plants around the world

Results

The works of Dr. Makay regarding pump troubleshooting have been collected in this volume with updates by Gates. Significant developments and corrective actions for high-energy-input pumps in U.S. power plant applications since 1965 are the primary subjects of this report. This discussion of high-speed, high-energy-input pumps includes such machines as boiler feed pumps (BFPs), nuclear feed pumps, high-pressure injection pumps, feed pump turbines, water lift pumps, condensate pumps, and nuclear reactor or main coolant pumps. The nuclear coolant pumps (all vertical, single-stage) are examined when evaluating the root causes of shaft breakages and vane passing frequency and its multiples. These pumps are known as the “highest outage causing” rotating equipment in nuclear plants.

Subjects discussed include hydraulically and dynamically induced instabilities, rotor seizure, dynamic balancing, assembly, and axial alignment of multi-stage rotors, optimization of impeller to diffuser/volute geometry, minimum flow requirements particularly for nuclear safety-related pumps, and the damaging occurrence of vane passing frequency and its multiples caused by Gap B geometry or acoustic resonance and pump component failures.

Volume 2 will be issued in late 2000. It will be a practical application of many of the principles defined in Dr. Makay’s works and will provide basic pump diagnostic information and guidelines for many levels of the plant organization from the new system engineer to the experienced pump mechanic. Collection of this information provides a valuable reference for future use.

EPRI Perspective

The information contained in this guide represents a significant collection of technical information, including case studies and implemented solutions, related to the troubleshooting of pump and pump-related problems in power plants by Dr. Makay. This report provides a single point of reference for pump troubleshooting information for power plant personnel, both in the present and in the future. The intended audience of Volume 1 of this guide includes component, maintenance, and system engineers involved in maintaining, operating, and troubleshooting pumps. This guide will be helpful in evaluating pump application problems in existing systems, selecting new and replacement pumps/pump components, and understanding pump performance and reliability.

Volume 1 is being issued in the first quarter of 2000, and Volume 2 will be issued in late 2000.

TR-114612-V1

Keywords

Design engineers
Plant support engineering
Plant maintenance
Plant operations

ACKNOWLEDGMENTS

EPRI would like to recognize the contribution of Mr. Will Gates of Southern Company, who was a colleague of Dr. Makay, in the development of this guide. His efforts to provide the various elements required to assemble the topical matter contained herein and his review and technical input contributed greatly to the successful completion of this publication.

The project manager would also like to express his appreciation to Lisa Perry, Brian Perry, and Annette Stephenson of the Charlotte Graphics group for their efforts in putting this project together.

ABSTRACT

Introduction

The following report was originally prepared by Dr. Elemer Makay and Mr. Will Gates for presentation at the Utility Pump Troubleshooting Symposium in March of 1995. The report represents a compilation of Dr. Makay's extensive research in the field of pump troubleshooting diagnostic methods. EPRI is privileged to make this important research available to its members at this time. The technical subject matter has undergone only minor editorial revisions so as to preserve its original intent. As such, the user should understand that the information has not been updated in any way to include research and developments recorded since 1995.

Original Abstract

Significant developments and corrective actions for high-energy-input pumps in U.S. power plant applications from 1965 to 1995 are the subject of this report. This discussion of high-speed, high-energy-input pumps includes such machines as boiler feed pumps (BFP), nuclear feed pumps, high-pressure injection pumps, feed pump turbines, water lift pumps, condensate pumps, and nuclear reactor or main coolant pumps. The nuclear coolant pumps (all vertical, single stage) are examined when evaluating the root causes of shaft breakage and vane passing frequency and its multiples. These pumps are known as the "highest outage causing" rotating equipment in nuclear plants.

Subjects discussed in this report include the following:

- Hydraulically and dynamically induced instabilities
- Rotor seizure (especially on turning gear)
- Dynamic balancing, assembly and axial alignment of multi-stage rotors
- Optimization of impeller to diffuser/volute geometry, minimum flow requirements (particularly for nuclear safety related pumps)
- The damaging occurrence of vane passing frequency and its multiples caused by Gap B geometry or "acoustic resonance"
- Pump component failures

Seven of the most common and typical vibration components are listed. Dynamic and hydraulic instabilities in the subsynchronous frequency range are emphasized. A large number of failures are caused by these two phenomena without actually realizing that their frequency ranges

overlap, resulting in misjudgment of the real causes. Exhaustive research has been done in the area of "rotor-dynamic-instability," while very little work to understand "hydraulic instability" has been performed due to the complexity of the subject and lack of funding by users and OEMs. For that reason, the detection and elimination of hydraulic instability receives the major emphasis in this report.

The root causes and damaging mechanisms of vane passing frequency and its multiples are reported. The importance of optimization of Gap A, as well as its Overlap (Overlap Ratio), Gap B, and their interrelationship are thoroughly explored based on almost three decades of systematic field data collection. Their influence on axial thrust stabilization, as well as their impact on how to gain pump efficiency during such geometry modifications, are pointed out.

Numerous field case histories are discussed in each of the seven vibration frequency ranges. Combination cases are explored where two or more of the frequency ranges are present, as well as how to separate them and how to pin down the root causes of the individual frequencies. Appropriate corrective modifications are given with post-modification test results showing root-causes and the proper remedy that eliminated these instabilities.

Sufficient references are given at the end of this report for more details if further explanation is needed on individual subjects.

INTRODUCTION

Power Plant Pump Troubleshooting State-of-the-Art Overview

The size of electric generating stations grew rapidly in the late 1960s and a large number of nuclear plants under construction were getting closer to start-up. The size of generating stations being designed grew almost daily, without the benefit of operating experience in the smaller units. The demand for very large feed pumps, as well as the competition among pump manufacturers, was the greatest in history. Initially, low speed, multistage feed pumps were offered, which had a more or less known performance history. Subsequently, large, high-energy-input feed pumps were quickly designed by pump vendors to replace the low speed, multistage designs. This was not an engineering decision; instead, it was a marketing move to remain competitive in the lucrative new nuclear business. Low speed (1200 to 1800 rpm) booster pump designs were quickly scaled up to speeds over 5000 rpm without the benefit of proven performance and reliable operation. A new monster was created: high-energy-input, single-stage, double-suction pumps for nuclear application.

The damage was done, and the utilities that owned these pumps were left with the task of making them operate. A new era started for high head-per-stage designs that carried over into boiler feed pump designs, as well as large injection pumps for the oil fields. The first large nuclear plant owners were committed to an accelerated pump research program by necessity through the numerous failures of the early designs. The 11 large nuclear facilities listed in Table I-1 are an example of those who contributed heavily to the state of the art of the present high-energy-input feed pump designs.

Table I-1
Nuclear Facilities That Were Pioneers with Large, High-Energy-Input Feed Pumps

These nuclear power stations permitted Energy Research and Consultants Corporation (ERCO) to initiate pump technology improvements due to major failures in new pump applications. This new technology drive also improved feed pumps for fossil-fuel applications.

Number	Utility	Nuclear Station	Year	MW (a)
1	NSP	Monticello	1970	540
2	CECO	Dresden 2, 3	1971	2 x 800
3	NUSCO	Millstone 1	1972	650
4	CECO	Quad Cities	1972	2 x 800
5	Y. A.	Maine Yankee	1972	900
6	NSP	Prairie Island 1, 2	1973	2 x 650
7	P.S. WISC.	Kewaunee	1973	650
8	CECO	Zion 1,2	1973	2, 1100
9	RG&E	Ginna	1974	500
10	DECO	Enrico Fermi 2	1974	1300
11	PECO	Limerick 1, 2	1986	2 x 1150 (b)

a) All modified by the author.
b) Described in References 1 and 11 and at the end of this paper.

During this same time period in England, an ambitious program was undertaken to design a new "stiff-shaft," 4000 ft/stage pump, which was planned as the standard for their large fossil units. Hydraulic models are expensive, the technology is very complex, and it can take decades to obtain meaningful results; on the other hand, rotor-dynamic models are inexpensive, and the results are available much faster. Therefore, with the added influence of academia, rotor-dynamic considerations won over hydro-dynamic considerations and were considered first while hydraulics took a distant second place. As a result, hydraulic research was weak and practically non-existent.

Coinciding with the utility industry requirements for high-energy-input feed pumps in the large 900 to 1300 MW power generating units, oil field applications also demanded a new pump design for injection service. As a result of management decisions, oil field production had accelerated, and the pump designs were simply extrapolated by the pump manufacturers. Due to the urgency to prepare proposals for the oil companies, R&D in the hydraulic area was again neglected. With the improper rotor-dynamic behavior, utility and oil field applications could not even start up with these large pumps; however, the effects of poor hydro-dynamic design could go undetected and take years to surface. For example, pumping cold water at these high energy

levels made cavitation erosion an unexpected monster. The concept of net positive suction head (NPSH) quickly became known to everyone. Not yet known, however, was how and with what financial support the necessary hydraulic research would be done.

We quote from a 1970 publication [3]: "Competition in the boiler feed pump (BFP) market has created a situation where desired pump efficiencies are exceeding current technological capabilities. Though performance figures appear somewhat inflated now, competitive position in the future demands that higher efficiencies be delivered without creating operational problems." This blind drive for efficiency overshadowed the real technology shortcomings in high-energy-input, multistage pump designs, particularly at reduced pump capacities.

The previously lucrative pump market started to shrink as the economy slowed in the 1970s. This resulted in periodic layoffs and the loss of experienced personnel to retirement, which quickly decimated the available expertise in the area of pump design and particularly field troubleshooting. For the first time in pump history, the original equipment manufacturers (OEMs) received competition from non-OEM repair facilities for the repair of feed pump rotors. The non-OEM repair shops were not spoiled by the lucrative business, were not burdened with large overhead costs, and were willing to underbid the OEM by as much as 10 times just to get the business. More layoffs followed at the OEMs, the market kept shrinking, early retirement programs were offered, and the number of well-trained, conscientious workers in this specialized field continued to shrink. This made competition even easier for the small non-OEM repair shops. But it also brought into the marketplace poor quality OEM and non-OEM shops who were unable to deal with the precision required for feed pump repair. At the same time, the only R&D going on was in the field, financed by the utilities and guided by ERCO.

Cancellation of nuclear projects started in the late 1970s and went into full swing following the March 28, 1979, Three Mile Island accident. By then, new pump sales were almost at a complete halt in both the utility and oil field markets. The only business that remained was the repair work that quickly received a new, better sounding name: "after-market service" or "after-market engineering."

Many large fossil-fired units, originally designed and built for base load operation, switched to cycling service as the number of large nuclear units in operation increased and the growth in electric power consumption decreased. Some units as large as 900 MW, not only operated in cycling mode, but also shut down daily. Major problems started to surface immediately in the pumps and the feedwater systems. Pump manufacturers looked to the piping designers, who questioned the integrity of the control system, and it was finally concluded that cyclic mode operation required more experienced people in the control room. Eventually, the plant operators accepted the idea that it is an "operating procedure" problem, and not a basic, inherent pump or system design efficiency.

EPRI, founded in 1972 to sponsor R&D projects for the utility industry, stepped in to provide partial support for the neglected R&D for power plant components. Feed pump research began in 1975 due to the persuasion of ERCO. Initially, a general survey of field failures was conducted that identified failure modes, generic failure root causes, and solutions to some of these major problems. The results of the first survey were published in a 1978 EPRI report by Energy Research and Consultants Corporation (ERCO) titled, "Survey of Feed Pump Outages" [4], and followed by other EPRI efforts [5, 6] also by ERCO. Boiler feed pumps turned out to be

one of the largest outage causing power plant components. The survey results were surprising to the utilities and gave enough incentive to EPRI, in conjunction with the Edison Electric Institute (EEI) Prime Movers Committee, to broaden the scope of this work.

The three major technology problem areas identified as being responsible for the major portion of all high-energy-input feed pump failures but previously never understood, tackled, or solved were:

- Feedwater (FW) system instability at part-load operation
- BFP "hydraulic instability" at part-load operation
- Axial thrust generated by a pump stage

The results of many years of research and development, supported in-house at ERCO and performed at many power station sites across the United States, point out that these problem areas are not only directly related but can stem from the same source. With the users' financed R&D, the efforts were strictly field problem oriented. More was accomplished in a decade in the "big research laboratory" (East Coast to West Coast, Texas to Canada) than ever before. All major improvements in feed pump technology since about 1970 are due to utility efforts systematically guided by ERCO, all financed by the utilities and partially by ERCO.

CONTENTS

LIST OF FIGURES

LIST OF TABLES

1
HIGH-ENERGY CENTRIFUGAL PUMPS

Through the years, new developments in materials and hydraulics have enabled designers to produce pumps that can withstand the stresses of higher power density. In fact, a logical definition of high-energy pumps is that they will experience stresses great enough to demand special engineering attention in the design phase. Such stresses increase directly with pressure rise per pump stage and become a reliable indicator of pump energy level.

On this basis, the power plant feed pumps with the highest energy level are the multistage barrel pumps that supply supercritical boilers using as few as four centrifugal impellers in series. These machines have single- or double-suction first-stage impellers, depending on the net positive suction head (NPSH) supplied by the plant. In the nuclear feed service, where the feedwater pressure requirements are not as great, high-energy, single-stage, double-suction pumps are used.

Most successful high-energy feed pump designs are the result of a gradual evolution. They are typically based on past designs that have proven successful throughout years of operation. As energy levels of feed pumps increased, as shown in Figure 1-1, with higher flow and pressure requirements, original equipment manufacturers (OEMs) extrapolated past hydraulic and mechanical designs in an attempt to deliver successful and reliable feed pumps to the utilities. The extrapolation of the past design continued without proper research to determine the limitations of the past designs, leaving the power stations to be the ultimate test or research facility for the new generation of high-energy-input pumps.

The high-energy-input centrifugal pumps in power plant applications are the primary topic for discussion in this report. The large forces generated in these pumps cause inherent problem areas, for example, design or manufacturing errors, to surface much more dramatically and more often than in lower energy pump applications. In the case of a machine failure, the physical damage to components is much more devastating in appearance than a low-speed, low-energy-input rotating machine. Also, high-energy-input pumps are generally the most critical to reliable power production at a generating plant. Thus, a failure of one of these pumps usually results in plant shutdown or significant plant load reductions. The highest stressed (that is, highest energy input pumps) today are:

- Boiler feed pumps (BFP)
- Nuclear feed pumps (NFP for PWR or RFP for BWR plants)
- Primary coolant/reactor recirculating pumps (PCPs, RCPs, or RRPs, various names used by nuclear plant owners, OEMs, and consultants)
- Condenser/cooling tower circulating water pumps

The design configuration of the first two pump applications noted above varies among pump manufacturers, sales personnel, and designers within the OEMs. Although there are similarities and common features within all pumps, the subtle differences require that each problem case be handled independently. A tabulation of the boiler feed pumps sold in the U.S. is provided in Table 1-1. The various pump configurations include:

- Multistage or single stage
- Single-suction (SS) or double-suction (DS) first-stage impeller design
- Diffuser-type or volute-type design
- Horizontal or vertical orientation

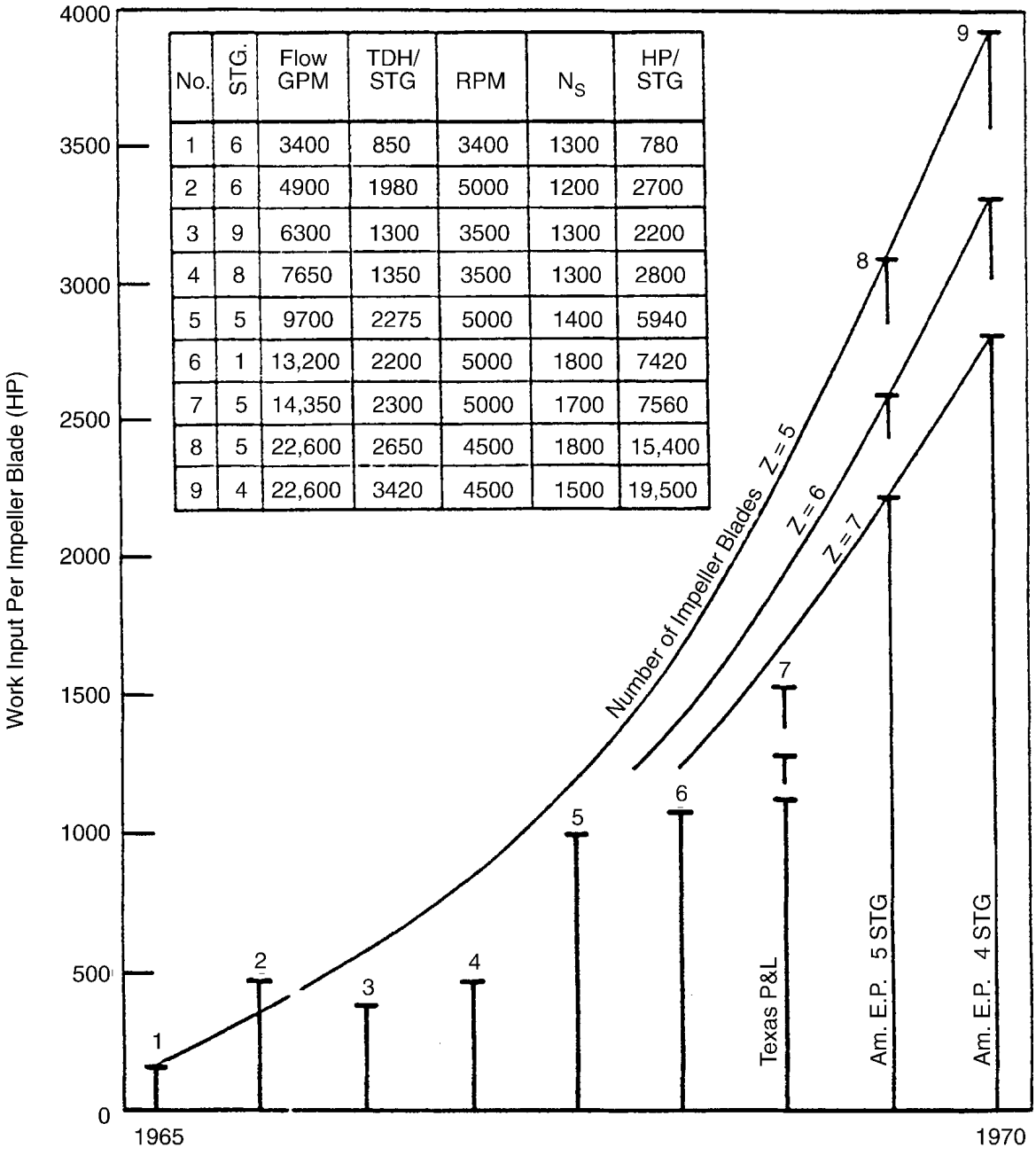

No.	STG.	Flow GPM	TDH/ STG	RPM	N_S	HP/ STG
1	6	3400	850	3400	1300	780
2	6	4900	1980	5000	1200	2700
3	9	6300	1300	3500	1300	2200
4	8	7650	1350	3500	1300	2800
5	5	9700	2275	5000	1400	5940
6	1	13,200	2200	5000	1800	7420
7	5	14,350	2300	5000	1700	7560
8	5	22,600	2650	4500	1800	15,400
9	4	22,600	3420	4500	1500	19,500

Figure 1-1
Increase of Horsepower per BFP Impeller Vane in Five Years in U.S. Utilities (No Further Development Since 1970)

Table 1-1
Tabulation of Main Coolant Pumps in the U.S. BWR and PWR Nuclear Plants

	Type	Plant	Company	MW	OPER	NSSS	PCP	#	GFM	RFM	H (FT)	SIZE/TYPE	Z2	Z3	Motor	HP
1	BWR	Arnold	Iowa E.L&P	550	1974	G.E.	B-J	2	27000	1650	550	22x22x30 DVSS			G.E.	
2	BWR	Browns Ferry #1	TVA	1065	1974	G.E.	B-J	2	45000	1650	710	28x28x36			G.E.	8000
3	BWR	Browns Ferry #2	TVA	1065	1974	G.E.	B-J	2	45000	1650	710	28x28x36			G.E.	8000
4	BWR	Browns Ferry #3	TVA	1065	1978	G.E.	B-J	2	45000	1650	710	28x28x36			G.E.	8000
5	BWR	Brunswick #1	Carolina PW&L	820	1978	G.E.	SING	2	45000	1650	500	RV			G.E.	
6	BWR	Brunswick #2	Carolina PW&L	820	1975	G.E.	SING	2	45000	1650	500	RV			G.E.	
7	BWR	Clinton	ILL. PW.	360	1986	G.E.	SING	2								
8	BWR	Cooper	Nebraska PPD	800	1974	G.E.	B-J	2	45000	1860	500	28x28x30			G.E.	
9	BWR	Dresden #1	CECO	200	1980	G.E.	B-J	2	1700	1750	130	6x6x13			G.E.	
10	BWR	Dresden #2	CECO	800	1970	G.E.	B-J	2	45000	1860	570	28x28x30	7		G.E.	
11	BWR	Dresden #3	CECO	800	1971	G.E.	B-J	2	45000	1860	670	28x28x30	7		G.E.	
12	BWR	Erico Fermi #2	Detroit Ed. Co.	1300	(1980)	G.E.	B-J	2	45000	1860	710	28x28x36			G.E.	8000
13	BWR	Fitzpatrick	PW. Auth. NY	850	1975	G.E.	B-J	2	45000	1860	500	28x28x30			G.E.	
14	BWR	Grand Gulf #1	Miss. PW&L	1250	1985	G.E.	B-J	2	45000	1780	770	28x28x36 DVSS (HS)				
15	BWR	Hatch #1	Georgia PW.	800	1974	G.E.	B-J	2	45000	1650	630	28x28x30			G.E.	8000
16	BWR	Hatch #2	Georgia PW.	800	1979	G.E.	B-J	2	45000	1650	630	28x28x30			G.E.	8000
17	BWR	Hope Creek	PSE&G	1100	1986	G.E.	B-J	2		1680		28x28x36				
18	BWR	La Salle #1	CECO	1100		G.E.	SING	2								
19	BWR	Lenstadt	KKL			G.E.	B-J	2	45000			28x28x36 DVSS (HS)				
20	BWR	Limerick #1	PECO	1100		G.E.	B-J	2	45000	1650	710	28x28x36				
21	BWR	Limerick #1	PECO	1100		G.E.	B-J	2	45000	1650	710	28x28x36				
22	BWR	Millstone #1	NUSCO	650	1970	G.E.	B-J	2	45000	1060	370	28x28x28	7		G.E.	
23	BWR	Monticello	NSP	550	1971	G.E.	SING	2	32000	1060	402	RV	7		G.E.	
24	BWR	Nine Mile Pt. #1	Niagara Mohawk	610	1969	G.E.	B-J	5	30000	840	120	28x28x32			G.E.	
25	BWR	Nine Mile Pt. #2	Niagara Mohawk	900		G.E.	SING	2								
26	BWR	Oyster Creek	Jersey Central	640	1969	G.E.	B-J	5	32000	840	126	28x28x30			G.E.	
27	BWR	Peach Bottom #2	PECO	1066	1974	G.E.	B-J	2	45000	1650	710	28x28x36 DVSS			G.E.	8000
28	BWR	Peach Bottom #3	PECO	1066	1974	G.E.	B-J	2	45000	1650	710	28x28x36 DVSS			G.E.	8000
29	BWR	Perry #1	Cleveland Elec.	1200	1987	G.E.	B-J	2	45000	1780		28x28x36 DVSS (HS)				
30	BWR	Pilgrim #1	Boston Ed.	650	1972	G.E.	B-J	2	45000	1860	380	28x28x28			G.E.	
31	BWR	Quad Cities #1	CECO	800	1972	G.E.	B-J	2	45000	1860	670	28x28x30			G.E.	
32	BWR	Quad Cities #2	CECO	800	1972	G.E.	B-J	2	45000	1860	670	28x28x30			G.E.	
33	BWR	River Bend	Gulf States	940		G.E.	SING	2				20x20x33				
34	BWR	Susquehanna #1	PP&L	1100		G.E.	B-J	2	45000	1860	710	28x28x36				
35	BWR	Susquehanna #2	PP&L	1100		G.E.	B-J	2	45000	1860	710	28x28x36				
36	BWR	Vermont Yank.	Yankee Atomic	520	1972	G.E.	B-J	2	32000	1860	340	28x28x26			G.E.	
37	BWR	Zimmer	Cincinn. Elec.	1300	*	G.E.	SING	2	32000	(80)	800	RV			G.E.	
38	PWR	Ark. Nuclear One	Arkansas PW.	850	1974	B&W	B-J	4	88000	1180	362	33x33x38 DFSS			A-C	8250
39	PWR	Ark. Nuclear Two	Arkansas PW.	950		C-E	B-J	4	80000	900	248	36x34x42 DFSS				5800
40	PWR	Beaver Valley #1	DUQ. P&L	850	1973	W	W	3	88000	1180		93-A			W	
41	PWR	Beaver Valley #2	DUQ. P&L	850		W	W	3	88000	1180		93-A			W	
42	PWR	Bellefonte #1	TVA	1300		B&W	SING	4	104000	1180		RDV			AEG	
43	PWR	Bellefonte #2	TVA	1300		B&W	SING	4	104000	1180		RDV			AEG	
44	PWR	Braidwood #1	CECO	1120		W	W	4		1180		93-AS			W	
45	PWR	Braidwood #2	CECO	1120		W	W	4		1180		93-AS			W	
46	PWR	Byron #1	CECO	1200		W	W	4		1180		93-AS			W	
47	PWR	Byron #2	CECO	1200		W	W	4		1180		93-AS			W	
48	PWR	Callaway	Union Elect.	1160		W	W	4		1180		93-A1			W	
49	PWR	Calvert Cliffs #1	Baltimore G&E	850	1976	C-E	B-J	4	8180	900	300	34x34x43 DFSS			G.E.	7000
50	PWR	Calvert Cliffs #2	Baltimore G&E	850	1977	C-E	B-J	4	8100	900	300	34x34x43 DFSS			G.E.	7000
51	PWR	Catawba #1	Duke PW. Co.	1160		W		4		1180		93-AS			W	
52	PWR	Catawba #2	Duke PW. Co.	1160		W		4		1180		93-AS			W	
53	PWR	Comanche Peak #1	Texas Utilities	1150		W	W	4		1180		93-A			W	
54	PWR	Comanche Peak #2	Texas Utilities	1150		W	W	4		1180		93-A			W	
55	PWR	Conn. Yankee	NUSCO	675	1968	W	W	2	82000	1180		83			W	
56	PWR	Cook #1	AEP	1050	1975	W	W	4	88000	1180		93-AS			W	
57	PWR	Cook #2	AEP	1050	1977	W	W	4	88000	1180		93-AS	7	12	W	
58	PWR	Crystal River #3	Florida PW.	880	1977	B&W	B-J	4	88000	1180	362	33x33x38 DFSS			G.E.	8250
59	PWR	Davis Besse	Toledo Ed.	900	1977	B&W	B-J	4	88000	1180	362	33x33x38 DFSS			W	9000
60	PWR	Diablo Canyon #1	PG&E	1100		W	W	4		1180		93-AS	7	12	W	
61	PWR	Diablo Canyon #2	PG&E	1100		W	W	4		1180		93-AS	7	12	W	

Table 1-1 (cont.)
Tabulation of Main Coolant Pumps in the U.S. BWR and PWR Nuclear Plants

	Type	Plant	Company	MW	OPER	NSSS	PCP	#	GFM	RFM	H (FT)	SIZE/TYPE	Z2	Z3	Motor	HP
62	PWR	Farley #2	Alabama PW	860	1977	W	W	3	88,000	1180		93-AS	7	12	W	
63	PWR	Farley #2	Alabama PW	860	1981	W	W	3	88,000	1180		93-AS	7	12	W	
64	PWR	Forked River	GPU	1100		C-E	KSS	4	104,000	1180	387	RER-710			A-C	
65	PWR	Fort Calhoun	Omaha	495	1973	C-E	B-J	4	47,000	1180	260	28x28x34			G.E.	
66	PWR	Ginna	Rochester G&E	490	1970	W	W	2	82,000	1180		93			W	
67	PWR	Indian Pt. #2	Con. Ed	900	1973	W	W	4	82,000	1180	272	93			W	
68	PWR	Indian Pt. #3	NY State	965	1976	W	W	4	82,000	1180	272	93			W	
69	PWR	Kewaunee	Wisc. PS	540	1974	W	W	2	83,000	1180		93-AS			W	
70	PWR	Maine Yankee	Yankee Atomic	500	1972	C-E	B-J	3	108,000	1180	280	40x40x38 DFSS			A-C	9000
71	PWR	Marble Hill #1					W					93-A				
72	PWR	Marble Hill #2					W					93-A				
73	PWR	McGuire #1	Duke PW	1180		W	W	4		1180		93-AS			W	
74	PWR	McGuire #2	Duke PW	1180		W	W	4		1180		93-AS			W	
75	PWR	Millstone #2	NUSCO	830	1975	C-E	B-J	4	83,000	900	300	35x35x34 DFSS			G.E.	7000
76	PWR	Millstone #3	NUSCO	1150		W	W	4		1180		93-A1			W	
77	PWR	North Anna #1	VEPCO	340	1977	W	W	3	88,000	1180	279	93-A			W	
78	PWR	North Anna #2	VEPCO	340	1978	W	W	3	88,000	1180	279	93-AS			W	
79	PWR	Oconee #1	Duke PW	830	1973	B&W	W	4	88,000	1180	372	93-AS			W	
80	PWR	Oconee #2	Duke PW	830	1974	B&W	SING	4	88,000	1180	372	RQV			W	
81	PWR	Oconee #3	Duke PW	830	1974	B&W	SING	4	88,000	1180	372	RQV			W	
82	PWR	Palisades	Consumers PW	800	1971	C-E	B-J	4	83,000	1180	260	35x36x45			A-C	6500
83	PWR	Palo Verde #1	Arizona PS	1300	1985	C-E	KSS	4		1180			6	11		
84	PWR	Palo Verde #2	Arizona PS	1300	1986	C-E	KSS	4		1180			6	11		
85	PWR	Palo Verde #3	Arizona PS	1300	1987	C-E	KSS	4		1180			6	11		
86	PWR	Prairie Island #1	NSP	540	1974	W	W	2	83,000	1180		93-AS	4		W	
87	PWR	Prairie Island #2	NSP	540	1975	W	W	2	83,000	1180		93-AS	4		W	
88	PWR	Pt Beach #1	Wisc. E PW	500	1971	W	W	2	83,000	1180	262	93			W	
89	PWR	Pt Beach #2	Wisc. E PW	500	1973	W	W	2	83,000	1180	262	93			W	
90	PWR	Ranch Seso	SMUD	320	1975	B&W	SING	4	96,000	1180	282	RQV			A-C	
91	PWR	Robinson #2	Carolina PW	700	1971	W	W	3		1180		93			W	
92	PWR	Salem #1	PSE&G	1100	1977	W	W	4		1180	270	93-A			W	
93	PWR	Salem #2	PSE&G	1100	1979	W	W	4		1180	270	93-A			W	
94	PWR	San Onofre #1	So. Cal Ed	430	1965	W	W	3	83,000	1180		63			W	
95	PWR	San Onofre #2	So. Cal Ed	1140		C-E	B-J	4	99,000	1180	290	36x38x38			A-C	
96	PWR	San Onofre #3	So. Cal Ed	1140		C-E	B-J	4	99,000	1180	290	36x38x38			A-C	
97	PWR	Seabrook #1					W					93-A1				
98	PWR	Seabrook #2					W					93-A1				
99	PWR	Sequoyah #1	TVA	1150		W	W	4				93-AS			W	
100	PWR	Sequoyah #2	TVA	1150	(80)	W	W	4	88,000			93-AS			W	
101	PWR	Shearon Harris	Carolina PW&L	300		W	W	4				93-A			W	
102	PWR	So. Texas Proj. #1	Houston L&P	1250		W	W	4				100-A			W	
103	PWR	So. Texas Proj. #2	Houston L&P	1250		W	W	4				100-A			W	
104	PWR	St. Lucie #1	Florida P&L	860	1978	C-E	B-J	4				35x36x43 DFSS			A-C	
105	PWR	St. Lucie #2	Florida P&L	850		C-E	B-J	4				35x36x43 DFSS			A-C	
106	PWR	Summer	S. Carolina E&G	900		W	W	4				93-A			W	
107	PWR	Surry #1	VEPCO	800	1972	W	W	3	88,000			93-A			W	
108	PWR	Surry #2	VEPCO	800	1973	W	W	3	88,000			93-A			W	
109	PWR	TMM #1	MET ED	820	1974	B&W	W	4	88,000			93-AS			A-C	6500
110	PWR	TMM #2	MET ED	900	1978	B&W	SING	4	88,000			RQV			A-C	6500
111	PWR	Trojan	PGE	1130	1976	W	W	4				93-AS			W	
112	PWR	Turkey Pt #3	Florida PW&L	725	1972	W	W	3				93			W	
113	PWR	Turkey Pt #4	Florida PW&L	725	1973	W	W	3				93			W	
114	PWR	Vogtle #1	Georgia FW	1120		W	W	4				93-A1			W	
115	PWR	Vogtle #2	Georgia FW	1120		W	W	4				93-A1			W	
116	PWR	Waterford #3	Louisiana	1165		C-E	B-J	4	39,000			38x38x42			G.E.	
117	PWR	Watts Bar #1	TVA	1120		W	W	4				93-AS			W	
118	PWR	Watts Bar #2	TVA	1120		W	W	4				93-AS			W	
119	PWR	Wolf Creek	Kansas	1150		W	W	4				93-A1			W	
120	PWR	Yankee Rowe	Yankee Atomic	175	61	W	W		24,000			CANNED			W	
121	PWR	Zion #1	CECO	1100	1973	W	W	4	83,000			93-A			W	
122	PWR	Zion #2	CECO	1100	1975	W	W	4	83,000			93-A			W	

The third pump category noted above, PCP, is typically vertical, single-stage, single-suction, diffuser-type pumps with a water-lubricated journal bearing above the impeller. These pumps are included in this report because they were declared the highest outage-causing components in nuclear plants [29], particularly due to shaft breakage or seal and bearing failures [29–32]. A tabulation of the PCPs sold in the United States is provided in Table 1-1. The fourth category noted above usually entails a vertical pump design, but a large number of horizontal applications are in service.

The boiler and nuclear feed pumps have radial flow impellers as characterized by their specific speed (N_S), which is defined by the equation:

$$N_S = (RPM)(GPM)^{½} / (H)^{3/4}$$

The pump-specific speed defines the shape of the impeller and the expected efficiency versus flow requirements, as shown in Figure 1-2. Most power plant pumps have a specific speed in the range of:

$$1000 \leq N_S \leq 3000$$

except for the large circulating pumps and most PCPs, which are in the vicinity of 4500.

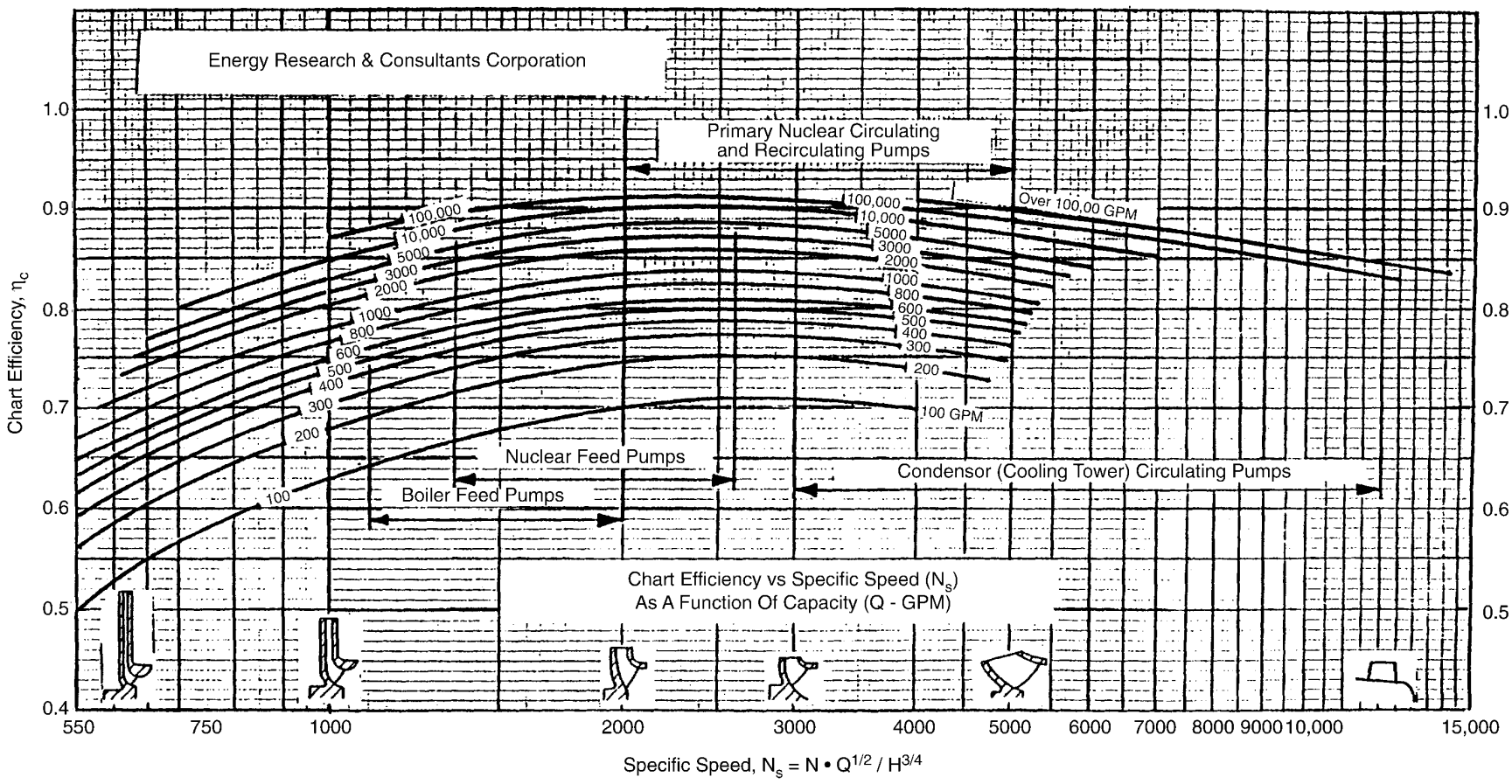

Figure 1-2
Expected Centrifugal Pump Efficiency as a Function of Specific Speed, Flow, and Impeller Geometry

All technology that applies to high-energy-input boiler feed pumps applies on a smaller scale to other industry pump types such as injection pumps (oil fields), chemical process pumps, and descaling pumps in the steel industry, and to other power plant pumps, such as:

- Feed water boosters (single-stage, double-suction)
- Condensate and heater drain (normally multistage, vertical)
- Nuclear safety-related pumps, such as charging/safety injection and auxiliary feedwater

A systematic survey of various pump geometries and design parameters was conducted by Energy Research and Consultants Corporation (ERCO) throughout the past 20 years to arrive at optimum hydraulic channel geometries, especially for part-load hydraulic stability. Some of the main targets of this long-range work were the understanding and control of:

- Rotor axial thrust
- Vibration characteristics
- Effects on efficiency
- Machine reliability increases through improved manufacturing/repair practices
- Proper rotor assembly/installation procedures

Modifications were introduced in a large number of nuclear and fossil power plant applications and in various ranges of pump parameters.

Many of the modified pumps were properly tested under the guidance of ERCO. A large number of cases included laboratory-type testing, especially to establish optimum dimensions for Gap A and its Overlap-Ratio (X), and Gap B, including analysis of the effects on loss or gain of efficiency as these parameters were rigorously varied. Ranges of some of the quantities investigated by ERCO are presented in Table 1-3. In order to appreciate the large number of modifications performed during the last few decades, the number of pumps modified in three select areas is shown in Figure 1-4.

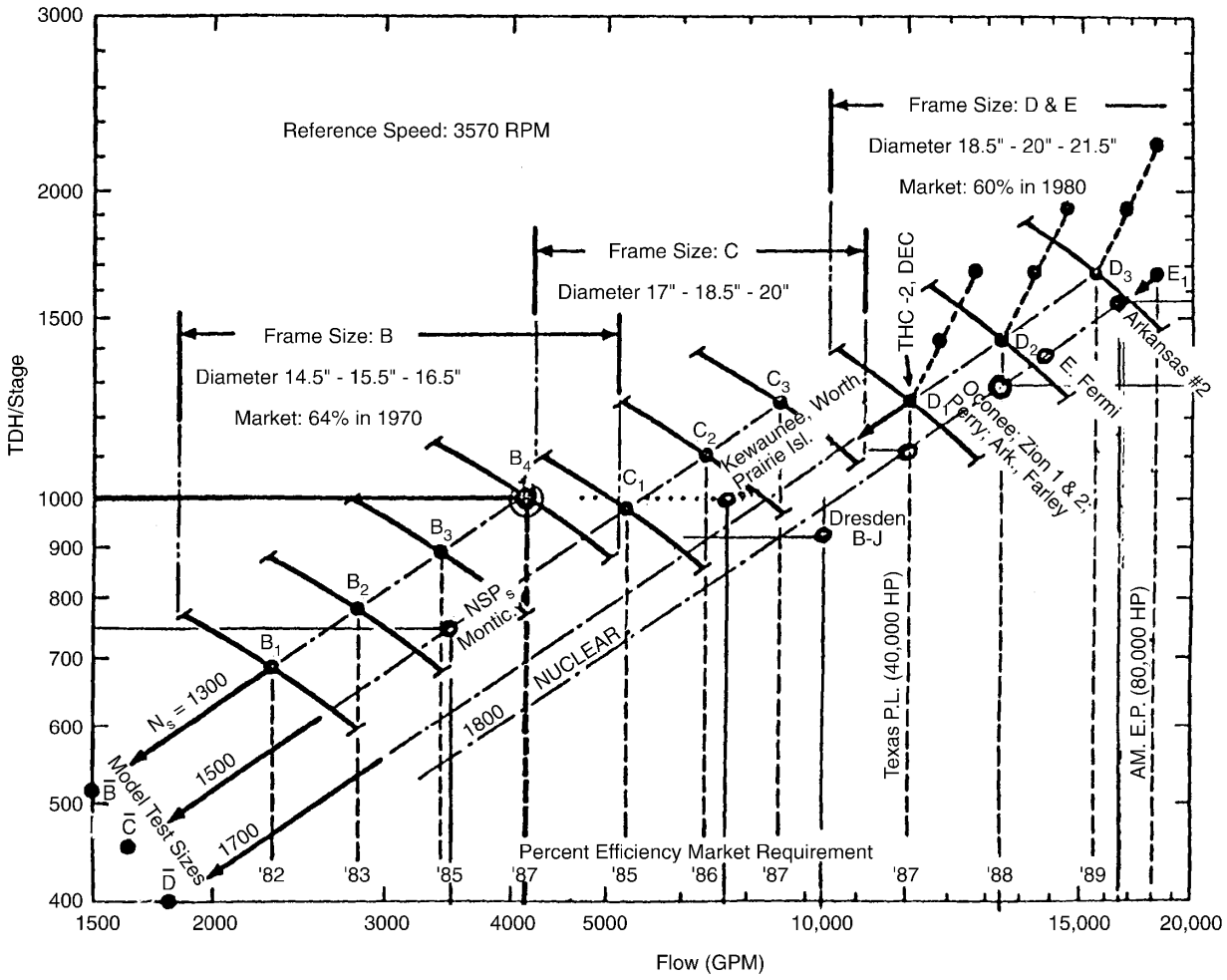

Figure 1-3
Customary Flow, Head, and Specific Speed Ranges for BFPs in U.S. Fossil Stations

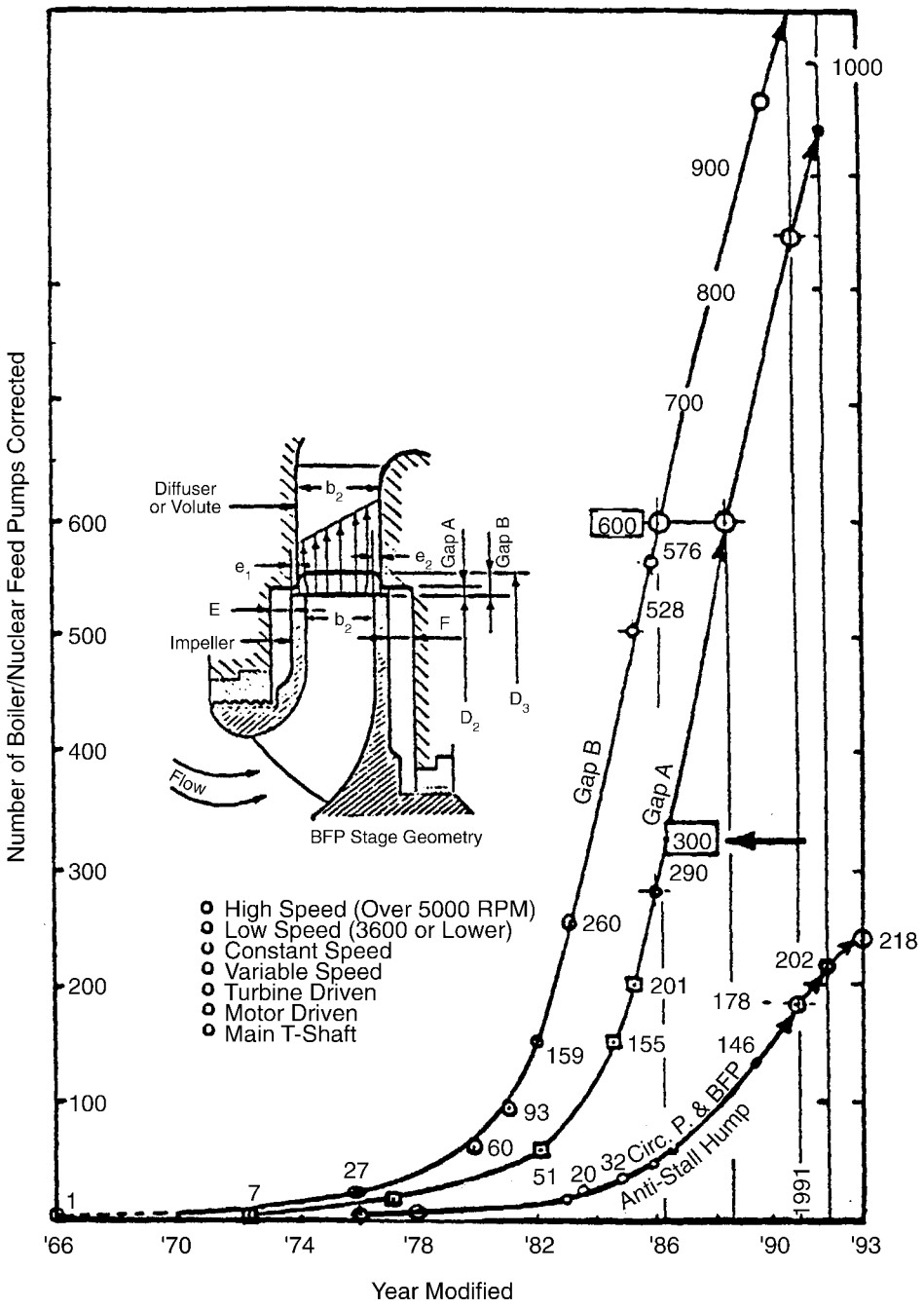

Number of troublesome boiler/nuclear feed pumps BFP/NFP modified with ERCO assistance for optimum Gap A, the Overlap, and Gap B during the past years. Also circ. pump modifications with impeller back-filing and application of the anti-stall hump to eliminate inlet cavitation damage and to increase flow capacity (if needed). The hump was also applied to several high-energy-input BFP/NFP first stage impellers with very high success.

Figure 1-4
ERCO History of Gap A, Gap B, and Anti-Stall Hump Modifications for Utilities

Table 1-2
Tabulation of U.S. Boiler Feed Pumps by Manufacturer

AL-CH/Sulzer Type: HPT/HPTX							
Size	24	30	32	34	35	40	Total
Qty.	30	10	19	8	10	5	82

Byron Jackson Type: HDB/HSB						
Size	6x8x13 10x10x13 10x12x13	8x10x14 10x12x14 12x12x14	10x12x15 16x12x15	14x14x16	16x16x18 12x16x19 12x16x21 20x20x21/22	Total
Qty.	21	156	32	101	18	328

DeLaval Type: A/B/C/D					
Size	A	B	C	D	Total
Qty.	48	261	31	2	342

Ingersoll-Rand Type: CHTA/CA												
Size	5 6 8 12	40 50 56 60	65	75	80	84 85 88	95	100	120 125	130	20 x 25	Total
Qty.	32	14	45	46	59	26	21	17	8	50	8	326

Pacific Type: BFI								
Size	6 in.	8 in.	10 in.	12 in.	14 in.	16 in.	18 in.	Total
Qty.	430	136	22	66	43	15	5	717

Worthington Type: WNC/WNCD						
Size	6	8	10	12	14	Total
Qty.	47	109	32	41	34	263

Table 1-3
Various Dimensions and Parameters Tested and Compiled by ERCO in Nuclear and Fossil Power Stations

Minimum (In/mm)	Parameter	Maximum (In/mm)
8/203	D_2	100/2540
0.75/19	b_2	9/228
0.9	b_3/b_2	1.5
0.024/.6	Gap A	0.3/7.62
0.4%	Gap B	34%
0.07/1.8	Gaps E&F	1.0/25.4
0	X=O/A	16
500	RPM	13,500
1,100/21	N_S	2,200/42
8,000/152	S_S	13,500/257

1.1 Developments Over the Past 20 Years

Hydraulic, rotor-dynamic, and system instabilities, particularly feedwater systems caused by centrifugal pumps, have caused many problems for large generating power plants and substantially influenced the availability and reliability of those plants. However, when compared to the research performed on other types of rotating equipment, such as compressors and turbines, only a limited amount of true research has been completed to improve the performance of centrifugal pumps.

Hydraulically induced vibration and pressure pulsations are now known to be major causes of pump failures, but they remain the least understood phenomenon associated with centrifugal pumps. The results and understanding of hydraulic instability explain a large range of observed problems, such as:

- Breakage of pump internal components
- Failure of external components
- Feedwater system complications or instabilities
- Malfunction of control valves and control systems
- Frequent plant trips
- Rotor dynamic and bearing instabilities
- Subsynchronous, running speed and blade pass (multiples of blade pass) vibration frequencies

One of the most important causes of failures in centrifugal pumps is the geometric relationship between the impeller exit and diffuser/volute inlet, (that is, hydraulic geometry or configuration). This geometry has the greatest influence on rotor vibration, axial thrust (static and dynamic components), hydraulic performance of the pump and its efficiency, feedwater piping, and the stability of the entire feedwater system. The influence of the hydraulic geometry has been validated by retrofit modifications on a very large number of boiler feed pumps, feedwater booster pumps, and nuclear feed pumps. It has also been demonstrated that the results apply to both diffuser- and volute-style pumps. Also, the secondary benefits of correcting the pump's hydraulic geometry have been a major reduction in noise generated by the pump and improvement of pump efficiencies.

The following is a list of significant developments and corrective actions in the area of centrifugal pumps that have occurred since 1970:

- Major advances in instrumentation for detecting and analyzing vibration and for machinery protection. However, most utilities, until recently, have not taken full advantage of the technology, and many do not use the technology.
- Elimination of seizures in boiler feed pumps through research, testing, and experimentation in materials, hardness, and wear surface geometry.
- Elimination of floating ring seals, because of their high maintenance and the cost of spare parts, with the gradual conversion to labyrinth-type seals.

- Use of tilting pad journal bearings to replace dynamically unstable journal bearings, especially in power stations where rotor-dynamic instability has caused high maintenance or recurring failures in feed pumps and other rotating machines (see Section 14).
- Introduction of the taper to the vertical face of the axial-thrust balancing disk, significantly increasing disk load carrying capacity. This eliminated recurring failures and also prevented failures in many new applications (see Section 11) [1, 2, 4, 9,16].
- Large variations in axial thrust, thrust reversal, and axial dynamic instability were discovered, explained, and corrected in many field applications. The relationship between axial thrust, Gaps A and B, and the backflow catcher [19] was discovered and applied.
- Four vane impellers were eliminated in double volute feed pumps, both in nuclear and fossil plant applications.
- Discovery and explanation of unfavorable impeller-to-diffuser/volute vane combinations in existing units and the effect on pump failure rates, maintenance, certain system instabilities, and plant availability (for example, avoid 6-8, 6-9, 6-10, and 6-21 vane combinations). If these cannot be avoided, proper impeller-to-diffuser geometry modifications may be required to improve pump performance and reliability.
- Determination of ways to increase existing BFP capacity to increase power plant output and to extend the life expectancy of older designs.
- Determination of ways to increase the capacity of circulating water pumps and thus prevent the derating of plants or load reductions during hot summer months.
- Development and application of the antistall hump to eliminate major cavitation at the impeller inlet of large circulating pumps without redesigning the impellers or without purchasing new replacement castings. This is also applicable to the inlet portion of vanes in any hydraulic channel of any pump type.
- Continuing extensive research on the damping effects of hydraulic components (for example, balancing drum, impeller wear rings, and the impeller itself combined with diffuser geometry) on rotor-dynamic behavior with field applications of the results being made to solve destructive subsynchronous vibration problems.
- Successful applications of the swirl break to boiler feed pumps to eliminate balancing-drum-piston-caused instability [12]. This was tested in a laboratory for impeller wear rings to improve rotor-dynamic stability. However, it has not been reported how much pump efficiency is sacrificed by the installation of a swirl break behind the impeller shroud, and the effects on static and dynamic axial forces at off-design flows have not been evaluated.
- Continued search for the interrelationship between rotor-dynamic and hydraulically induced forces. The issues are how much can damping control these forces and how great is the energy input that gives the hydraulic forces an overriding or dominant effect or influence. A crossover point between rotor-dynamic and hydraulic forces and their interaction as a function of energy input level is being sought using both laboratory measurements and actual field applications.
- Discovery of the effectiveness of Gap A and its overlap as a significant contributor to rotor dynamic damping when properly optimized. This conclusion is based on data collected from a large number of field installations before and after the modifications were performed.

- Establishment through field applications that Gap A and its overlap eliminate or at least greatly reduce internal and external hydraulic instabilities, in particular axial shuttling of the rotor.
- Explanation and correction of axial thrust, thrust reversal, and dynamic instability in a large number of field modifications by utilizing the relationship that was discovered between axial thrust, Gap A and its overlap, and Gap B.
- Discovery and demonstration of the relationship between axial thrust and the backflow deflector through laboratory measurements [11, 19].
- Discovery and proof through field demonstrations that Gap A and its overlap fully control the static and, more important, the dynamic components of axial thrust developed by the hydro-dynamic action on rotor components.
- Demonstration that full control over the static and dynamic axial forces permits application of the conventional thrust calculation methods to multistage boiler feed pumps. The discrepancies between the predicted results and various calculation methods had led to a long and unresolved dispute among researchers. These discrepancies can now be considered resolved.
- Extensive investigation of the influence of rotor axial positioning on static and dynamic axial forces was explained and eliminated with proper impeller-to-diffuser geometry, and was applied in several field cases. This implies a heavy influence on BFP availability and has reduced maintenance and made rotor assembly much easier.
- Complete elimination of axial thrust in very high-energy-input, double-suction pumps used in nuclear feed, booster, and other pump applications. This was eliminated by the discovery of the influence of impeller-to-diffuser geometry and hydraulic forces. The discovery not only ended disputes regarding the calculation method used but, more important, eliminated the need for such calculations because the static and dynamic forces were completely suppressed by these modifications.
- Elimination of internal hydraulic recirculation and hydraulic instability through the proper application of Gap A with its overlap. The results were:
  - Straightening of the head curve to eliminate the dip in the head curve
  - Significant improvement in efficiency
  - Elimination of rotor axial shuttling
- Recognition and demonstration of the backflow deflector (or backflow catcher) to eliminate low flow hydraulic instability in high-suction specific-speed designs, including inducers [11, 14, 15].
- Discovery of the relationship between Gap A and the backflow catcher and agreement by the inventors. Both eliminate hydraulic instability in the reduced-flow operating regime; Gap A in low-suction specific-speed applications (BFP, nuclear feed, booster, etc.) with high energy input, and the backflow catcher in high-suction specific-speed applications with low energy input [1, 14, 15, 19, 34, 42].
- Determination through a survey that the majority of the boiler feed pumps in older and especially smaller installations have insufficient impeller sideplate thicknesses and/or an

inadequate b_3/b_2 (diffuser width/impeller width) ratio. They are, therefore, sensitive to axial alignment and prone to thrust reversal due to insufficient Gap A and Gap A Overlap. If the power input is large enough, all of these characteristics may contribute to hydraulic instability. In very small units, this condition is not of great concern because the dissipated energy is insufficient to cause system instability. It may, however, cause unnecessary or increased maintenance.

- Discovery of the relationship between feedwater system instability Gap A, and Gap A Overlap, and Gap B has been demonstrated in many power station applications with excellent results. This is considered a very powerful development in centrifugal pump design.
- Demonstration through field applications that hydraulic instability at reduced capacities can be further reduced by application of the latest technologies in impeller hydraulic design methods [11, 34, 42].
- Determination that external damages and various failures resulted from inadequate Gap B.
- Achievement of major noise reductions for several high-speed boiler feed pumps through proper application of Gap B, which has contributed to improved working environments for maintenance personnel.
- Revision of the old design philosophy for Gap B standards. Formerly, it was believed that an increased gap reduced efficiency, but if the modifications have been properly implemented, the opposite has been shown through numerous field applications.
- Demonstration of significant improvement in pump efficiency through proper application of the impeller-to-diffuser/volute geometry (that is, the combination of Gap A, its overlap, and Gap B). This was an unexpected benefit from the long-range research and development program, which was conducted continuously for almost two decades to explain the causes for hydraulic instability.
- Convincing demonstrations that most of the foregoing advances apply equally to diffuser- and volute-style pumps.
- Continuing progress made on power plant life extension programs by EPRI and some architect engineers.

1.2 Impeller-Diffuser/Volute Definitions

All relevant impeller-diffuser/volute dimensions and geometry for a typical modern BFP are shown in Figures 1-5 and 1-6.

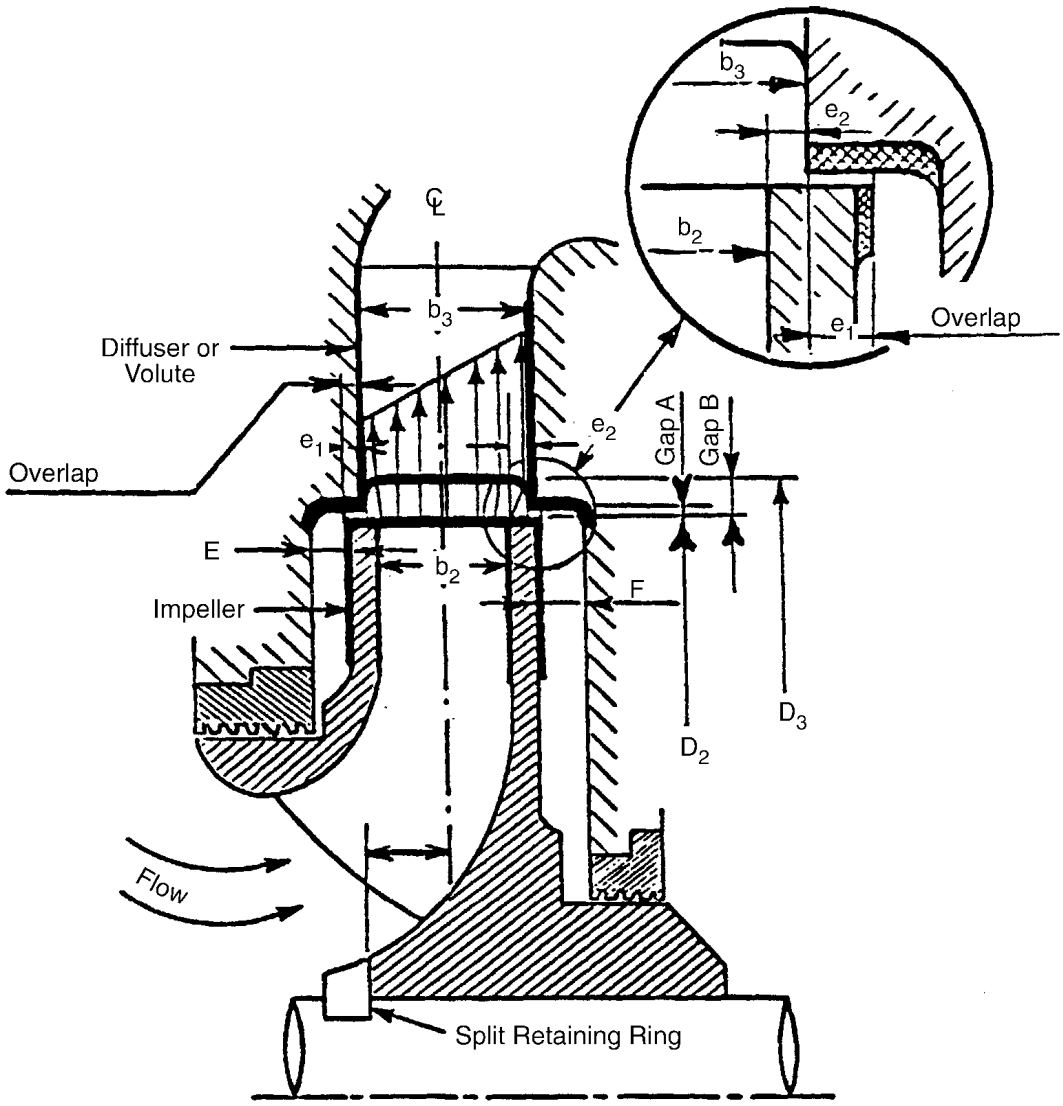

Meridional cross-section view and basic nomenclature of an impeller stage for a multistage boiler feed pump with a diffuser or a volute.

Figure 1-5
Meridional Cross-Sectional View of a Diffuser-Style BFP Stage With the Appropriate Nomenclature

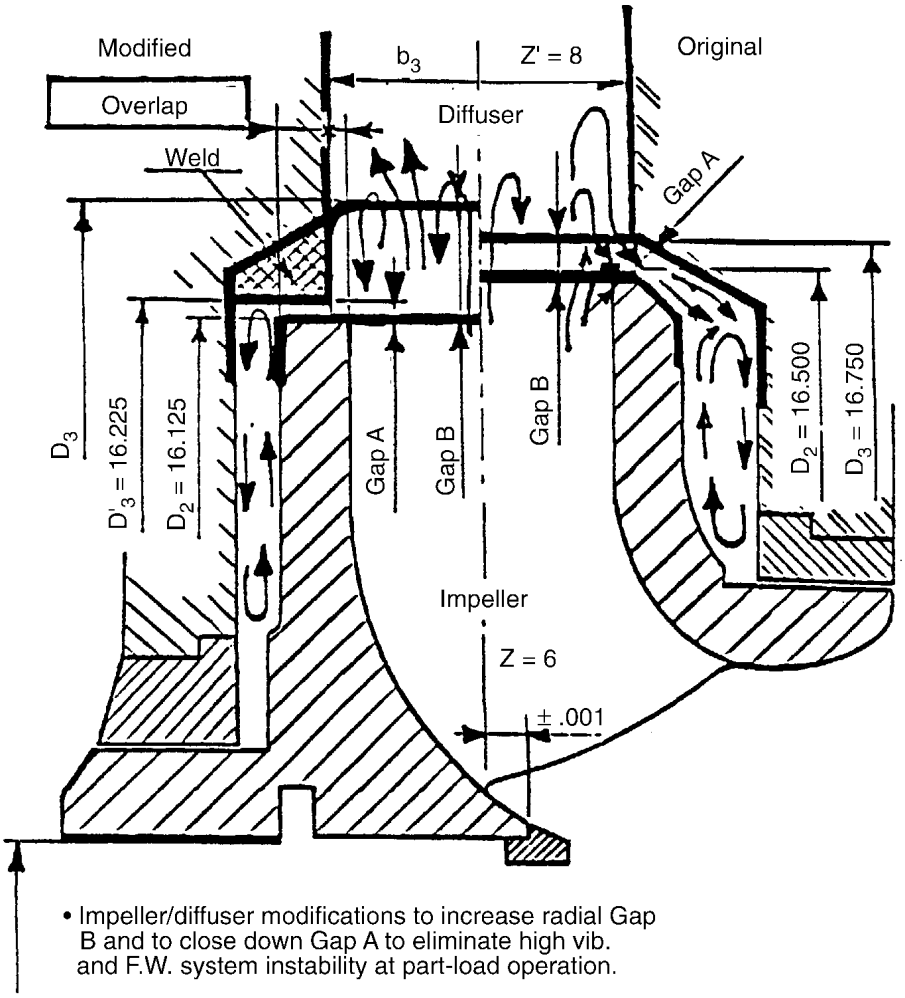

- Impeller/diffuser modifications to increase radial Gap B and to close down Gap A to eliminate high vib. and F.W. system instability at part-load operation.
- Flowpath that upsets axial thrust behind impeller sideplates during part load operation is shown before and after geometry modifications.
- Sacred dimensions shown: Shrink fit and impeller axial position.

Figure 1-6
Meridional View of a BFP Impeller/Diffuser Stage Before and After Proper Gap A and Gap B Modification

Meaningful definitions for Gap A, Gap B, and a new dimension, Gap A Overlap and its important overlap-ratio, have not appeared previously in pump design technology other than in publications by ERCO:

- Gap B is the radial clearance between the impeller vanes at the outer diameter (D_2) and the diffuser or volute vanes at the inner diameter (D_3). It is always given as a percent of D_2.
- Ratio b_3 / b_2 is between the hydraulic widths of the diffuser inlet (b_3) to the impeller exit (b_2). This ratio is very critical for a good hydraulic flow pattern and for rotor axial positioning, especially in pumps with a large number of stages. A general rule in diffuser-type pump hydraulic design requires this ratio to have a minimum value of not less than 1.15. For a volute design, a larger number is preferred.
- Rotor axial positioning actually means centering between the hydraulic channels of the impeller exit and diffuser/volute inlet. Figures 11-3 and 11-6 show various configurations. In Figure 11-6, they range from good to very poor.
- Gap A is the radial clearance between the outer diameter of the impeller sideplates, both hub and shroud, and the inner diameter of the diffuser/volute channel sideplates. Gap A is given in inches or more commonly in mils (for example, 50 mils = 0.050 in.). Usually, this dimension does not exist in OEM volute designs, suggesting strongly that its importance was not previously recognized.
- The axial overlap of Gap A is the effective axial length of overlap between the narrow hydraulic passage between the impeller and diffuser/volute sideplates (O). The recognition of its major technological significance in pump hydraulic design is a major breakthrough. It has a very large controlling effect on both the static and dynamic components of the rotor axial thrust, damping developed by the impeller from rotor motion, pump hydraulic stability, feed water system stability, BFP turbine drive governor stability, and pump efficiency.
- Overlap-ratio (X=O/A) is the ratio of overlap and Gap A. This parameter is very important. If incorrect, it can make Gap A ineffective even though the numerical value of Gap A has been selected correctly, as shown in Figure 8-5.
- Gaps E and F are the axial spaces behind the impeller shroud and hub, respectively (see Figure 1-5). This clearance can have a great effect on friction losses, axial thrust, efficiency, and the overall effectiveness of Gap A (see Figure 8-5). If these gaps are too small, boundary layer forces may dominate the flow region as well as diminish the effectiveness of Gap A.
- Impeller sidewall thickness (S) has a major effect on all of the above geometries. Performance of the pump with optimum Gap A dimensions can be degraded if, for example, grinding of the sidewalls during dynamic balancing extends to the impeller OD.
- Swirl break, if introduced behind the impeller sidewalls as shown in Figures 10-14 and 10-15, will alter the flow pattern in those areas; therefore, friction losses, efficiency, and axial thrust will also be altered. The purpose of swirl break is added rotor-dynamic stability of the rotor with the aid of the close clearance cylindrical surfaces such as wear rings and balancing disks/drums.
- A modified Lomakin Effect wear-ring geometry added for rotor-dynamic stability is discussed in Section 10.4 and References 16, 34, 44, and 45.
- The number of vanes, the vane combination between impeller and diffuser/volute, and Gap B all have a significant influence on the flow pattern at Gap A and on its effectiveness.

1.3 Determining Where Problems May Originate

During the late 1960s and through the 1970s, larger and larger power plants meant that the speed and size of rotating machinery increased. As the output requirements of this equipment were increased, the design decisions became more critical, and the question of operational reliability arose, with rotor, bearing, and seal failures being all too common in new units. Rotor dynamics became an important factor in the design stage of the rotating machinery and warranted close scrutiny by the end user. The dynamics of the hydraulic forces generated by these high-energy-input pumps came to the forefront only after the rotor-dynamic technology was no longer able to solve or explain the problems being experienced.

The problems that arose at the power stations had a variety of origins. The magnitude of the problems experienced could usually be related to how many of the possible problems resulted from a given application, design, manufacture, and installation for a power station. The successful design and manufacture of high-energy-input pumps depends on a thorough coordination of a series of events. If any link of the chain is broken, trouble starts. The possible sources for pump problems are:

- Sales: Pumps sold for the wrong application (wrong size, type, NPSH)
- Incorrect basic hydraulic research predictions (for example, academia, research institutes, and OEM's research facilities)
- Basic engineering design errors
- Manufacturing errors
- Assembly errors at the OEM
- Installation errors at the plant
- Operational errors and part-load operation at the power station
- Utility purchasing departments having the lowest bidder theory during both the initial purchase and later during repairs/refurbishment
- Most frequently, lack of feedback from field service to OEM's design engineering

Typically, when a pump is specified for an application, the designers or engineers at the OEM are not a part of the process that selects a pump for a given application. The sales and marketing groups review the utility specifications, choose a pump for the application, and submit a bid to the utility. Usually, only after the contract has been awarded, do the OEM designers and engineers get involved, with the instructions to make the pump work in the application.

During the time when most of today's high-energy-input pumps were purchased and designed (during the 1960s and 1970s), cost was the primary measuring stick that the utility used in choosing a pump for an application. As discussed in Section 1.0, this often forced manufacturers to push the existing designs to their mechanical and performance limits without proper research. Hydraulic and mechanical modifications to meet the horsepower and efficiency requirements were made based on predicted outcomes instead of research test results. Proper research would have added cost to the job, which in essence left the power stations as the research facilities for the modifications. However, instead of approaching the problems with a researcher’s mentality

to identify and eliminate the root cause of the problems, attention shifted to the spare parts required to keep the pumps on line because the parts are a major source of revenue for the manufacturers.

The problems were compounded when pumps that had previously been properly applied (and thus had no history of failures) began to fail. The manufacturers often claimed that they had never seen that particular problem before and sold the power station replacement parts with the same design or manufacturing flaws. The sad part is that, 20 years later, the manufacturers still make the same statements and continue to promote the same problems. However, significant strides have been made by ERCO and the utilities to eliminate the design and manufacturing problems, all done with little assistance from the manufacturers. The problems have required hydraulic modifications, precision parts and balancing, and proper assembly and installation.

The utilities' policy of awarding contracts to the low bidder can be a major source of problems at power stations. If the policy does not create a problem initially, it most certainly will later during the repair and refurbishment of the pumps. The key to low cost pump (and ultimately plant) operation is a quality repair at a fair price. These do not always go hand in hand. The repairs must be performed by diligent people who understand the importance of precision and quality in high-energy pumps. As shown in Figures 1-7, 1-8, and 1-9, one cannot escape the fact that **"Cheap Meat Makes Cheap Soup."** For example, an **Expert Bicycle Shop** performed a Gap B modification on a 20,000 hp BFP. The diffusers were cut back to increase the original 1% Gap B to 6%. The improper cutting back of the diffuser channels resulted in major loss of pump efficiency.

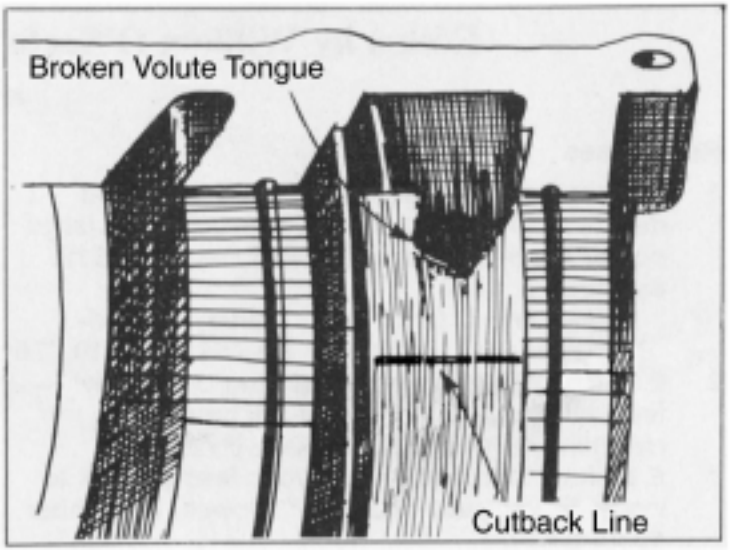

Figure 1-7
"Bicycle Shop" (Usually the Lowest Bidder): "Cheap Meat Makes Cheap Soup"

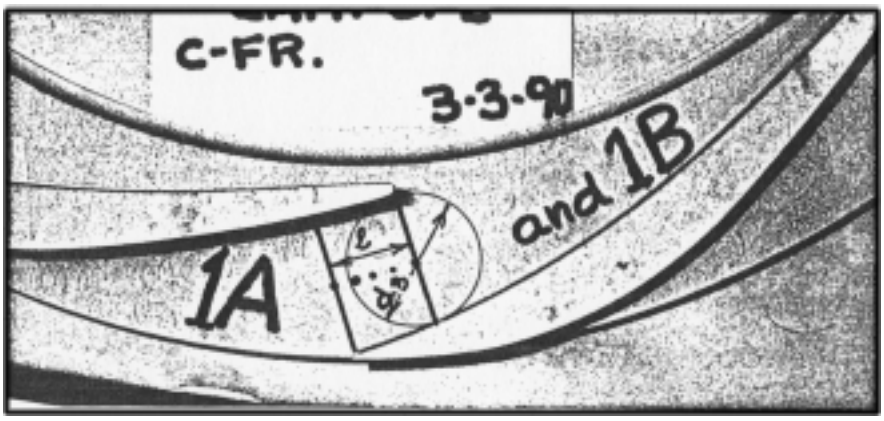

Figure 1-8
Original First Stage Diffuser L/d3 = 3.6; Cut to 0.6, Which Resulted in Major Efficiency Loss

Figure 1-9
Original Normal Stage Diffuser L/d3 = 4.0; Cut to 1.5, Which Resulted in Major Efficiency Loss

The final links in the chain relate to the design and operation practices of the utilities and architect engineers (AEs). Historically, the required pump design points specified to the pump OEMs were not the conditions at which the pumps were operated. The boiler feed pumps were required to operate at flows as low as 25% of the pump's best efficiency point (BEP). Meanwhile, the nuclear plants required pumps to provide two functions, normal operation and emergency operation. A nuclear pump would be sized to meet the emergency flow conditions, but it would operate 90% of the time at the normal operating flow conditions (for example, at 30% of the emergency flow) or would be operated only during surveillance testing at minimum or recirculation flow conditions. The existing technology and design of the pumps could not accommodate such a wide range of operating conditions.

When purchasing or troubleshooting high-energy-input pumps or other large rotating machinery such as main turbines, you must understand the effects of hydraulic and rotor-dynamic instabilities. They are separate issues with different solutions, but they are related and are often mistaken for each other. This is particularly true with hydraulic instabilities, which usually are diagnosed as rotor-dynamic problems. When purchasing rotating machinery, potential stability problems often can be minimized through good communication between the buyer and the vendor or consultant and with detailed quality control programs. The buyers should clearly specify design basis requirements, particularly hydraulic geometry and rotor-dynamic performance, when obtaining price quotes. They should make sure that any deviations from a "standard design" are specifically covered in the bidder's specifications. A performance history of models with comparable horsepower, speed, and service requirements as the equipment being specified should be obtained and evaluated. If the equipment specified is the largest ever made of a given model, then **BUYER BEWARE**.

Finally, the utility should not look upon quality control as an unnecessary expense. A good design does not guarantee that your equipment will perform properly. Remember that manufacturing is independent of design in many respects. Problems originating in the machine shop, foundry, or pattern shop or during assembly can occur without the knowledge of the design engineers. If ignored or not properly dispositioned by the OEM, it may ultimately lead to failures at the power station. It is not in a utility's best interest to accept equipment that does not meet the requirements or tolerances of the design documents.

The intent of this report is to provide you with the necessary tools to ensure that the rotating machinery installed at your power station performs as intended and as reliably as possible. The information provided may be used either as a guide for evaluating new equipment or troubleshooting existing equipment. The basic principles and technology are the same; however, you can save considerable expense if the problems are corrected prior to installation.

2
CENTRIFUGAL PUMP DESIGN

The troubleshooting of pump problems requires, at a minimum, a basic understanding of pump design and its governing principles. In this chapter, a simplified technique has been used to illustrate the design of a typical multistage diffuser-style pump. The method uses predominately graphical techniques to predict pump stability and to determine impeller size, diffuser size, and the optimum number of impeller blades. An example has been used to illustrate the method.

2.1 Selection of Basic Dimensions

In a typical application, two parameters are specified: pump head (H) in feet and flow (Q) in gallons per minute (GPM). In this example, the conditions specified are Q = 1800 GPM and H = 575 ft/stage, that is, multistage design).

The speed was not specified, but the speed selection chart, Figure 2-1, can be used to select a speed. Where the head and flow intersect, point A, move along the diagonal line to whatever speed is desired, and note the specific speed (N_S). The specific speed is calculated from the formula:

$$N_S = N (Q^{1/2} / H^{3/4})$$

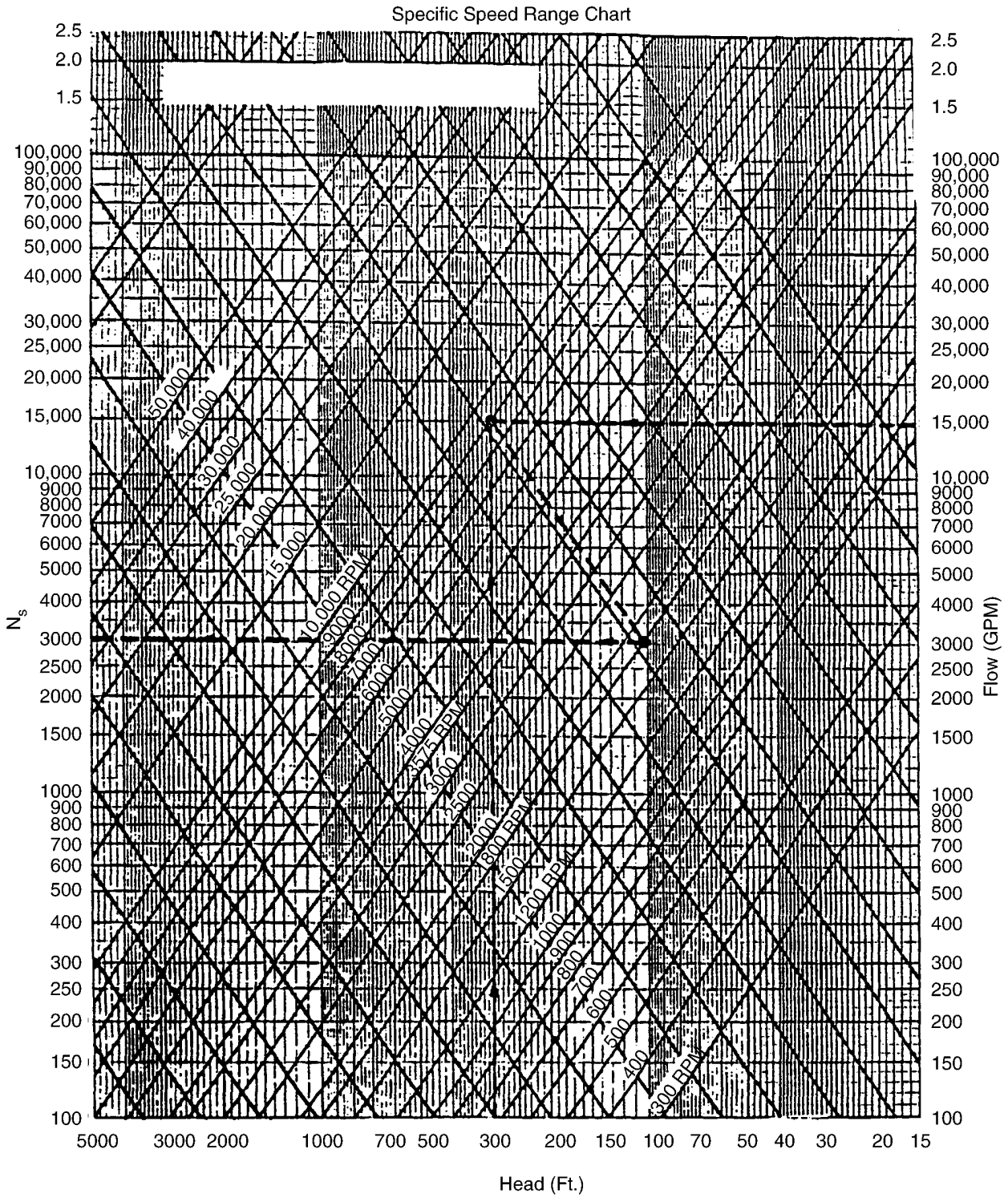

Using Chart: Plot head-capacity point. Move from this point, parallel to heavy lines, to correct speed. From there, move horizontally to the left and read specific speed.

Example: (Dashed lines) H = 300 feet, Q = 15,000 GPM, N = 1800 RPM ⟶ N_s = 3058

Figure 2-1
Chart for Choosing Rotational Speed and Specific Speed

For example, if pump speed (N) = 3600 RPM (point A), N_S = 1300. At 1800 RPM (point B), N_S = 650, and at 10,000 RPM (point C), N_S = 3600. Actually, any convenient speed can be chosen to fulfill most head and flow requirements as long as N_S is within a satisfactory range. The suitability can be judged in part by the efficiency chart shown in Figure 2-2. The higher the efficiency, the better the impeller shape is for the design conditions.

Specific speeds for average pumps may be between 600 and 4000. For a high-energy-input multistage pump, the recommended customary range for N_S is 1000 to 2000. Therefore, a pump speed of 3600 RPM, yielding N_S = 1300, has been chosen for this example.

The specific speed chosen appears to have been selected somewhat casually or arbitrarily and in fact, it was, as it will be with other parameters yet to be determined. When the values N, H, and Q are selected, the pump is, in effect, designed and can then be tested on paper. If the design proves to be inadequate, the values selected can be varied and a correct or optimized design prepared. Therefore, the design technique is strongly iterative, permitting quick tests of somewhat arbitrary decisions.

An initial impeller diameter can now be selected with the aid of the empirical data in Figure 2-3. The head parameter, K_{U2} is defined as:

$$K_{U2} = (D_2)\ (N) / 1{,}838\ H^{1/2}$$

If a prerotation angle (that is, direction of fluid velocity at the impeller entrance with respect to the axis, α_1) of 15° is used, then from Figure 2-3, K_{U2} = 1.013. The impeller diameter D_2 can be found from:

$$D_2 = 1{,}838\ (H^{1/2})\ (K_{U2}) / N$$

For example,

D_2 = (1,838) (1.013) (23.979) / 3,600 = 12.40 or approximately 12 ½ in.

If a different prerotation angle is selected, then a different head parameter is found and a different impeller diameter calculated (for example, D_2 = 12.24 in. and 12.67 in. for prerotation angles equal to 0° and 45°, respectively). It can be seen that assuming no prerotation angle results in a smaller impeller diameter, but it will also result in not meeting design requirements if inlet flow pre-rotation occurs at the plant (usually piping induced). With the prerotation angles of 0° and 45° in this example, a 4% drop in flow and a 2% drop in head could occur. It is customary to assume a 15° to 25° prerotation angle if it is unknown or if flow straighteners are not used to prevent prerotation.

The experimentally derived diameter-ratio chart, Figure 2-4, yields an impeller outside-to-eye diameter ratio (D_2/D_0), from which the impeller eye diameter at the inlet (D_0), can be estimated:

D_0 = 12.5 / 1.93 = 6.48 or approximately 6.5 in.

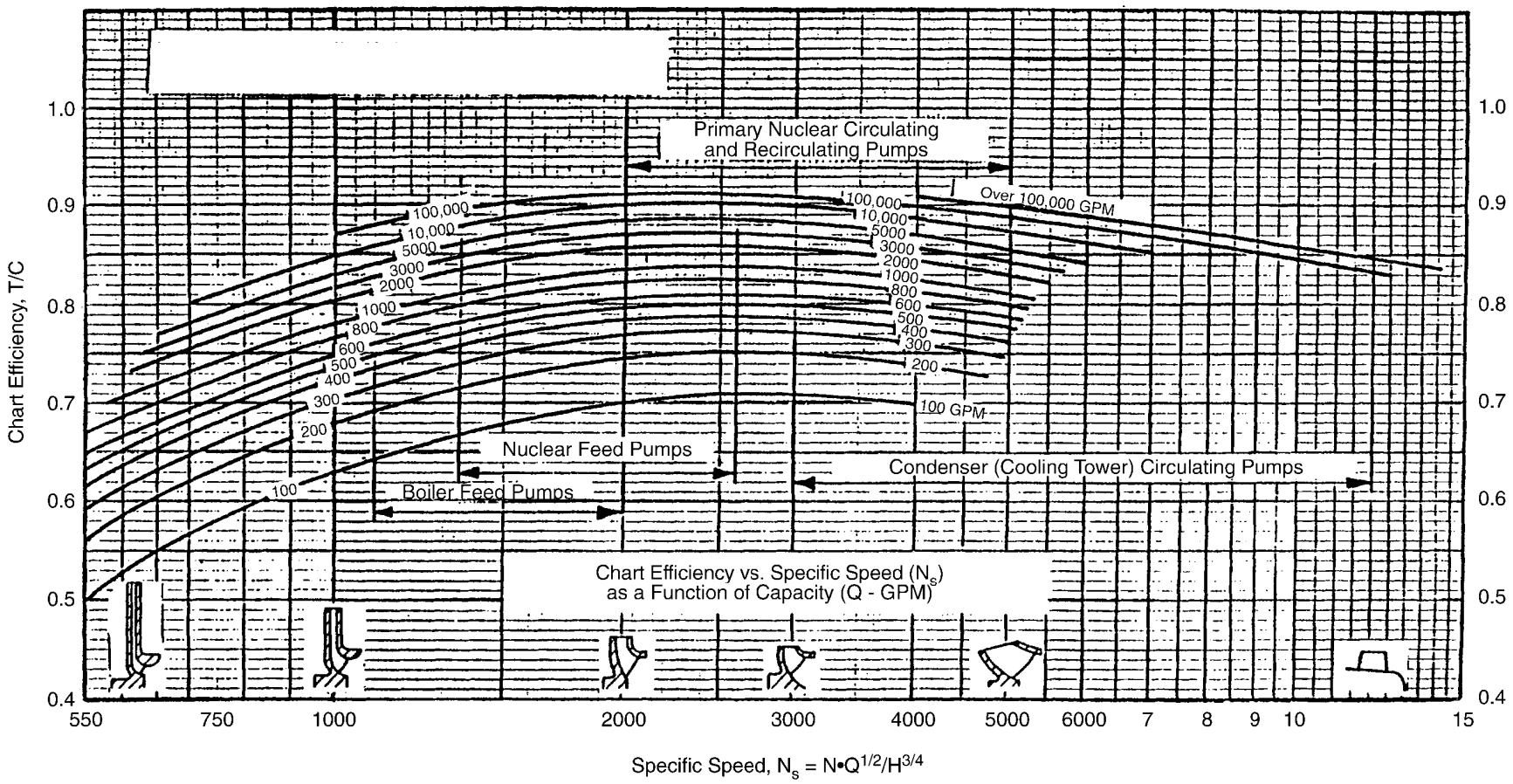

Figure 2-2
Chart Efficiency vs. Specific Speed as a Function of Capacity. As shown by the small insert drawings, specific speed implies (or determines) impeller geometry.

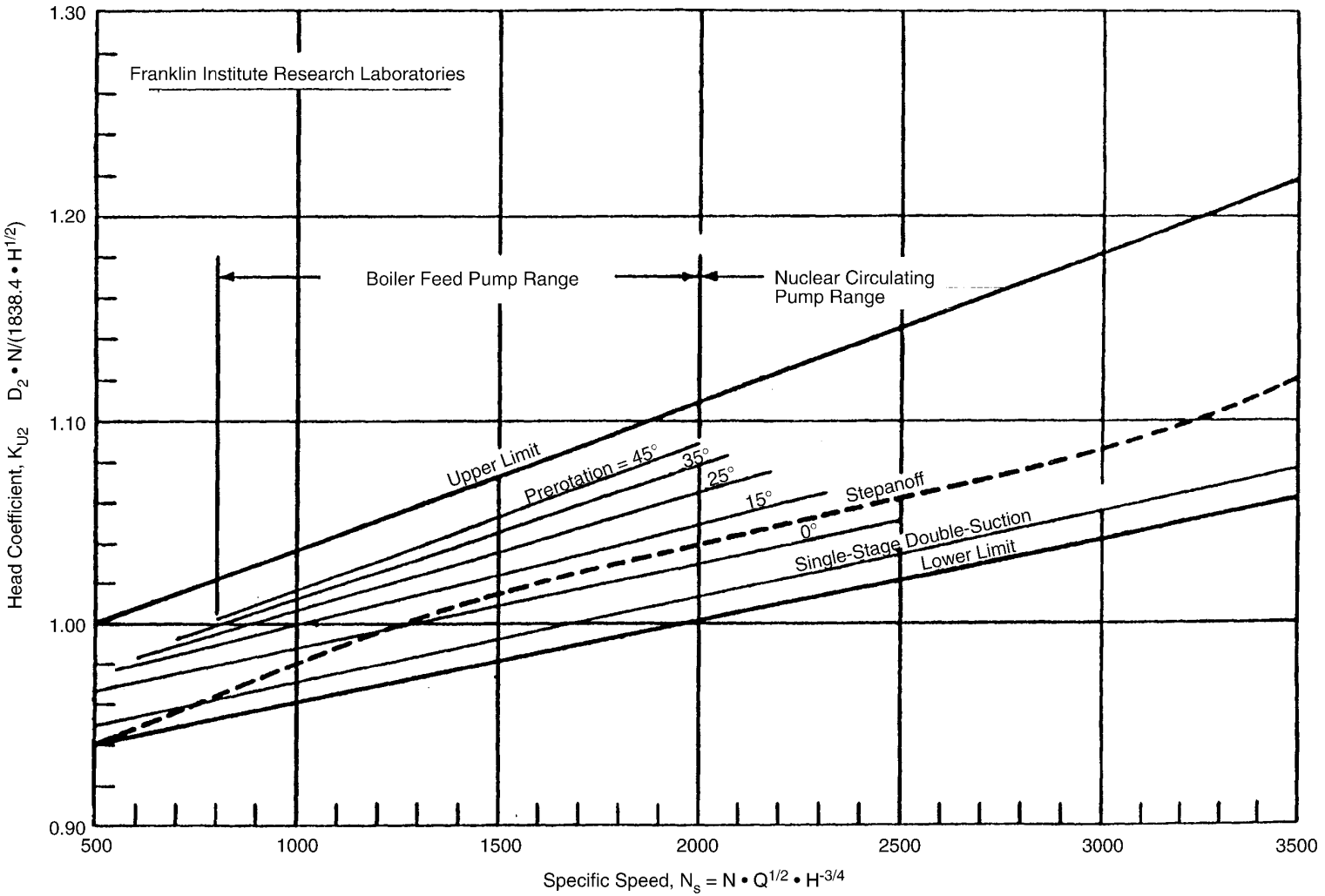

Figure 2-3
Head Coefficient vs. Specific Speed as a Function of Prerotation

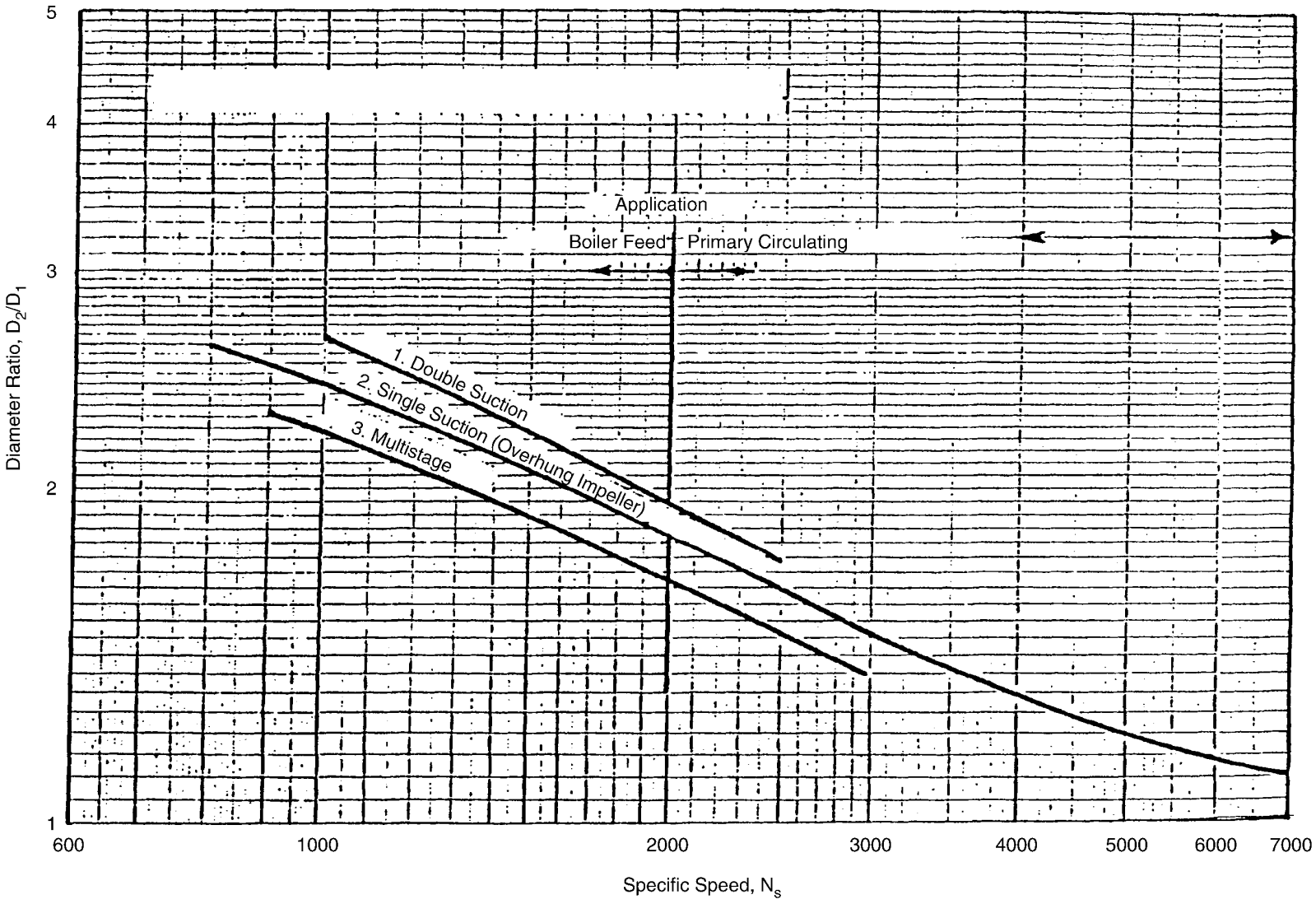

Figure 2-4
Diameter Ratio as a Function of Specific Speed

Similarly, the impeller width at the exit, b_2, can be obtained from the width-ratio chart, Figure 2-5:

$$b_2 = D_2 (b_2 / D_2)$$

Figure 2-5 gives a range of width ratios for a specific speed, $0.0646 \leq b_2 / D_2 \leq 0.08$, which results in a possible impeller width ratio of $0.807 \leq b_2 \leq 1.00$. The higher value results in a wider impeller, lower head rise from BEP to shutoff, and higher efficiencies than the lower value. For this example, we have chosen an intermediate value of $b_2 = 0.9$in.

At this point, the number of impeller vanes and the vane exit angle, β_2, can be selected. Although β_2 may vary from 14° to 29°, for a normal application without any special requirements, $\beta_2 = 22°$ is a good average choice. To determine the number of impeller vanes, Z_2, the vane exit angle can be divided by three for a quick guide. Thus, in this example, $Z_2 = 22 / 3 = 7.33$ or approximately seven vanes.

Within the specific speed limits discussed here (N_S = 1000 to 2000), the number of vanes usually required is four to eight. Higher numbers yield higher efficiencies, but when higher head rise is needed between full and part load as is the case at most power plants, it can be easily achieved by choosing a lower number of vanes, as shown in Figure 2-6. Therefore, in this example, the number of vanes chosen is six. A summary of the sample calculations has been provided in Table 2-1.

Table 2-1
Summary of Basic Impeller Calculations

Given	Selected	Calculated	Finalized
Q = 1800 GPM	N = 3600 RPM	N_S = 1300	N_S = 1300
H = 575 feet	α_1 = 15° β_1 = 22° β_2 = 22°	D_2 = 12.4 in. D_O = 6.47 in. Z_2 = 7 0.8 < b_2 < 1.0	D_2 = 12.5 in. D_O = 6.5 in. Z_2 = 6 b_2 = 0.9 in.

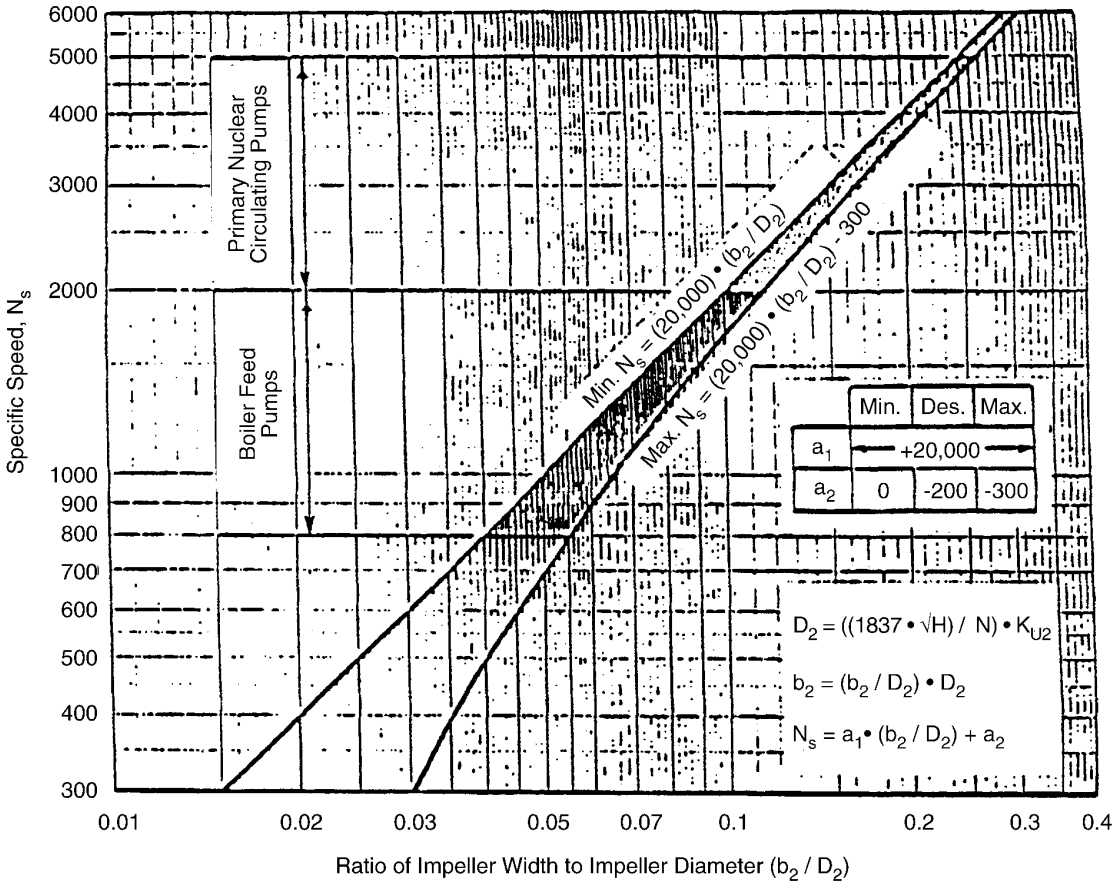

Figure 2-5
Specific Speed vs. Impeller Width/Diameter Ratio

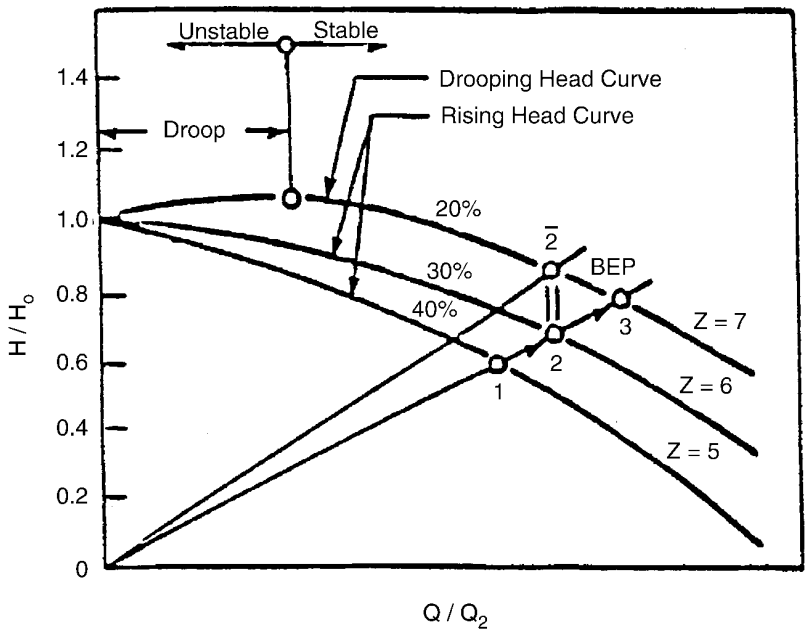

Figure 2-6
Effects of Vane Number on Head Rise for a Pump With Specific Speed N_s = 1500

2.2 Secondary Calculations

Now that the preliminary pump estimates are complete, some quick calculations are required to predict performance and to confirm some of the estimated size data. Primarily, a calculated value is needed for the impeller outside diameter (D_2), which is found from:

$$D_2 = 229 (U_2 / N)$$

where,

$$U_2 = C_{M2} /(2 \tan \beta_2) + (g H_T + (C_{M2} / 2 \tan \beta_2)^2 + U_1 C_{U1})^{½}$$

Most of these terms are defined graphically in the velocity triangles of Figure 2-7. In this formula, the definition of H_T (Euler head) is:

$$H_T = (1 + p) H / \eta_H$$

To find the Euler head, the hydraulic efficiency (η_H) and the slip factor (p) must be calculated. The hydraulic efficiency is defined as:

$$\eta_H = \eta / \eta_V \eta_M$$

where η is found from Figure 2-2 for N_S = 1300 or η = 0.828 for this example. If exact values of η_V and η_M are unavailable, they can be estimated from:

$$\eta_M = 0.99$$

and,

$$\eta_V = 0.94 + 0.0225 (N_S / 1{,}000) - 0.0025 (N_S / 1{,}000)^2$$

for the example, η_V = 0.965, thus η_H = 0.867.

The slip factor, p (Stodola correction), is an experimental correction factor that rectifies the discrepancy between the direction of the exit fluid velocity and the vane exit angles. These two would be equal, theoretically, if the number of impeller blades were infinite. If this were the case and if there were no hydraulic losses, then the head developed by the impeller would be H_T. Values of p can be obtained from Figure 2-8; for this example, p = 0.376. Hence, from the Euler head equation:

$$H_T = (1 + 0.376)(0.575) / 0.867 = 0.91$$

The meridional velocity component, C_{M2}, can be approximated as a function of the specific speed:

$$K_{M2} = C_{M2} / (2 g H)^{½}$$

Or, when enough information is available, as it is in this example, C_{M2} can be calculated directly:

$$C_{M2} = (0.1022 / b_2 D_2) (Q / \eta_v) ((\pi \ D_2 / Z_2) / (\eta_v \ D_2 / Z_2 - s / \sin \beta_2))$$

where "s" is the thickness of the impeller vane (assume s = .25 in.) and $D_2 = 12.5$.

For the example:

$$C_{M2} = (0.1022 / (0.9 \times 12.5)) (1{,}800 / 0.965) (1.1135) = 18.87 \text{ feet/sec}$$

Now, U_2 can be calculated from the equation presented earlier in this section. For the example, assume that $C_{U1} = 0$, which means the liquid is approaching the impeller axially without prerotation. Then at first approximation, $U_2 = 196.29$ feet/sec. To refine this estimate, construct an inlet velocity diagram, similar to that in Figure 2-7. From that diagram, $C_{U1} = 8$ feet/sec, rather than 0. Returning to recalculate speed, $U_2 = 198.3$ feet/sec.

The new calculated values are: $D_2 = 12.28$ in. (without prerotation), $D_2 = 12.61$ in. with 15° prerotation, and $D_2 = 13$ in. with 45° prerotation.

This calculation process should be repeated at least once by replacing D_2 with the newly calculated value to obtain the final impeller outside diameter, yielding a slightly different diameter than the previous value. If high accuracy is needed, then the process needs to be repeated one or more times to obtain an iterative solution.

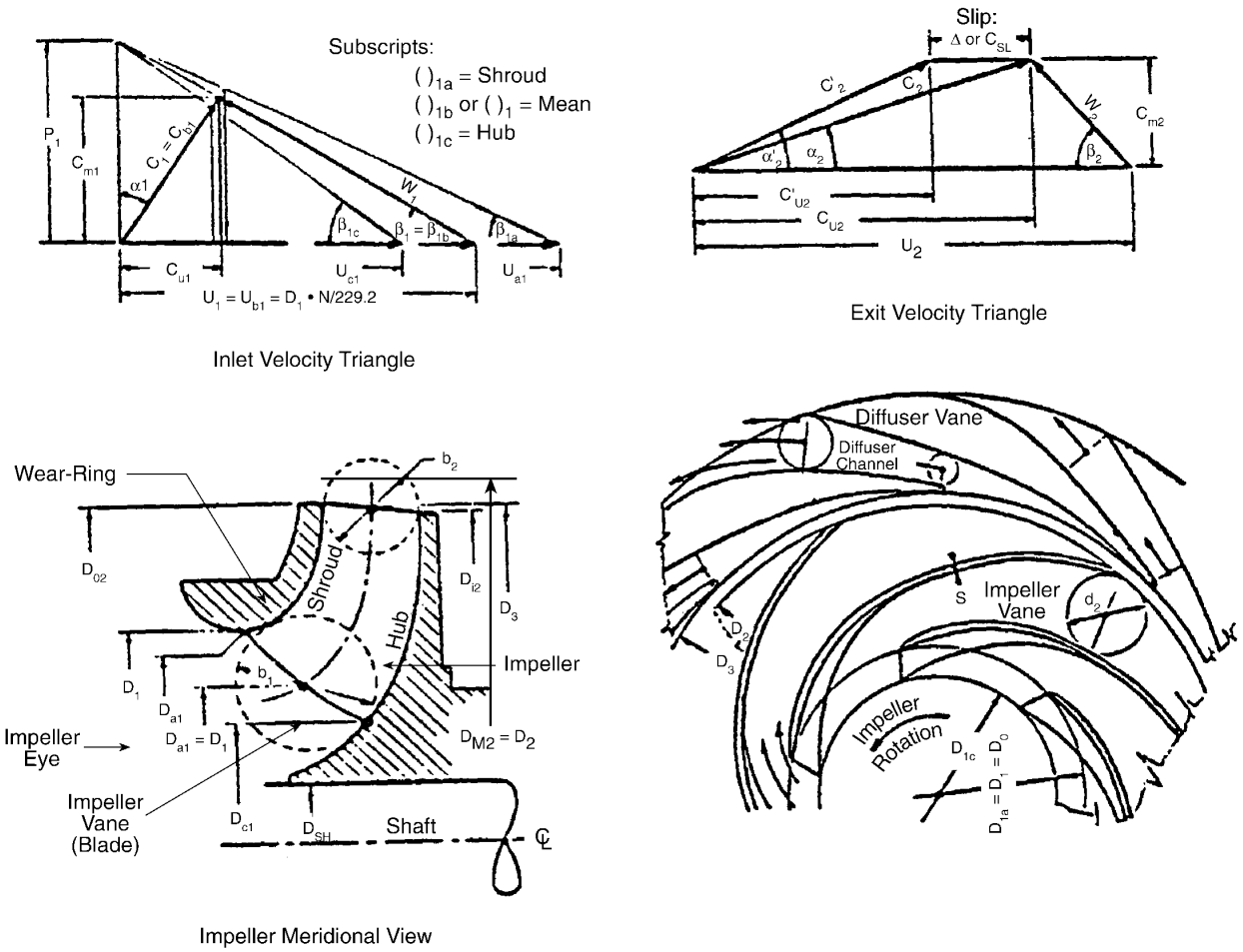

Figure 2-7
Inlet and Exit Velocity Triangles for a Pump, With Pump Views Included to Define Dimensions

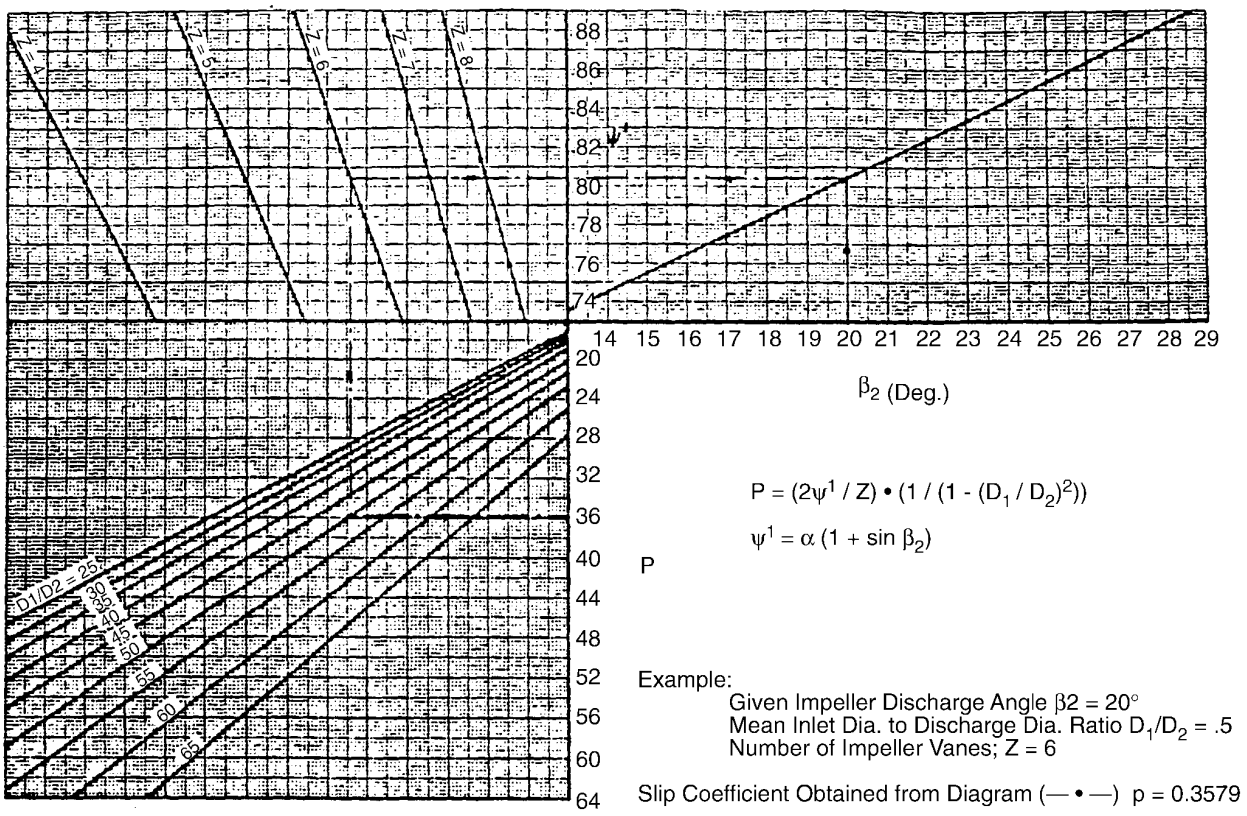

Figure 2-8
Chart for Determining Slip Coefficient

2.3 Diffuser Calculations

The next step in centrifugal pump design is to calculate the diffuser dimensions. Normally, diffuser values are determined from complex calculations. These complex methods have been distilled into an area-ratio chart, Figure 2-9, to simplify the design process.

The most important value is the diffuser (or volute) throat area because it is one of the geometries most responsible for hydraulic instabilities. Figure 2-9 gives experimentally verified values of impeller exit to diffuser throat area ratio. When the area ratio is incorrect, the result is lowered efficiency, hydraulic instability, higher noise level, and mechanical vibration.

Assume that for the example impeller, an existing diffuser is available with the following dimensions: diffuser width b_3 = 1.00 in., diffuser inlet diameter d_3 = 0.80 in., and number of vanes Z_3 = 8. Accordingly, the diffuser throat area is :

$$A_3 = Z_3 \, b_3 \, d_3 = 6.4 \text{ square in.}$$

The impeller exit area, A_2, is given as:

$$A_2 = k_3 \, \pi \, D_2 \, b_2 \, \sin(\beta_2) = 12.63 \text{ square in.}$$

for the example of $k_3 = 0.95$.

The area ratio, Y, for this example is:

$$Y = A_2 / A_3 = 2.00$$

In contrast, Figure 2-9 yields a much lower number:

$$Y_{DESIGN} = 1.60$$

Resulting in a normalized area ratio of:

$$Y^* = Y / Y_{DESIGN} = 1.25$$

This parameter is useful to check stability in Figure 2-10. We move up on the $D_2^* = 1.0$ curve to $Y^* = 1.25$. This suggests that $N_S^* = .935 = N_S / N_{S\,DESIGN} = N_S / 1300$. Therefore, the pump has a specific speed of 1220, instead of 1300 as planned.

Other consequences of pump operation can be read directly from Figure 2-10:

- Droopy head curve, implying difficulty for parallel operation.
- Higher noise level, so sound insulation might be needed.
- Hydraulically excited vibration at part load. Piping and other component failures or impeller sideplate and diffuser inlet vane fatigue could occur.
- Lower efficiency than expected.
- Lower specific speed, so BEP occurs at lower flow.

To overcome these faults, a different diffuser, with the throat area changed to yield Y* closer to 1.0, must be used.

Therefore, starting with Figure 2-9, the optimum area ratio for this example is 1.6, giving:

$$A_3 = A_2 / Y_{DESIGN} = 12.63 / 1.6 = 7.89 \text{ in.}$$

The next important dimension is the width of the diffuser channel (b_3). The b_3 dimension should always be larger than b_2 (impeller channel width), with a recommended range of:

$$1.15 \leq b_3 / b_2 \leq 1.30$$

For this example, $b_3 / b_2 = 1.15$ was chosen; therefore, $b_3 = 0.9 \times 1.15 = 1.035$ in.

Also, stable hydraulic performance of the pump, particularly at low flows, depends on Gap A between the impeller and diffuser sideplates and its overlap ratio between the sideplates. Since b_3 and b_2 are known, the impeller sideplate width can be calculated. Figure 2-11 shows that the optimum overlap ratio is 4. Gap A can range from .050 in. to .080 in. depending on the impeller

diameter (for example, for a larger diameter impeller, say 20 in., one may choose values on the high side of this range). For this example, Gap A was selected as .050 in. Therefore, the impeller sideplate thickness can be calculated:

$$S = [(b_3 - b_2) / 2] - .200 = 0.268 \text{ in.}$$

Assuming the impeller vane and sideplate diameter are equal, 12.5 in., the diffuser sideplate diameter is calculated from the following:

$$D_3' = 12.5 + 2 \text{ (Gap A)} = 12.6 \text{ inches}$$

The diffuser inlet vane diameter is dependent on Gap B (the ratio of impeller vane and diffuser vane diameters). For this example, Gap B has been selected as 6%; therefore:

$$D_3 = D_2 + D_2 \text{ (Gap B)} = 12.5 + 12.5 (.06) = 13.25 \text{ in.}$$

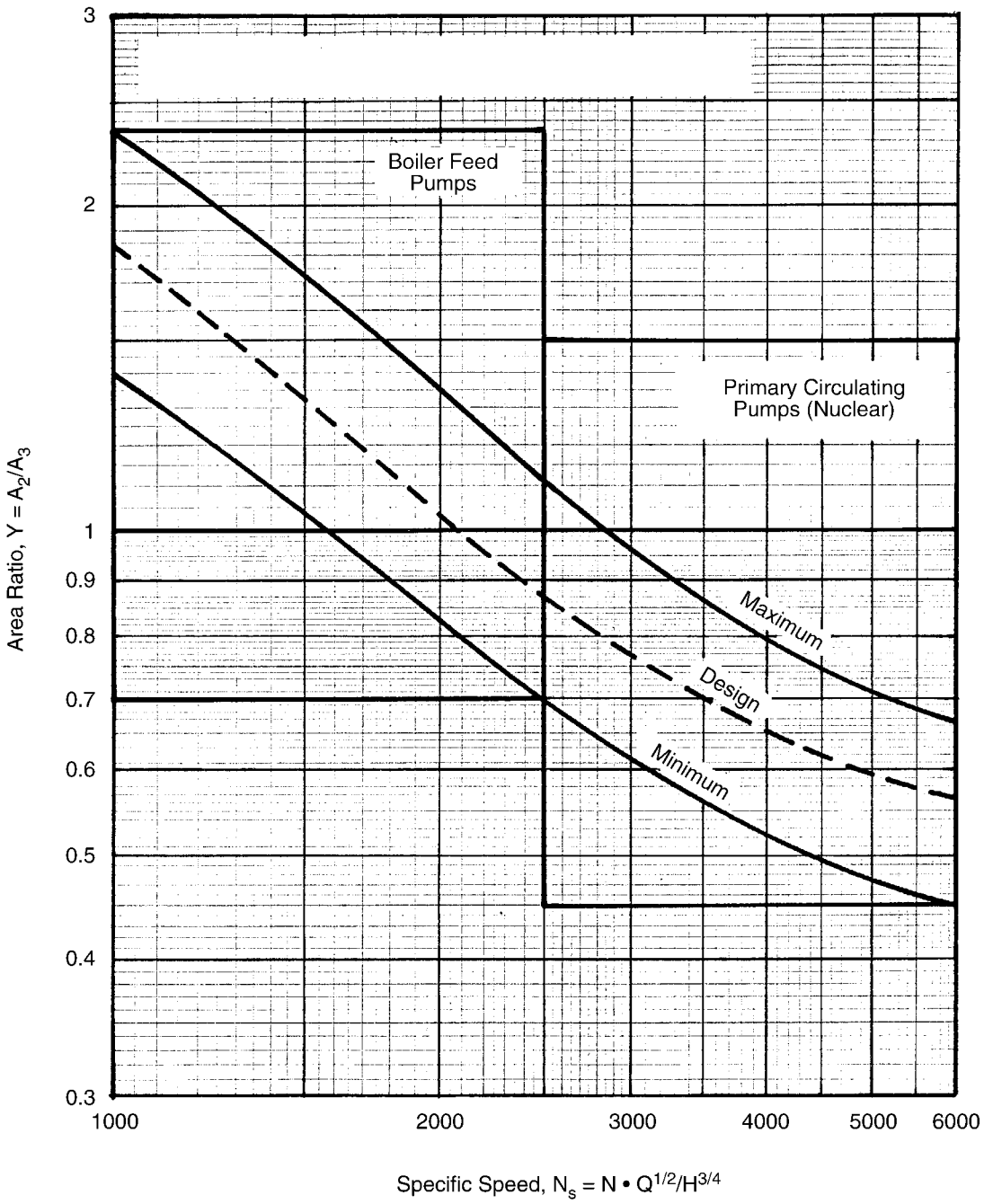

Figure 2-9
Area-Ratio Chart

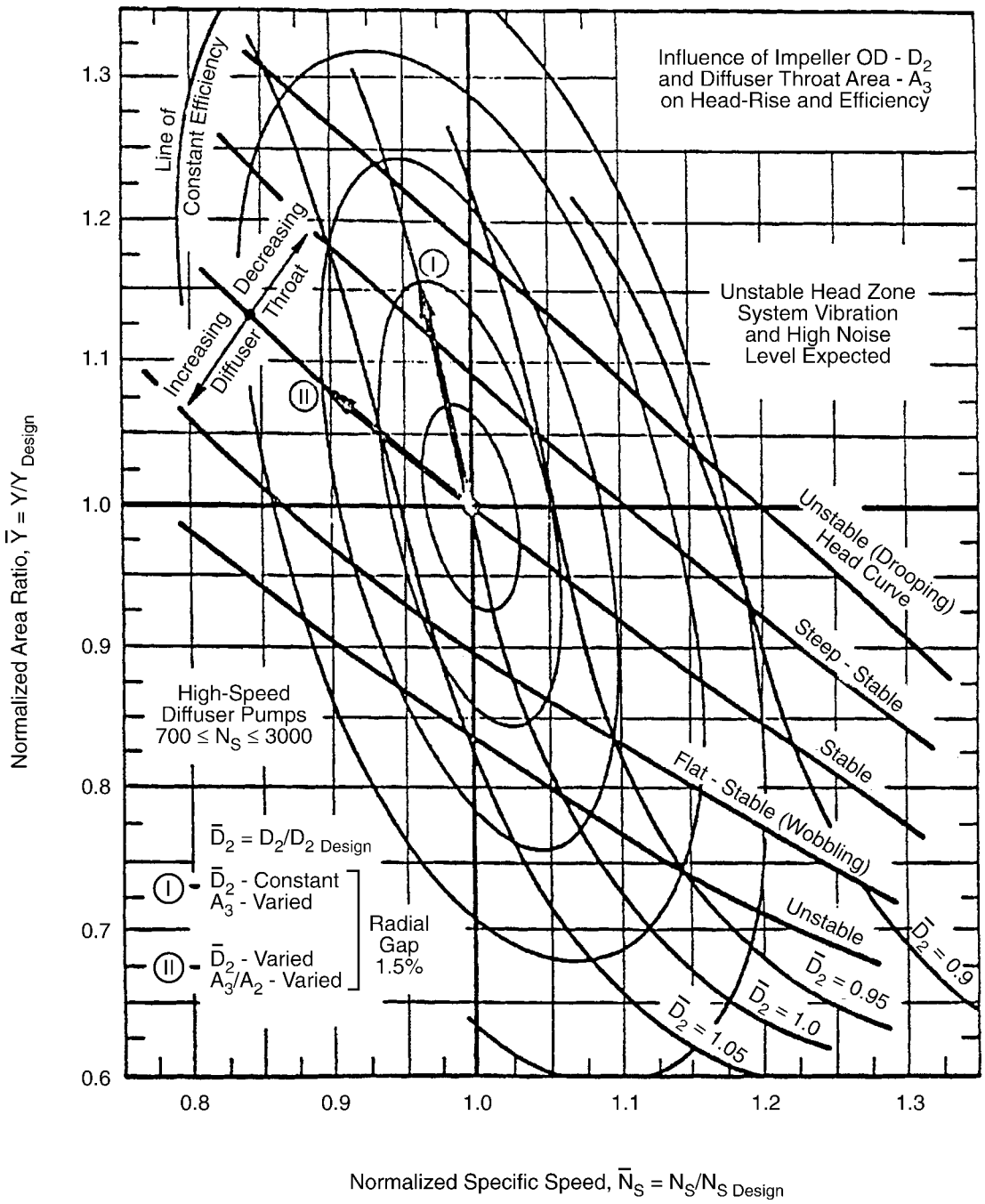

Figure 2-10
Normalized Area Ratio vs. Normalized Specific Speed

From our references, the optimum number of diffuser vanes for a six vane impeller, to minimize the potential for blade pass frequency vibration problems, would be eight (Z_3). Now, the diffuser channel height (d_3) can be calculated from the following:

$$d_3 = A_3 / (Z_3 \times b_3) = 7.894 / (8 \times 1.035) = 0.953 \text{ in.}$$

The active diffuser channel length (L) is dependent on the channel height, with the optimum ratio being 4. Therefore,

$$L = d_3 \times 4 = 3.813$$

The outside diameter (D_4) and exit angle (β_4) of the diffuser are not controlling factors in the diffuser design and will not be calculated. These dimensions are generally derived by factors such as pump size or available space and consequently by the economics of designing a cost-competitive pump. Also, the diffuser inlet angle (β_3) has not been a factor in the diffuser design. Typically, the diffuser inlet angle will be 11° to 12°, but modifications to this angle may be required if cavitation is experienced at the diffuser inlet. A summary of the diffuser and impeller calculation is provided in Table 2-2.

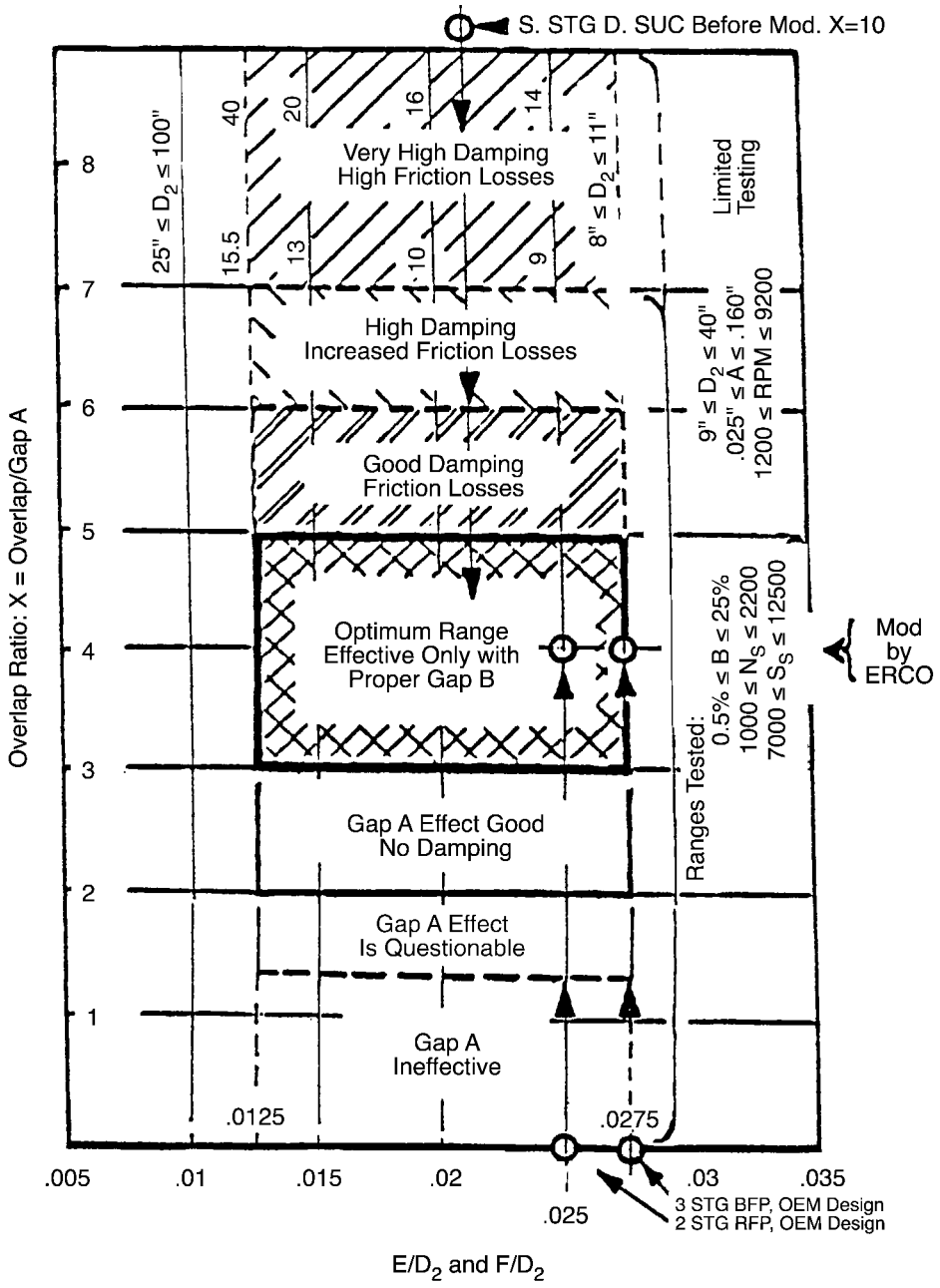

By applying the basic design charts, three specific applications are shown above: (1) Large single-stage, double-suction nuclear reactor feed pump with an overlap ratio of 10, (2) Two stage nuclear reactor feed pump, and (3) Three-stage bolier feed pump, both applications with zero overlap. In all three cases, ERCO recommended optimum ratio of 4 with Gap A = 0.050 in. The modifications since have been incorporated resulting in excellent vibration behavior and hydraulic stability.

Equally applicable to diffuser and volute designs, single and multistage, and single twin and double suction pump designs. However, all three of the above applications are of the diffuser type.

Figure 2-11
General Design Chart for Impeller to Diffuser Sideplate Overlap Ratio

Table 2-2
Summary of Diffuser and Impeller Calculations

Given	Selected	Calculated	Finalized
Q = 1800 GPM	N = 3600 RPM	N_S = 1300	N_S = 1300
H = 575 feet	α_1 = 15°	D_2 = 12.4 in.	D_2 = 12.5 in.
	β_1 = 22°	D_O = 6.47 in.	D_O = 6.5 in.
	β_2 = 22°	Z_2 = 7	Z_2 = 6
		$0.8 \leq b_2 \leq 1.0$	b_2 = 0.9 in.
			S = 0.268
			Z_3 = 8
			D_3 = 13.25 in.
			D_3' = 16.6 in.
			d_3 = 0.953 in.
			b_3 = 1.035 in.
			A_3 = 7.894 in.
			L = 3.813

3
TYPICAL VIBRATION FREQUENCIES

Vibration, as well as pressure pulsation amplitudes, is meaningless without knowing the frequency of vibration or pressure pulsation. The seven most common vibration frequencies for high-energy-input and high-speed pumps with a flexible rotor geometry are shown in Figure 3-1. A flexible rotor geometry means that the rotor operating speed is above its first lateral critical speed. If the operating speed is below the first critical speed, it is called a "rigid" rotor.

The main objectives of Sections 3, 4, 5, 6, 7, and 8 are how to determine which vibration frequency is responsible for the rotor, piping, or system damage; the determination of its root cause; and how to find the most appropriate solution.

After discussing the seven vibration components, a combination section follows where two or more of the frequency components are present.

Vibration in general can be put into two major categories:

- Forced vibration—speed dependent:
  - Unbalance (dynamic or hydraulic: 1 x N)
  - Vane passing, (hydraulic: Z x N)
- Self-exciting vibration—independent of speed, always at some fraction of speed, usually less than N (subsynchronous), such as:
  - Oil-whip (journal bearing related, also called bearing instability)
  - Friction or rubbing induced
  - Hydraulic instability (percent of design flow dependent)

3.1 Vibration Data Collection and Analysis

Many times, vibration measurements are taken without actually knowing what to look for. Often it is known what to look for, but the measurements' meaning is unclear. The objectives during data collection are to:

- Determine the usual vibration or pressure pulsation frequencies in a centrifugal machine
- Determine the root causes and what they mean
- Determine the logical remedy (fix), if any

Sometimes, only one vibration component is present. Frequently, a combination of two or more vibration components develop. How can they be separated to determine which one is the root cause of the problem, especially if the vibration frequency is in the vicinity of 0.6 x N? This subject receives major focus in this report.

Typical vibration frequencies in high-speed, high-energy-input boiler feed pumps (BFP) are listed in Figure 3-1 (note the text in the upper part of Figure 3-1). These frequency components are:

- Rotational (synchronous: 1 x N).
- Two times rotational (first harmonic: 2 x N).
- Half-frequency (in the vicinity of 1/2 x N [0.35 to 0.6], often called half-frequency whirl, subsynchronous whirl, oil-whip).
- Subsynchronous around 0.65 x N (0.35 to 0.9). This component can be either 3 or 4 or the combination of both. Most difficult to determine the root cause.
- Very low frequency, usually below 10 Hz, occasionally somewhat higher (Gap A).
- Vane passing: number of impeller vanes (Z) times rotation (Z x N) (Gap B).
- Multiples of vane passing (n x [Z x N]) (IMP and DIFF vane combination coupled with Gap B).
- Combination of two or more of the above. How to determine which is the **root cause**?

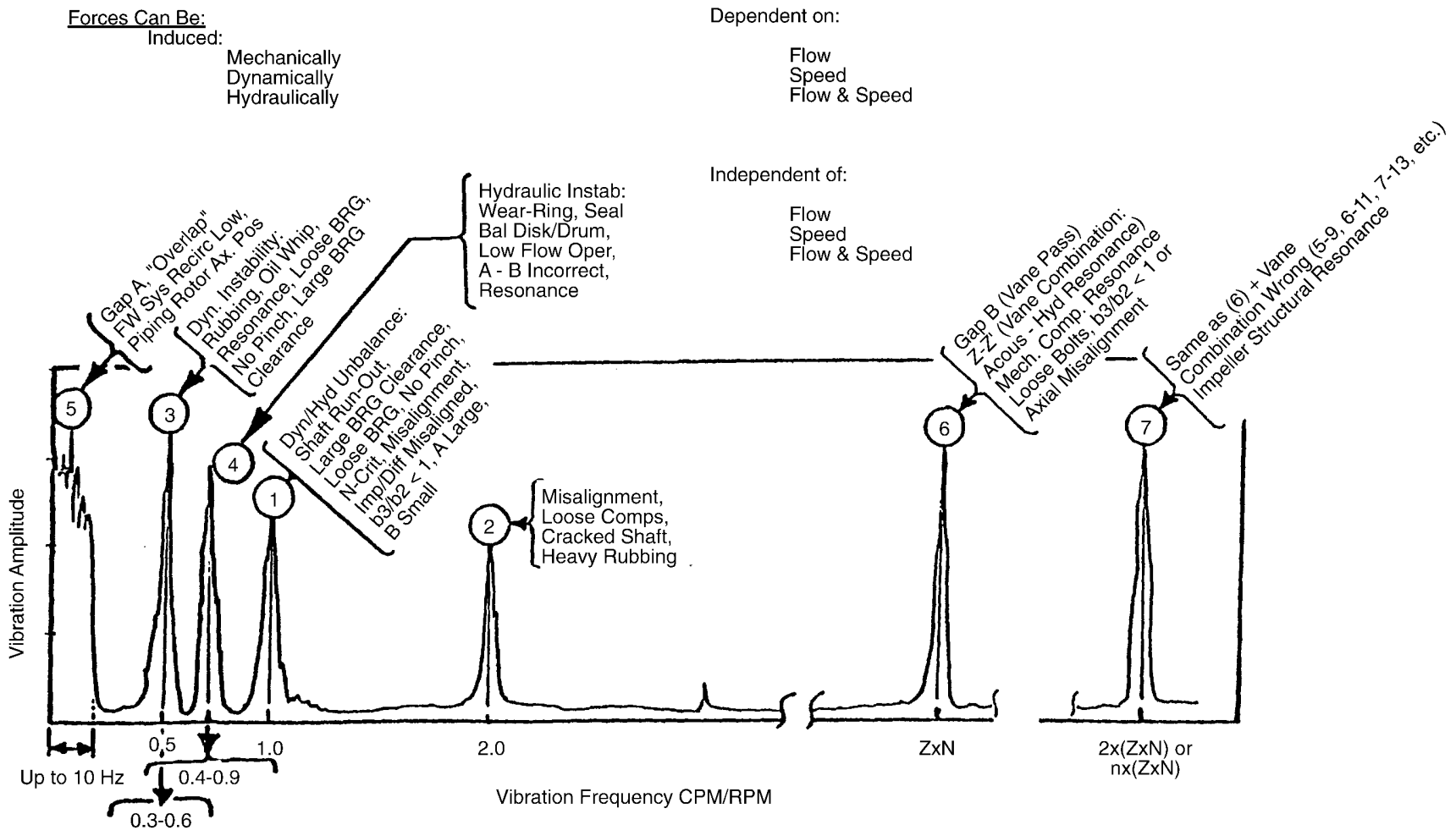

Expected hydraulically and dynamically induced vibration components in high-energy-input centrifugal pumps (all large utility pumps included)

Figure 3-1
Typical Vibration Components Measured in Large Centrifugal Pumps

Typical Vibration Frequencies

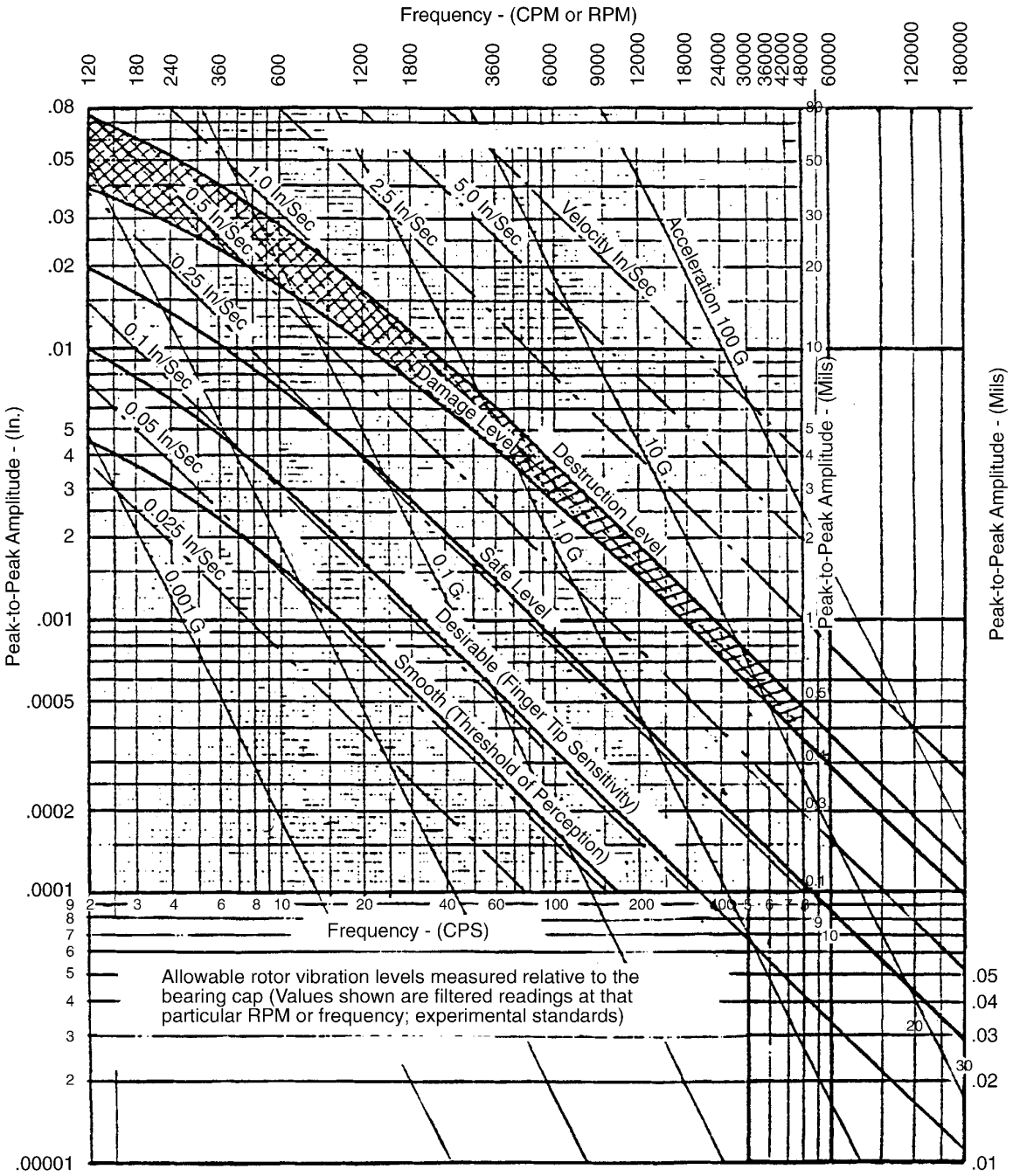

Dynamic Balancing: MILSPEC 167 (Maximum Allowable)
$U_{(MAX)}$ = 4xW[Lbs]/N[RPM] = {Oz-In}
Preferred: U = 1x W/N [Oz-In] (ERCO/EPRI Std.)

1 Oz-In = 28.35 Gm-In = 720 Gm-Mm

Figure 3-2
Vibration Severity Chart (Source: ERCO File)

4
SYNCHRONOUS VIBRATION FREQUENCY

There are many sources of synchronous or operating speed vibration amplitudes. The synchronous vibration amplitudes experienced in a pump can be the result of dynamic or hydraulic forces. When troubleshooting an operating speed vibration problem, usually hydraulic forces are not considered, and the problem continues after repeated attempts to correct the problem with precision balancing.

Dynamic forces are the result of mechanical unbalances in the rotor. Mechanical unbalances are caused by improper balance tolerances, loose parts, improper shaft keys, bowed shaft, or excessive grease in a geared-type coupling. These problems can be corrected by proper rotor assembly and installation and precision balancing of the rotor.

Hydraulic unbalances cannot be corrected on the balance machine, by proper assembly, or by installation because it is a hydro-dynamic problem and surfaces only when the pump is in service. Hydraulic unbalance results from uneven spacing of the impeller vanes, usually caused by poor casting quality or a core shift during the casting process. When troubleshooting synchronous vibration problems, inspect the impeller for equal vane spacing and uniformity.

4.1 Balancing Standards

In general, four balancing standards are used for hydraulic machinery:

- ISO (International Standards)
- API 610 (Petrochemical Industry)
- MILSPEC 167 (Military) [39]
- ERCO Standards

In terms of rotor weight (W-lbs. or M-kg) and maximum operating speed (N-RPM), the maximum permissible balance criteria from each standard, expressed in ounce-inches (oz-in and gm-cm), are provided in Table 4-1.

Table 4-1
Balancing Standards Used for Hydraulic Machinery

Balance Standards	Unbalance (oz-in)	Unbalance (gm-cm)	Comments
ISO -Grade 2.5	15 W/N	2300 M/N	Not adequate for high-speed BFP applications
ISO - Grade 1.0	6 W/N	920 M/N	Better but not good enough
API 610	4 W/N	610 M/N	Petrochemical industry only
MILSPEC 167	4 W/N	610 M/N	Clearly say: not to exceed
ERCO Standard	1 W/N	150 M/N	Not a problem to obtain with hard bearing balance machines

For example, the LCRA-Ferguson BFP rotor would have the following balance criteria:

ISO Grade 2.5	3.6 oz-in.	102.24 gm–in.	260 gm-cm
ISO Grade 1.0	1.4 oz-in.	39.76 gm–in.	105 gm-cm
API 610	.97 oz-in.	27.55 gm–in.	70.0 gm-cm
ERCO Standard	**.24 oz-in.**	**6.82 gm–in.**	**17.3 gm-cm**

The rotor was balanced to U = 0.1 oz-in. = 2.84 gm-in = 7.2 gm-cm. This precision certainly paid off. During startup, the machine was subjected to all possible conditions such as minimum to maximum flows and minimum to maximum speed, and the highest vibration amplitude did not exceed 0.5 mil (0.0005").

4.2 Dynamic Unbalance

The importance of dynamically balancing a rotor is often underestimated, toned down in the literature, and misunderstood. A frequent, but not readily apparent, error occurs when attempts are made to correct a hydraulic induced unbalance by dynamic balancing of the rotating assembly. This is particularly true for RCP nuclear applications, where counterbalance weights are added to the pump/motor coupling and create a very large bending moment at the lower journal, as shown in Figure 4-5. Four examples of simple dynamic unbalance are presented below. These examples emphasize the importance of proper dynamic balancing and demonstrate typical mistakes encountered during pump troubleshooting.

Alberta Power-Sheerness 1 & 2 Start-Up BFP (Type 6 x 13 CA-4): This is a constant speed pump operating at 3600 RPM. A purely synchronous vibration frequency (Figure 4-1) grew rapidly during startup until major damage occurred. The rapidly increasing synchronous vibration component indicated a large unbalance was in the rotating assembly. During inspection

of the rotor, it was discovered that the coupling key height was .125 in. less than the coupling keyway (Figure 4-2).

The unbalance caused by the missing key was calculated as follows:

Weight, W = 49.8 gm = 1.750 oz Shaft radius, R = 1.875 in.

Unbalance, U = W x R, therefore: U = 93.375 gm-in = 3.29 oz-in

Maximum permissible unbalance: U_{MAX} = 4 W/N = 0.60 oz-in

Recommended maximum unbalance: U = W/N = 0.15 oz-in

The unbalance created by the missing key material resulted in a rotor unbalance force 5.5 times greater than the maximum permissible balance criteria.

In addition to correcting the rotor unbalance, Lomakin grooves were added to the impeller, (Figure 4-3). The purpose of the Lomakin grooves is to provide increased rotor damping and to reduce the amount of potential seizure surface.

The pump was restarted on 6-13-88 after the proper coupling key had been installed and the rotor had been balanced to:

U = 6 gm-in = .21 oz-in

The resultant vibration amplitudes, at any flow between recirculation and full flow, were:

O.B. = 0.35 mils maximum, and I.B. = .70 mils maximum.

Alberta Power-Sheerness No. 2 Main BFP (Type 75CHTA-4): This a turbine-driven pump with a full speed of 5750 RPM. During witness testing at the OEM, a purely synchronous vibration component kept increasing to levels that would not permit the pump to reach full test speed.

The pump was shut down and the coupling key was inspected. The key was found to have 1/2 in^3 of material missing (Figure 4-4).

The unbalance calculated for the missing key was:

Weight, W = 0.142 lb. = 2.272 oz Shaft radius, R = 2.75 in.

Unbalance, U = W x R = 6.248 oz-in

Also, the initial bearing clearance of the inboard bearing was found to be 3.5 mils. Normal clearance for a shaft having a 5.5-inch diameter would be 6 to 7 mils. The very tight bearing clearance offered greater rotor damping than the normal clearance. During testing, the clearance

increased to 6 mils, which permitted the vibration amplitude to increase as the bearing damping decreased.

A third problem was found that required correction when it was determined that the bearing shell was 6 mils loose in the bearing housing, that is, the bearing did not have the required .5 to 1.5 mil pinch.

These three items were corrected, and the BFP was able to operate at full speed with acceptable vibration amplitudes.

Alberta Power-Sheerness No. 1 Main BFP (Type 75CHTA-4): This case involved one 100% pump for a 400 MW unit. The plant suffered from vibration problems for 18 months. As a result, two rotors had been damaged during operation. Vibration amplitudes as high as .87 in/sec had been experienced, which then prompted an investigation to determine the source of the high vibration.

A check of the rotors found extremely high dynamic unbalance. As received from the factory, the unbalance in the rotors was:

Rotor 1: U = 14.7 oz-in = 418 gm-in, or 93 W/N

Rotor 2: U = 8.00 oz-in = 227 gm-in, or 51 W/N

The unbalance was corrected to:

U = .035 oz-in = 1 gm-in (U_{max} = .63 oz-in = 18 gm-in)

In addition, the following design and manufacturing problems were found:

- The axial position of the last stage impeller was offset from its optimum or proper position (impeller CL to diffuser CL) by 0.205 in., which required correction.
- The impeller vane width to diffuser vane width ratio was incorrect; $b_3 / b_2 = 1.75 / 1.67 = 1.05$ instead of a minimum of 1.15. The ratio was optimized by chamfering the diffuser inlet to provide $b_3' = 1.85$ in.
- The diffuser castings were found to be eccentric ($14.3 \text{ in.} \leq D_3 \leq 14.76 \text{ in.}$), which resulted in a varying Gap B of 2% to 6%. Closer inspection determined that the castings were not finish-machined at the diffuser vane inlets. A large casting core shift caused the diffuser to be eccentric. The diffuser geometry was corrected by machining the diameter of the inlet vane to $D_3 = 14.76$ in., which provided a uniform Gap B of 6%. The diffuser vanes were hand-machined as much as possible to provide equal and uniform channels.
- An incorrect journal bearing type was applied for this application. The narrow land of the Tri-Lobe bearing was already damaged because it could not support turning gear operation or high vibration. The damage had wiped the small land that controls bearing damping and resulted in poor, unstable bearing performance.
- Rotor seizures had occurred several times. The impeller eye wear-ring surface was inspected and found to be eccentric on all four stages: Stage #1 - .005 in., #2 - .006 in., #3 - .007 in.,

and #4 - .005 in., even after heavy rubbing. The wear rings were remachined to a maximum runout of .003 in. Also, the wear ring clearance was increased from .014 in. (diametral) to .018 in. (18 to 22 mils).

- The wear-ring surface of the balancing disk was incorrect, which also permitted seizures. The balance disk wear-ring surface was corrected.
- The balancing disk vertical face did not have the necessary taper, which had permitted five disk failures to date. This problem was not corrected during this work, but it was recommended for future balance disks.

Results: The BFP was started up on 7-25-87 and the plant achieved 405 MW. However, on 7-28-87, the pump seized after an emergency plant trip, unrelated to the pump (that is, a plant trip resulted in pump seizure). The pump was unseized by the so-called thermal shock procedure and placed back in service. The plant returned to 400 MW with the pump performing satisfactorily and with acceptable vibration levels.

LCRA-Ferguson Plant Main BFP (Type HPTX-40, 3 stg., 6000 RPM Max): This case was purely one of synchronous vibration, where material missing in the coupling key was found as shown in Figure 4-2.

4.3 Hydraulic Unbalance

Casting inaccuracies of pump impellers or a bad core shift in the impeller, such as a vane, can create a large hydraulic force that rotates with the impeller. It will appear as dynamic unbalance but actually is a hydraulic unbalance. In many cases, the hydraulic unbalance can overshadow the dynamic unbalance and cannot be balanced out in air or in a vacuum. Frequently, this can be found in large circulating pump and RCP impellers because of their size. However, proper machining and good quality casting (precision cast) and milled or precision cast diffusers can prevent this problem.

Synchronous Vibration Frequency

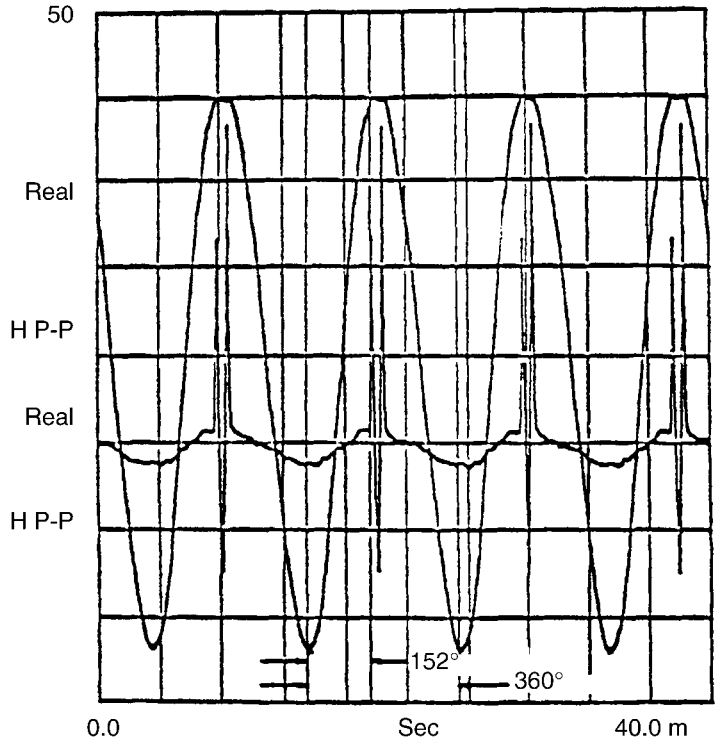

Figure 4-1
Rapidly Increasing Synchronous Vibration Results in Rotor Destruction

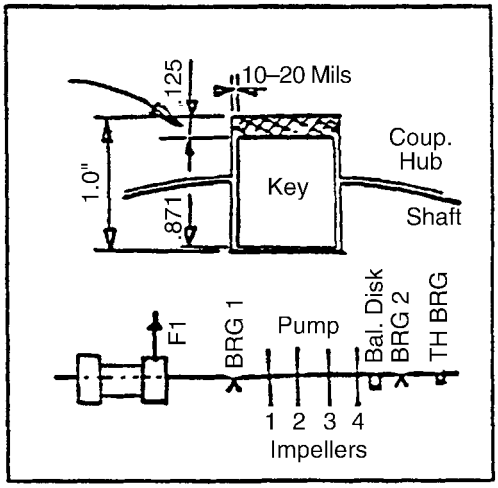

Figure 4-2
Coupling Key Missing 0.125 In. of Material

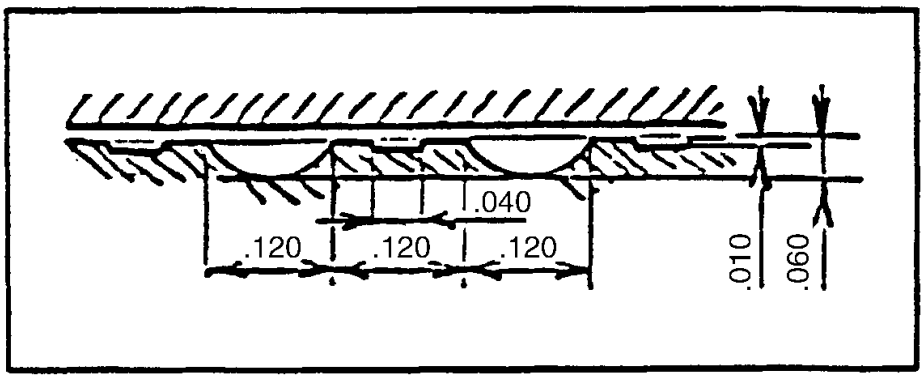

Figure 4-3
Existing Wear-Ring Geometry Modified to Include Lomakin Grooves

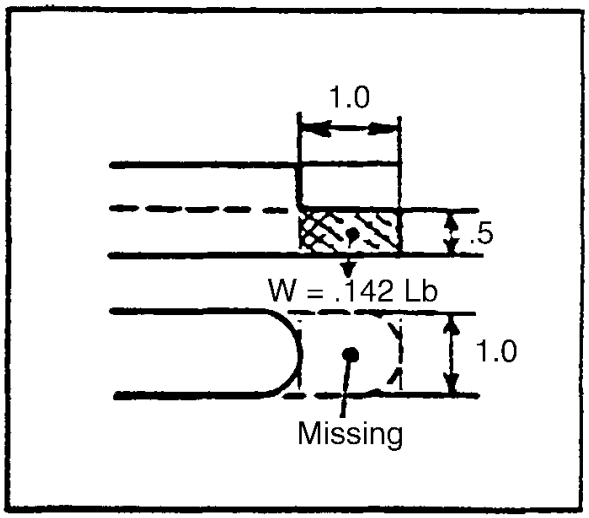

Figure 4-4
Improper Key With Missing Material

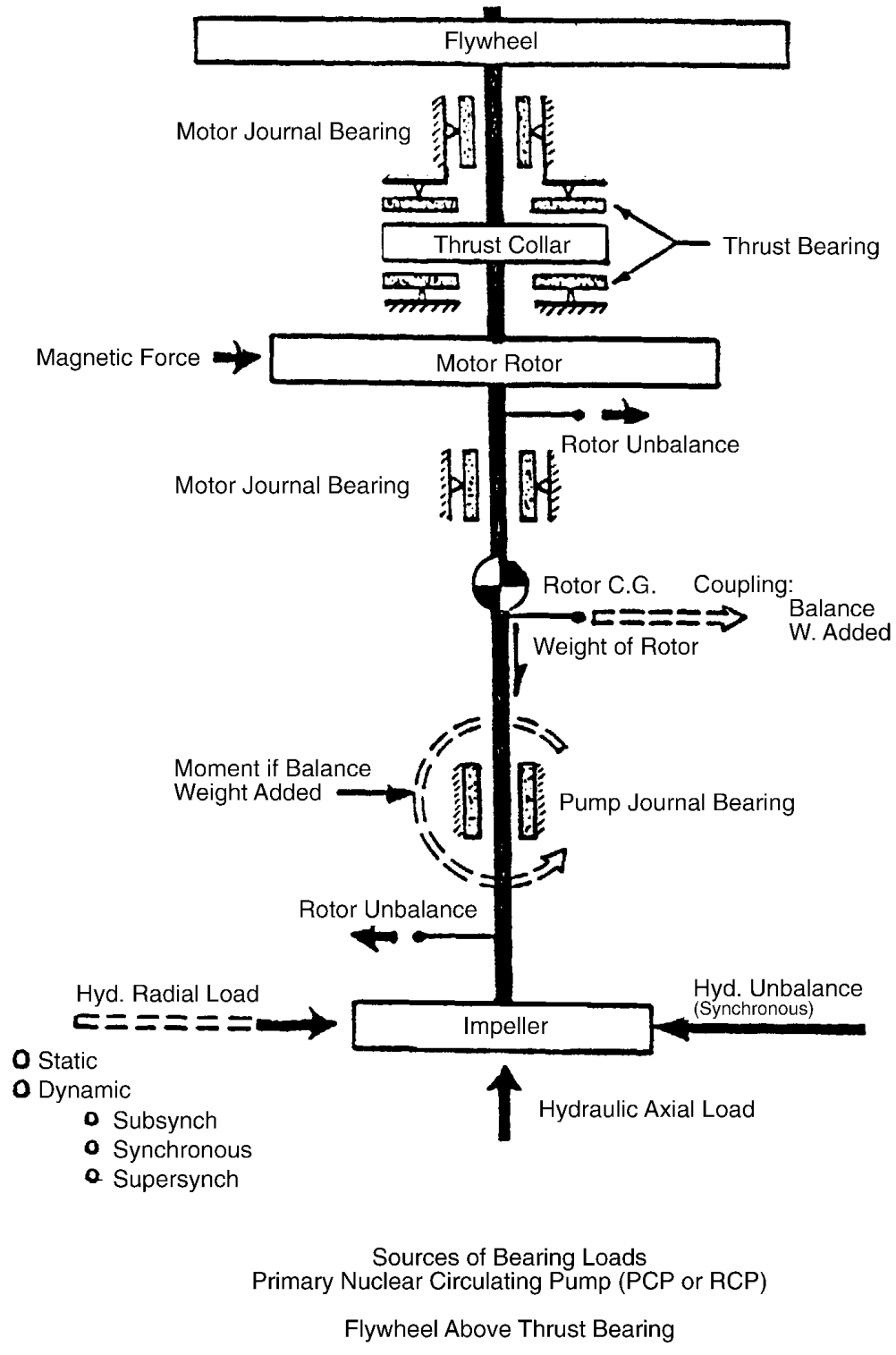

Figure 4-5
Sources of Bearing Loads and Shaft Stresses in Primary Coolant Pumps

5
SUBSYNCHRONOUS VIBRATION FREQUENCY

Subsynchronous vibration is the most damaging and unstable type of vibration that can occur in a rotating machine. Subsynchronous vibration amplitudes have been detected at frequencies ranging from 0.3 to .9 times operating speed (Figure 3-1). The first and most difficult step in troubleshooting subsynchronous vibration problems is making the distinction between rotor-dynamic and hydro-dynamic, or hydraulic, induced instability. This is a very difficult task and for years hydro-dynamic induced instabilities were not considered when a subsynchronous vibration problem was investigated. Rotor-dynamics was considered to be the source of all subsynchronous vibration frequencies, resulting in many elaborate and expensive rotor modifications that did not solve the problem. When this occurred, the problem was considered a phenomenon and was left unresolved. With the help of the utilities, hydraulic modifications were made by ERCO that solved the problems and failures experienced, and the phenomena became well-understood occurrences.

Frequency 3: This vibration component appears in the vicinity of 1/2 x RPM (0.3 to 0.6). It is a self-excited, bearing-induced vibration instability. It is very damaging, and if it surfaces will result in rotor destruction, often without warning. A basic requirement for this to develop is a lightly loaded journal bearing, which is the case for most centrifugal pumps, particularly for vertical applications such as reactor coolant pumps (RCP, PCP, or RRP).

Frequency 4: This vibration component appears in a wider range of frequencies, 0.35 to 0.9 x RPM. It is the result of hydraulic forces developed when operating a centrifugal pump off or away from its best efficiency point (BEP) flow. Examples are given below with distinct frequencies as low as 0.35 and as high as 0.92 x RPM.

Combination of 3 and 4: This is the most difficult case to analyze. If the vibration frequency is about 0.6 x RPM, it could be dynamic, hydraulic, or a combination of the two.

Vertical pumps, such as the RCP in nuclear applications, have very lightly loaded journal bearings and, hence, are prone to bearing instability. If the hydraulic excitation is just right, it will put the pump in the Frequency 3 category. The result of this phenomenon can be:

- Frequent shaft seal failure (the most delicate part of the RCP)
- Journal bearing damage
- Shaft damage
- Shaft breakage

In order to counteract instability, more stable types of journal bearings are needed for these RCP applications. Above the pump, in the electric motor, tilting-pad-type bearings are applied

(Figures 14-6 to 14-9). However, many motors are found with fitted bearings (Figure 14-9), which are a misapplication and have been attributed to age. Most BWR applications also have plain cylindrical journals in the electric motor, which result in the most unstable rotor-dynamic combination. This combination (that is, vertical pumps with plain cylindrical pump and motor bearings) is responsible for many pump failures, resulting in outages in large nuclear plants. These pump types are discussed in greater depth in References 29 to 33. Reference 33 is a design book for these pumps.

Several field examples are discussed in the remaining portion of this section. The main objectives are:

- Identify the problem.
- Find the root causes.
- Apply the correct modification to eliminate these very damaging, built-in design discrepancies.

New England Electric, Brayton Point Unit No. 3: The 100% BFP Model 95-CHTA-5 with a 31,000 hp Westinghouse turbine drive was tested after three failures. Rapid increase of the 1/2 x RPM component did not permit the unit to go on-line. This component was already over 20 mils at 2400 RPM (see Figure 5-1) with the operating speed at full load over 5000 RPM.

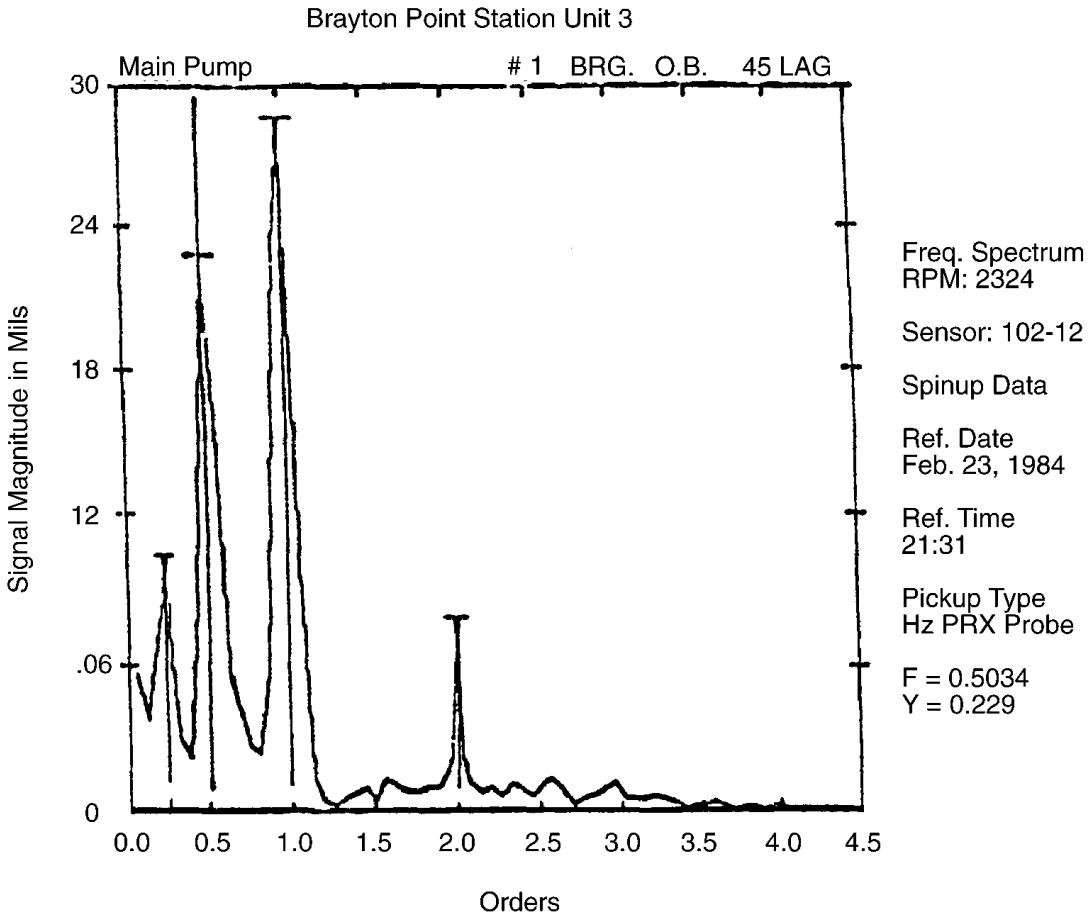

Figure 5-1
Oil-Whip Development in 95 CHTA-5, 32000 HP High-Speed BFP

An investigation was conducted with the following conclusions or findings:

- The rotor was out of balance by 72 oz-in; corrected to 0.2 oz-in.
- Bearing clearance was 15 mils; corrected to 7 mils (D=6.5 in.).
- 16 mils looseness was found between the bearing upper half and bearing housing (no pinch). The looseness was corrected to one mil pinch by shimming.

After correcting the above three items, the pump vibration became 0.8 mil maximum in any operating mode, and there was a complete absence of any subsynchronous vibration components.

Louisville Gas & Electric Company, Cane Run Power Station: The onset of a subharmonic resonance as detected in the inboard horizontal component of the No. 61 boiler feed pump, model HPT-35-12 stages, as shown in Figure 5-2. The magnitude of this subharmonic component rapidly increased to above 7 mils, necessitating a unit shutdown.

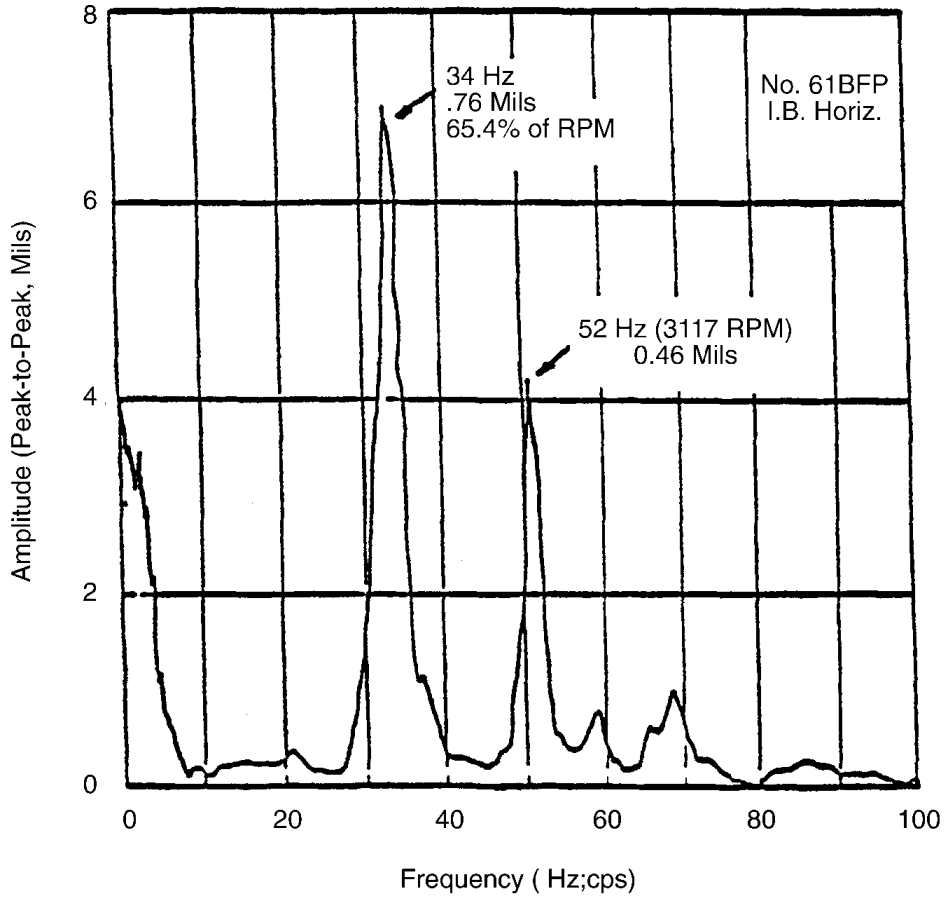

Figure 5-2
Destructive Subsynchronous Vibration Component

Changing to tilting-pad-type journal bearings did not eliminate the harmful subsynchronous vibration component. This indicated that the root cause of the problem was hydraulic instability and not just rotor-dynamic instability; perhaps it was a combination of two phenomena. The subsynchronous vibration component, at .654 of running speed is in an area where the two instabilities (hydraulic and rotor-dynamic) overlap, both claiming to be responsible for the difficult vibration problem.

Pennsylvania Power &Light, Montour No. 1: The 1B BFP (14-WNC-156, six stages) experienced a typical case of hydraulic instability at part load, which previously had been mistaken as a rotor critical speed problem. More details and precise description can be found in Reference 26. The vibration was clearly identified during well-organized testing as a function of feedwater flow, and not speed or any other parameter. The pump became unstable at 62% of BEP flow regardless of the pump speed. The instability was completely eliminated as shown in

Figure 5-4 by ERCO hydraulic modifications. All failures had occurred when the startup of large new nuclear units required the plant to cycle based on system load demands.

Conclusion: The clear root cause of the problem was hydraulic instability induced at 62% of BEP. Hydraulic modifications (see Figure 5-3) to optimize Gap A and Gap B alleviated the problem. The modifications also stabilized the axial thrust (see the before and after modification test data shown in Figures 5-5 and 10-8).

Lower Colorado River Authority (LCRA), Ferguson Station: This is a 400 MW power station with one 100%, Model HPTX-40, three-stage BFP. The damaging subsynchronous vibration frequency was at or around 0.6 x RPM as shown in Figure 5-6. A strong amplitude at vane passing frequency was also present, and hence Gap B was increased from the original 2% to 6% (see Figures 5-6 and 5-7).

To increase rotor dynamic stiffness, the Lomakin Effect serrations were added at the balancing disk cylindrical section and in all impeller wear rings (See Figure 5-7), and a swirl break was added upstream of the balancing disk (see Figure 10-17). In all, a total of 22 items were corrected simultaneously, summarized as follows:

- Balanced rotor 36 x better than the ISO standard recommended by Sulzer.
- Changed both couplings (badly worn) and fine balanced.
- Replaced incorrect BFP coupling key, which had resulted in a 5.6 oz-in unbalanced.
- Changed the Sulzer journal bearing design to tilting pad, because the subsynchronous whirl frequency was 0.6 x RPM.
- Put the Makay taper into the balancing disk (minor dimensional corrections).
- Redesigned the retaining procedure of balancing disk (removed copper shim and replaced with stainless).
- Changed impeller wear-ring geometry. Added Lomakin Effect labyrinths in:
  - Impeller wear rings (Figure 5-7)
  - Balancing disk (Figure 10-16)
- Changed impeller wear-ring material and hardness to current ERCO standards (420°F and minimum 10 Rc difference between rotating and stationary surfaces).
- Added the swirl-break in front of the balancing disk (Figure 10-16).
- Found many cracks in seal housings, weld repaired, and re-machined.
- Found many cracks in impeller vanes at the eye. Welded vanes, and returned hardness to present standards.
- Vertical faces, or fits, in pump barrel were out of perpendicular by as much as 50 mils. The pump barrel was re-bored.
- Re-shaped all diffuser channels to the proper geometry.
- Found kicker stage installed backwards (that is, wrong rotation) and corrected.

- Welded up diffuser sideplates and impeller ODs for proper Gap A and Gap A Overlap.
- Opened up Gap B to proper dimensions.
- Introduced proper shrink-fit between impellers and shaft.
- Changed original shaft seals to Durametallic mechanical seals just prior to the above changes. Since flow from seal to the balance disk leak off chamber no longer existed, the monitor leak off flow could now be monitored.
- Controlled final rotor assembly as good as possible.
- Master alignment at the plant between turbine-BFP-gear booster.
- Pinch-checked all bearings. Some were way out.
- "Blued" coupling bores to shaft to obtain proper contact surface.

Results:

Vibration levels never exceeded 0.2 mil (.05 mm) on any of the bearings in all flow ranges.

Efficiency: Excellent data were taken at 300 MW before and after modifications were made. A clear 3.8% improvement in efficiency was achieved.

Booster pump: The previously heavy axial vibration (shuttling) was completely eliminated due to the changes in Gaps A and B and the Overlap ratio.

Although the problem was completely solved, the root cause of the subsynchronous vibration must be considered inconclusive. Rotor-dynamic and hydraulic modifications were made simultaneously, which prevented concluding what contribution each had on the poor performance of the pump (for more details, see Reference 15). However, the HPTX-40-3 boiler feed pump is now an up-to-date machine. The machine is more efficient than ever and is good for the next 40 years of operation.

Future Action:

The booster pump impeller has unusually large eye geometry, resulting in heavy suction piping vibration at very low flows. Gap A change eliminated the heavy axial shuttling of the rotor, but the booster pump needs one of the following:

- New impeller design
- The backflow deflector (eye catcher, see Figure 9-2). Note: A new impeller design is always risky, while the eye catcher has been proven to be effective.

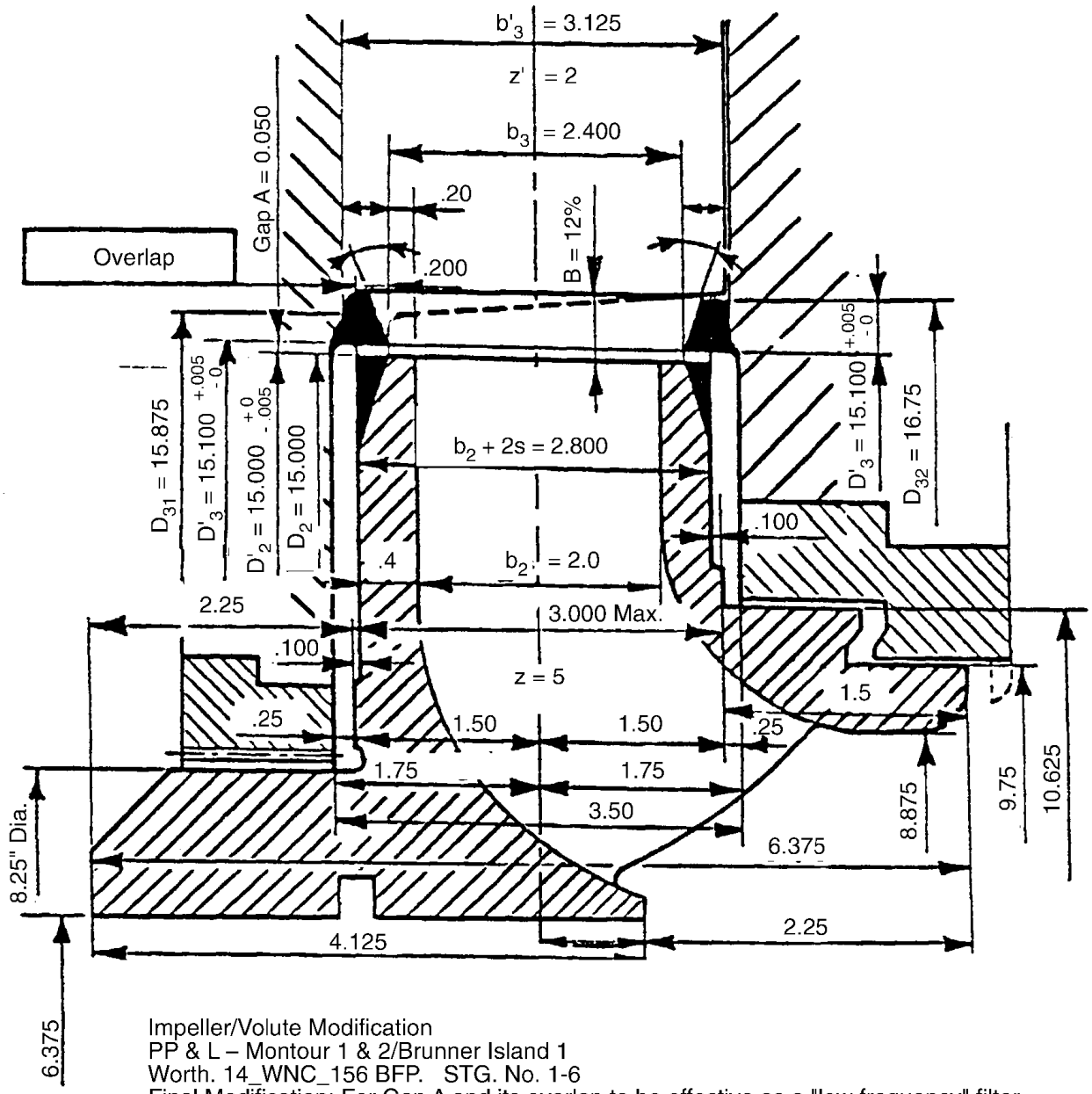

Impeller/Volute Modification
PP & L – Montour 1 & 2/Brunner Island 1
Worth. 14_WNC_156 BFP. STG. No. 1-6
Final Modification: For Gap A and its overlap to be effective as a "low frequency" filter, the impeller sideplates and the volute inlet should be welded up as shown above.

Note: When ordering new impellers from Worthington, give instruction on the P.O. not to chamfer the impeller sideplates.

Axial Float Per Design = [(0.250) + (0.250)] = 0.500
Measured = _____

Stage Spacing = 7.375 in.
Underfile All Impeller Vanes to x = .25 in. Land
Journal Bearing Diameter = 5.500 in.

Figure 5-3
Boiler Feed Pump Gap A and B Modification

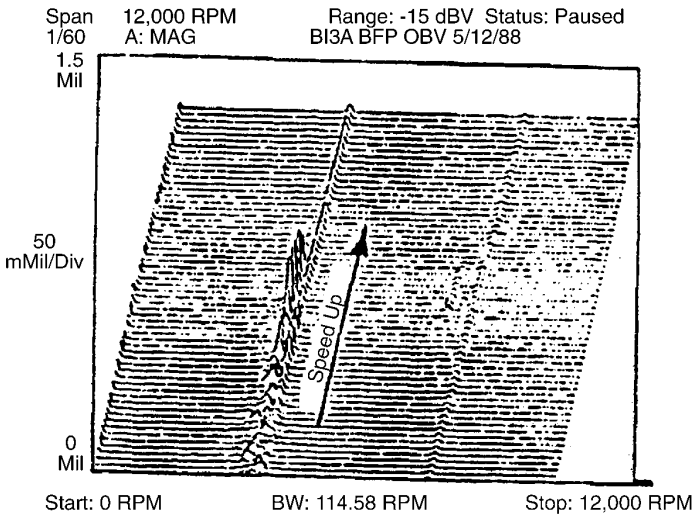

Data taken on 5/12/88 in 3-second intervals during speed increase from 4370 RPM to 4500 RPM. Instability between 4400 and 4440 RPM.

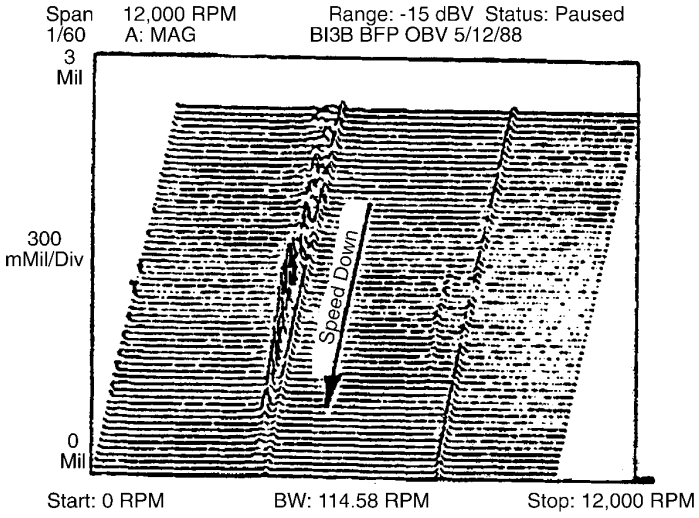

Data taken on 5/12/88 in 3 second intervals during speed decrease from 4500 RPM to 4390 RPM. Instability between 4440 and 4400 RPM.

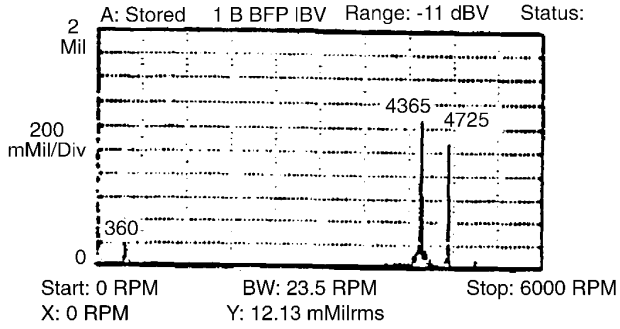

Data taken on 7/26-7/27/88 at the Montour Unit No. 1, No. 1-B boiler feed pump. Flow at 61% BEP.

PP&L - Montour Ses No. 1 BFP Test.
Worthington, Type: 14 WNC-156 BFP

Figure 5-4
Hydraulic Instability at 62% BEP Before Introducing Proper Gap A and B

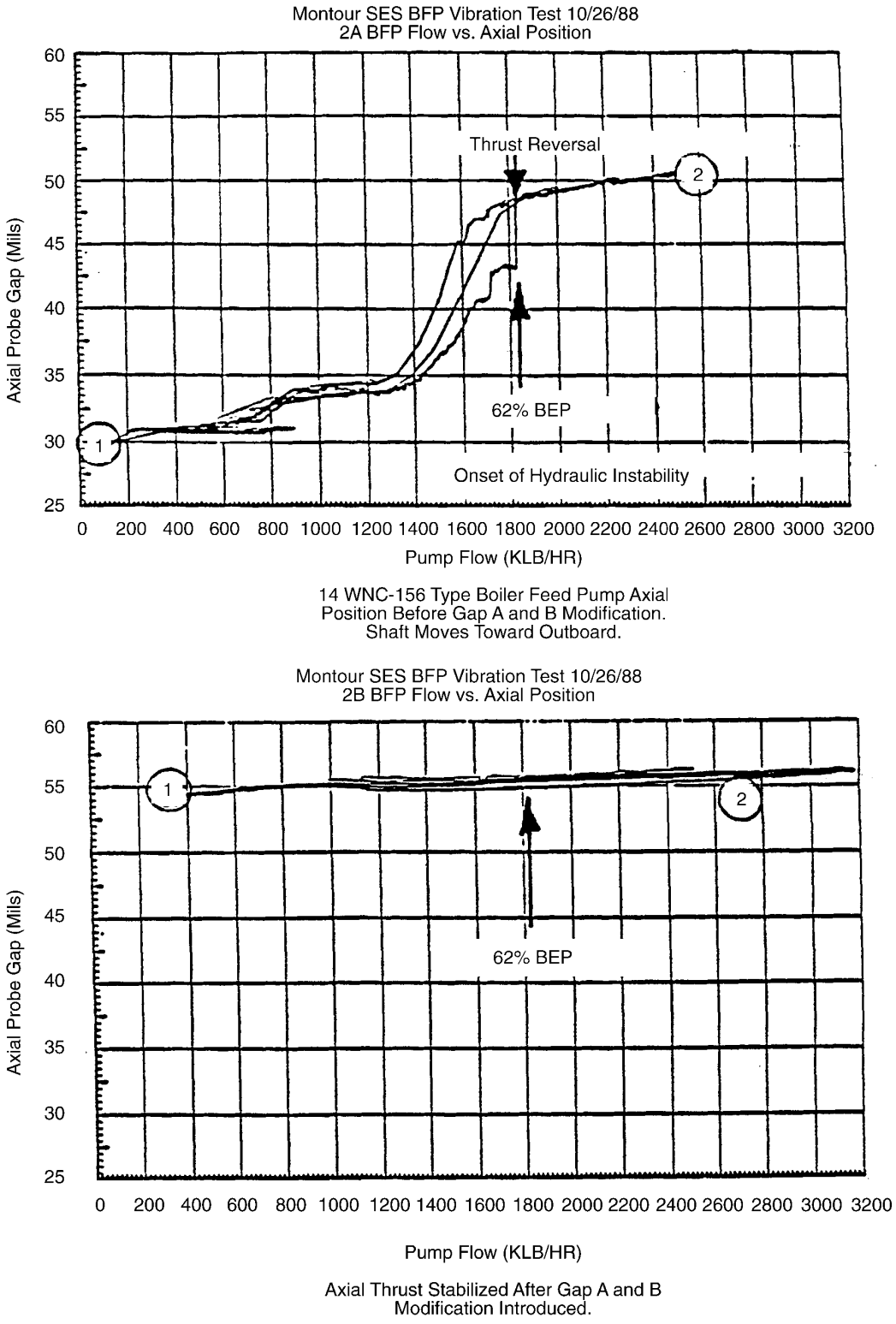

Figure 5-5
Boiler Feed Pump Vibration Tests Showing Axial Thrust Stabilized After Gap A and B Modification

Subsynchronous Vibration Frequency

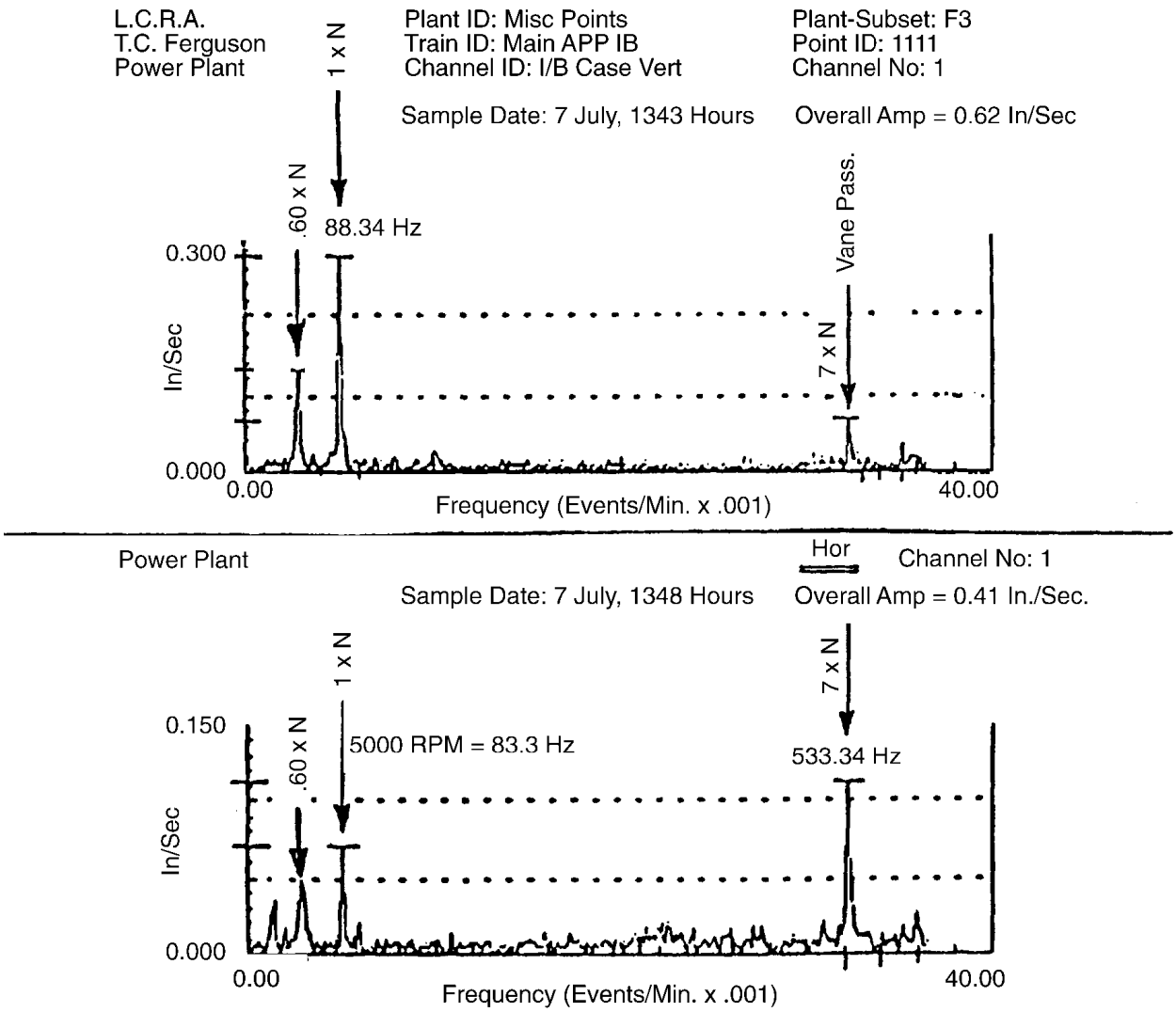

Figure 5-6
Boiler Feed Pump, Type HPTX-40, 3 Stage Plus Kicker Stage

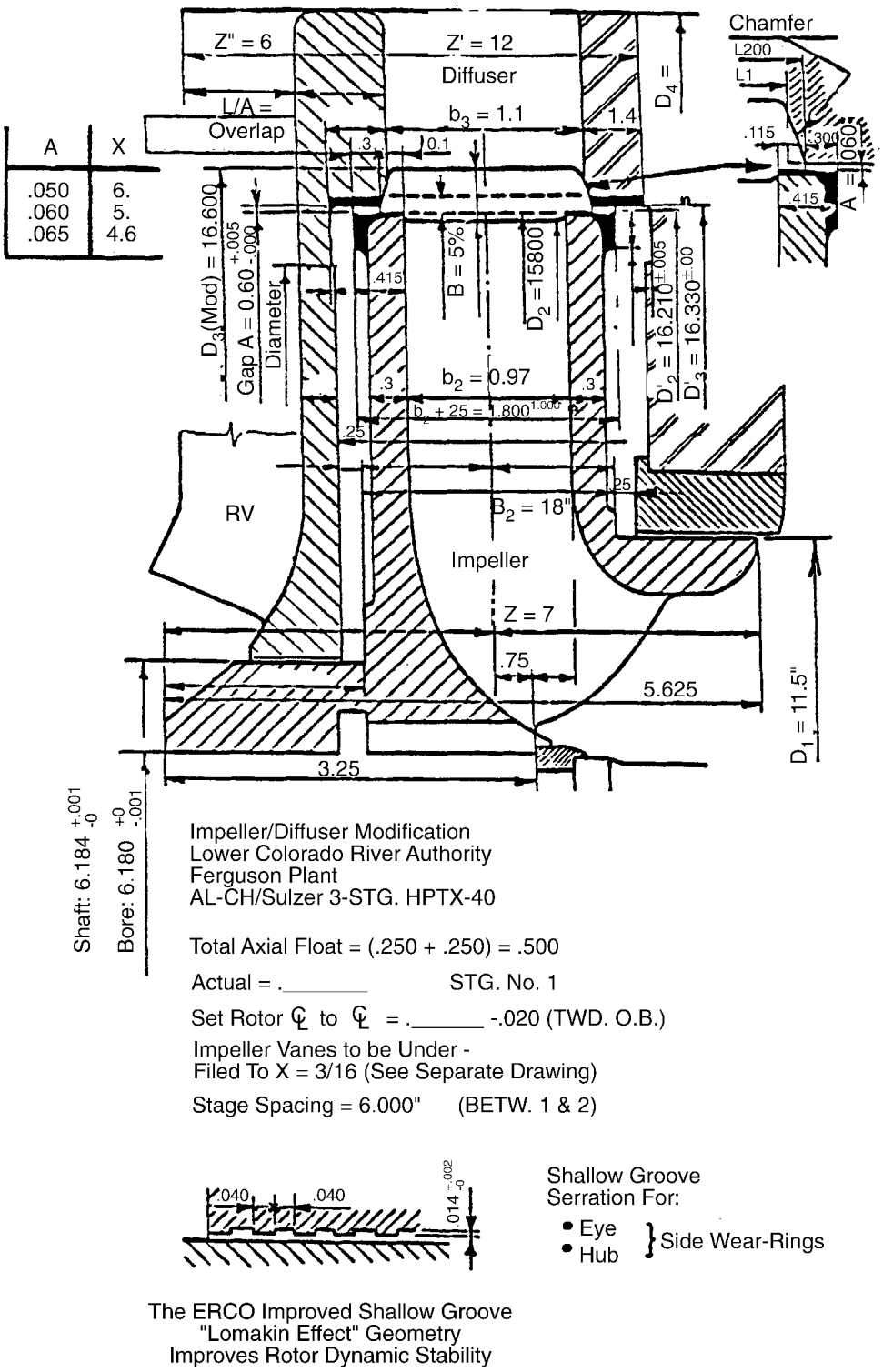

Figure 5-7
Impeller/Diffuser and Wear-Ring (Lomakin) Modification

6
COMBINATION EXAMPLES

For vibration components 1, 2, 3, and 3-A (for component numbers see Figure 3-1), two cases are presented below. Both are De Laval-made boiler feed pumps. Although the number of stages and operating speeds are quite different, the symptoms and root causes of problems, as well as the solutions, are similar.

6.1 Case 1: 6060 RPM, Five-Stage BFP, City of Los Angeles

A long failure history and the similarity between this case and the next case created much interest in this in-house study of rotor critical speeds. A simple mathematical model with spring and dashpot (spring and damping coefficients) is shown in Figure 6-1. It shows how the spring and damping effect influences the location of the critical speed and the amplitude of vibration. Figure 6-2 shows the actual rotor response calculation with changing the spring and damping coefficients as inputs. It becomes obvious from Figure 6-2 that, when rotor internals begin to wear out, the critical speed sinks into the operating speed and the vibration amplitudes grow until destruction of the rotor occurs. The rotor dimensions of Cases 1 and 2 are identical; except in Case 1, the feed pump had five stages, whereas Case 2 presents a nine-stage BFP.

6.2 Case 2: 3570 RPM, Nine-Stage BFP, City of Henderson

The symptoms and remedies are similar for both cases. Case 2 is much more pronounced; therefore, it is presented below. Test data are shown below (Figures 6-3 to 6-5). After 22 major failures in two years after startup (four pumps, two per unit), an investigation started. Usually the rotor failed in the axial direction (axial thrust at part load). In one failure case, by the time failure occurred, internal clearances grew from a nominal 16 mils to as high as 75 mils at the location of maximum deflection.

Journal bearings were plain cylindrical two-axial groove sleeve type. The first change was to replace the journal bearings with five pad, preloaded tilting-pad-type bearings (pre-load: C/C'=0.75, for explanation, see Figures 14-7 and 14-8 and the last paragraph of Reference 7). The 0.47 x N vibration component did not recur at the beginning, but it reappeared when other components became excessive. After changing to tilting-pad bearings, the 0.54 x N vibration component set in during low flow operation and vanished above 67% of BEP (where the kink in the H-curve began from high to lower flows or onset of hydraulic instability). When rotor internal clearances opened up beyond a certain amount, this component remained up to full flow, and the 0.47 component also reappeared.

Several other changes followed by necessity:

- Gap B was changed from 1.3% to 6%.
- The cast iron inner bearing housing was changed to heavy-walled cast steel.
- The coupling was changed to a flexible dry diaphragm type.
- The balancing disk was replaced by the new ERCO design to avoid axial thrust failure.
- The rotor was properly balanced to W/N standard and realigned.
- The shaft geometry was changed at the location of the balancing disk to increase shaft stiffness
- The diffuser channels were redesigned for more stable flow characteristics. Some other minor changes were made.

6.2.1 Conclusions

The root cause of all failures was a combination of the following items:

- Journal bearing permitted (or contributed to) rotor-dynamic instability (see Figure 6-5, left side).
- Hydraulic instability at and below 67% of BEP-induced rotor instability (see Figure 6-5, right side).
- Insufficient Gap B and bearing housing resonance induced high vane-pass amplitudes.
- High residual dynamic unbalance exaggerated the vibration amplitudes.
- Incorrect axial balancing disk dimensions permitted several failures. Assembly and alignment discrepancies made this more pronounced.
- The shaft was more flexible than desired due to the heavy undercut at the balancing disk location.
- Rapid wear of the close clearance surfaces resulted in:
  - Loss of pump hydraulic performance
  - Lowered second critical speed came close to the operating speed, as shown in Figure 6-2 for Case 1, making the wear phenomenon even more rapid.

6.2.2 Follow-Up and Summary of the 1976 Major BFP Design Modifications on Units 1 and 2 (Two Pumps per Unit, Total of Four Motor-Driven BFPs)

Also provided is the summary of the last two of 23 failures and the end results of the modifications:

- June 27, 1976: Vane passing (9 x RPM) and 1/2 x RPM vibration components grow rapidly; destroyed rotor (22nd major failure in two years from start-up).
- June 28: Changed rotor, put in new element. Same story (ERCO now present), both vibration components are growing. Ramped up unit to 70% load, 1/2 component disappears completely above 67% load, indicating that we are dealing with a flow-related problem called hydraulic instability.
- July 23: Journal bearings changed to tilting-pad type.
  - 09:14 Startup. Slight sign of 1/2 x N vibration component discovered in both journal bearings but only at 0.54 x N frequency.
  - 13:51 1/2 frequency component grows rapidly. Vane passing also grows with it.
  - 13:56 Out of control, emergency shutdown, rotor destroyed. Taped all channels during failure.
  - 14:51 After shutdown, replay tape to see what the 1/2 frequency component looked like. There is a fork (see Figure 6-3 and especially 6-4), one component at 28 Hz (0.47 x N) and one at 32 Hz (0.54 x N).
  - 15:17 Made corrections as described below.
- Startup on Oct. 25, 1976: OK in all flow ranges, no sign of subsynchronous or vane passing vibration components (upper part of Figure 6-3). Synchronous component was 1 mil maximum at low flows and less at full load.

6.2.3 Summary of Conclusions

Table 6-1
Summary of Conclusions

Changes Made	Conclusions
1. Replaced bearings with tilting pad	Did not help too much by itself.
2. Put in new balancing disk (Designed by ERCO)	No change in vibration frequency, but prevented catastrophic failures.
3. New shaft geometry (eliminated deep undercut at the balancing disk)	Increased rotor stiffness, hence moved up critical speed (Figure 6-2).
4. Corrected Impeller to diffuser radial Gap relation (Gaps A and B), changed I.B. bearing housing to stainless steel casting	Removed/decreased hydraulically induced instability and vane passing shocks, also I.B. bearing resonance.
5. Modified diffuser channels	Further increased hydraulic stability at reduced capacities (Part load).

A combination of changes 1 to 5, plus some other changes such as good dynamic balancing, changing to flexible coupling, and proper assembly (axial line-up of impellers to diffusers), eliminated all harmful vibration frequency components.

6.2.4 Conclusions

Failures were caused by a combination of hydraulic and dynamic instability, design, service, and assembly errors. Closeness of the rotor second lateral critical speed to operating speed accelerated the failures when internal clearances started to wear.

Fluid film journal bearing caused oil whip (0.47 x N) and the rubbing caused whip. It is very rare to observe both at the same time. When changing to tilting-pad bearings, the 0.47 component did not recur initially (see Figure 6-5. Hydraulic instability induced flow forces (at part load), and the large forces created by the very small Gap B resulted in rubbing of the rotor, which in turn created dry friction whip. Therefore, the root cause was hydraulics, and the apparent effect was dry whip.

An explanation of the two subsynchronous vibration components is offered in the paper by Ehrick [23] and is illustrated in Figure 6-5.

A. When changed to a tilting-pad-type bearing, this component did not recur until heavy rubbing increased the internal clearance, resulting in loss of rotor damping. The two (0.47 and 0.54) then jointly destroyed the rotor during the twenty-third failure.

B. When changed to tilting-pad-type bearings, this component did not change in frequency, but the amplitude kept increasing until destruction of the rotor (see the final state of failure as shown in Figure 6-3).

The user should review the critical speed (N_{crit}) of a rotor as a function of k_{ij} and c_{ij} (spring and damping coefficients). Then the effect on N_{crit} of the rotor can be seen in each case:

- Frequency-(k_{ij})
- Amplitude (c_{ij})

For simplification, approach the problem as a single degree of freedom mathematical problem. For example, a single mass with a spring and a dashpot, as shown in Figure 6-1. The equation of the motion is:

$F = m \bullet a = -m \bullet x$

$= -C \bullet Vel = -C \bullet x$

K = Spring coefficient of the spring

C = Damping coefficient of the dashpot

m = Rotor mass = W/g

W = Weight of the rotor

K = dF/dx [lbs/in]

C = -F/x [lb-sec/in]

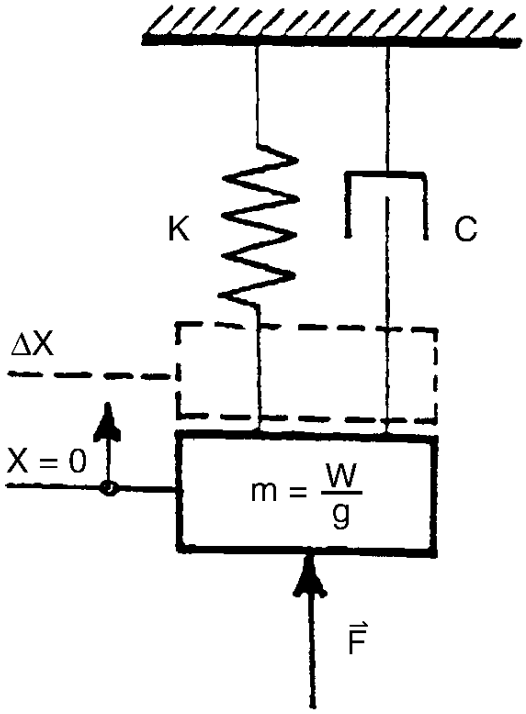

Figure 6-1
Simple Mathematical Model

Natural Frequency of the System:

$N_{crit} = (k/m)^{1/2}$

If: k up, then N_{crit} up

If: m up, then N_{crit} down

Vibration Amplitude:

A = 1 / C

If: C up, then A down

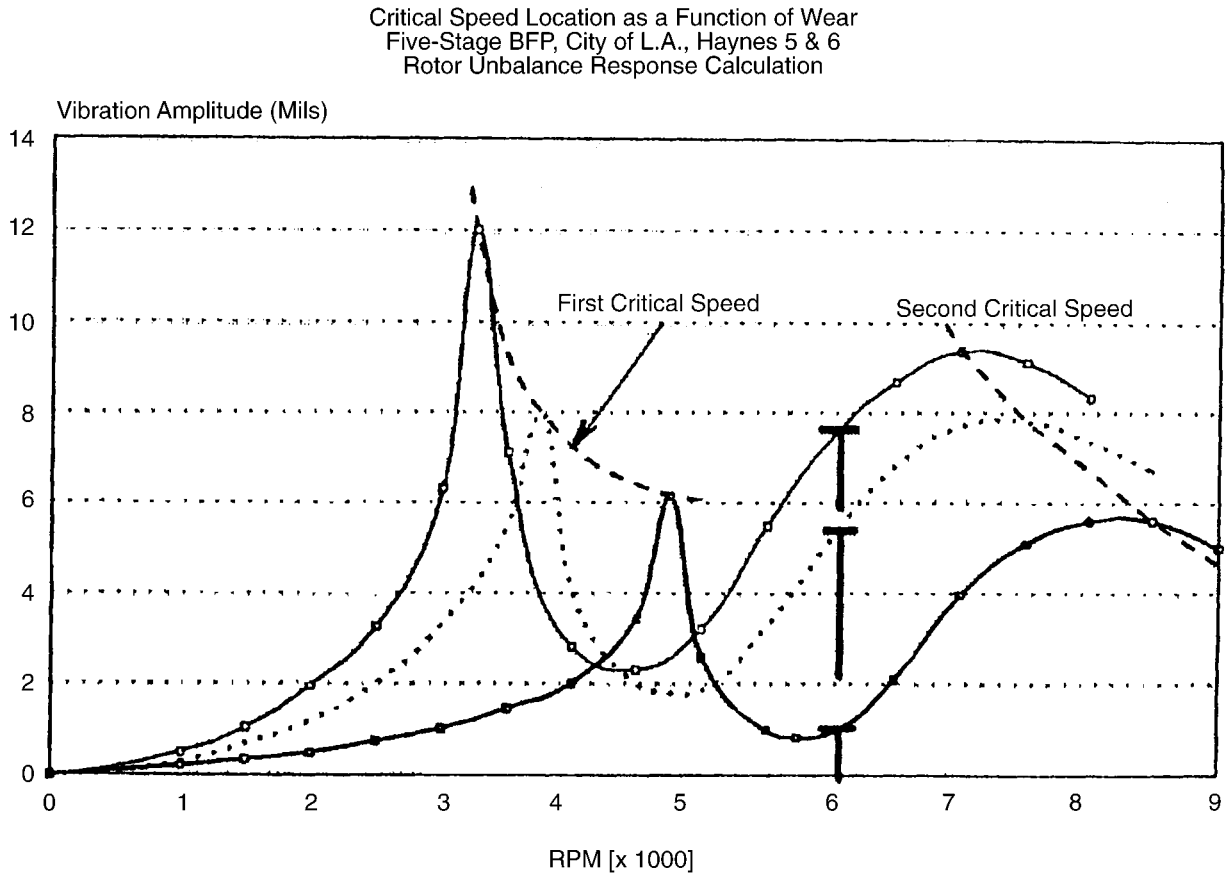

Figure 6-2
Change of Critical Speeds as a Function of Rotor Wear

Combination Examples

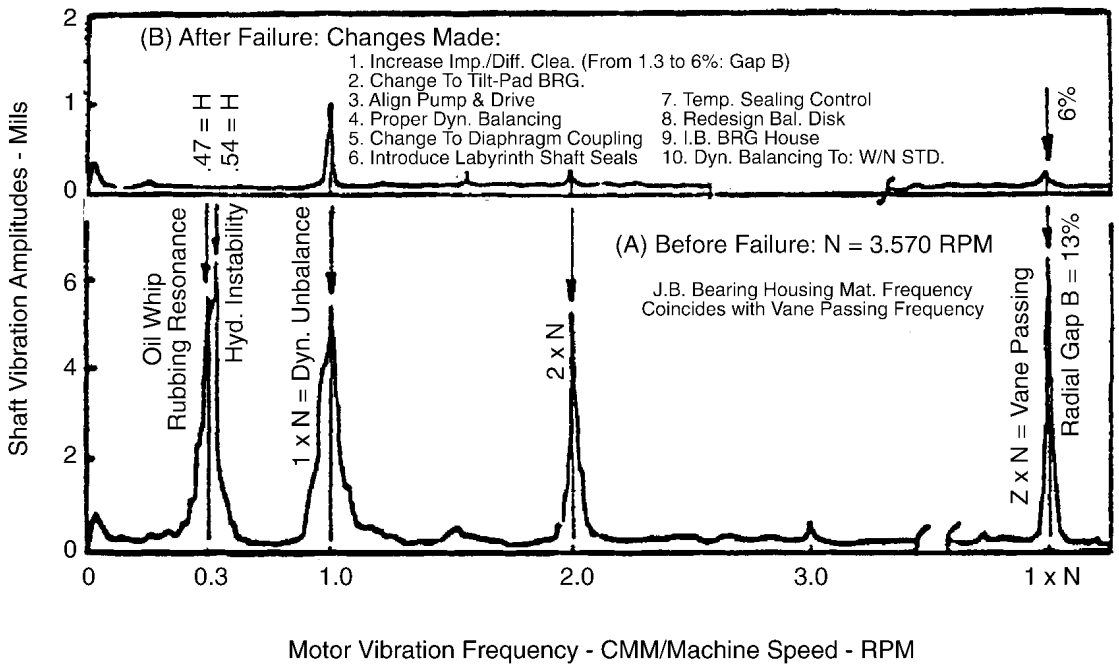

Figure 6-3
City of Henderson Shaft Vibration History

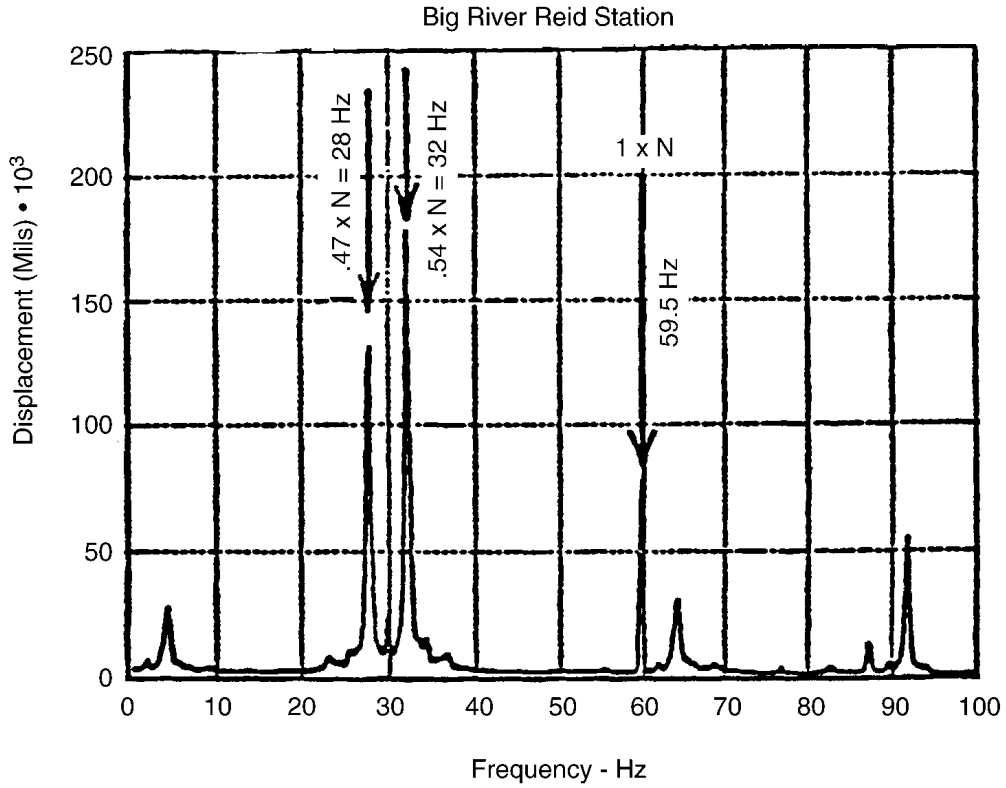

Figure 6-4
Double Vibration Amplitude at ½ x N

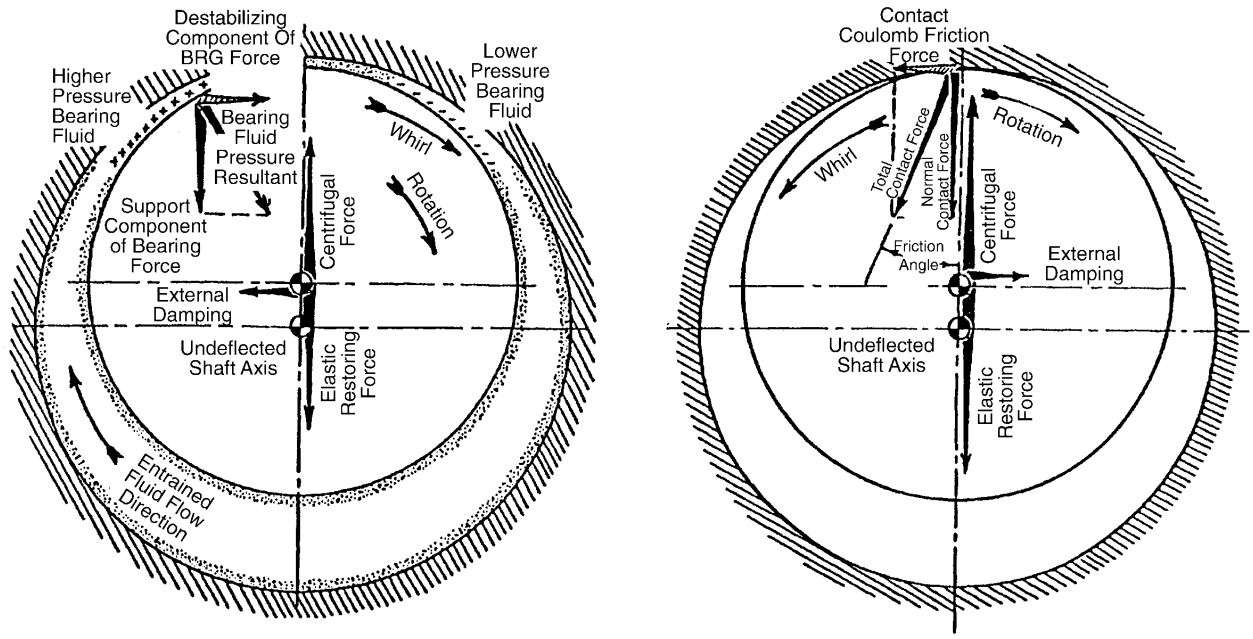

Fluid Bearing Whip
When changed to tilting-pad-type journal bearings, this component did not recur.

Dry Friction Whip
When changed to tilting-pad, this component did not change in frequency, but amplitude increased to destruction of rotor.

Figure 6-5
Bearing Instability: (A) Bearing Whip, (B) Dry Friction Whip

6.3 Case 3: Boiler Feed Pump Type: 8-WNC-95 (Five STGS)

P.S. Oklahoma, Northeastern 1 & 2, 1984 startup, and several other units across the U.S. such as PSE&G, NJ (Mercer Station) have the above BFP type at very high operating speed ranges (8800 to 9250 RPM). The unusually high speed resulted in hydraulic instability at part-load operation that caused many severe failures. Maximum operating speed at the Northeastern Station was 9250 RPM. A summary is given below.

High maintenance costs and many major failures were experienced at every station. The subsynchronous vibration component, as shown in Figure 6-7, is always present and dominant.

The original Worthington plain sleeve journal bearing was changed to Centritech-made tilting-pad type. This had little or no effect in alleviating the problem. Vibration components are described in Figures 6-6 to 6-8.

Complete hydraulic modifications were introduced at two stations: P.S. Oklahoma; by ERCO as shown in Figure 6-9 (inexpensive and not a time-consuming modification) and the Mercer County Station by the OEM (a complete redesign of the internal assembly, which was expensive, time consuming and risky).

The ERCO modification permits the user to determine the root cause of the problem, while the other modification does not.

Northeastern started up shortly after the June 1991 EPRI Pump Symposium held in Tampa, Florida, where the above subject was discussed by Oral Newell and Elemer Makay. The subsynchronous vibration component was absent at that time and the pump overall vibration was excellent.

6.3.1 Conclusion

The root cause of pump vibration and system instability was determined to be hydraulically induced. The problem was solved, hence the case is closed for Public Service Oklahoma. As of today, we have several years of successful operating experience at the Northeastern station. The same cannot be claimed for the users of the other similar pumps.

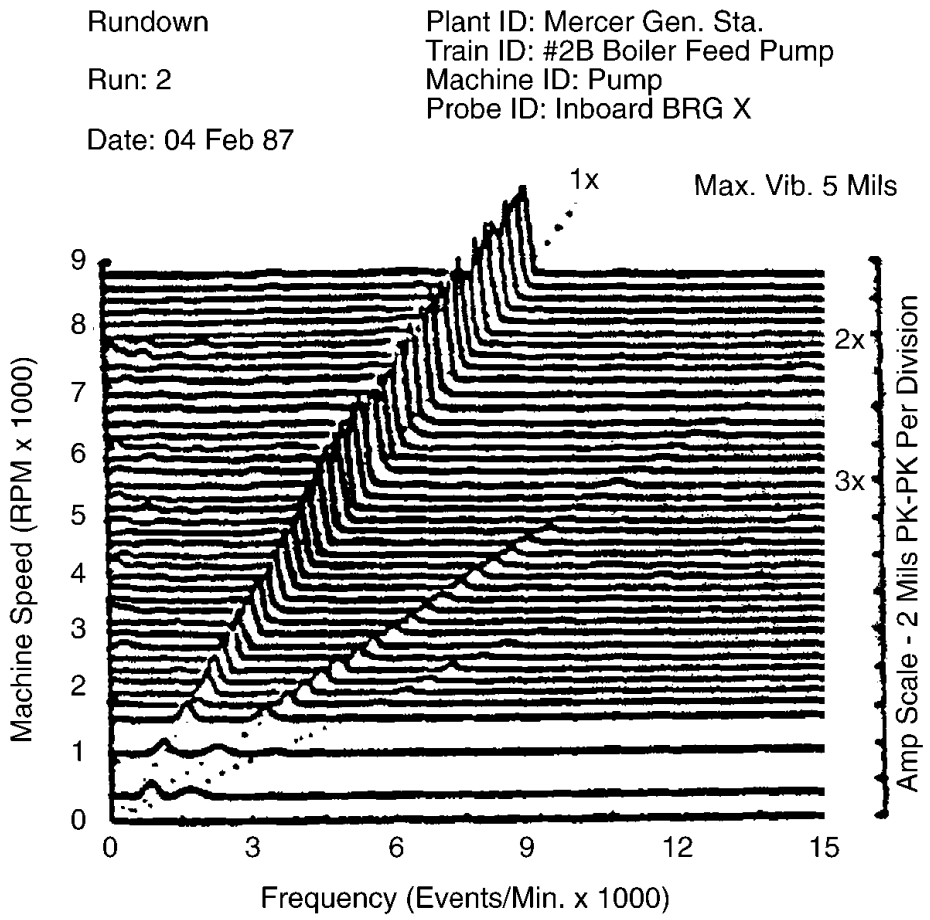

Figure 6-6
Newly Repaired Rotor Startup

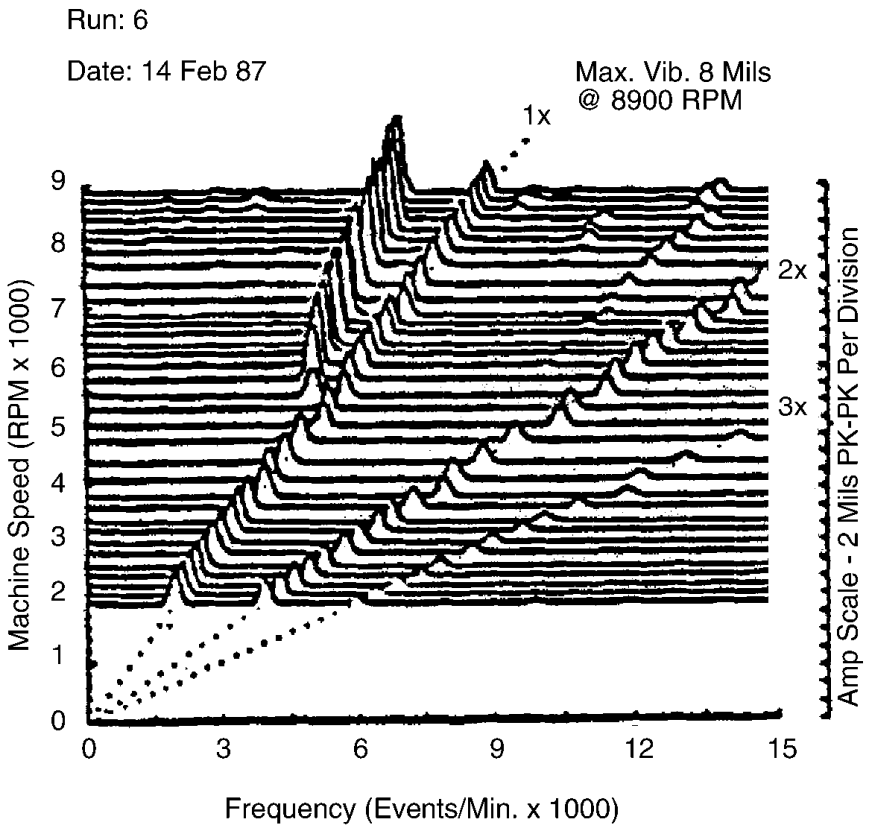

Figure 6-7
Subsynchronous Vibration (8 Mils)

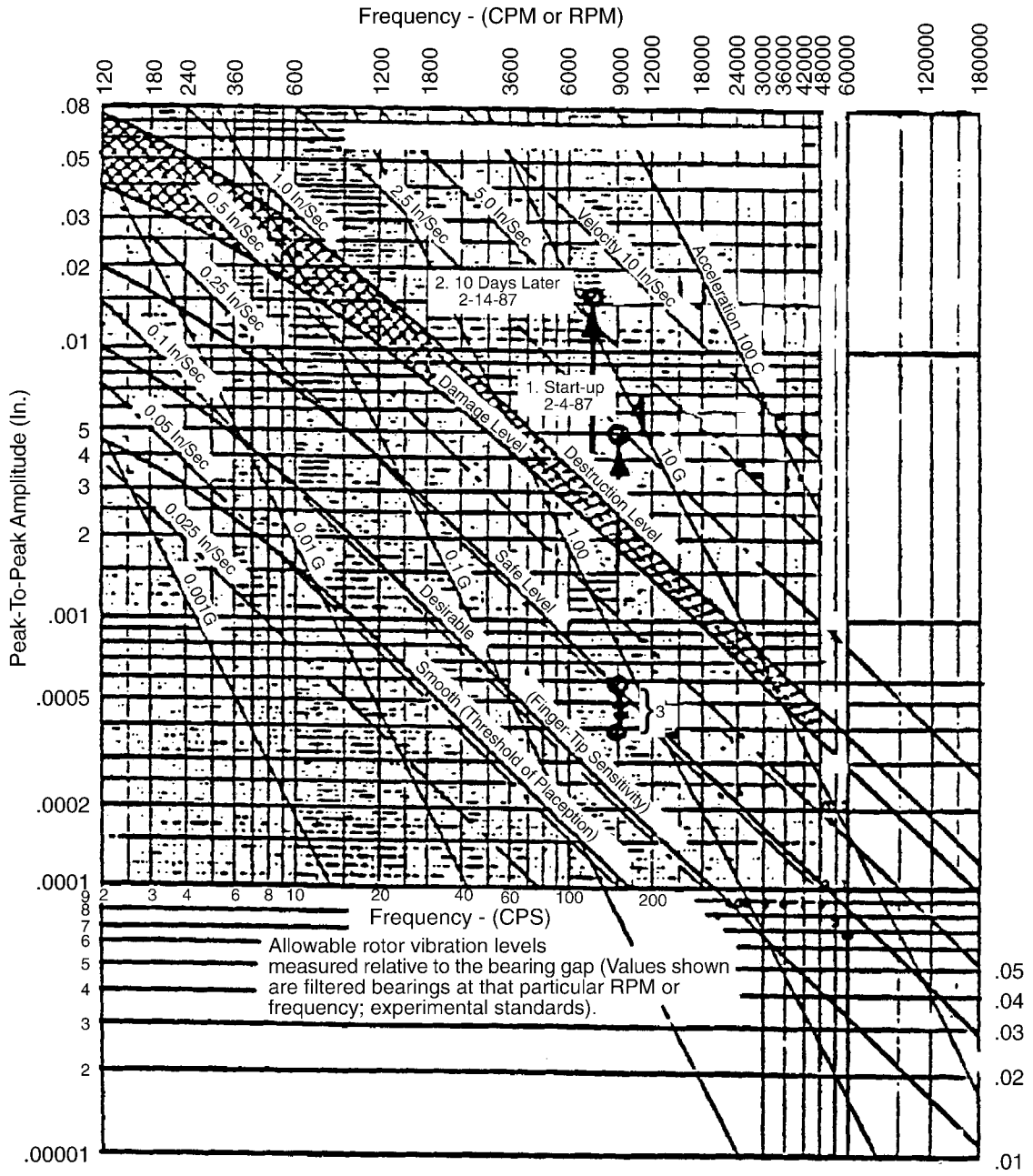

Figure 6-8
Vibration Amplitudes Before ERCO Modifications [2,4]

Dynamic balancing: MILSPEC 167 sets $U_{(Max)}$=4xW(lbs)/N(RPM)=(oz-in) as the maximum permissible unbalance. ERCO preference is U=1xW/N(Oz-In), which can be easily achieved on a hard bearing balancing machine. Balancing to the ERCO standard eliminates one possible dispute when trying to determine the root cause of the vibration.

Combination Examples

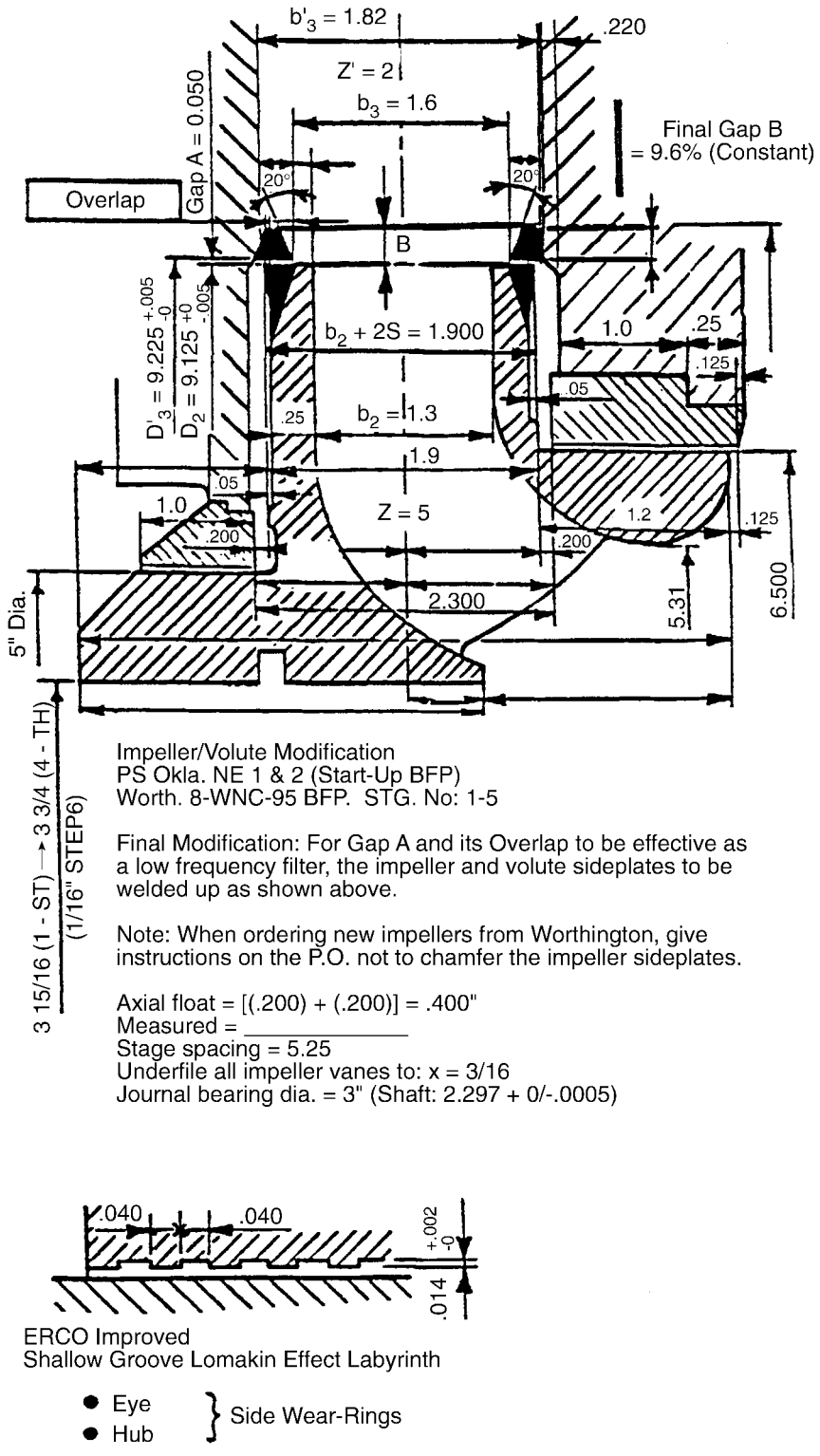

Figure 6-9
Impeller/Volute Modification of the Startup BFP

7
VANE PASSING FREQUENCY AND ITS MULTIPLES IN HIGH-ENERGY-INPUT CENTRIFUGAL PUMPS

This section concentrates on preventing equipment damage from vibration frequencies associated with vane passing and its multiples, or frequencies 6 and 7 in Figure 3-1 in new designs, or correcting it in existing applications. Over 20 years, field modifications were performed and design technology developed by ERCO to optimize the impeller-to-diffuser geometry. Before and after tests in the field, on the test stand, and in the laboratory proved that the geometry can be optimized to eliminate or minimize the effect of vane passing frequencies. After the geometry was optimized and the vane passing frequency still persisted, there remained a puzzling occurrence and only in later years was it related to acoustic responses. The effects of acoustic vibration and the role it plays in exciting the rotor and pump structure is technology that can now be applied to field problems.

The root causes of vane passing frequencies and its multiples have been assembled based on past experiences. Refer to Figure 3-1 when reviewing the list:

1. Tight radial gap (internationally called Gap B) between the impeller and diffuser vanes, giving rise to a hydraulic shock at the vane passing frequency or its multiples, as shown in Figure 7-1.

2. An unfavorable geometry between the impeller sideplate OD and the diffuser sideplate ID (internationally called Gap A). This geometry has a very strong influence on almost all vibration and pressure pulsation components, particularly in the low flow operating range (that is, below approximately 70% of BEP) as shown in Figure 1-6 and in Figure 8-10.

3. An unfavorable impeller-diffuser vane number combination (see Figures 7-1 and 7-2):
   - An even number of impeller and diffuser vanes (such as 4-2, 6-2, 6-8, 6-12, giving rise to high shock forces resulting from vane-to-vane pressure waves at vane passing frequency as shown in Figure 7-1. This is a pressure shock wave and not acoustic resonance as referred to in Figure 7-2.
   - A multiple combination of impeller and diffuser vanes (such as 6-9, 5-10, 4-8, giving rise to a strong force with vane passing and/or multiples of vane passing frequency. The same principle applies to this as described above (not an acoustic resonance phenomenon).
   - The diffuser vane number is one less than twice the number of impeller vanes (such as 5-9, 6-11, 7-13) giving rise to a strong force with 2 times (or other multiples of) the impeller vane passing frequency. This component is frequency-dependent, which

means speed; therefore, it is load-dependent (if a turbine or variable-speed drive). Examples are given in Figures 7-8 and 7-15. This is an acoustic resonance problem.

– The diffuser vane number is one more than the number of impeller vanes (such as 7 and 8) giving rise to strong pressure pulsation and vibration at vane passing frequency such as shown in Figures 7-12 to 7-14. Redesigning the impeller or the diffuser with a different vane number is the proper solution. Redesigning the diffuser is easier and much more economical. The lower parts of Figures 7-13 and 7-14 show the dramatic results achieved by changing the number of diffuser vanes from 8 to 12 for a large nuclear reactor feed pump. This is also an acoustic resonance problem (See Figure 7-2).

4. Axial misalignment between the impeller and diffuser, or impeller vane width greater than the diffuser vane width ($b_3/b_2 \leq 1$), giving rise to several vibration frequencies (vane passing, synchronous as well as subsynchronous components). Such geometry is shown in Figures 8-11 and 11-6 and labeled as incorrect.

5. A bad combination of Gap A and Gap B. This can be disastrous in all flow ranges, but particularly in the low flow operating range.

6. Loose internal components, allowing vibration components at various frequencies to develop. Such an example is shown in Figure 7-7 where the 3 times and 4 times vane passing was excited when internals of that three-stage high-speed boiler feed pump were loose in the barrel. The components were greatly reduced after the looseness was eliminated.

If there is an acoustic resonance or natural frequency at a specific, troublesome frequency, the problem will be much more pronounced, and it will be frequency-dependent; therefore, it will be speed- and load-dependent for a turbine-driven pump. Other frequent acoustic or mechanical resonance causes can be:

7. Acoustic resonance of the cross-over channel in a pump with opposed impellers as shown in Figure 7-16. The cross-over channel length should be measured as shown in Figure 7-17. The length, hence the resonance frequency, depends on the pump frame size, the number of stages, and whether the pump has a kicker stage in the middle of the rotor for the desuperheater.

8. Acoustic resonance of other internal hydraulic channels (other than impeller and diffuser, as discussed in item 3 above).

9. Impeller structural resonance. An example is given in Figure 7-5 using a Campbell diagram.

10. Bearing or seal housing resonance excited by the vane passing (or multiples of vane passing) frequency as shown as in Figure 7-16.

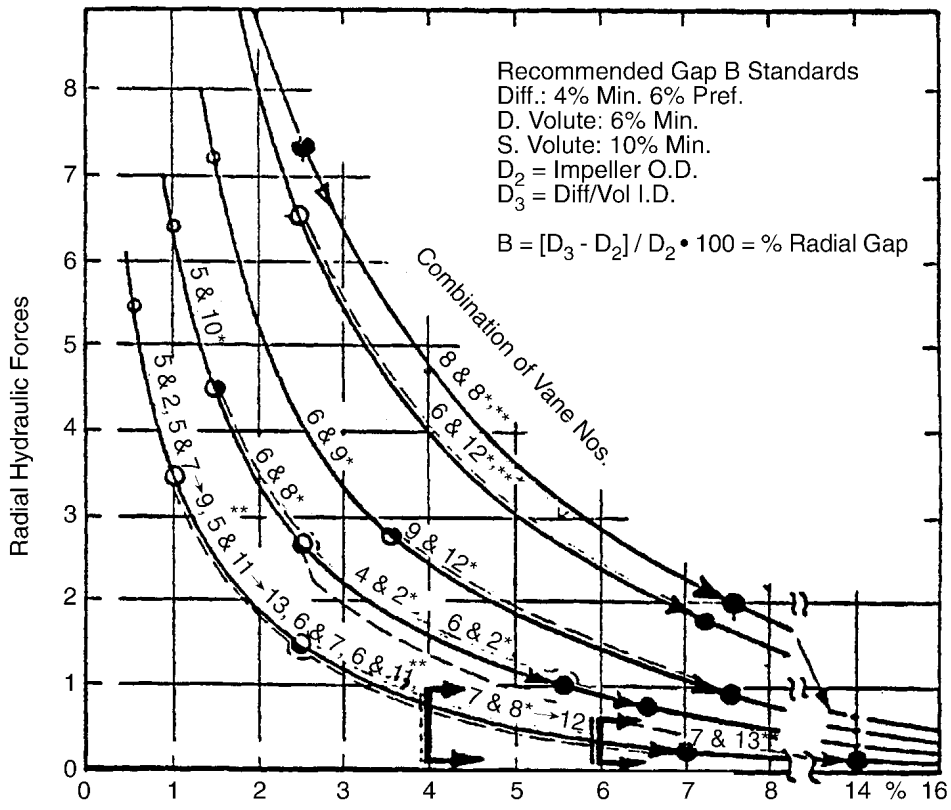

* Branded as "Bad" combinations in general.

*,** Such vane combinations are not permitted for high-energy-input (such as BFP) pump designs for troublefree operation in power plant applications.

○ "Bad" vane combination may require large Gap B or design change of vane number combination.

● This table does not apply to harmonics of vane passing and/or to cases when the source of origin is acoustical.

Figure 7-1
Impeller/Diffuser Combination Chart. Dominant Pressure Pulsation Due to Impeller-to-Diffuser/Volute Vane Number Combinations.

		Number of Impeller Vanes/Vane Pass Frequency Multiples																			
DIFFUSER VANES and ORDER		3	2nd	3rd	4th	4	2nd	3rd	4th	5	2nd	3rd	4th	6	2nd	3rd	4th	7	2nd	3rd	4th
	2	1				2															
	2nd	1	2			0				1				2							
	3rd		0			2	2			1				0				1			
	4th		2				0				2			2				1			
	8		2	1			0				2			2				1			
	2nd								0			1				2			2		
	3rd																0				
	4th																				
	9			0			1				1							2			
	2nd								2				2			0					
	3rd																				1
	4th																				
	10			1	2		2	2			0				2						
	2nd												0			2				1	
	3rd																				2
	4th																				
	11			2	1			1			1				1						
	2nd												2				2			1	
	3rd																				
	4th																				
	12				0			0			2				0				2		
	2nd																0				
	3rd																				
	4th																				
	13				1			1				2			1				1		
	2nd																2				2
	3rd																				
	4th																				

Z_2 (Z_3) = # Impeller (Diffuser/Volute) Vanes, K = 1, 2, 3, 4, etc.
P_2 (P_3) = K x Z_2 (Z_3)

If M = 0 Strong pressure pulsation is expected. It can excite any part of the system, such as casing, piping, control system, etc. If strong enough, it can be picked up as rotor vibration.

If M = 1 Rotor radial vibration is expected.

If M = 2 Rotor resonance at the natural frequency of the rotor is expected.

If M • 3 Generally of little consequence.

Figure 7-2
Impeller/Diffuser Combination Chart. Calculated Predominant Pressure Pulsation Frequencies Due to Impeller-to-Vane Combinations.

The main objective of this discussion is to explain and especially to simplify this otherwise very complex phenomenon. If it occurs, how to:

- Recognize the phenomenon
- Clarify if it is hydraulic shock caused by Gap B's being too tight or if it is an acoustical problem.
- Find the appropriate, most effective, and most economical solution.
- Implement the solution and prove that the modification was successful.
- Determine the natural frequencies of the rotor or other components, such as bearing housing and seal housing.

Some significant and often reported cases are:

- Grand Coulee Pumping Plant, 1951 [49, 50, 51].
- Palo Verde Nuclear Plant primary coolant pumps, 1983
- Havasu Pumping Plant, transfer pumps, 1990 [39]
- Numerous other cases where the author was involved between 1965 and 1995

ERCO collected field data on this and related subjects for almost three decades from many power stations and other applications as well as from laboratory measurements. Their appearance, type of damage, how to recognize, how to explain, and most important, how to troubleshoot and correct the damage were stored systematically on ERCO files and serve as the basis of the discussions to follow.

Variation of radial forces/pressure pulsation with Gap B as a function of impeller/diffuser or volute vane number combination.

Vane interaction: Pressure pulsation is intensified if multiples of impeller vane numbers are equal to the number of diffuser vanes or differ by one (such as 5-9, 6-11, or 7-13).

7.1 Gap B

Gap B refers to the distance between the impeller vane exit and the diffuser vane inlet (or volute tongue) and is normally expressed as the percentage of the impeller radius. Gap B generates vibration amplitudes at the vane passing frequency and its multiples. A tight Gap B (for example, less than 6%) results in shock waves being generated each time an impeller vane passes a diffuser vane. Because of the finite thickness of the vanes at the impeller exit and the formation of a boundary layer adjacent to each impeller vane, a pressure wake originates that is interrupted as the vane passes each diffuser/volute vane. The interaction between the wake and the diffuser creates a dynamic force that can be particularly great at part-load conditions. The magnitude of the force is a function of the gap between the impeller exit and diffuser inlet. The variation of this force is a function of the percent gap, or Gap B, and is also responsible for the noise generated within a pump. The frequency of the force depends on the number of impeller vanes times RPM or multiples of this number.

The shock wave and pressure pulsations can be so great that the diffuser inlet vanes will fail in fatigue (Figure 7-3) or the pump flow control system can become unstable (Figure 10-4). The larger the gap, the longer the free unguided flow path of the liquid becomes, which increases the possibility for the flow to find a more favorable (that is, shockless) path into the diffuser, especially under conditions of high incidence angles that occur at reduced capacities. An example is given in Figure 7-3 when in addition to the diffuser tip breakage, flow induced incidence angle caused stall resulted in major cavitation damage ultimately breaking off the diffuser inlet tips. Figure 7-3 is an important of an actual failed diffuser. The proper Gap B is highly dependent on the impeller and diffuser vane combination, which in some cases has resulted in increasing the clearance from 2% to greater than 20%. It is interesting to note that, contrary to classical thinking [2], the efficiency of the pump is not reduced and in most cases is improved when a proper Gap B modification is performed. Many examples are given below and in Reference 1.

For a high-energy-input pump, such as a modern BFP, the gap must not be less than a certain minimum value to minimize the hydrodynamic forces. A smaller gap can induce forces that:

- Fracture components such as diffuser vane tips (see Figure 7-3), impeller sideplates (see Figure 12-9), and diffuser retaining bolts
- Cause failures of many other minor or major components internal and external to the pump
- May also introduce severe flow instability problems to the feedwater system such as a reactor water level control problem for a BWR nuclear unit

In previous EPRI publications, a 3% minimum gap was recommended for reasonable operation. Later publications called for at least 4%, but preferably 6% or more. Now much greater gaps are being recommended, depending on the impeller-to-diffuser vane combination.

In conclusion, when Gap B is incorrect, especially if it is too small, and the energy input into a pump stage is high, the pump generates excessive:

- Noise levels (at vane passing frequency or its multiple).
- Pressure pulsations (at vane passing frequency or at its multiples) that propagate through the feedwater system at the speed of sound and can give the impression that it originated at a place other than the pump hydraulics.
- Vibration amplitudes that (if strong enough) can be picked up anywhere in the feedwater system. This can be the root cause of many major and minor failures (shaft breakage, impeller disintegration, pipe vibration and breakage, seal injection line fatiguing, and nuclear reactor water-level malfunctioning).

Our statistically collected data clearly prove that boiler feed pumps do not have to be noisy. However, Gap B has to have optimum dimensions for the given design and application. In general, a 4% absolute minimum, 6% preferred, is quoted [1, 2, 4, 5, and 11], but the magnitude of Gap B really has to be evaluated for each feed pump that generates more noise or various modes of failures than desired.

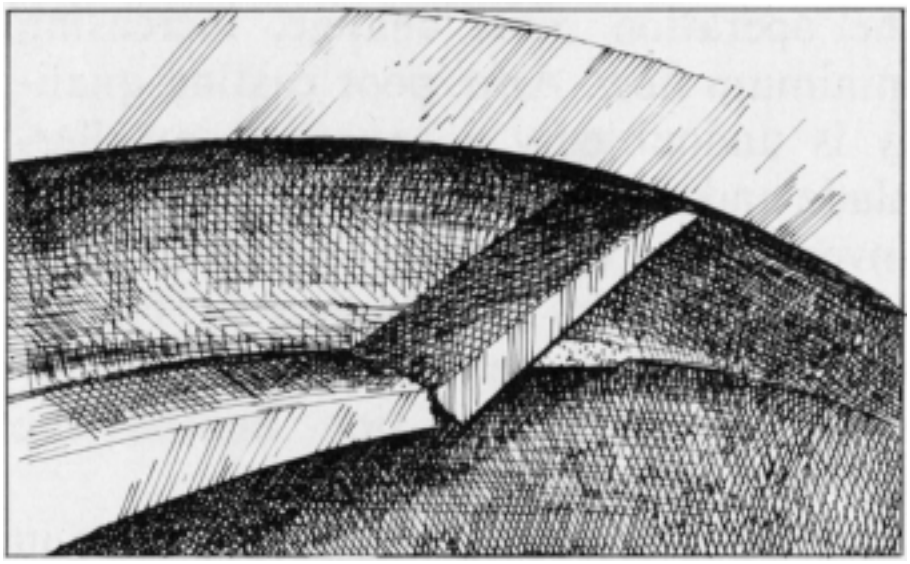

Figure 7-3
Broken Diffuser Vane Inlet Tips - Small Radial Gap B (1%), Hydraulic Instability at Low Flow, and Stall at the Diffuser Inlet

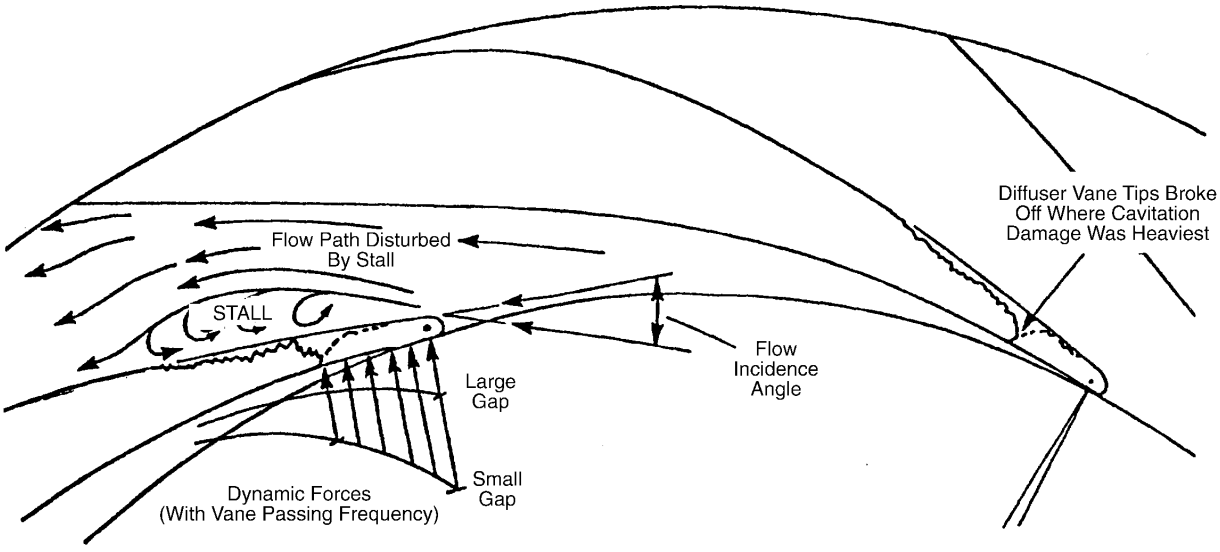

Origin of Failure Mechanism:

Flow Incidence Angle Induced Stall

Development of stall, cavitation damage, and diffuser inlet tip failure of a first-stage boiler feed pump vaned diffuser. Several identical failures in various power stations. No failure or damage since the diffuser tips were cut back to the point of breakage. Elimination of stall substantially improved pump efficiency. This drawing was made as an imprint from the actual diffuser.

Figure 7-4
Flow Incidence Angle Induced Stall Resulting in Cavitation and Mechanical Damage of Diffuser Vane Inlet Tips

7.2 Gap A

Gap A refers to the radial distance between the impeller sideplate OD and the diffuser sideplate ID and is discussed extensively in Section 8.

7.3 Interaction Between Gaps A and B and the Overlap

Gap A, its Overlap ratio, and Gap B are involved in fluid mechanical actions in the area between the impeller exit and diffuser inlet; therefore, these geometries cannot be considered independently. The interaction of these geometries is very strong and distinct, and the results apply equally to diffuser and volute pumps. The design range for effective application of Gap A and its Overlap is limited by the specific speed and suction-specific speed of high-energy-input utility pumps. The effectiveness of Gap B applies to any centrifugal pump design and to all N_S and S_S values used in utility pumps.

The combination "fix" for boiler feed pumps and other high-energy-input pumps has become a powerful design modification to eliminate failures and to control various system problems that were previously not connected to pump component design. This has also proven to be the least expensive modification in most instances. Rotors with fundamental hydraulic design deficiencies often require frequent overhauls caused by failures, or they are high maintenance components. With a small additional effort during overhauls or rebuilds, corrective modifications can be performed to eliminate the root cause of the problem and improve equipment reliability. Performing an overhaul without correcting the design deficiencies leaves the potential for continued failures and unnecessary maintenance.

7.4 Vane Number Combination

The subject of pump blade pass frequencies and their multiples is complex due to the number of variables that affect their occurrence and their strength. The dynamic components of the forces generated have not been widely studied because the energies at the higher frequencies were not believed to be significant or to have an impact on the reliable operation of the pump and system. The high-energy-input pumps of the utility industry forced a reevaluation of this position. The understanding of this technology should provide significant insight into the troubleshooting of pump operating problems and providing or identifying designs that provide trouble-free operation.

The hydrodynamic phenomenon of vane passing frequencies comes from a rotating component (such as the impeller vane tip at the exit) passing by a stationary item (such as diffuser or volute vane inlet tip) resulting in a shock or pressure wave. Its strength at the point of the shock initiation depends mainly on the distance between the stationary and rotating vanes (called Gap B). The larger the gap, the weaker the generated shock for a given flow velocity and capacity. This phenomenon is well documented [1] and is well understood.

The impeller and diffuser vane combination is extremely important when evaluating the proper Gap B. Figure 7-1 shows the relationship between the vane combinations and the proper Gap B. It can be seen, for example, that a 5 and 2 vane combination with a Gap B of approximately 3%

and a 6 and 9 vane combination with a Gap B of approximately 7.5% produce basically the same radial hydraulic forces.

As a last resort and in extreme cases, the only way to correct a bad vane combination may be to change the combination. In a diffuser-style pump, either the diffuser or the impeller can be changed; however, changing the diffuser usually is the preferred option due to the expense and performance uncertainties of new impeller castings. In choosing a different number of diffuser vanes, care should be taken to select a number that will not create new or additional problems. For example, if the diffuser vane number chosen is one less than twice the number of impeller vanes, a troublesome acoustic vibration at 2 times vane pass could develop as discussed later in this section. The only option for changing the vane combination of a volute-style pump may be to change the number of impeller vanes because the number of volute vanes is fixed in the casing. Finally, choosing a new vane combination should include reviewing the natural frequencies of pump attachments, such as bearing housings and seal or lube piping. If the natural frequency of these components corresponds to the new blade pass frequency, high vibration could remain as a problem, just at a different frequency, due to the resonance frequency of the attached components being excited. For typical examples, see Figures 7-5 and 7-16.

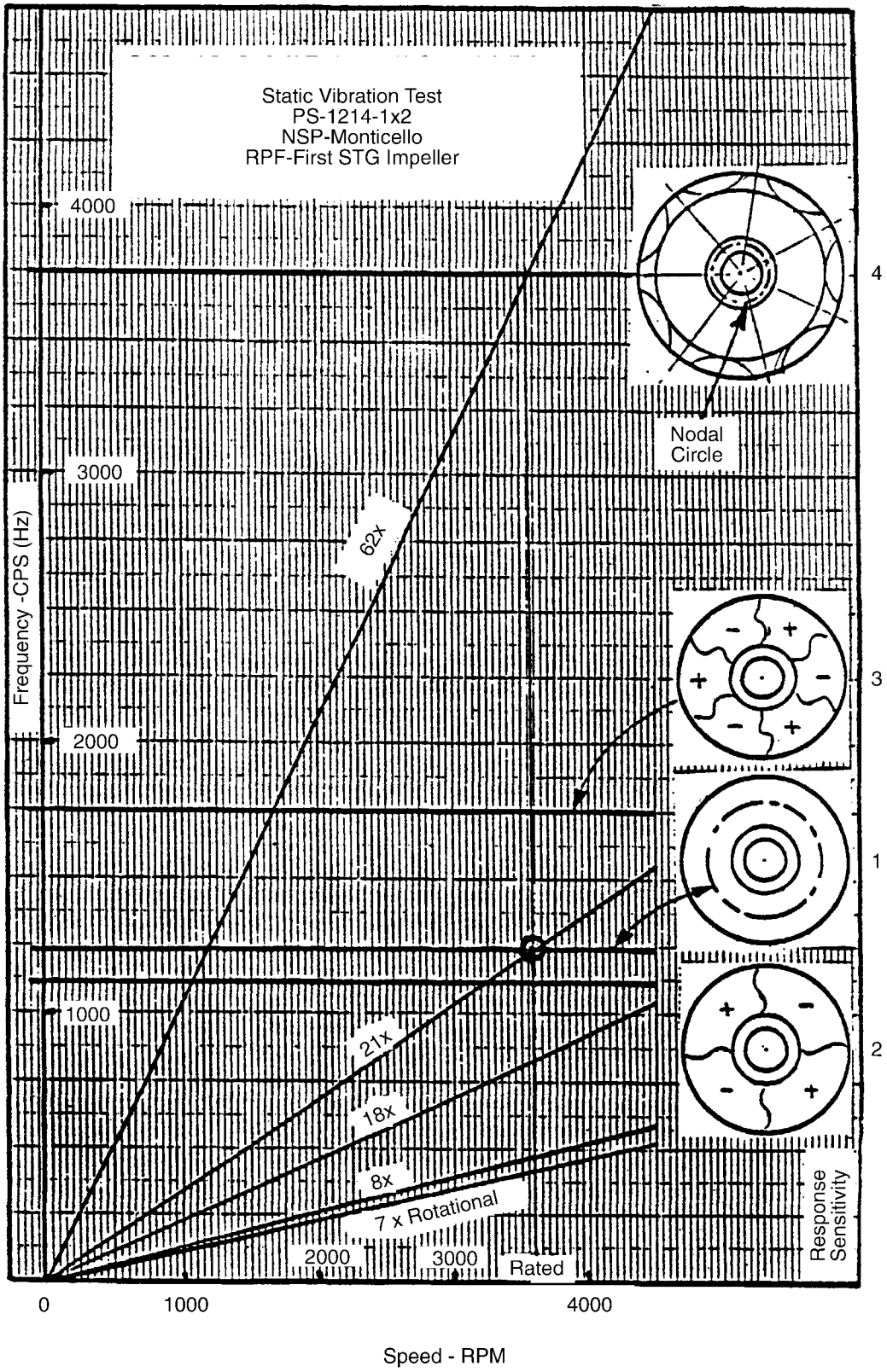

Figure 7-5
Campbell Diagram of Seven-Vane Impeller

The upper harmonic vibrations or pressure pulsations, and many times the vane passing component, are acoustical, that is, pressure waves generated at different points and at different times, which strengthen or cancel each other, creating harmonics of the original frequency. After a shock has been created, its strength can be magnified due to the geometry of the diffuser or volute vanes and passages. Many times, multiples of the vane pass frequency appear with larger amplitudes than at vane passing. Harmonics of concern usually are limited to two, three, or four times the vane passing frequencies, since above the fourth harmonic sufficient energy to damage the pump or the feedwater system components usually does not exist. Parameters that control this acoustical phenomenon can be:

- Speed of sound (pressure waves in the liquid travel with that speed)
- Tip speed of the impeller (determining phase velocity)
- Geometry of flow channels
- Vane number combination (periodicity)
- Gap B (determining the strength of the initial shock wave) combined and optimized with Gap A

Professor Den Hartog published a most convincing and thorough paper in the *Journal of ASME* [37] that went unnoticed or was forgotten until a research project on the Hitachi pumps at the Havasu pumping station forced a reactivation of the subject. The impeller-to-diffuser vane combination (7 and 13) of the Havasu pumps developed an unusually strong 14 x RPM (that is, 2 times vane passing) vibration component that produced the "singing rock wall" at the pumping station. It was determined that the geometry of the volute casing (note that this pump had a diffuser in a single volute discharge casing) in combination of the rotating speed with the pump and the vane combination, matched perfectly to amplify the 2 times vane passing vibration.

In most of the cases, enlarging Gap B should eliminate or substantially reduce the vane passing amplitudes. However, a hydraulic channel geometry can be so sensitive that the smallest amount of hydraulic disturbance can be amplified into major harmonic vibration or pressure pulsation components. These major harmonic components give rise to very large excitation forces that can damage plant components far away from the origin of the shock waves. On the other hand, there are cases where all the ingredients are present to have a bad case, but the impeller tip speed is far away from the threshold area and no problems occur due to acoustic resonance in those hydraulic channels.

The tabulation described in Figure 7-6 [18] can be used to predict potentially harmful vane pass frequencies and their harmonics for a given blade combination. The tabulation was developed based on the velocity-pressure field interactions between the rotating impeller and stationary diffuser vanes. This interaction was reduced to its components of the Fourier series, resulting in the periodicity and phase velocity relationships. Several impeller and diffuser vane combinations with known vibration or pressure pulsation characteristics have been used by ERCO to test the usefulness of the tabulation. This tabulation can be a very useful tool during field troubleshooting. If nothing else, this tabulation provides the frequency range for field troubleshooting and vibration analysis. In one case, the tabulation identified the rotor critical speed (Figure 7-7). This is a nice substitute for otherwise expensive and not always reliable calculation methods or other techniques such as bump tests and shaker tests where the rotor is at

zero speed. The rotor critical speed identified as a result of the tabulation includes the influence or spring and damping coefficients of journal bearings, seals, etc., and hence provides a more accurate location for the rotor critical speed.

	Periodicity				**Phase Velocity**			
	P_{I1}	P_{I2}	P_{I3}	P_{I4}	Ph_1	Ph_2	Ph_3	Ph_4
P_{D1}	m_{11}	m_{21}	m_{31}	m_{41}	C_{11}	C_{21}	C_{31}	C_{41}
P_{D2}	m_{12}	m_{22}	m_{32}	m_{42}	C_{12}	C_{22}	C_{32}	C_{42}
P_{D3}	m_{13}	m_{23}	m_{33}	m_{43}	C_{13}	C_{23}	C_{33}	C_{43}
P_{D4}	m_{14}	m_{24}	m_{34}	m_{44}	C_{14}	C_{24}	C_{34}	C_{44}

P_{IN} = Impeller vane pass harmonics = No. impeller vanes x N N = 1, 2, 3, 4

P_{DM} = Diffuser vane pass harmonics = No. diffuser vanes x M M = 1, 2, 3, 4

m_{NM} = Periodicity magnitude = $|P_{IN} - P_{DM}|$
(Note: List values of 0, 1, or 2 only)

Ph_N = Phase velocity harmonic (Same as impeller vane pass harmonic)

C_{NM} = Phase velocity magnitude = m_{NM} / P_{IN}

The periodicity for the various combinations of impeller and diffuser vanes and harmonics should be calculated:

If $m_{NM} = 0$ Strong pressure pulsation is expected. It can excite any part of the system, such as casing piping, control system, etc. If strong enough, it can be picked up as rotor vibration.

If $m_{NM} = 1$ Rotor vibration is expected.

If $m_{NM} = 2$ Rotor resonance at the natural frequency of the rotor is expected.

If $m_{NM} \geq 3$ Generally of little consequence.

Note: Only periodicity values of 0, 1, and 2 should be placed in the tabulation, since these will identify the vane pass frequencies of interest.

Calculation of the phase velocities for the periodicities of interest are performed to obtain a feel for the strength of the corresponding impeller vane pass frequency.

Figure 7-6
Tabulation to Predict Potentially Harmful Vane Pass Frequencies and Their Harmonics

7.4.1 6 and 8 VANE COMBINATION: HL & P - CEDAR BAYOU NO. 5 BFP Type 3BB1I512

Table 7-1
Running Speed vs. Periodicity and Phase Velocity (6 and 8 Vane Combination)

	PERIODICITY				PHASE VELOCITY			
	6	12	18	24	1	2	3	4
8	2	-	-	-	3	-	-	-
16	-	-	2	-	-	-	9	-
24	-	-	-	0	-	-	-	00
32	-	-	-	-	-	-	-	-

The tabulation identifies three vane passing frequencies of concern:

- 1 times (6 times running speed - N)
- 3 times (18N)
- 4 times (24N)

The periodicity value of m = 2 for the 1 and 3 times vane passing frequencies identifies rotor resonance as a potential problem, but the greatest potential for a problem occurs at the 3 times vane passing frequency due to the higher phase velocity. The periodicity of m = 0 for the 4 times vane passing frequency identifies a potential for strong pressure pulsations, particularly if Gap B is tight.

Field vibration data, measured in velocity (in/sec), was taken in the radial direction at the pump outboard bearing. They are shown in Table 7-2 below and in Figure 7-7.

Table 7-2
Field Vibration Data (Measured in Velocity)

RPM	1N	6N	12N	18N	24N
5370	.24	.03	.00	.10	.24
4932	.40	.15	.00	.60	.10
4880	.25	.06	.05	.50	.05
4791	.24	.04	.00	.00	.25

The 1N (pump running speed) and 24N (4 times vane passing) frequencies had the dominant vibration amplitudes at 4791 and 5370 RPM, while the 18N (3 times vane passing) frequency had the dominant amplitude at 4880 and 4932 RPM. In fact, the 18N component at 4932 RPM was 2.5 times the largest 1N and 24N component at any running speed.

An investigation was performed to determine the root cause of the high vibration at the different frequencies. It was determined by calculation that the rotor first critical speed was approximately 4900 RPM. Rotor inspection found that Gap B was 1.5% and that internal looseness existed in the rotor. Gap B was increased to 6.2% (reducing radial hydraulic forces by a factor of six as can be seen in Figure 7-1), and the internal rotor looseness was corrected. Also, the rotor was dynamically balanced to the ERCO standard (U=1W/N) to minimize the possibility of exciting the rotor first lateral critical speed. During subsequent testing, the vibration amplitudes remained below 0.1 in / sec, at all loads, speeds, and vane passing frequencies and were not able to excite the critical speed to any visible degree.

This case demonstrates that vibration at the vane passing frequency or its multiples is clearly a function of the forces or pressure pulsations generated by the impeller and diffuser interaction and that a tight Gap B can produce the forces necessary to excite these frequencies, including a rotor critical speed.

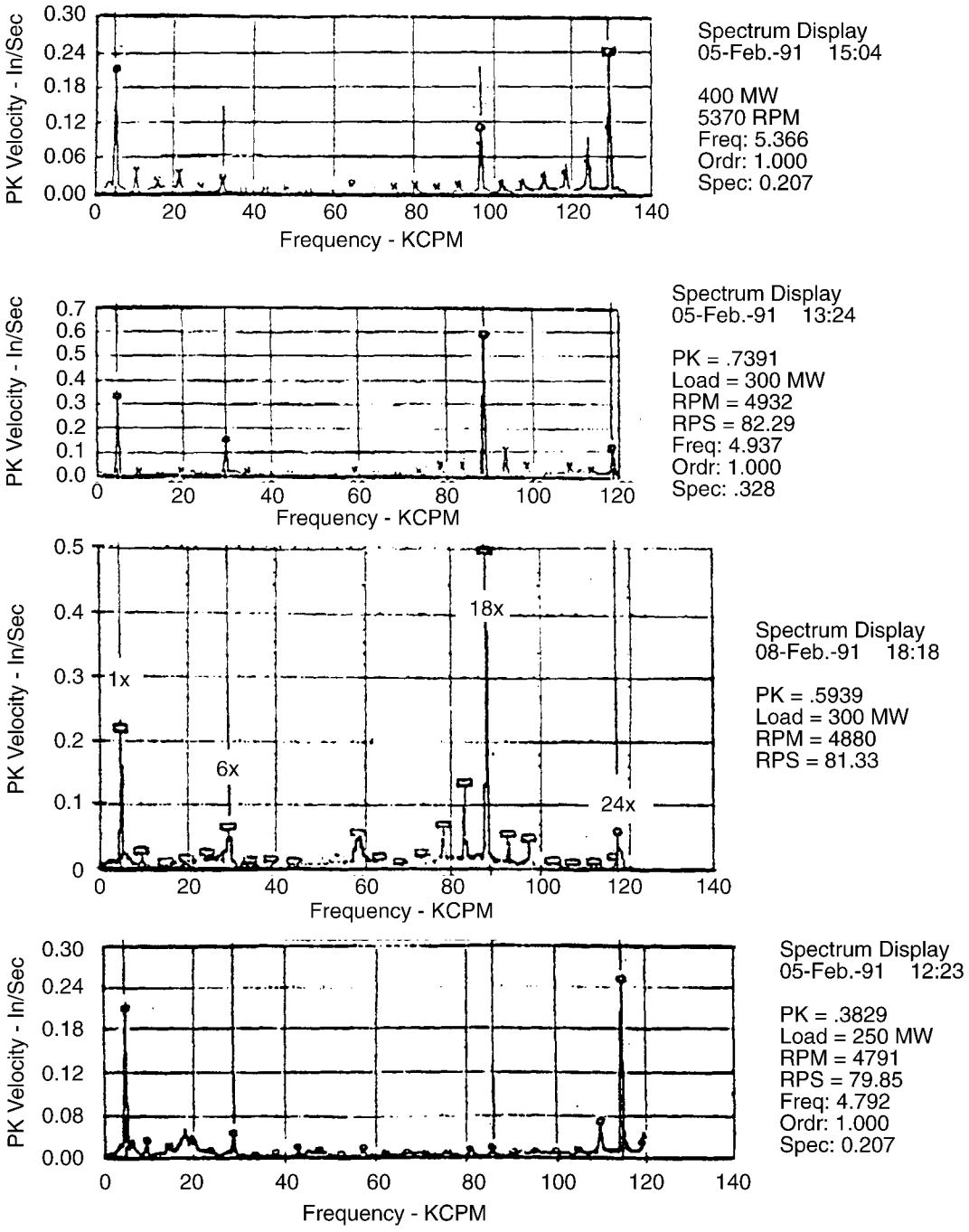

X = Operating speed of pump (RPM or RPS)
V = 6x = Impeller vane passing freq. (CPM or CPS)
V, 3V, and 4V are speed, flow, therefore load (MW) dependent frequencies for this particular case

Figure 7-7
Vibration Spectra from a Type 3BB1I512 Pump Showing Change in 3 and 4 Times Vane Passing Frequency Vibration With Speed

7.4.2 7 and 13 Vane Combination: Central Arizona-Havasu Station Hatachi Single-Stage, Single-Suction Vertical Pump

Table 7-3 identifies two vane passing frequencies of concern: 2 times (14N) and 4 times (28N). In this case, the pump experienced a strong 2 times vane passing frequency, as shown in Figure 7-8 and as would be expected by m = 1 in the tabulation. Vibration or pressure pulsations at 4 times vane passing frequency was not evident, but with m = 2 (that is, rotor resonance) and the pump being constant speed, it would not be expected.

Table 7-3
Running Speed vs. Periodicity and Phase Velocity (7 and 13 Vane Combination)

	PERIODICITY				PHASE VELOCITY			
	7	14	21	28	1	2	3	4
13	-	1	-	-	-	14	-	-
26	-	-	-	2	-	-	-	14
39	-	-	-	-	-	-	-	-
52	-	-	-	-	-	-	-	-

A series of tests was conducted to see how the pressure pulsation amplitudes at vane passing frequency developed and why extremely strong 2 times vane passing amplitudes evolved that make the 800-foot rock wall at the pump station resonate to that frequency. The pump has both a diffuser- and a volute-style casing. The tests were performed with various configurations of Gap A, Gap B, and diffuser inlet camber angles, as shown in Figures 7-9 and 7-10. It was determined that pressure pulsations generated at the impeller and diffuser interface increased in magnitude as they progressed through the volute and, again, the magnitude of the vibration was dependent on the force developed by the impeller and diffuser interaction strength of the force or pressure pulsation.

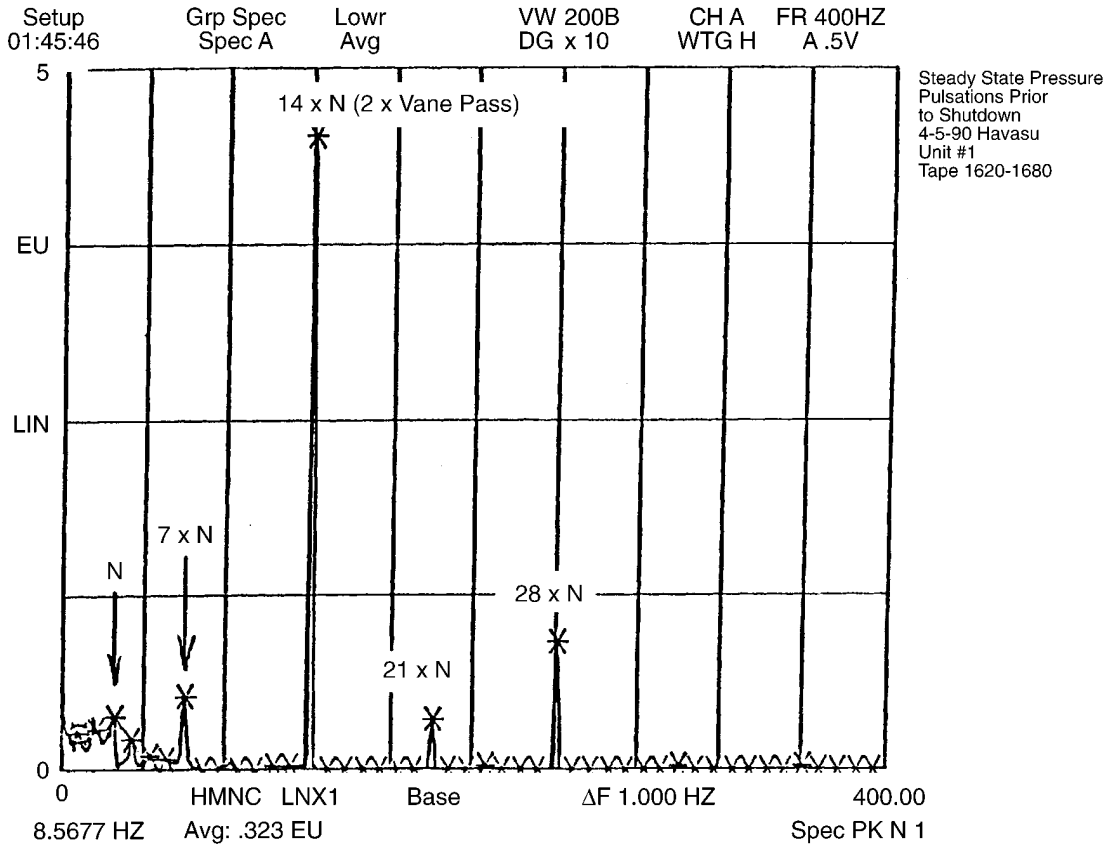

Figure 7-8
Vibration Spectrum From Havasu Station Showing Strong 2 Times Vane Passing Frequency Vibration

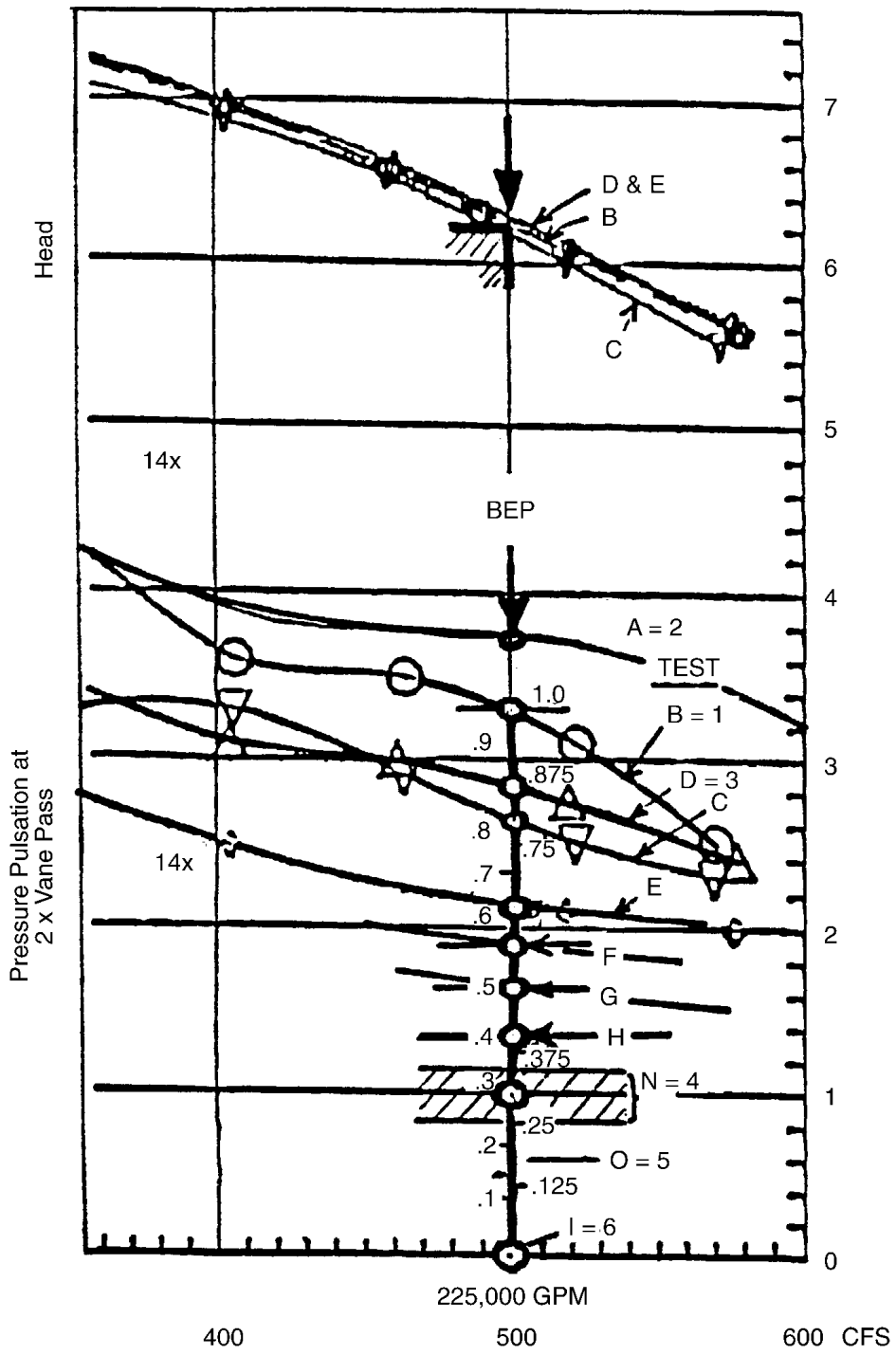

Figure 7-9
Reduction of Pressure Pulsations at 2 Times Vane Passing Frequency With Modifications to Diffuser Inlet

Changes made to the diffuser included:

- Gap A: Small (0.30 in.) vs. large (0.115 in.)
- Gap B: 2, 4, 5, 6, 12, and 30% (diffuser taken out)
- Diffuser vane inlet angle changed by under and over filing

These modifications changed the strength of pressure pulsation at 2 times vane passing frequency as shown in Figure 7-9. The pressure pulsation amplitudes are normalized for easy overview. Magnitude 1 is the present or original configuration of the pump. Magnitude zero is with the diffuser taken out:

- 1.0 (normalized) to 0.32 (B=2% to 12%)
- 1.0 (normalized) to 0.0 (B=2% to 30%, diffuser taken out)

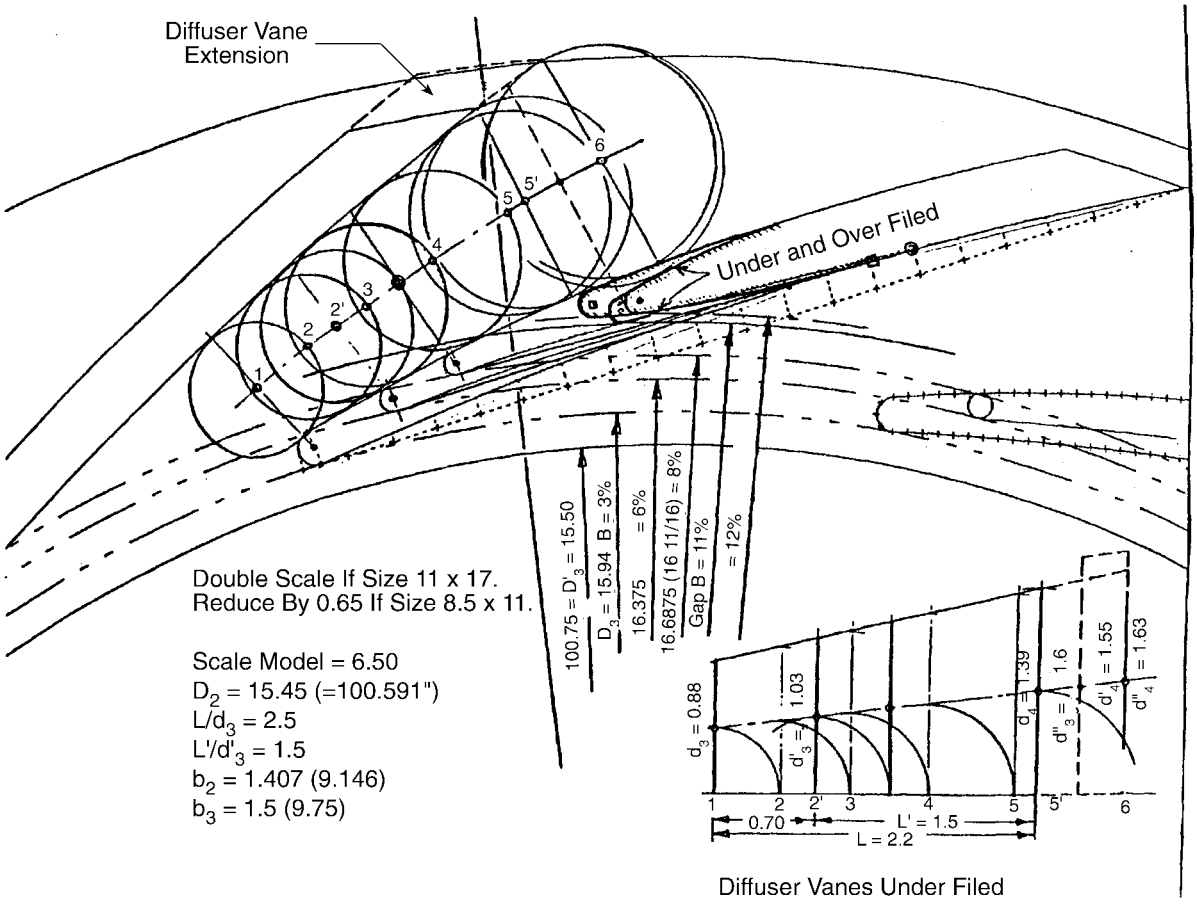

Figure 7-10
Modifications Performed at the Diffuser Inlet That Reduced Pressure Pulsations and Stabilized the Head Flow Curve

While performing the modifications to reduce the pressure pulsation amplitudes at 2 times vane passing frequency, it was observed that changes made which reduced pressure pulsations also had a stabilizing effect on the head-flow curve at low flows as can be seen in Figure 7-11. This supports previously published data showing that hydraulic and flow instabilities are a function of the geometry between the impeller exit and diffuser inlet, if vibration or pressure pulsations at the vane passing frequency and its multiples are observed.

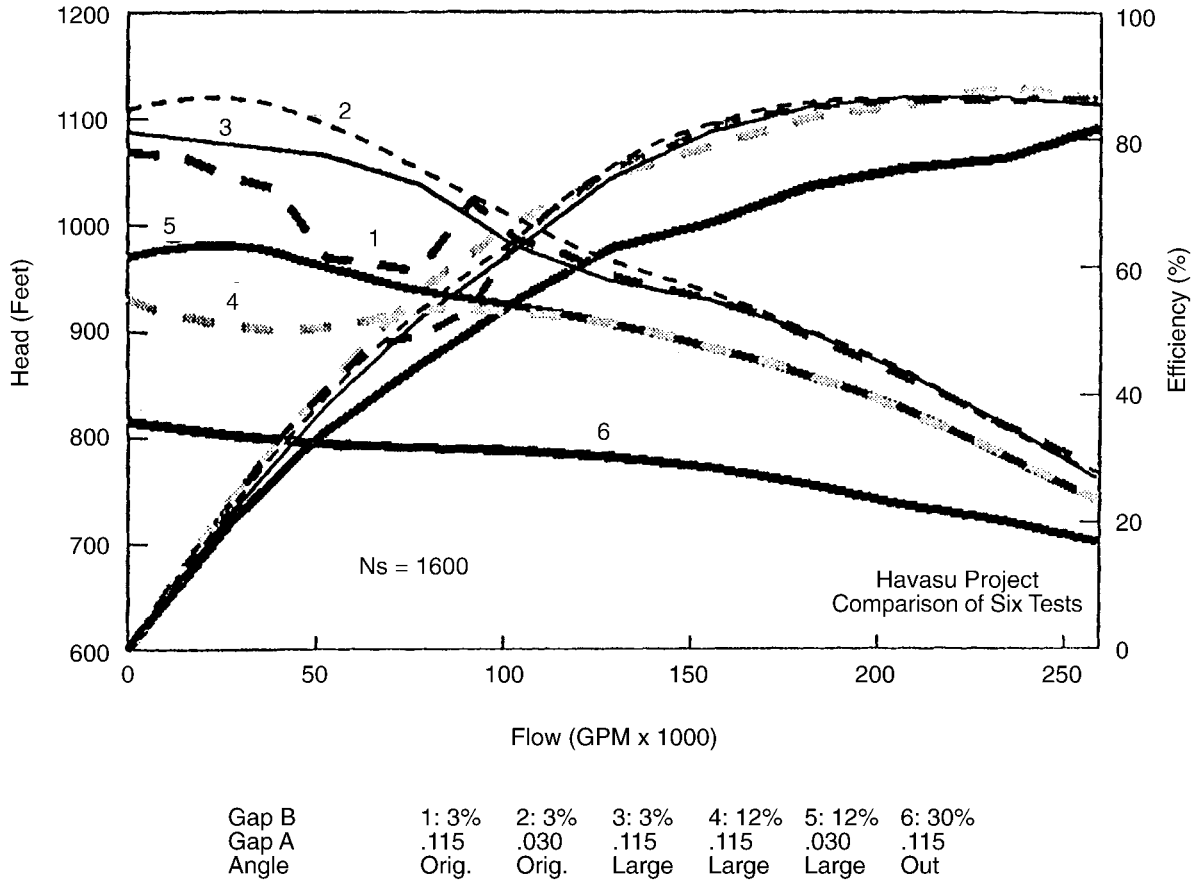

Figure 7-11
Head-Flow Curve Showing Stabilizing Affect of Modification to the Diffuser Inlet

7.4.3 7 and 8 Vane Combination: Nuclear Reactor and Boiler Feed Pumps BFP Frame Size 1BSXI516

Table 7-4
Running Speed vs. Periodicity and Phase Velocity (7 and 8 Vane Combination)

PERIODICITY					PHASE VELOCITY			
	7	14	21	28	1	2	3	4
8	1	-	-	-	7	-	-	-
16	-	2	-	-	-	7	-	-
24	-	-	-	-	-	-	-	-
32	-	-	-	-	-	-	-	-
	7	14	21	28	1	2	3	4
12	-	2	-	-	-	7	-	-
24	-	-	-	-	-	-	-	-
36	-	-	-	-	-	-	-	-
48	-	-	-	-	-	-	-	-

The 1BSX type nuclear feed pumps with a 7 and 8 vane combination experienced a high 1 times vane passing frequency vibration, as shown in Figure 7-12. The 1 times vane passing frequency would be expected based on m = 1 in the above tabulation. However, the high vibration persists even with Gap B increased to 25% (Note: In Figures 7-13 and 7-14, Gap B was 21%), indicating that the geometry of this pump was very sensitive to the forces or pressure pulsations generated by the impeller and diffuser interaction. It was determined that the vibration was the result of acoustic resonance in the diffuser channels, with a resonant frequency of some stationary components being excited by the vane passing frequency and its multiples. It is interesting to note that, with vibration amplitudes of .3 to over one inch/second experienced at vane passing frequency, only a very few major failures of these pumps have been reported. Most failures were minor, such as seal injection line and instrumentation line fatigue, bearing damage, seal damage, and internal bolt breakage.

The vane passing frequency vibration has been successfully eliminated at the Perry nuclear plant by replacing the 8-vane diffuser with a 12-vane diffuser as shown in Figures 7-13 and 7-14. As shown in the tabulation above, the 7- and 12-vane combination is a better combination than 7 and 8, because m=1 is eliminated at 1 times vane passing and m=2 exists only at 2 times vane passing frequency. The m=2 component at 2 times should not create a concern for the 7 and 12 combination since it also existed with the 7 and 8 combination without a problem. These rotors have a 4.5-inch shaft at the journal bearings and only a 4-foot bearing span; therefore, the rotor first critical speed would be above 6000 RPM. All these pumps are outfitted with pre-loaded tilting-pad-type journal bearings (with five shoes).

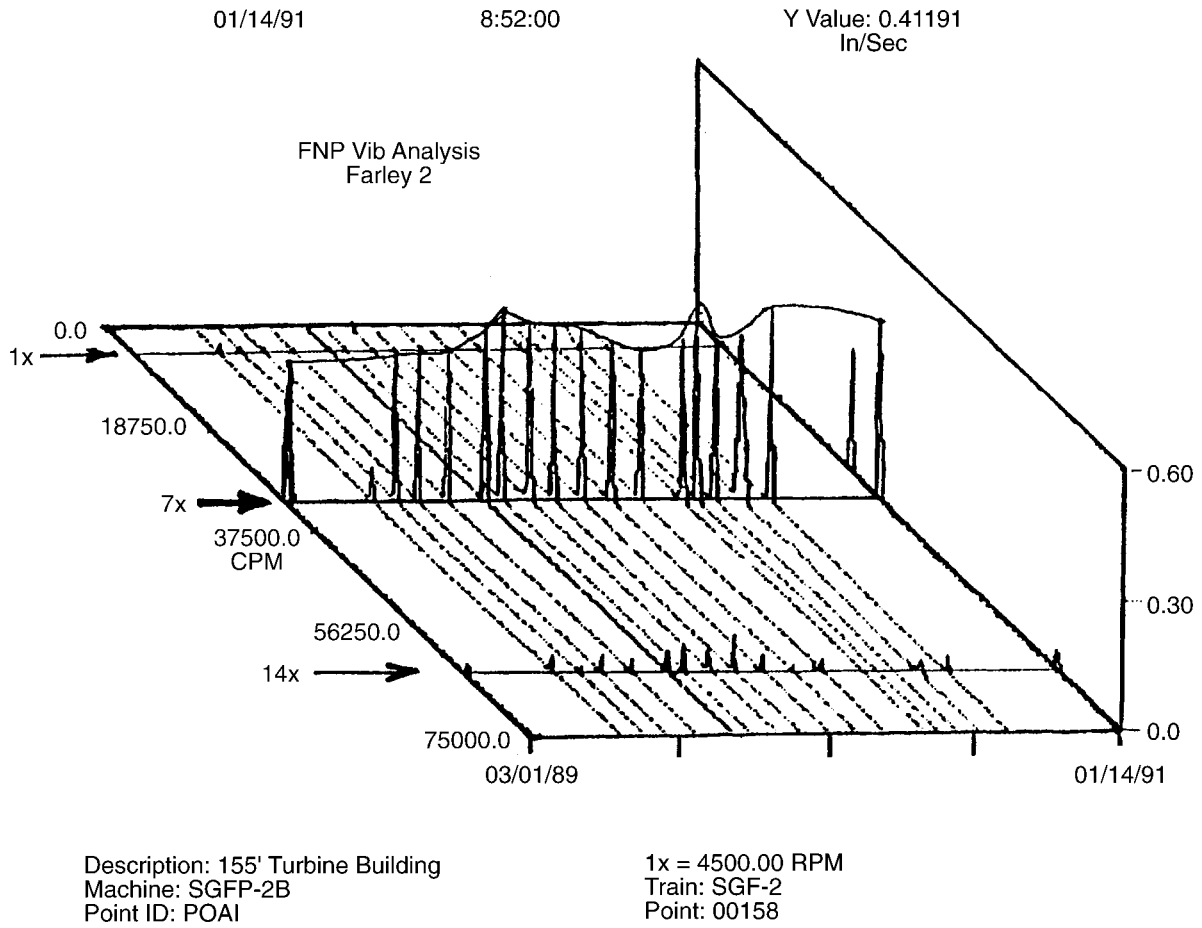

Figure 7-12
Vibration Spectrum for DeLaval 1BSXI516 With a Seven-Vane Impeller and Eight-Vane Diffuser

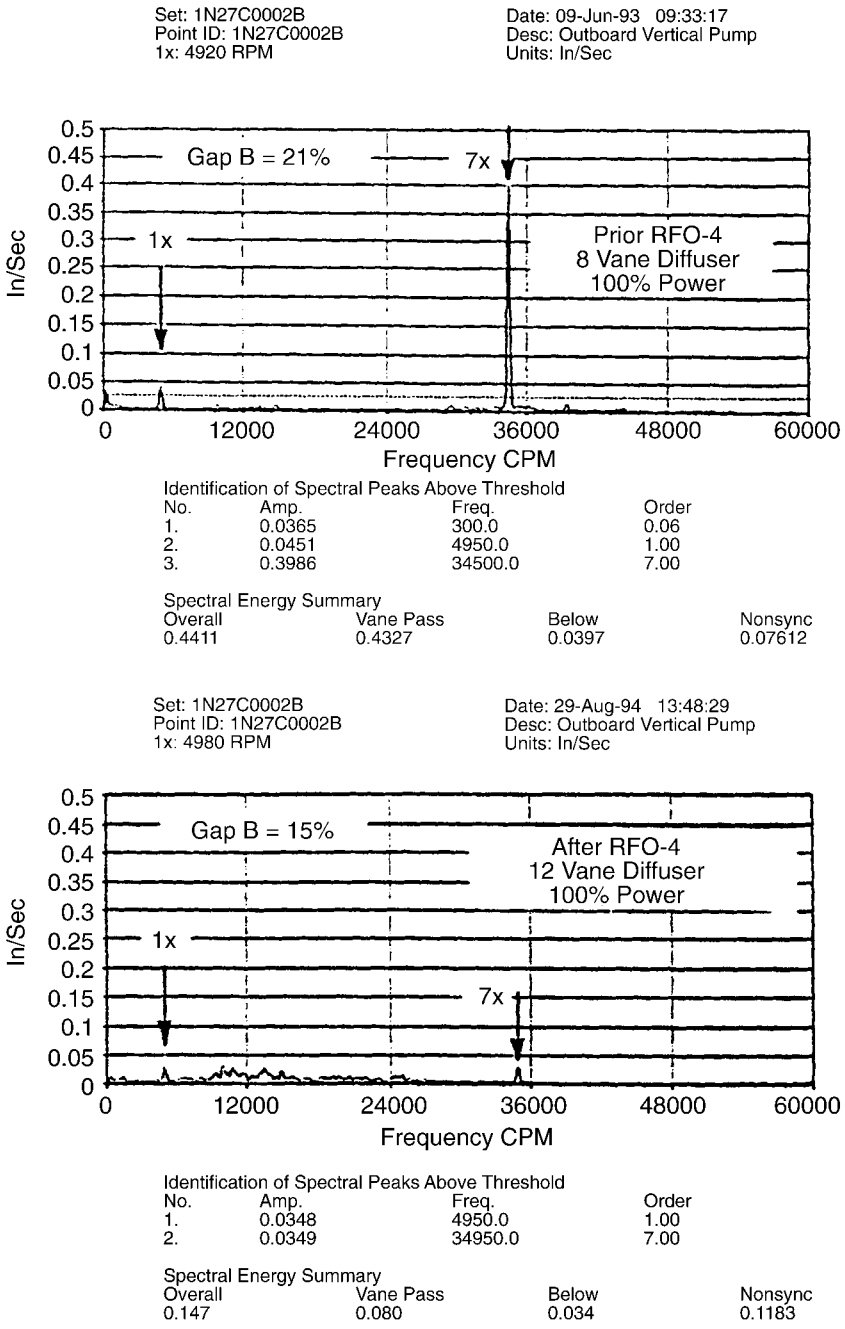

Vibration of RFP No. 2 measured on the O.B. bearing housing at the Perry Nuclear Plant before and after diffuser modification. Vibration amplitudes at the frequencies shown are similar in all other directions and locations.

Figure 7-13
Comparison of Vibration Amplitudes at Impeller Vane Passing Frequency Before and After Diffuser Design Modification

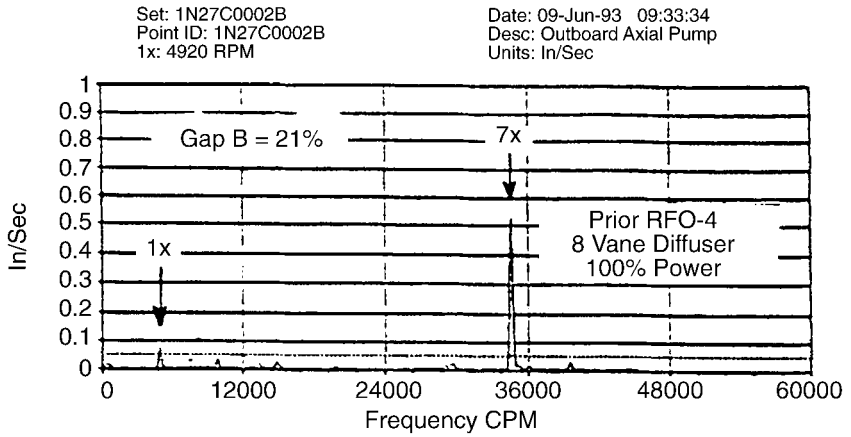

Identification of Spectral Peaks Above Threshold

No.	Amp.	Freq.	Order
1.	0.0798	4950.0	1.00
2.	0.5319	34650.0	7.00

Spectral Energy Summary

Overall	Vane Pass	Below	Nonsync
0.6151	0.5932	0.03365	0.1591

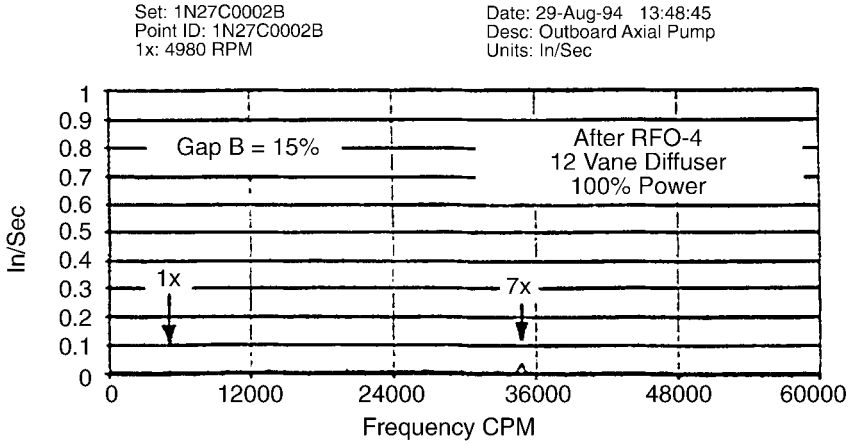

Identification of Spectral Peaks Above Threshold

No.	Amp.	Freq.	Order
1.	0.0206	4950.0	1.00
2.	0.0423	34800.0	7.00

Spectral Energy Summary

Overall	Vane Pass	Below	Nonsync
0.113	0.062	0.0252	0.091

Vibration of RFP No. 2 measured on the O.B. bearing housing at the Perry Nuclear Plant before and after diffuser modification. Vibration amplitudes at the frequencies shown are similar in all other directions and locations.

Figure 7-14
Comparison of Vibration Amplitudes at Vane Passing Frequency Before and After Diffuser Design Modification

Nuclear Reactor Primary Coolant Pumps, Arizona P.S.-Palo Verde Nuclear Plant

PCP-manufactured by KSB: $Z_2 = 6$ $Z_3 = 11$

Original Configuration: Gap B = 2%

Vane Passing: Strong

2X Vane Passing: Predominant

Solution: Open up Gap B to 6%

Figure 7-15 shows test results before and after modifications of the Gap B configuration. Peak-to-peak pressure pulsation amplitudes are shown at 1X, 7X, and 14X. Before modifications, the 2 times vane passing amplitudes were dominant. They were reduced by a factor of five after the increase of Gap B at both vane passing and, more important, at the 2 times vane passing frequencies. The modification was tested first with the 1/3-scale model test stand and later verified during the 600 hours endurance test on the full scale pump, both appropriately instrumented.

7.4.4 5 and 2 Vane Combination: Two STG Reactor Feed Pumps at Dresden 2 and 3

The reactor feed pumps are motor-driven, constant speed (N = 4500 RPM). Therefore, once a problem, always a problem. Exaggerated at lower flows by the hydraulic instability, due to smaller than recommended Gap B and non-existent Gap A, the typical B-J volute type should be closed down to Gap A = 0.050 in. (similar to the modifications performed for the Louisa Station in Iowa).

Two impeller designs exist: (1) $Z_2 = 5$ $Z_3 = 2$

(2) $Z_2 = 7$ $Z_3 = 2$

Before any change is made, the phase velocity should be examined to see which impeller is more favorable for the application such as speed range, temperature, number of stages, and with/without kicker stage.

7.4.5 5 and 2 Vane Combination: Boiler Feed Pumps, Wansley Units 1 and 2

Figure 7-16 shows the acoustic and mechanical resonance interaction with the cross-over channel and the outboard bearing housing at the Wansley power station for the 16x16x18 HDB-5 type boiler feed pumps. Other pump sizes shown are:

12x12x14

14x14x16

16x16x18

20x20x21

20x20x22

All show the same basic acoustic resonance problem. The frequency of resonance will depend on various items such as the number of stages or whether the pump can operate with or without a kicker stage. All of these reflect on the length of the crossover channel, consequently on the frequency of resonance. The temperature of the feedwater has a strong influence on the frequency because the speed of sound changes as the temperature varies. The quality of the casing sandcast also has some influence because of the dimensional variation, which again alters the resonant frequency. Be careful when changing from five to seven vanes because the change may introduce bearing housing, seal housing, or other component resonance, or it may excite the previously avoided rotor critical speed. Therefore, before the impeller vane number is changed, the above subject should be investigated so as not to incur more trouble than what had originally been experienced. Bearing and seal failures are frequent trade-offs with this change.

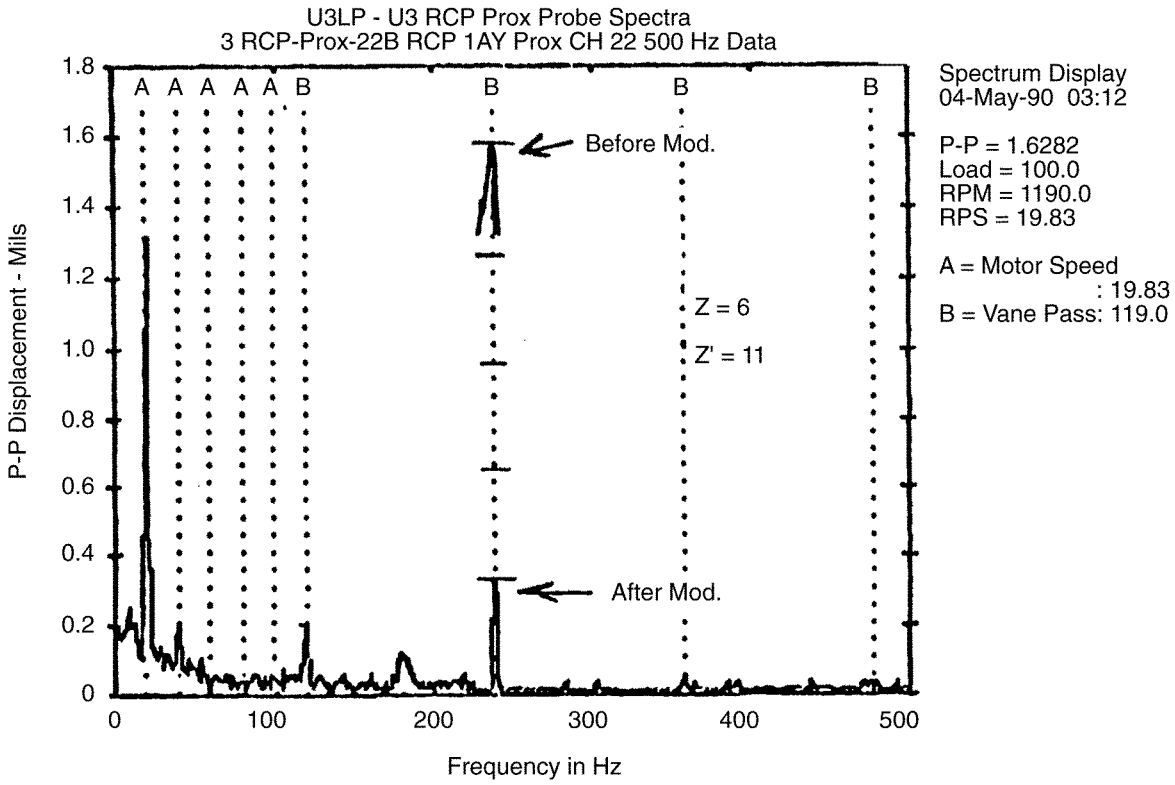

Figure 7-15
Damaging Amplitudes at 2 Times Vane Passing Frequency, Palo Verde, 3 Times 1300 MW PWR (RCP, Four per Loop, Total of 12 Pumps)

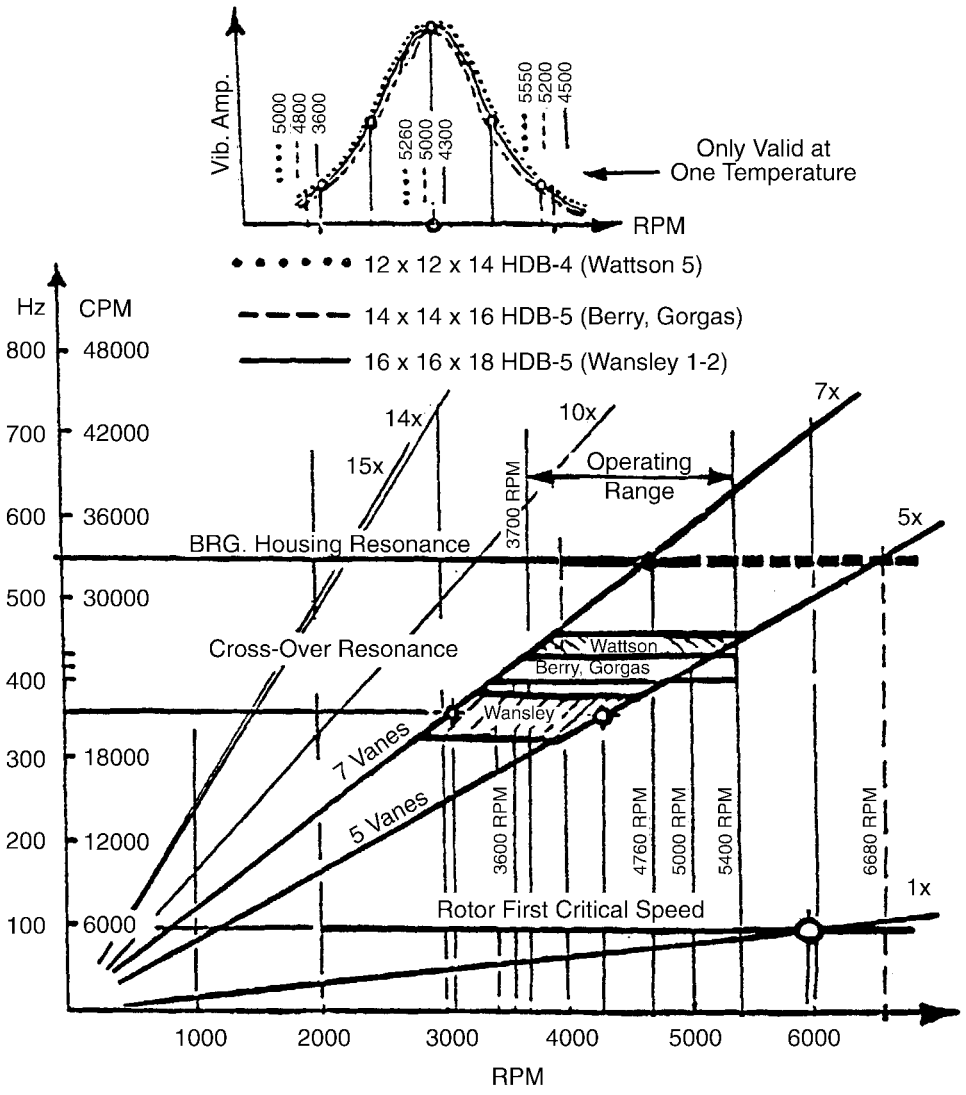

Acoustic and Mechanical Resonances
With 5 and 7 No. of Impeller Vanes

12 x 12 x 14 HDB and HSB (Wattson 5, Field Measurements)

14 x 14 x 16 HDB and HSB (Barry, Gorgas, etc.: Field Measurements)

16 x 16 x 18 HDB (Wansley, Measurements Before and After Major Failure)

20 x 20 x 22 HSB-2 (9 MI PT)

Figure 7-16
Acoustic and Mechanical Resonance With Five- and Seven-Vaned Impeller: First Rotor Critical Speed, Cross-Over Channel, and Bearing Housing Resonance Is to Observe for Trouble.

Cross-Over Channel Dimensions
For B-J Made HDB and HSB Type BFP-S

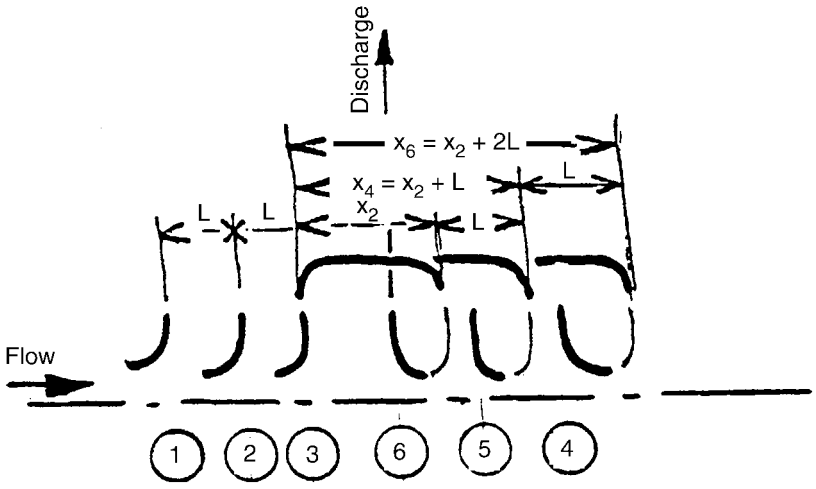

	B-J BFP Frame Size			
	12x12x14	**14x14x16**	**16x16x18**	**20x20x22**
Stg. Spacing: L =	6.0	7.5		
$K = X'_2 - X =$				
	Without Kicker Stage			
$X_2 = X_2 + 0$				
$X_4 = X_2 + L$				
$X_6 = X_2 + 2L$				
	With Kicker Stage			
$X'_2 = X_2 + K$				
$X'_4 = X'_2 + L$				
$X'_6 = X'_2 + 2L$				

Figure 7-17
Acoustic Length of the Cross-Over Channels for the Two, Four, and Six-Stage HDB and HSB Models, With and Without Kicker Stage for Various Size Opposed-Impeller-Type BFP

8
VERY LOW FREQUENCY VIBRATION

The Gap A geometry has a very strong influence on almost all vibration and pressure pulsation components, particularly in the low flow operating range (below approximately 70% BEP). An improper Gap A will typically be picked up in the 4 to 10 hertz (Hz) range on the vibration spectrum and will be most dominant when monitoring the axial direction. However, due to the axial movement of the rotor, Gap A can also cause elevated vibration at the vane pass frequency. When required to operate at reduced flows, a proper Gap A is essential for acceptable operation of the pump. For a high-speed boiler feed pump, Gap A typically should be 0.050 in. and have impeller-to-diffuser sideplate overlap of 0.200 in. to be effective. This is measured as Overlap Ratio, for example, 0.200/0.050= 4.0 for the above case, which is optimum for most cases [1].

8.1 Gap A

The frequency discussed below is less than 10 Hz in most cases; most frequently, the component is between 4 and 6 Hz. In a feedwater system, many components such as piping, foundation, and turbine drive governor can respond to this low frequency. However, the source of excitation lies within the pump itself. It is a hydraulically induced vibration component generated by unstable fluid flow at or below the onset of hydraulic instability. Actual field examples are given, demonstrating how pumps develop this frequency component. However, we will show how it can be controlled or eliminated with the proper geometry of the pump hydraulic channels at various locations:

- Impeller exit to diffuser/volute inlet: Gap A for high-energy-input, low-suction, specific-speed applications [S_S = RPM * Q $^{1/2}$/(NPSH-R) $^{3/4}$]. All feed pumps in the United States belong in this category.
- Impeller inlet (eye) for low-energy-input, high S_s impeller designs: Circulating water pumps and chemical process pumps are examples (see the backflow deflector, also called the eye-catcher, shown in Figure 9-3 and discussed in References 11, 14, and 15).

8.2 History of Gap A

- First application in the United States by Makay to a diffuser-type, single-suction, vertical pump was in 1974. See Figure 8-1.
- First application in the United States by Makay to a diffuser-type, double-suction, high-speed pump was in 1975.
- First application in the United States by Makay to a volute-type, double-suction, single-stage, booster pump was in 1976. See Figure 8-2.

- Makay coined the names Gap A and Gap B during EPRI research project FP 754 in 1976 (Published in 1978 and 1980 by EPRI [4,5].
- Hitachi patented Gap A in Europe in 1988. Withdrawn by Hitachi in 1989 due to Makay's prior publications and applications.
- As part of EPRI research project 1884-10, Sulzer literature search resulted in a one-page description on Gap A application in the Swiss Archive (no name was given to it). August 1941. No reasoning was given by the author in the article (Rutschi).

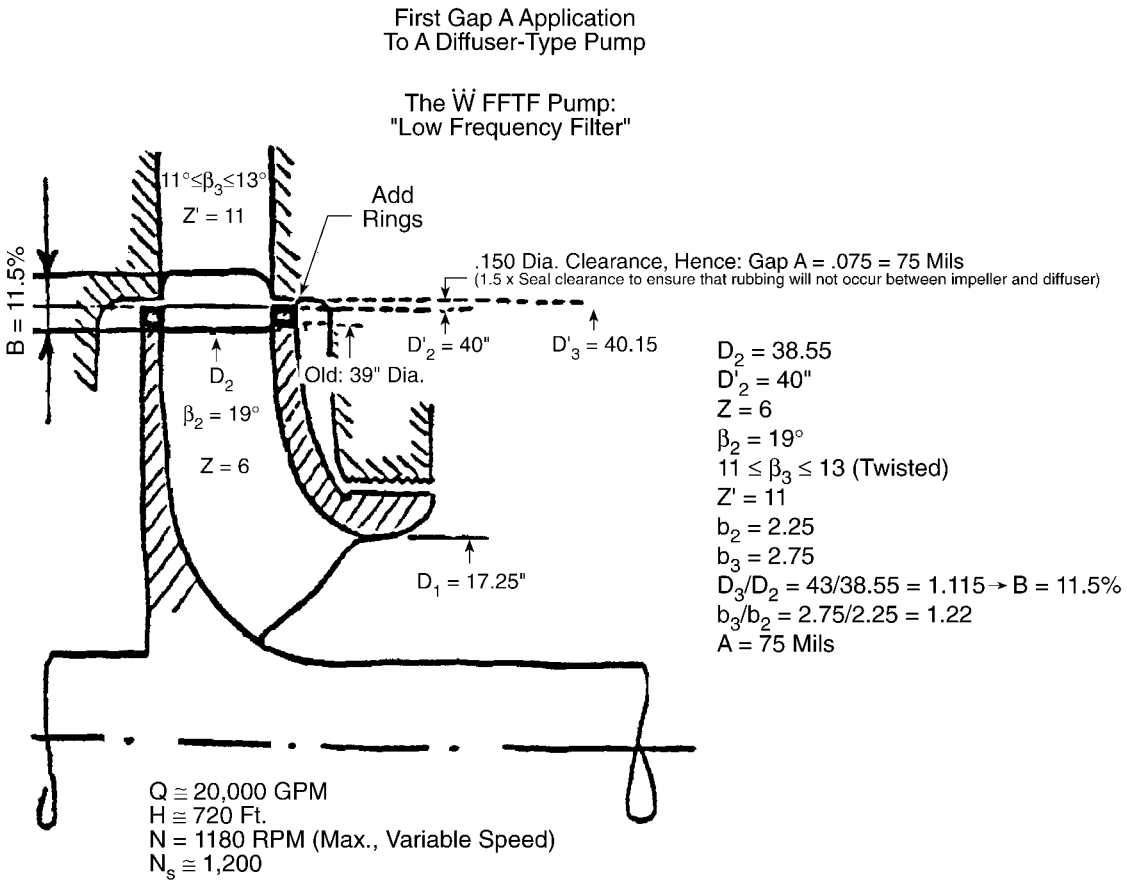

FFTF primary reactor coolant pump (PCP or RCP) meeting took place at Westinghouse on 4-4-74. The subject was unexplained very low frequency vibration and pressure pulsation that did not permit delivery of pumps to the Hanford FFTF site. Modification to the impeller exit to diffuser inlet geometry was suggested as shown above.

CONCLUSION: The very low frequency vibration component did not reappear after the installation of the Gap A rings (rings were welded to the impeller sideplates at the OD as shown above). All seven pumps passed the shop test successfully and were delivered to the Hanford nuclear site.

Figure 8-1
First Gap A Modification to a Diffuser-Type Pump

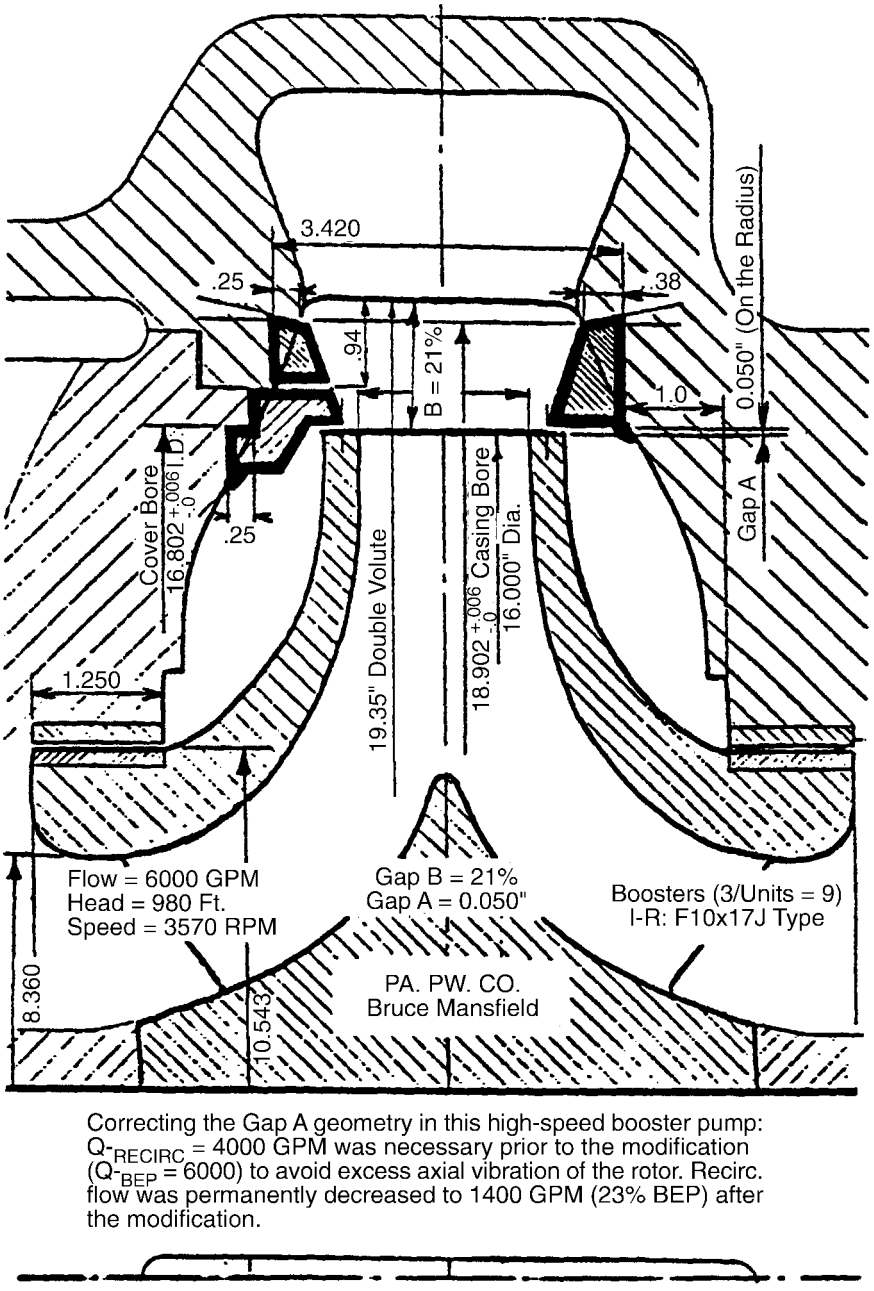

Correcting the Gap A geometry in this high-speed booster pump: Q_{RECIRC} = 4000 GPM was necessary prior to the modification (Q_{BEP} = 6000) to avoid excess axial vibration of the rotor. Recirc. flow was permanently decreased to 1400 GPM (23% BEP) after the modification.

First Modified: 4-20-77 at the Navajo Station

Figure 8-2
First Gap A Modification to a Volute-Type, High-Speed, Feedwater Booster Pump (I-R: F10X17J, Single-Stage, Double-Suction) Navajo Generating Station

8.3 Description of Gap A and the Overlap

Gap A and its overlap greatly influence fluid mechanical action at the impeller periphery, in the impeller channels and the diffuser passages, in the gap itself, and in the space behind the impeller sideplates. It also acts as a low-frequency filter between the active hydraulic channels and the space behind the impeller. Its effect can be quite different for various pump types, designs (such as vertical or horizontal, double-suction or single-suction impeller, single-stage or multistage, light or heavy rotor configurations), specific speeds (N_S), suction specific speeds (S_S), and energy per stage. It is most significant for high-energy pumps such as BFPs, NFPs, and high-head feedwater booster pumps.

Gap A is an effective filter for high-amplitude responses at very low frequencies (up to 10 Hz) for high-energy-input pumps. Its effect diminishes as S_S increases. For higher S_S pump designs, the high-energy concentration shifts toward the impeller eye at flows below BEP because of the dominating action of flow recirculation at the eye. When the S_S is very high, as in inducers, the backflow catcher [14, 15] is very effective for eliminating low-frequency flow oscillations and stabilizing the head curve at lower flows. There is a region between low- and high-suction specific-speed applications where both the Gap A with Gap A Overlap and the backflow catcher can be effective. Probably the combination of the two concepts would offer the most effective solution in eliminating hydraulic instability caused by low flow. Neither concept is recognized, understood, or accepted by most hydraulic designers. Current pump design philosophy is very conservative, especially for utility applications.

The comprehension and physical visualization of Gap A and its overlap is not as simple and apparent as that of Gap B. The complexity of the interactions between flows at the impeller exit, diffuser flow reversal, boundary layer effect, creation of a new flow pattern in Gap A, and the influence of the radial gap and its overlap in the axial directions is beyond simple visualization. The interaction between the impeller exit and diffuser inlet geometry and their connection with the effect of Gap B is a complex phenomenon. Publications on this subject are very limited.

Occasionally, the importance of this area is mentioned. However, the influence of Gap A and its overlap on pump stability behavior at part load, on system instability, on the static and dynamic components of axial thrust, or on the use of this geometry as a corrective device for the above items is found only in References 1, 2, 3, and 5.

The multiple effects of Gap A geometry and its overlap are strong and unique, especially when they are properly coupled with the Gap B geometry. Based on many field applications and measurements, they can be summarized as follows:

- Head-capacity curve stabilization. Introduction of the proper Gap A geometry in a pump, coupled with the proper overlap and vane-to-vane radial distance between impeller and diffuser/volute (Gap B), improves the head curve stability at part load, as shown in Figure 8-3. This improvement may eliminate or improve stability thought to be from pump, feedwater flow, feedwater control system, valve, and often BFP turbine-drive-governor instabilities. It can have a significant effect on piping vibration and on failures of major and minor components.

- Axial thrust stabilization. Stabilizing the axial thrust eliminated abrupt changes in the static magnitude and dynamic fluctuations of axial thrust. Therefore, it can eliminate such effects as the following:
  - Thrust-bearing overheating or failure, or any axial-thrust related problem
  - Part load instability of static and dynamic axial forces, especially for single-stage double-suction feed pump designs
  - Thrust reversal problems [17 and 26].
  - Balancing disk/drum leak-off flow fluctuations (unless seal injection flow control is not properly set).
  - Unstable balancing disk/drum performance (usually results in catastrophic failure).

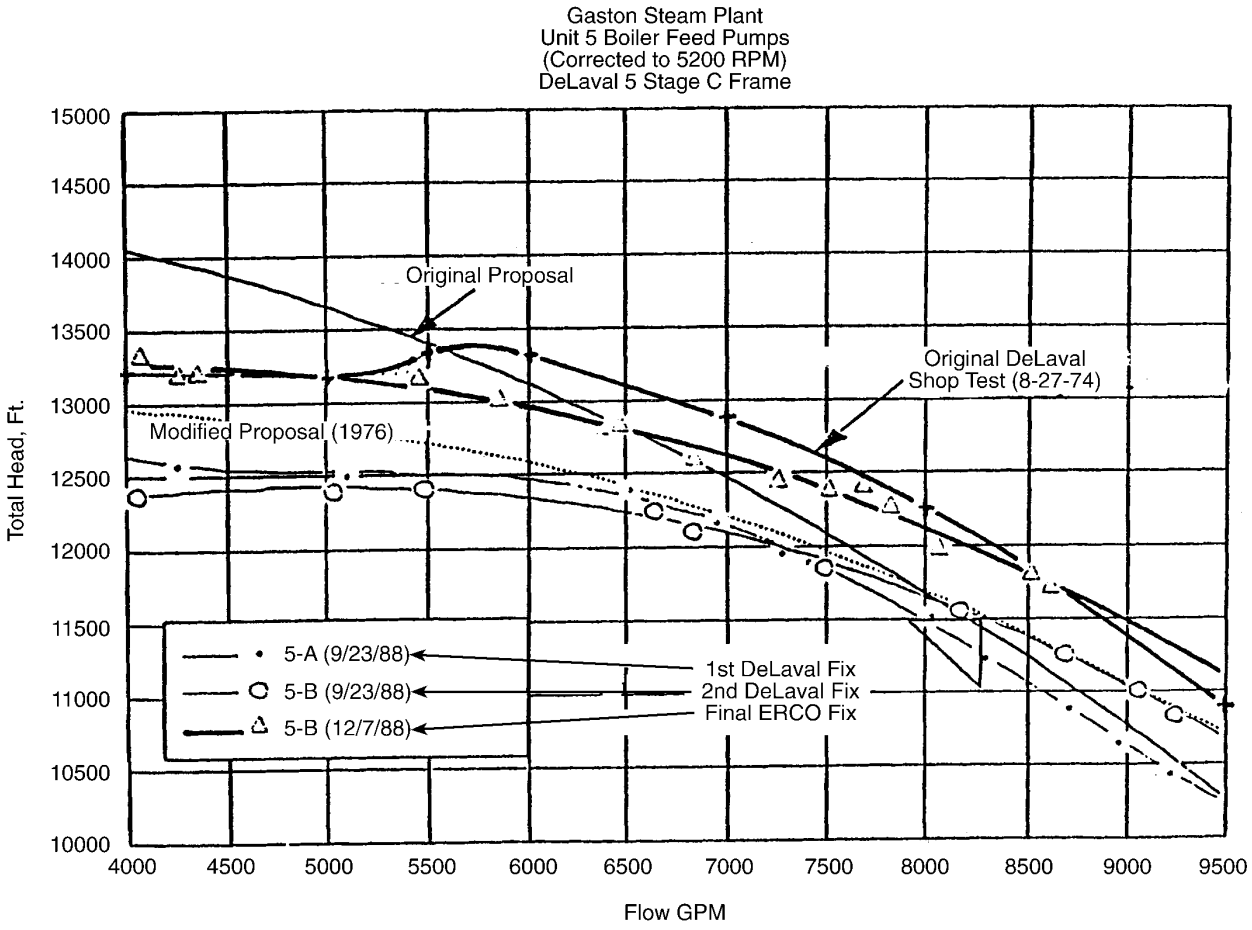

Figure 8-3
Head Curve Stabilized at Part Load by Introduction of Proper Gap A and Its Overlap

It is shown in Figure 11-13 how the rotor axial thrust changes as the percent of BEP flow varies and how axial misalignment of the rotor changes the thrust. The response of the axial balancing device is shown for the balancing drum and the balancing disk (without tapered face and with tapered vertical face). It is clear that the disk with the tapered face has superior performance.

- Rotor-dynamic improvement. Rotor dynamic improvement provides positive rotor-dynamic damping to stabilize motion, resulting in smoother running pumps, less rubbing and wear, fewer bearing and seal problems, and longer rotor life. Therefore, the result is less need for maintenance. This was not known until many field modifications showed repeated and consistent improvements of rotor behavior. The evidence is not based on theoretical calculations but on a long list of field applications.
- Feedwater system instability improvement. Elimination of feed pump instability reduces or, in many cases, completely eliminates the system instability problem. This is probably the most significant contribution to the development of pump technology.
- Increased pump efficiency. When the geometry modification is properly incorporated in the pump, the pump efficiency increases. This is a minor but significant contribution to the development of pump technology.

The foregoing are critical from an engineering perspective; however, the bottom line for the power stations is:

- Increased plant availability
- Significant decrease in maintenance efforts
- Decrease in operating cost
- Increased reliability of operation and system behavior, which is particularly important for cyclic operation of very large units
- Noise reduction when properly combined with Gap B modifications
- Increased pump efficiency

Many cases have shown that the concept works equally well for both diffuser-type and volute-type pumps. The effect of Gap A was first demonstrated on diffuser-type designs. The first full proof of applicability on volute-type pumps was in 1976 for single-stage, double-suction, high-energy-input booster pumps. All other pumps previously modified were diffuser types. This case opened a new road for research on volute-type pumps. Many single-stage, double-suction and single-suction, multistage, volute-type pumps now have been modified. These fully support the evidence that the technology applies to volute-type as well as diffuser-type pumps.

Radial changes of axial thrust as the rotor position changed were reported to create major unexplained problems. With sufficient overlap, the thrust variation becomes insignificant when the impellers are shifted in the axial direction. The overlap ensures that the gap will not be unsealed fluid mechanically and remains in full control for the flow path. When an impeller has a sideplate with an incorrect thickness, as in a very large number of older designs, the overlap and gap cannot be effectively used. Even if Gap A is reduced to a very small value, several problems exist:

- There is insufficient overlap to make it effective.
- If b_3/b_2 is incorrect, the flow catches on the diffuser sideplate when there is axial misalignment, causing thrust reversal and large vibration amplitudes.

Some designs specify a radius or a chamfer on the impeller sideplate at the OD or specify a very thin sideplate. This reduces the effectiveness of the gap. A wall thickness of not less than 3/8 inch is recommended, preferably 1/2 inch on large feed pumps. The available axial clearance behind the impeller sideplates also must be examined. Insufficient clearance greatly increases fluid friction and reduces pump efficiency. Axial float of the rotor may also become a problem.

Conclusions are that when properly applied, Gap A, in conjunction with the Overlap Ratio, Gaps B, E, and F (see Figure 1-5 for nomenclature), will result in the following performance, vibration, maintenance, and pump availability improvements:

- Head-stability always improves at part load. Its effectiveness decreases with increasing N_s and with reduced Gaps E and F. Below a critical value of E and F, pump performance is independent of Gap A. When performing Gap A modification, one must be sure that Gap B is also correct. Proper A and B Gap modifications eliminate the dip in the H-curve as shown in Figures 8-3, 8-4, and 8-12.
- The modification may eliminate feedwater system instabilities such as piping vibration, control system and/or turbine drive governor instabilities (for more details on feedwater instability, see Reference 1).
- It results in higher head at minimum (recirculation) flow. Effectiveness is the same as above.
- It usually has very little or no effect on head at BEP.
- A gain in efficiency is expected if the modification is done properly or correctly. A 4% efficiency gain at full load is reported in Reference 16. Another example is shown in Figure 8-12 where the OEM factory performance test showed 2% improvement in efficiency on their properly instrumented test stand [11]. Substantial efficiency gain is reported in several installations [25]. If the modification is executed improperly, a loss in efficiency may result such as reported in EPRI research project interim report RP 1884-10.
- Proper combination of Gaps A and B may eliminate subsynchronous vibration components in the range of 0.5 to 0.9 x RPM as shown in Figures 5-3 and 5-4 and reported in Reference 26.
- High vibration amplitudes are eliminated in the very low frequency range below 10 Hz [1, 2, 17].
- Damaging "axial shuttling" for single stage, double suction pumps is eliminated [1, 2, 4, 11, 17, 21]
- It has a strong stabilizing effect on rotor axial thrust. Also it can eliminate axial-thrust reversal at part load. Axial balancing disk/drum and/or thrust bearing failures or rotor destruction can be eliminated in some cases. An example for thrust reversal is shown in Figures 5-3 and 5-4 and is reported in Reference 26.
- It has no influence on vibration amplitudes above synchronous frequency.
- Up-lift for single-suction vertical pumps such as condensate and circulating water is eliminated.
- The probability of shaft breakage is reduced when it is a recurring problem, when the possibility is high that it is induced by hydraulic forces at part-load performance, which is quite frequent.

- Minor damage such as diffuser tip breakage, impeller cracking at the exit, diffuser retaining bolt or tie-rod breakage, internal gasket damage, and seal injection line fatigue failure is eliminated.
- It has a strong flow stabilization effect at the impeller inlet (eye).
- It reduces cavitation damage, if present, at the impeller inlet as described in the anti-stall hump (Section 14) for the Crystal River 4/5 main boiler feed pumps.
- It results in reduced maintenance and improved pump availability.

Each case has to be evaluated individually. Do not expect miracles from Gap A because there are many other parameters that can influence flow instability. There is such a thing as hopelessly bad hydraulic impeller or diffuser design or a combination of the two. These can be corrected only with newly designed components.

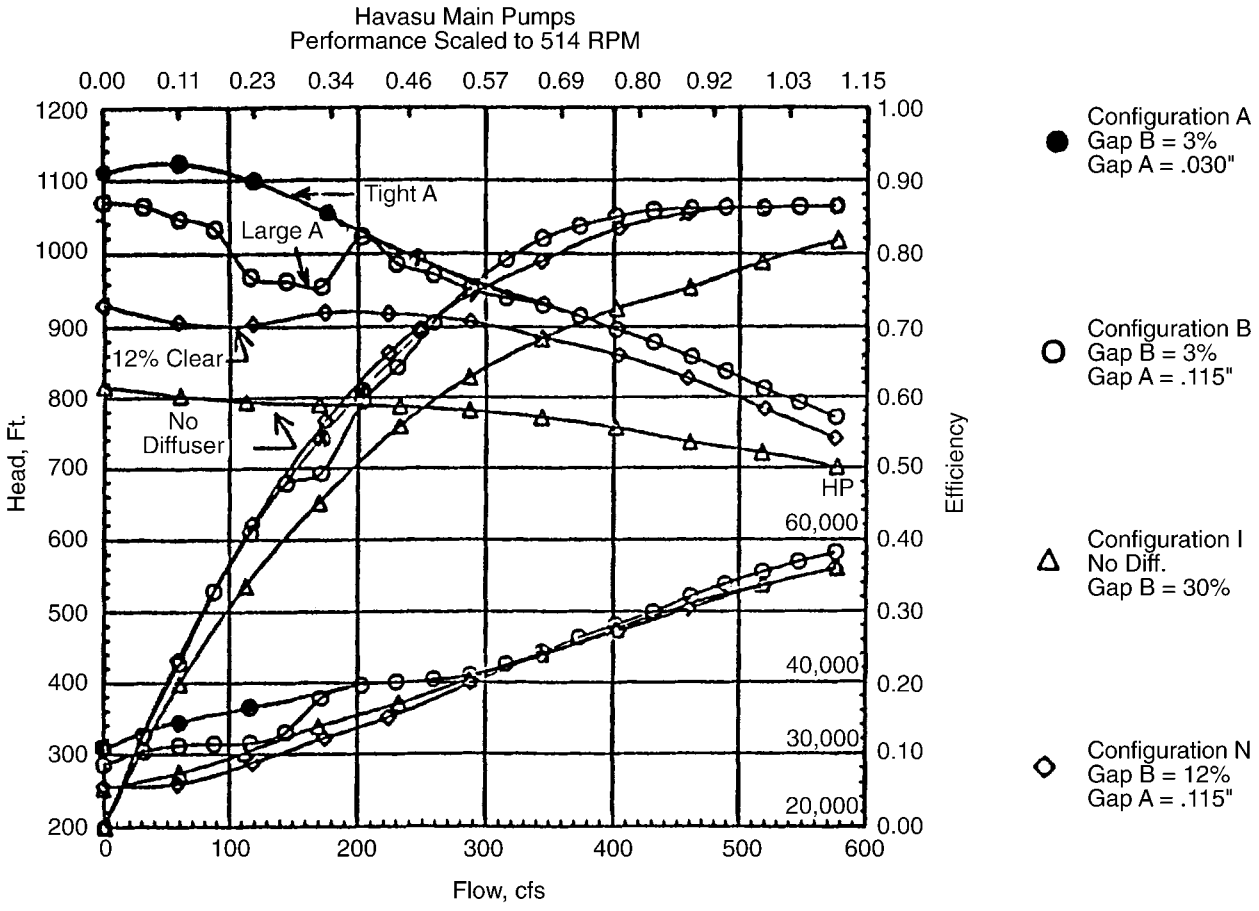

Figure 8-4
Three Ways to Stabilize the Head Curve of a Pump by Various Combinations of Gap A, Gap A Overlap, and Gap B

8.4 Design Criteria for Gap A and Its Overlap

The above changes in pump stage hydraulic geometry make it feasible to update an older pump to the standards of the latest technology. By incorporating the proper design modifications, one can essentially redesign a new pump for little (sometimes zero) investment and may end up with a year 2000 pump design.

Recommended Gap A and its Overlap Ratio ranges are given in Figures 8-5 and 8-6 as functions of various pump parameters. These values were systematically collected by ERCO from 1972 to the present, and, as shown in Figure 9-2, over 800 field modifications were performed on Gap A alone. Figure 8-5 exhibits a general design chart that is equally applicable to diffuser and volute type, single-suction and double-suction, single-stage and multistage pump designs. Once approximate values are estimated from Figure 8-5 for Gap A, go to the appropriate chart like Figure 8-6 to determine final values for that particular design. The chart will indicate optimum values and permissible ranges for that particular D_2 and N_S. There is no general chart of the Figure 8-6 type.

Actual field modification examples are given in the next few pages for various pump types and designs, including a calculation sample for Gap A, E, Overlap and X (=O/A) optimization.

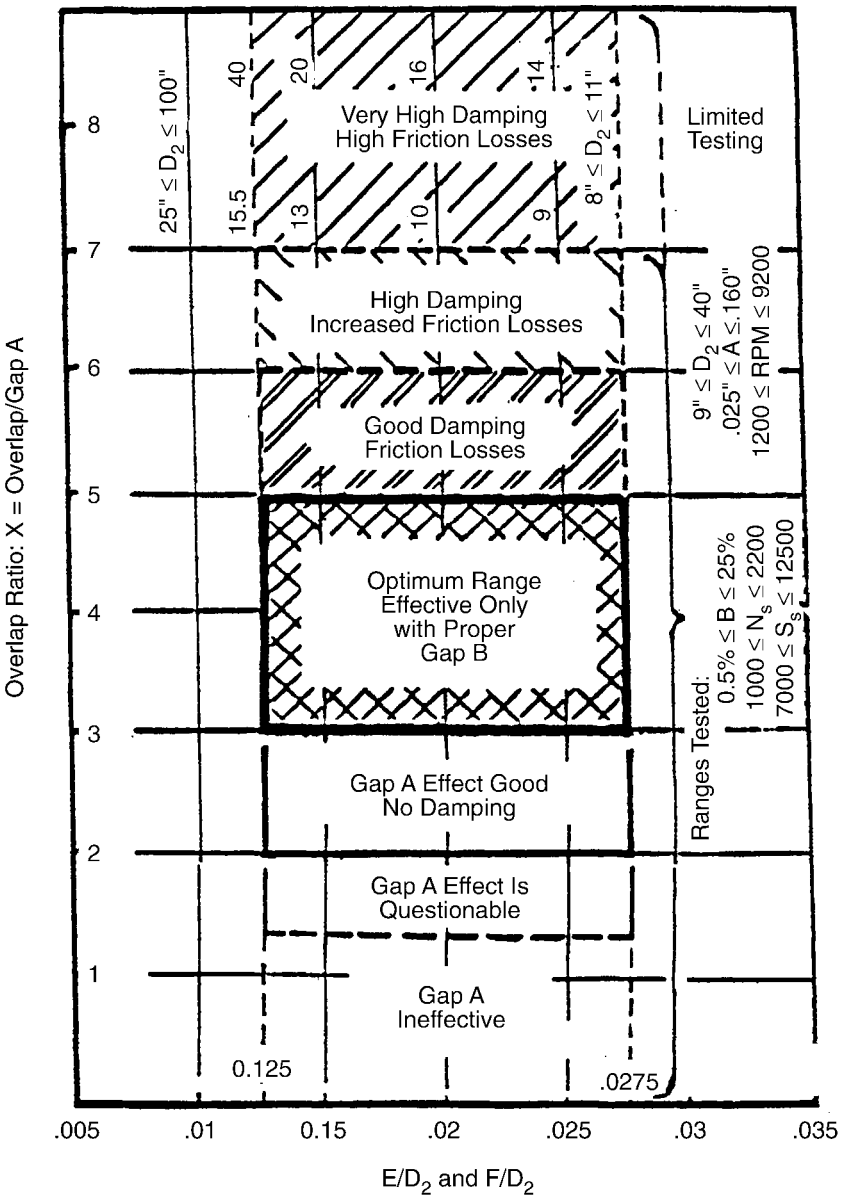

General design chart recommended for Overlap/Gap A ratio as function of impeller diameter, side plate clearances E and F, Gap B, specific speed N_s and suction specific speed S_s (statistical data collected by ERCO on over 800 pump modifications in nuclear and fossil power plants between 1972 and 1990).

Equally applicable to diffuser and volute designs, single and multi-stage, and single, twin and double suction pump designs.

Figure 8-5
General Design Chart for Gap A, Its Overlap, and Other Associated Impeller Geometries

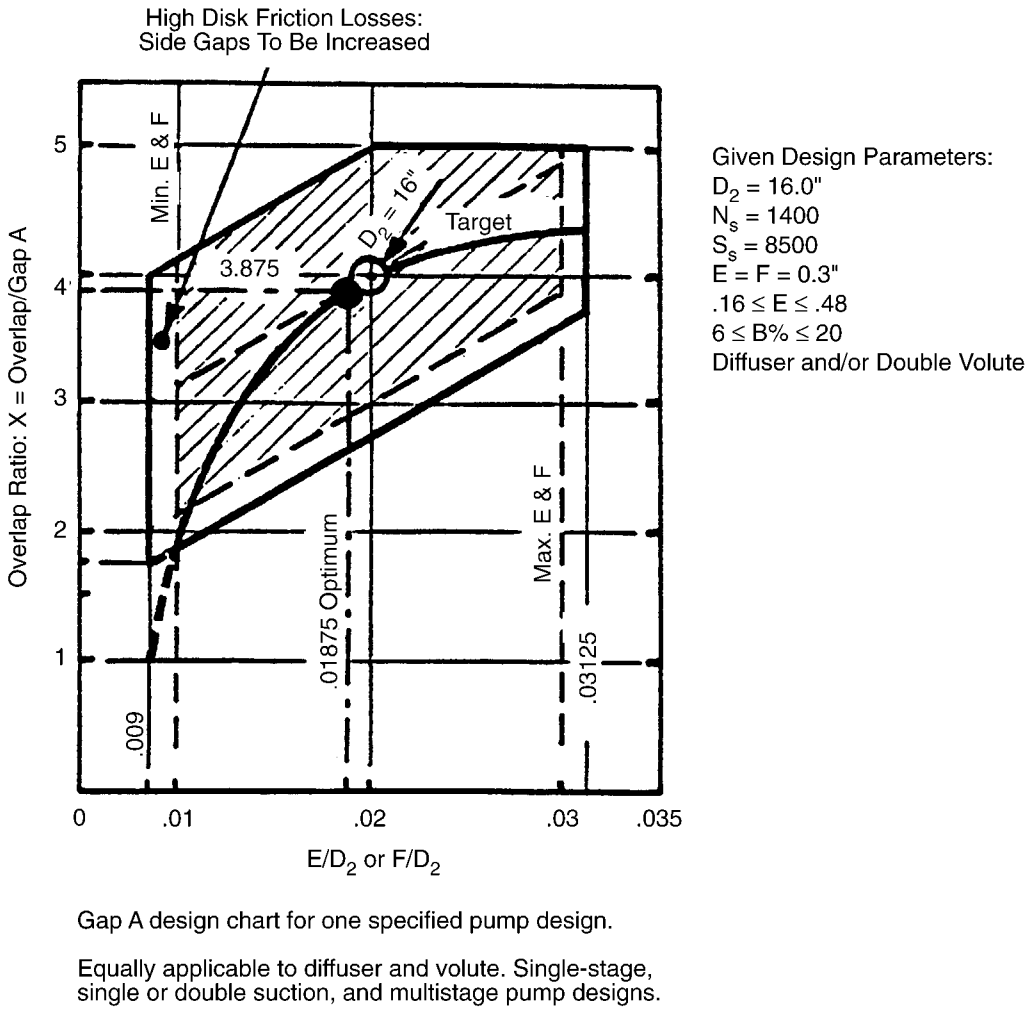

Gap A design chart for one specified pump design.

Equally applicable to diffuser and volute. Single-stage, single or double suction, and multistage pump designs.

Figure 8-6
Optimization Chart for Gap A and Its Overlap

8.4.1 First Diffuser-Type Modification

The first diffuser-type modification was performed in April 1974 on an FFTF coolant pump to filter out low-frequency rotor vibration. The pump, shown in Figure 8-1, was a single-stage, single-suction vertical type. The very low frequency vibration component disappeared completely after the installation of the Gap A rings welded onto the impeller OD as shown in Figure 8-1. This was the first Gap A modification performed by the author on a diffuser-type pump. The results opened a new era in centrifugal pump hydraulic research and development and prevented a large number of field failures in literally hundreds of power stations, both nuclear and fossil applications.

8.4.2 First Single-Stage, Double-Suction Booster Pump

The first single-stage, double-suction booster pump with double volute, of the type F10x17J, is shown in Figure 8-2. Severe axial vibration resulted from hydraulic instability in flow conditions below BEP. Initial 25% minimum flow was inadequate during plant start-up in 1972. Heavy vibration brought upon the whole feedwater system made it essential to add a second recirculation line, bringing the total required minimum flow to 60% of BEP. Even at this high recirculating flow, mechanical seal failure was a routine occurrence at the power station. Modifications made to the feedwater booster pumps are presented in Figure 8-2, reported in Reference 22, and further discussed in References 2, 4, and 11. Insert rings were installed to create a Gap A on both sides of the impeller exit. The new Gap A dimension, as shown in Figure 8-2, was 50 mils. After the recommended modifications were incorporated in the power station machine shop, the feedwater system instability was completely eliminated, and the previous 40 mils axial shuttling of the rotor was reduced to an amplitude so small that it could not be effectively measured. The frequency of the rotor vibration before the modification was 4 Hz, the same as the feedwater piping vibration frequency, and both were completely eliminated after the simple geometry change. The added minimum flow line was permanently removed. Mechanical seal failures stopped after the modification was performed. The geometry modifications apparently did not reduce pump efficiency at BEP, according to plant data, and efficiency at low flows has substantially improved. The present minimum (recirculating) flow is 25% of BEP.

8.4.3 Single-Stage, Double-Suction Booster Pump

Single-stage, double-suction booster pump of a double-volute type is shown in Figure 8-7. It is a 10x10x14 DVS type with a cast iron casing. This was the first volute-type pump modified by the author for Gap A. Dove-tail rings were used to close down Gap A to 50 mils on the radius. The results were very favorable. Axial shuttling that previously was responsible for several failures was completely eliminated. Later in 1973 a research project at the AUSTRO Research Institute in Graz, Austria, shed light on the subject (plexi-glass windows between the impeller exit and the diffuser inlet).

The above successful examples started a new way of thinking in hydraulic research for hydraulic component design of high-energy-input centrifugal pumps. A new era in hydraulic development had commenced.

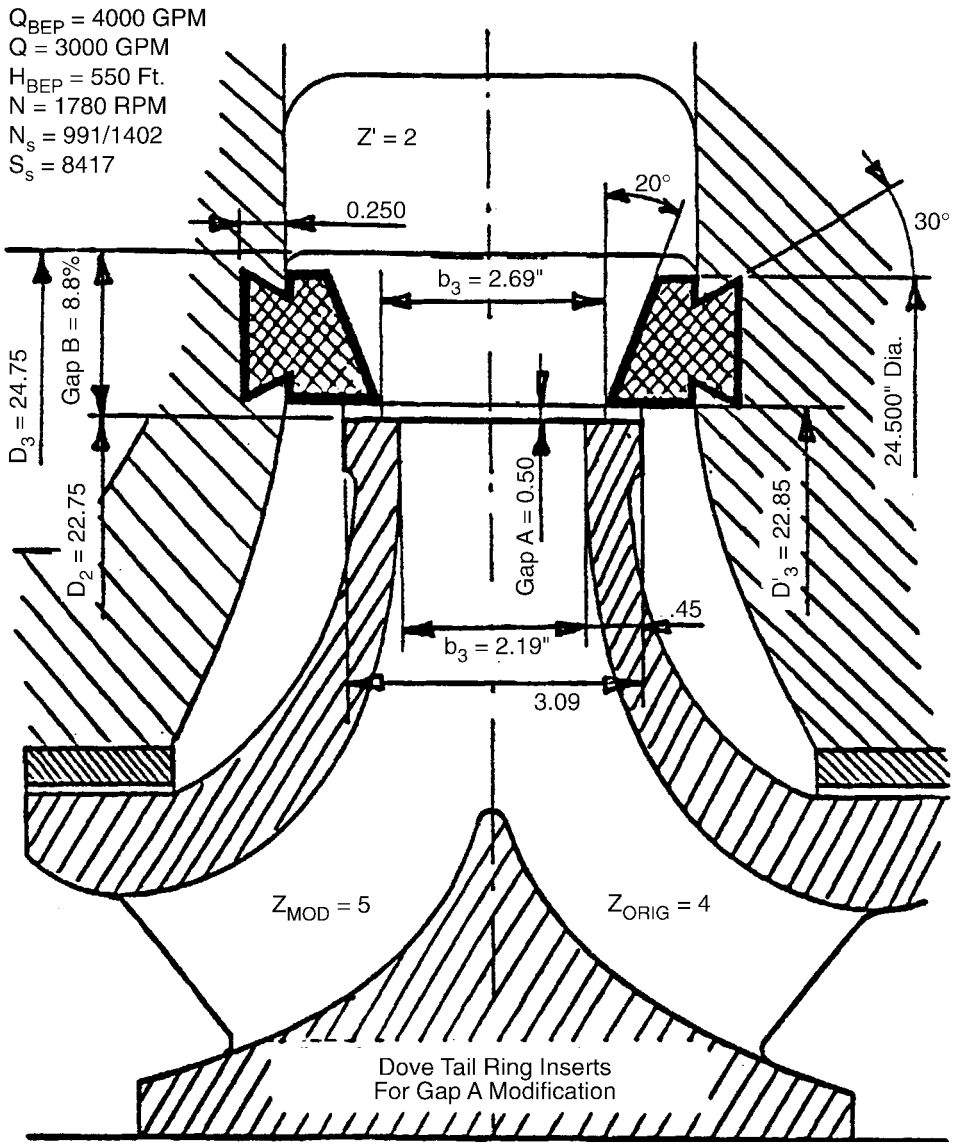

TU Electric Co.
Comanche Peak Nuclear Plant
Containment Spray Pump

Sulzer Bingham Co.
10 x 12 x 25 HSA

Gap A = 0.50
Gap B_{MOD} = 8.8%

Figure 8-7
Dove Tail Style Gap A Ring Insert (B-J at THC2 in 1976 and Sulzer/Bingham at Comanche Peak Proposed in 1993)

8.4.4 Boiler Feed Pump, Double-Volute Type

Boiler feed pumps, double-volute types, are shown in Figures 8-8 and 8-9. Pump and feedwater system instabilities prompted modification action on volute-type feed pumps. So far, mainly diffuser-type feed pumps were modified because modification of a diffuser-type pump is simple, but it can be very complex and costly for a volute-type pump. A double-suction first-stage Gap A modification was achieved by fabricating complex inserts that were attached to the volute casing and the inlet closing flange. Insert rings were welded to the casing in Figure 8-9 for the single-suction stages to create a previously nonexisting Gap A. Although Gap A modifications were stagnant in the past for volute-type boiler feed pumps due to the difficulties in the geometry (not because they were not needed), today, after overcoming the initial difficulties, more double volute types are being modified than diffuser-type feed pumps. Acoustic resonance of the inner hydraulic channels for volute-type pumps is quite frequent, where the Gap A modification can offer a quick and reliable solution in a most economical way.

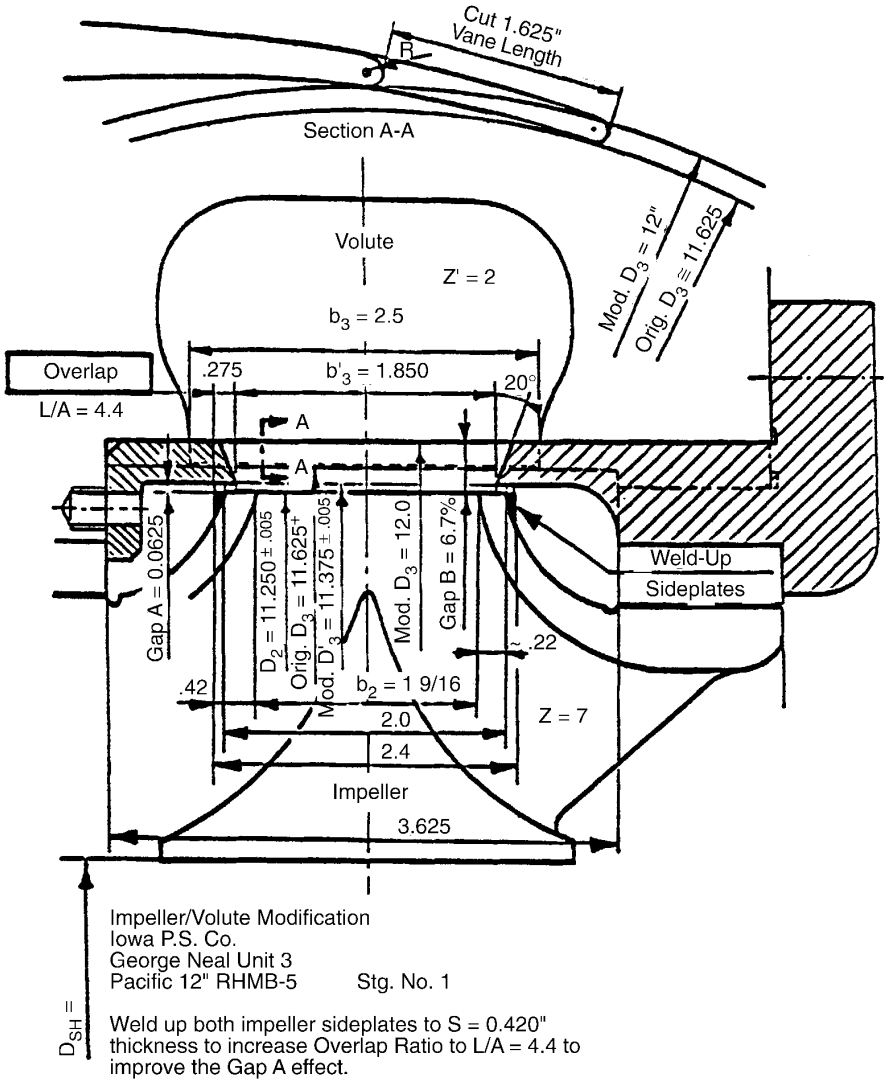

Figure 8-8
BFP Double Volute: Pacific 12 In. RHMB-5

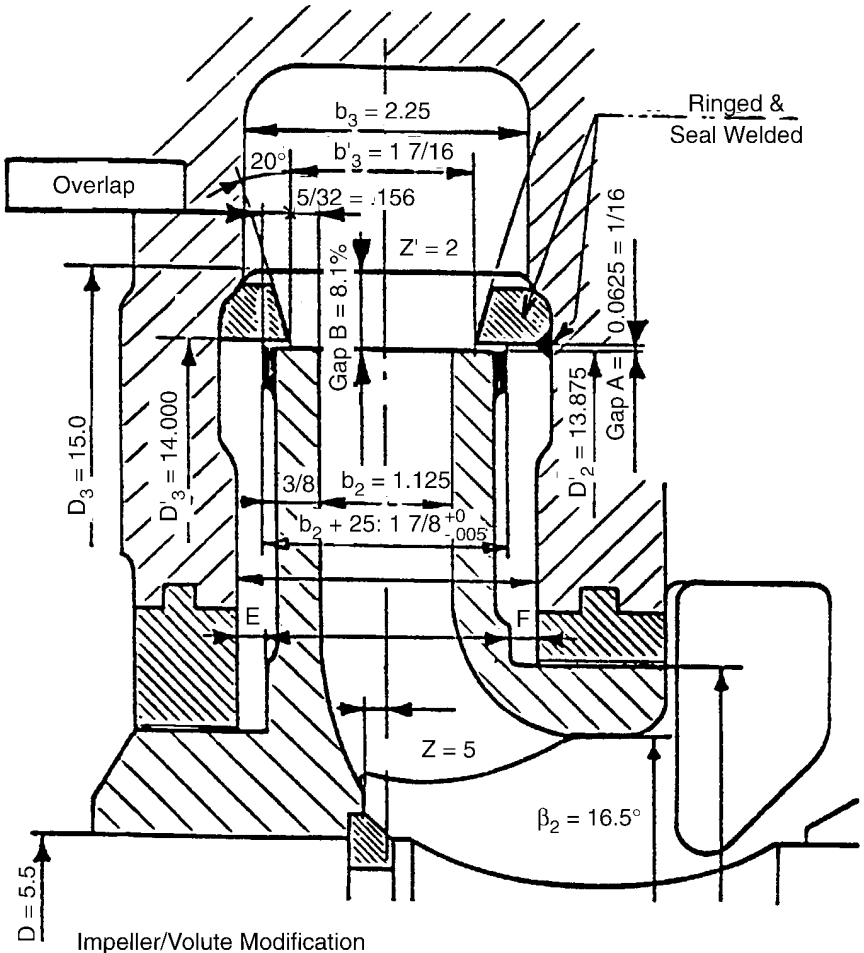

Impeller/Volute Modification
Louisville G & E - Trimble County
B-J: 12 x 12 x 14HDB-6 Stg. No. 2-6

Final Modification: For Gap A and its overlap to be effective as a low frequency filter, the impeller and volute side plates to be modified as shown above.

Note: When ordering new impellers from B-J, give instruction on the P.O. not to chamfer or radius the impeller side plates. Do not remove material from the Gap A side-rings during dynamic balancing of impeller.

Axial Float = [(E) + (F)] = .500"
Measured = _____
Stage Spacing = _____
Underfile All Impeller Vanes To: X = _____"
(See Separate Drawing For Under-Filing)
Journal Bearing Diameter = 5-14"

Figure 8-9
BFP Double Volute: B-J 12x12x14 HDB-6

8.4.5 Single-Stage, Double-Suction Nuclear Feed Pump With Diffuser Discharging Into a Double-Volute Casing

A single-stage, double-suction nuclear feed pump with diffuser discharging into a double-volute casing is shown in Figure 8-10 after modification by the OEM. Vibration history is also shown at various flows and speeds. As the flow was reduced below 65% of BEP, vibration amplitudes became excessive, even when the pump speed was greatly reduced. The new reduced vibration level, at 18% flow and full speed (5200 rpm), after modification of Gap A, is also presented in Figure 8-10.

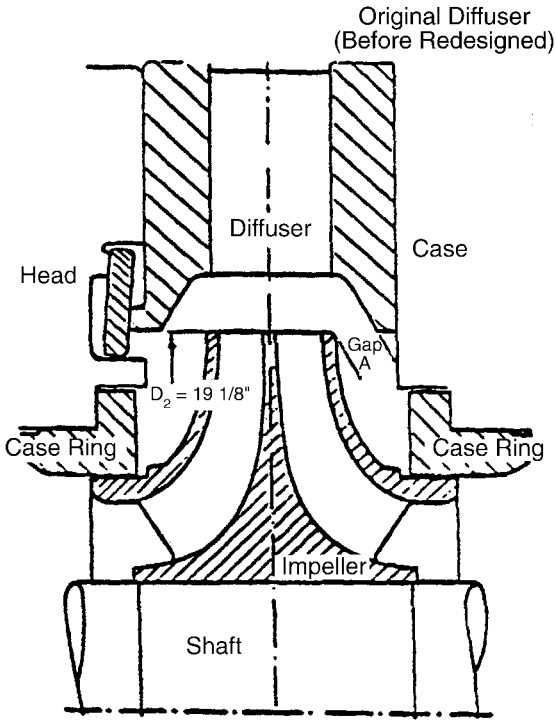

High-speed reactor feed pump before diffuser was redesigned. Axial vibration of rotor was 42 Mils at 26% of BEP at reduced speed of 4000 RPM.

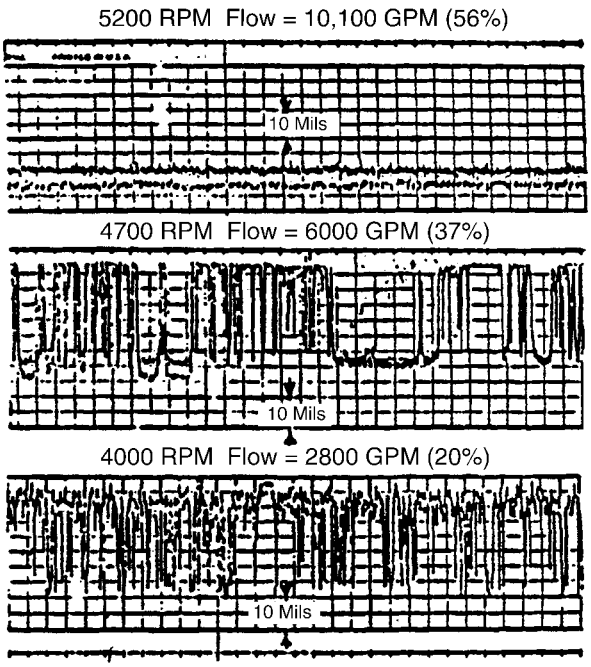

Shaft Axial Vibration = 0.042 In. = 42 Mils

Axial shuttling of a high-speed nuclear feed pump rotor. Rotor vibration level was normal at BEP (100% design capacity). Maximum vibration level was 42 Mils. Thrust bearing was 16 Mils. Shaft movement was clearly visible at minimum flow.

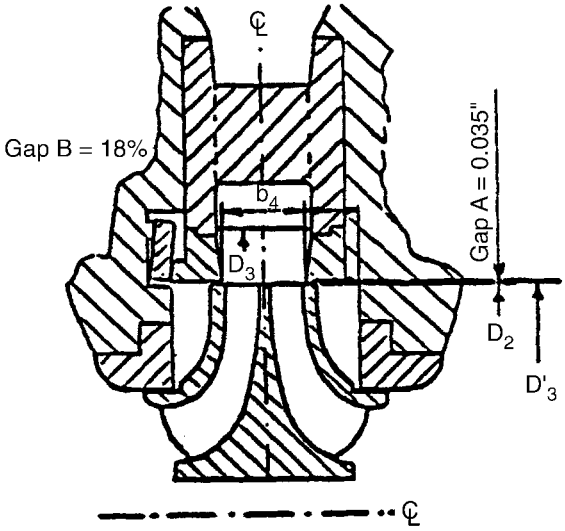

Axial vibration of a high-speed nuclear feed pump greatly reduces (from 42 Mils to 2 Mils maximum) at 18% of BEP minimum flow after the diffuser inlet geometry was redesigned with Gap A = 35 Mils.

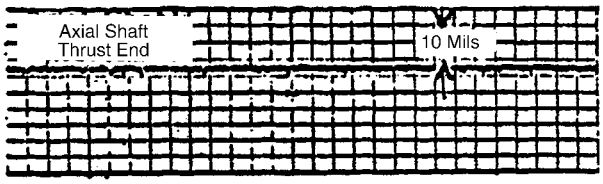

Figure 8-10
High-Speed Reactor Feed Pump Before and After Gap A Modification

8.4.6 Single-Stage, Double-Suction Reactor Feed Pump (Diffuser-Type, Volute Casing)

During startup of an 1100 megawatt BWR nuclear unit, feedwater system instability and high levels of radial and axial vibration occurred in a reactor feed pump at and below 60% of pump BEP. The plant required stable operating characteristics down to 46% BEP (at reduced pump speed). The pumps are single-stage, double-suction, diffuser type in a volute casing with very high energy input. An intensive investigation was started by testing one pump with its controversial suction piping configuration at the OEM's testing facilities with a well-instrumented test program. Test 1 was performed with the original full diameter impeller but is not shown in Figure 8-12. Test 2 was the benchmark test, where the impeller vanes were partially modified as shown with dotted lines in Figure 8-11. Test 2 was performed without modification of the impeller exit to diffuser inlet dimensions, Gap A, and without cutback of the leading edge of the diffuser vanes. The Test 2 geometry is shown in Figure 8-11 with dotted lines. The geometry for the Test 3 ERCO modifications are shown with solid lines.

A new impeller and diffuser were also designed and cast with special emphasis on low-flow stability. Sideplates were made wider at the OD for proper Gap A Overlap, and balance weight removal did not interfere with uniformity of the overlap. A diffuser center-dividing shroud was also introduced for more uniform flow distribution in the diffuser.

Full performance, vibration, and pressure pulsation were made between 130% and 25% of BEP flow at full speed (5100 RPM) and at reduced speed (4500 RPM) down to 15% flow. The head-capacity curve rose steadily toward low flows and was stable for both Tests 3 and 4, as shown in Figure 8-12. References 1 and 11 give more detailed description. The stability criterion was met at 30% flow with Test 3, and 25% flow with Test 4, both at full speed. The change in shaft axial vibration was similar to the results shown in Figure 8-10. There was a substantial improvement in rotor damping. Pump configurations are also shown in Figure 8-10.

A clear efficiency increase of 2% was measured during Test 3 for that configuration at the OEM's well-instrumented test floor. The Gap A overlap ratio was $X = O/A = 4.0$, carefully selected and optimized by the author (Figure 8-12). For a more detailed description, see References 1 and 11.

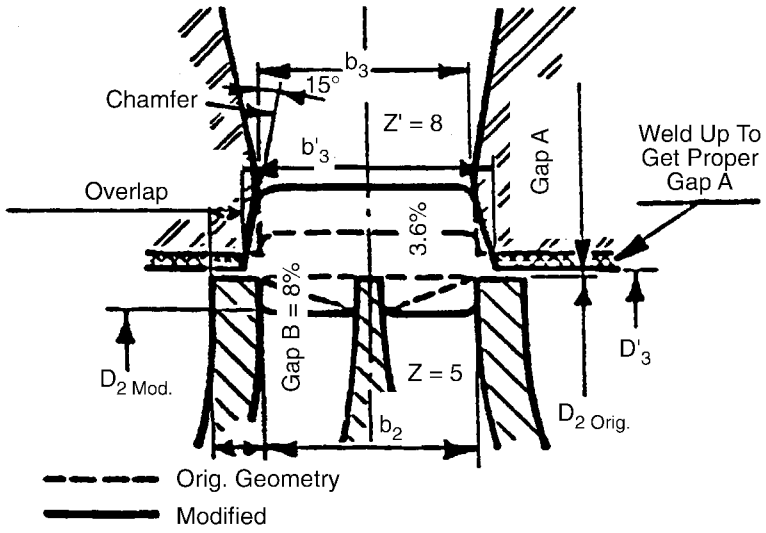

Nuclear reactor feed pump modifications. In addition to Gap A, its overlap, and Gap B modifications, the diffuser inlet is also to be chamfered 15° for:

- Better flow conditions into the diffuser channels
- Easier impeller-to-diffuser axial alignment during assembly

Figure 8-11
Nuclear Reactor Feed Pump Modification

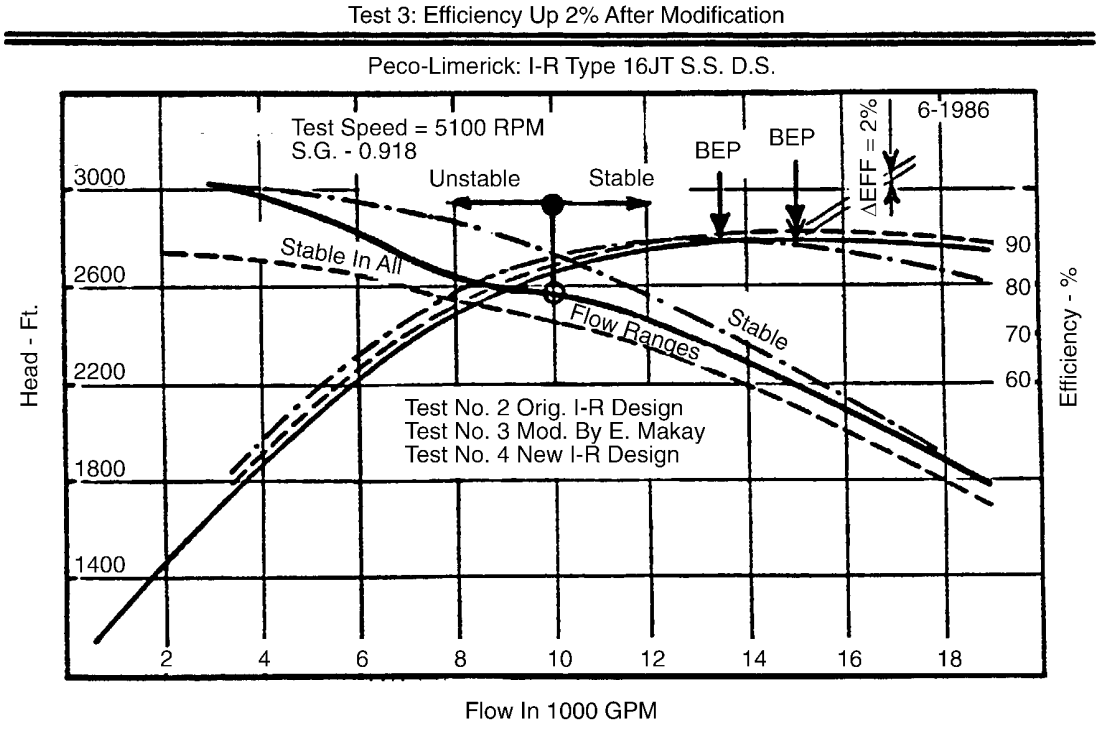

Figure 8-12
Nuclear Reactor Feed Pump Test Data Before and After Impeller-Diffuser Modification

8.4.7 Example

Selection of optimum Overlap Ratio X: LCRA-Ferguson Sta. HPTX-40-3 Stg. type. Dimensions from Figure 5-7:

D_2 = 16.210"	Z = 7	Z' = 12	Gap B = 5.1%
E = .265 to .300	F= .4	N_s = 1520 (Stg. 2-3)	S_s = 8500
E Side Plate:	Gap A = .0625	Overlap = .300	X (ratio)= 4.8
If Overlap decreased. to .285			
F Side Plate	Gap A = .0625	Overlap = .285	X (ratio)= 4.56

On the hub side, we are within optimum range in Figure 8-15. See Figure 8-15 for final selection: $E/D_2 = 0.3 / 16.21 = 0.0185$

Minimum overlap ratio needed to control Gap A effect is: X = 3.85 Min

Hence selecting X = 4.5, we are within the recommended range in Figure 8-15. If E is increased to 0.324, we have a perfect arrangement for the hub side, which will result in:

- Optimum control of hydraulic stability at part load
- Best possible efficiency
- Good damping effect for the rotor
- Proper control of axial thrust at part load

On the shroud side, $F = 0.4\text{-}F / D_2 = 0.025$ X = 5 is needed.

Final selection for both sides is: X = 4.75

It is impractical to select different values for the two sides from a machining practicality point of view. It is too expensive, and more mistakes can be made during the machining of the components.

8.5 Efficiency Gain or Loss When Gap A Modifications Are Introduced

When geometry corrections are applied to a multistage boiler feed pump, reactor feed pump, or any other pump type to control or regain hydraulic stability, if done correctly, an improvement in efficiency will accompany these modifications. Some engineers claim the opposite; namely, a loss of efficiency. Earlier work done in the 70s and 80s with the aggressive thinking of Texas Utilities resulted in consistent efficiency improvements in many of their power stations on a very large number of boiler feed pumps and booster pumps [1 and 2]. Similar results followed in the Southern Company stations for an equally large number of cases [25 and 28].

Figure 8-13 shows pump performance before and after modification by the OEM, showing a clear loss of 1.5% efficiency. After proper analysis of the modified geometry, the Overlap Ratio for Gap A was found to be X=10. The reason for this efficiency loss is quite clear from Figure 8-14, namely the excessive Overlap Ratio. High Overlap Ratio produces increased rotor damping, which was greatly reduced in this case by the labyrinth serrations put in by the OEM on the Gap A surface. Pressure pulsation at the vane passing frequency was very low because Gap B was increased to 18.5%. When the same modifications were introduced properly in similar pumps, an average of 2% increase in efficiency was experienced. Hydraulic stability, however, was achieved in all cases in the previously unstable flow ranges including stabilizing the axial thrust of the pump rotor. Carefully made corrections resulted in a clear 2% efficiency gain at the Limerick nuclear reactor feed pumps (see Figures 8-11 and 8-12) and were reported in detail in Reference 11.

A 4% efficiency gain was reported [16] after the thorough modification of the LCRA-Ferguson BFP. Gaps A, B, and the Overlap were carefully optimized as shown in Figure 5-7 and Section 8.2.7.

Many other cases could be quoted from the over 800 modifications introduced by the author just on Gap A dimensions (see Figure 9-1). A few cases where efficiency loss was reported can be analyzed for a possible explanation. Some of the sources of trouble can be traced to the following conditions:

- Incorrect Selection of Dimensions: A 1.5% efficiency loss was reported in Figure 8-13. An Overlap Ratio of X=10 was selected inadvertently and introduced very high friction losses.
- Casting Inaccuracies: These resulted in incorrect impeller/diffuser ratio of b_3/b_2 less than one (see Figure 8-18). Gap A did not work.
- Assembly/Q.A. Mistakes: Gap A insert rings were left out during pump assembly at the site (see Figure 8-17). Gap A did not work.
- Alignment: Misaligned impeller/diffuser resulted in high vibration (see Figure 11-16). It also resulted in high axial thrust at part-load operation (see Figure 11-13), causing major failures of the rotor.

The above and many similar cases are associated with loss of efficiency. When loss of efficiency is evident, it is easy to blame it on Gap A because it is more difficult to review the case on the drawing board, in the repair shop, or at the site. Gap A does not work without a bridge over those gaps, as shown in Figure 8-12.

Test 1: Original factory acceptance test (not shown)

Test 2: Pump re-tested

Test 3: Gap A and B modifications

Test 4: New impeller design for low flow stability and all modifications of Test 3

After obtaining approximate values for Gap A, the Overlap, and the Overlap-Ratio from Figure 8-14, and with the given dimensions of the pump to be modified, Figure 8-15 permits the user to optimize those dimensions depending on the goals of the modification, for example, higher efficiency, more damping, and stabilization of thrust forces. Both sides (hub and shroud) should be analyzed for optimum performance.

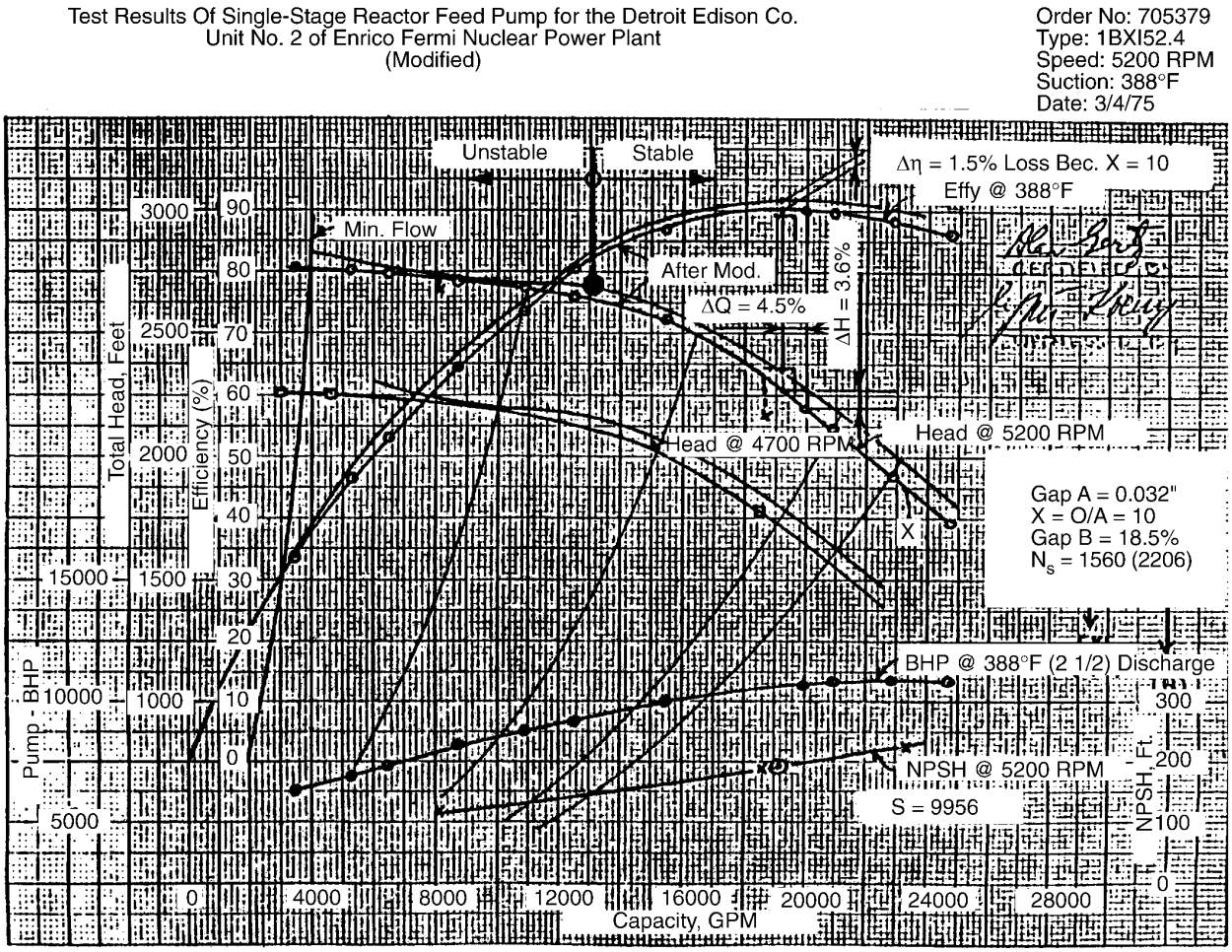

Figure 8-13
The OEM's Gap A Modification Results in 1.5% Loss of Efficiency Due to Excessive Gap A Overlap

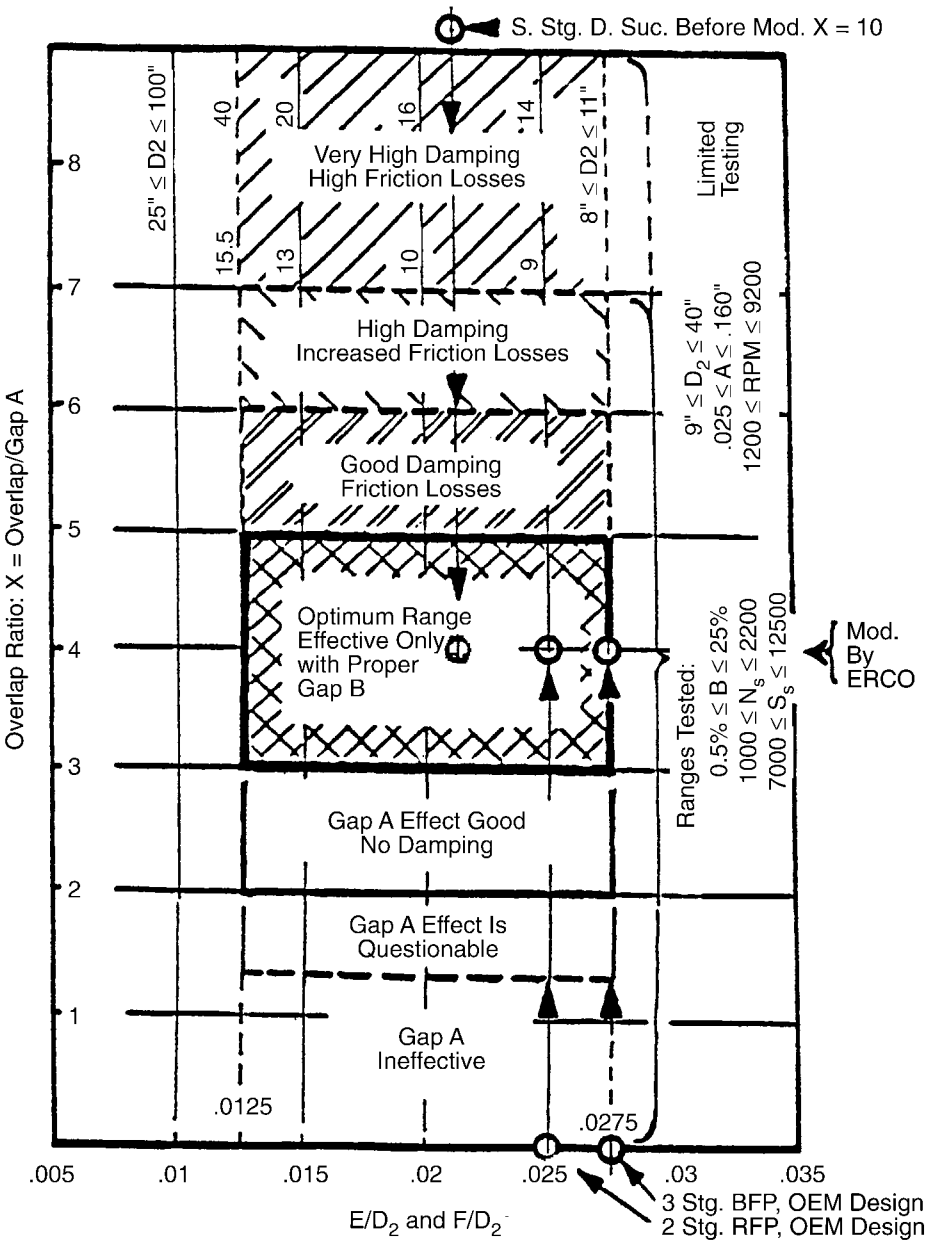

By applying the basic design charts, three specific applications are shown above: (1) Large single stage double suction nuclear reactor feed pump with an overlap ratio of 10, (2) Two stage nuclear reactor feed pump, and (3) Three stage bolier feed pump, both applications with zero overlap. In all three cases, ERCO recommended optimum ratio of 4 with Gap A = 0.050". The modifications since have been incorporated resulting in excellent vibration behavior and hydraulic stability.

Equally applicable to diffuser and volute designs, single- and multistage, and single, twin-, and double-suction pump designs; however, all three of the above applications are of the diffuser type.

Figure 8-14
Design Chart for Gap A and Its Overlap Ratio Applied to Three Specific Feed Pump Modifications

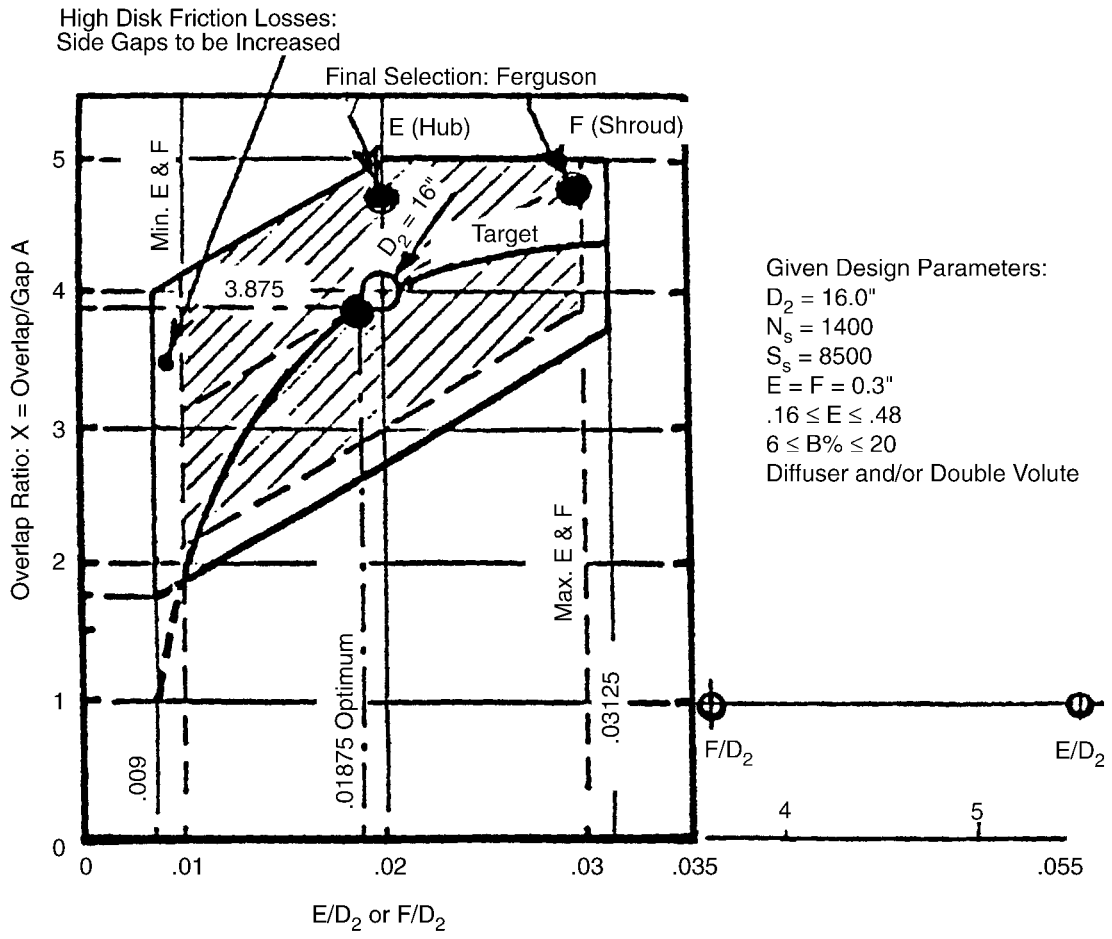

Gap A design chart to optimize one specific pump design modification.

Equally applicable to diffuser and volute designs, single- and multistage, and single, twin-, and double-suction impellers. The above design is a diffuser type.

Figure 8-15
Optimization Chart for Gap A Overlap Applied to One Specific Feed Pump Design Modification Figure

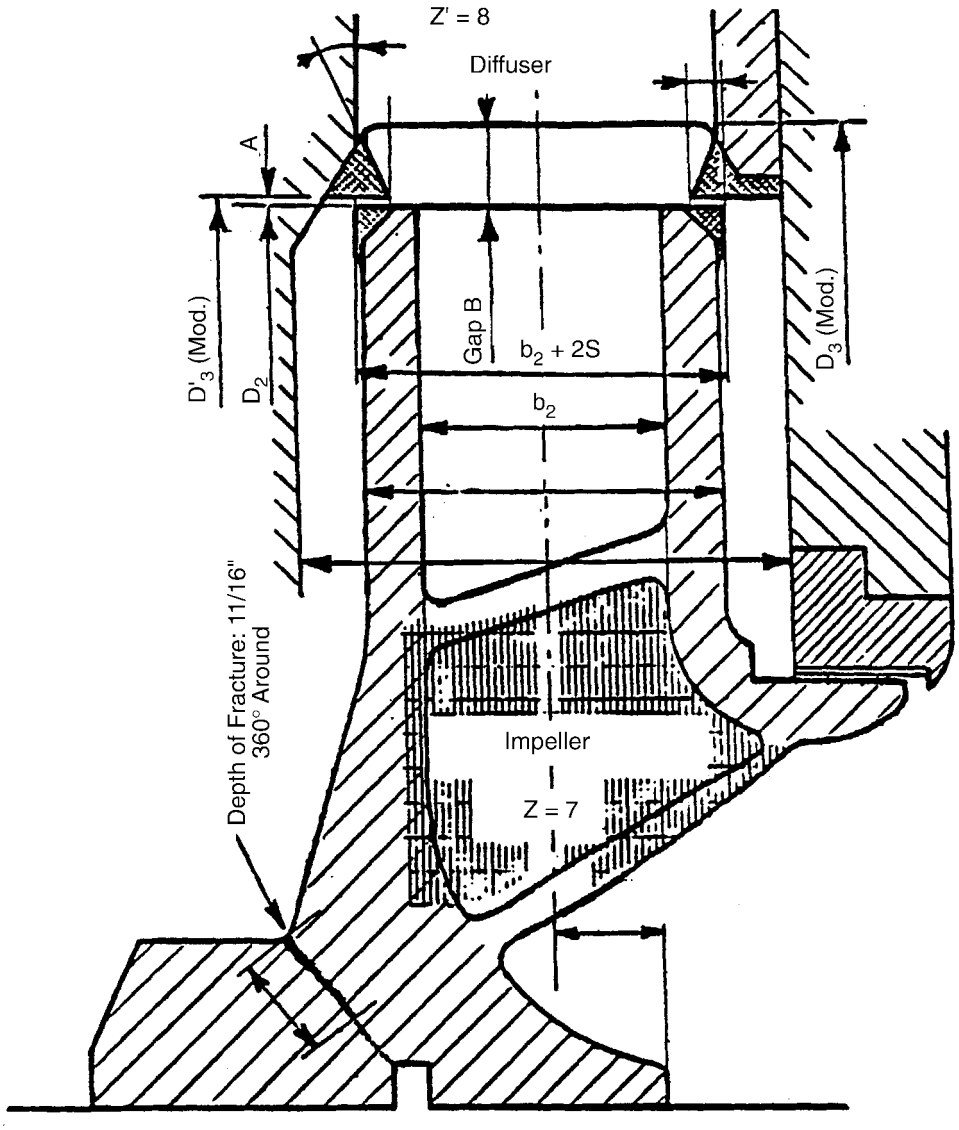

Nuclear reactor feed pump impeller breakage. Impeller-diffuser geometry modification to stabilize head-flow characteristics and to eliminate pressure pulsation behind the impeller sideplates, root cause of impeller breakage. Depth of fracture: 11/16", 360° around.

Figure 8-16
Multistage Nuclear Reactor Feed Pump Gap A and B Modification

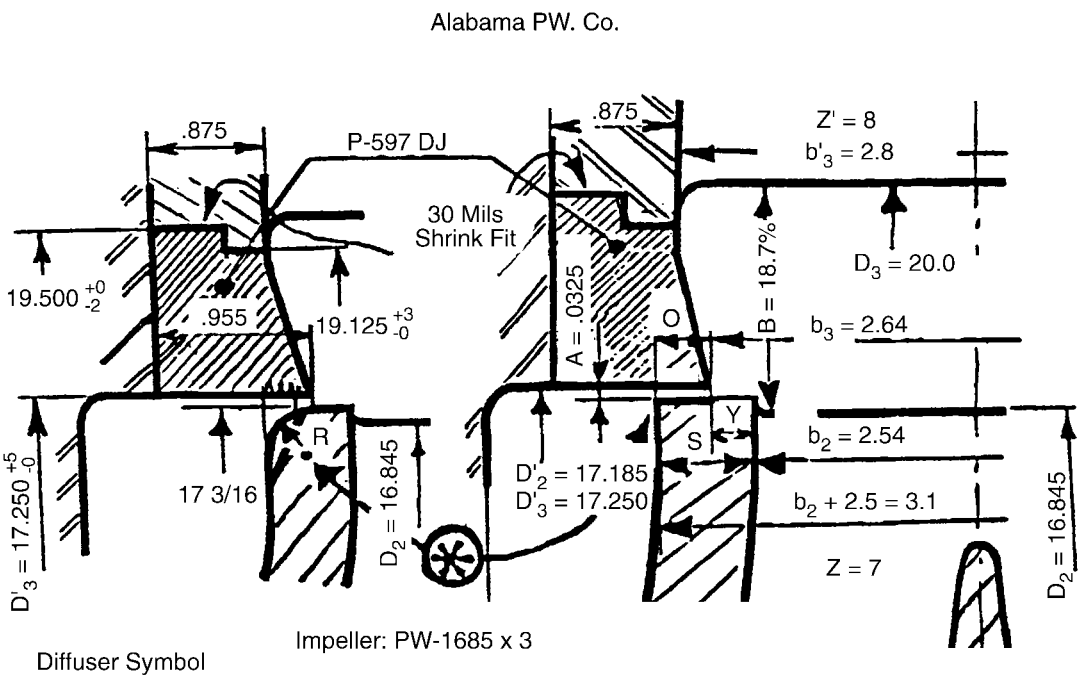

Impeller: PW-1685 x 3

Diffuser Symbol

- O Original: P-597DNx3
- O Modified: P-597 GPx2

- O Gap A and Overlap Ratio: X = O/A = .230/.0325 = 7.0
- O Y = 0.050 (Not enough rotor axial alignment is difficult: If b_3 = 2.74, then Y = 0.1 and X = .18/.045 = 4. Most ideal number, see Figures 8-5 and 8-6.)

- O Gap B: D_3/D_2 = 20.0/16.845 = 18.7%

⊛ Inspect if impeller shroud O.D. is radiused or chamfered. The X overlay ratio is critical for axial shuttling.

Inspected pump at the Farley Nuclear Plant with DeLaval representative and Alabama representative on 10-10-86. We found no radius or chamfer. The diffuser was machined to receive the Gap A ring, but was not put in place (In 1979). Good reason for the previous vibration history. Inspected pump again on 8-30-89.

D (Jour) = 4.500/4.494
DeLaval Assy. Drwg. No: F-10860/Rev. 17

Figure 8-17
Modification to a Nuclear Feed Pump with History of Rotor Axial Shuttling and Vane Passing Vibration

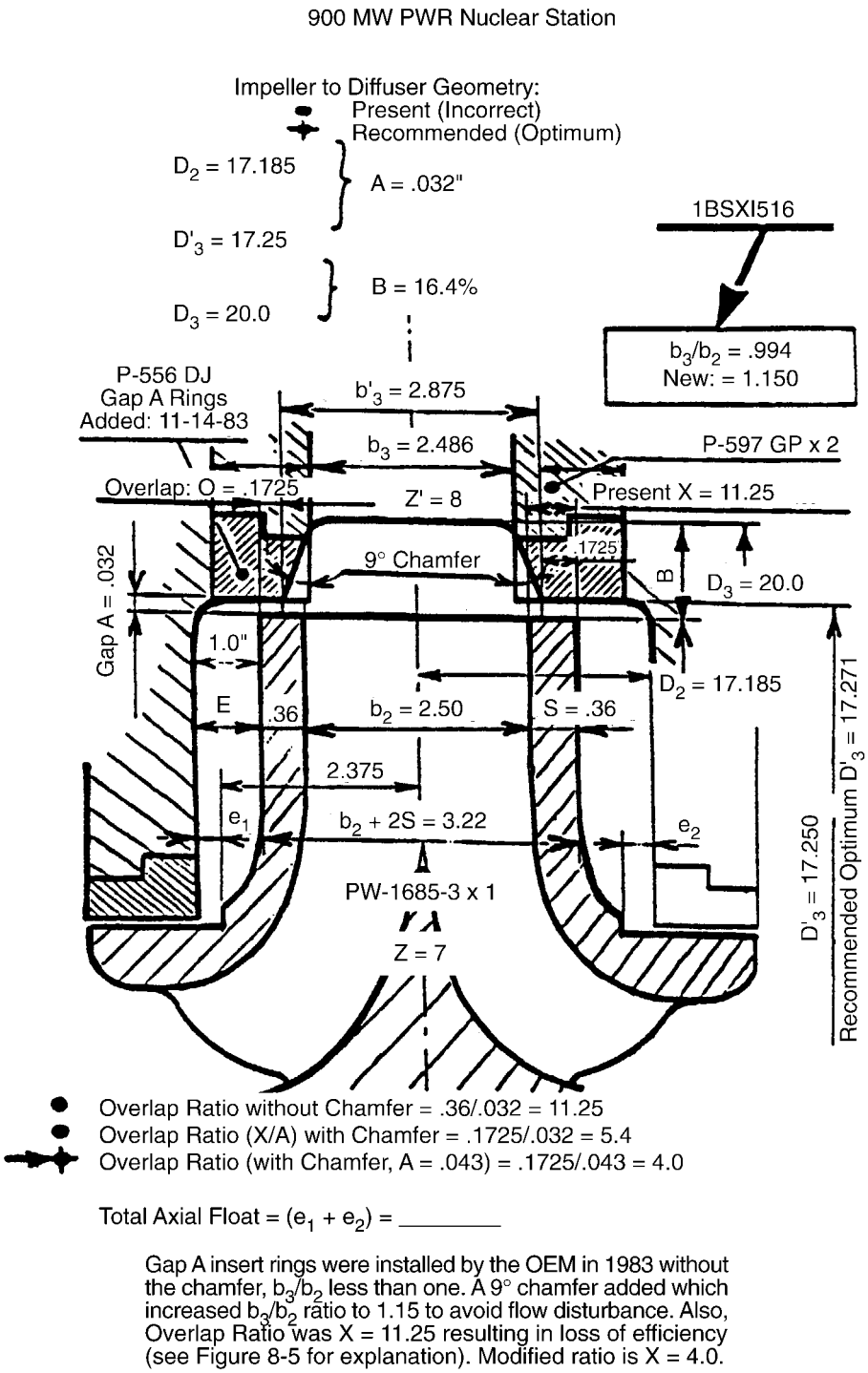

Figure 8-18
Gap A Rings With and Without Chamfer at the Diffuser Inlet for a Nuclear Reactor Feed Pump

9
SURVEY OF HYDRAULIC PARAMETERS

A systematic survey of various pump geometries and design parameters was conducted by ERCO throughout the past 25 years in order to arrive at optimum hydraulic channel geometries, especially for part-load hydraulic stability. Understanding and control of rotor axial thrust, vibration characteristics, effects on efficiency, improved machine reliability, and rotor assembly practices were some of the main objectives for this long range work. Modifications were introduced in a large number of nuclear and fossil power plant applications for various ranges of these parameters. Many of the modified pumps were properly tested under the guidance of ERCO. A large number of cases included laboratory type testing, especially to establish optimum dimensions for Gaps A and B, the Overlap-Ratio (X), and the effects on loss or gain of efficiency, as these parameters were rigorously varied. Ranges for several of the quantities tested by ERCO are presented in Table 9-1. In order to get a feel for the large number of modifications performed during the last few decades, the number of pumps modified in three select areas is shown in Figure 9-1.

Table 9-1
Various Dimensions and Parameters Tested and Compiled by ERCO in a Large Number of Nuclear and Fossil Power Stations

Parameter	Minimum (In/mm)	Maximum (In/mm)
D_2	8/203	100/2540
b_2	0.75/19	9/228
b_3/b_2	0.9	1.5
Gap A	0.024/.6	0.3/7.62
Gap B	0.4%	34%
Gaps E and F	0.07/1.8	1.0/25.4
X=O/A	0	16
RPM	500	13,500
N_s	1,100/21	2,200/42
S_s	8,000/152	13,500/257

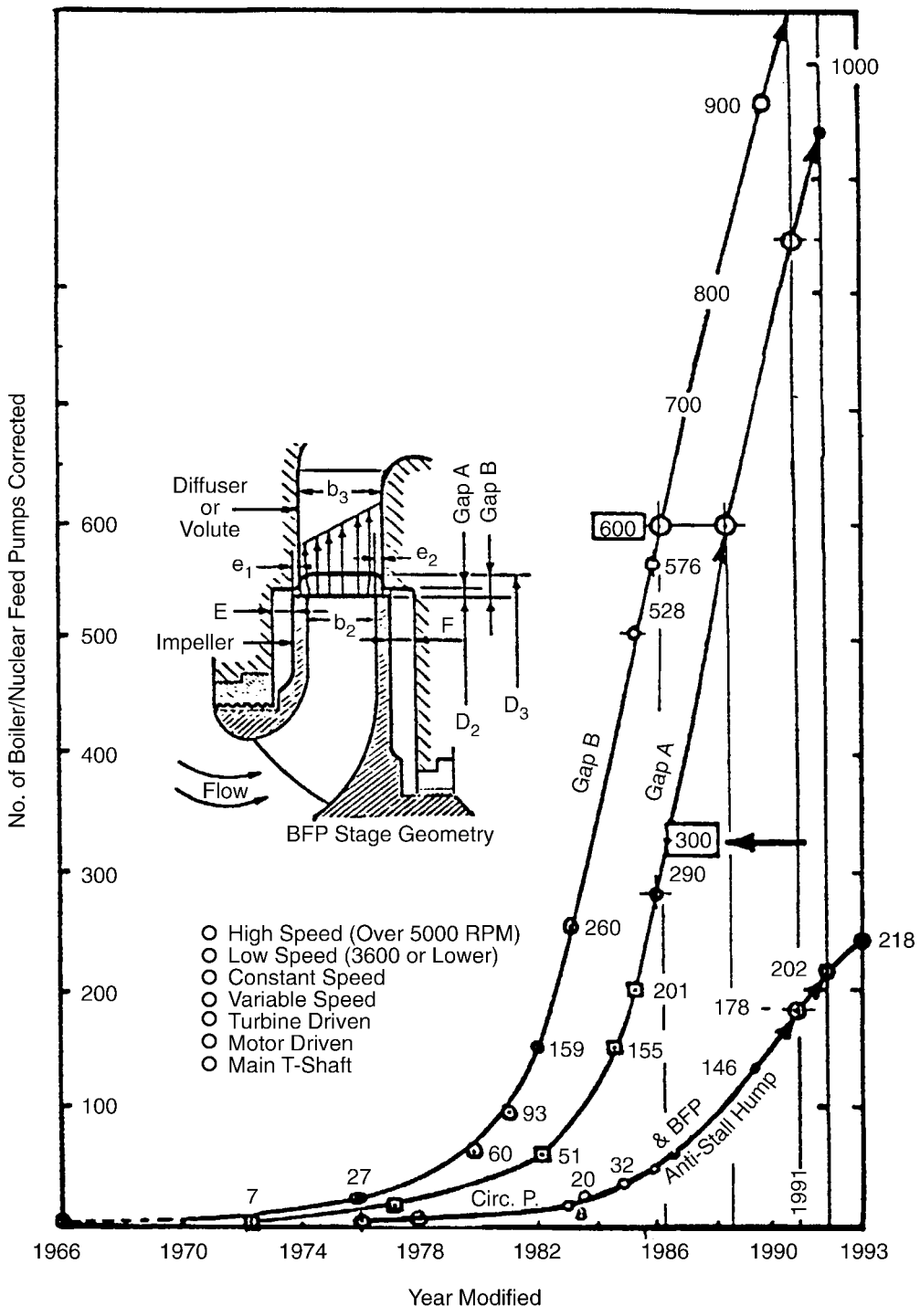

No. of troublesome boiler/nuclear feed pumps (BFP/NFP) modified with ERCO assistance for optimum Gap A, the Overlap, and Gap B during the past years. Also, circ. pump modifications with impeller back-filing and application of the anti-stall hump to eliminate inlet cavitation damage and to increase flow capacity (if needed). The hump was also applied to several high-energy-input BFP/NFP first stage impellers with very high success.

Figure 9-1
History of Gaps A and B and Anti-Stall Hump Modifications by ERCO for the Utilities

9.1 Backflow Deflector

The backflow deflector, as called by NASA since 1966 [14], called eye-catcher at ERCO, backflow recirculator as termed by Ingersoll-Rand since 1983 [15], is shown in Figure 9-2. The backflow deflector eliminates flow-induced vibration amplitudes, apparently in the same very low frequency range (below 10 Hz) as Gap A, in a large eye impeller design (that is, high suction specific speed, S_s). This proves that the origin of hydraulic instability is governed strongly by the S_s of the impeller design. A detailed discussion can be found in Reference 14, a program in which Dr. E. Makay was a reviewer for the *NASA Project Manager* in 1970 and 1971. For high-energy-input boiler feed pump (BFP) applications, the impeller design S_S is considered low; hence, gaps A and B are dominant. Detailed discussions on the deflector are given in References 11, 14, and 15 for high S_s designs; while for $S_s < 12{,}500$ (that is, low S_S designs), discussions are presented in detail in References 1, 2, 4, and 11.

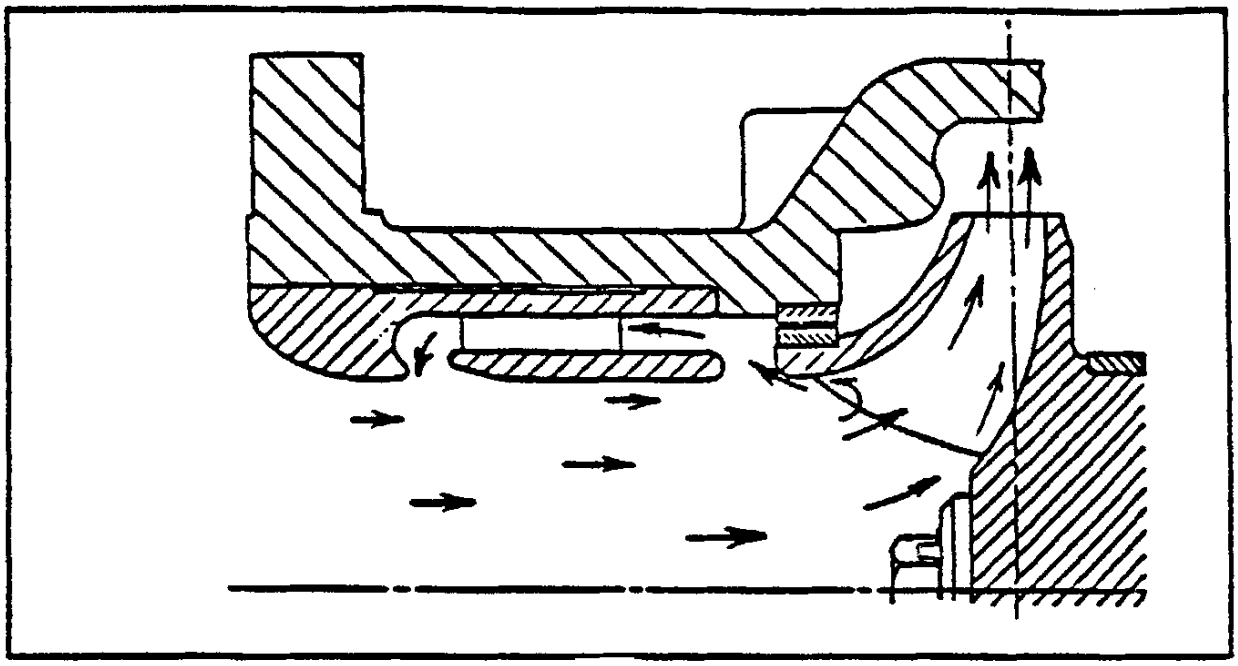

Figure 9-2
Backflow Deflector/Eye-Catcher [14, 15]

9.2 Eye Ring

The eye ring first appeared in the literature in 1969 as an ASME research paper by Murakami and Hey [60] to improve pump performance (stability at part load) of a high specific speed circulating pump with a mixed (almost axial) flow impeller by throttling the flow at the impeller eye. It was first introduced in the U.S. by Makay and Drechsler in 1973 in a large nuclear power plant for testing purposes only, as discussed in Reference 36 and as shown in Figure 9-3.

Later, in January 1991, the same concept was proposed by ERCO for the Vogtle and Farley nuclear plants to prove the presence of hydraulic instability in the low flow range of their residual heat removal (RHR) pumps during testing at Ingersoll-Rand as a research and development project. The eye-ring configuration is shown in Figure 9-4. The impeller suction specific speed (S_S) is close to 13,000, hence either or both the eye and the impeller exit (Gap A) can be responsible for the flow instability. The specific speed of the pump was 1650.

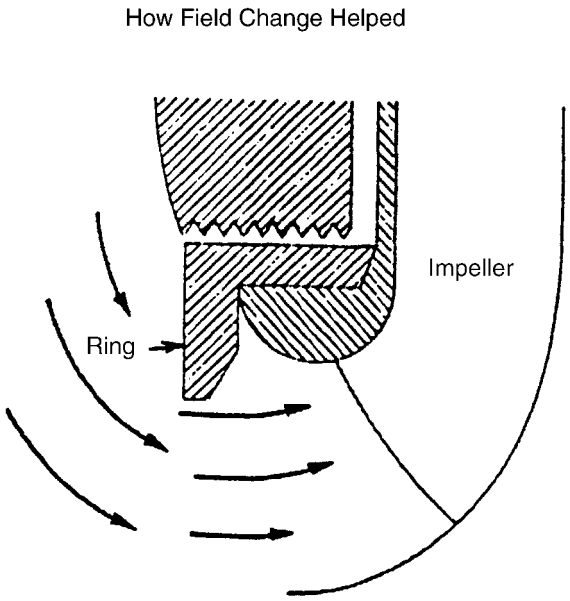

Figure 9-3
Impeller Eye Insert Ring [35]

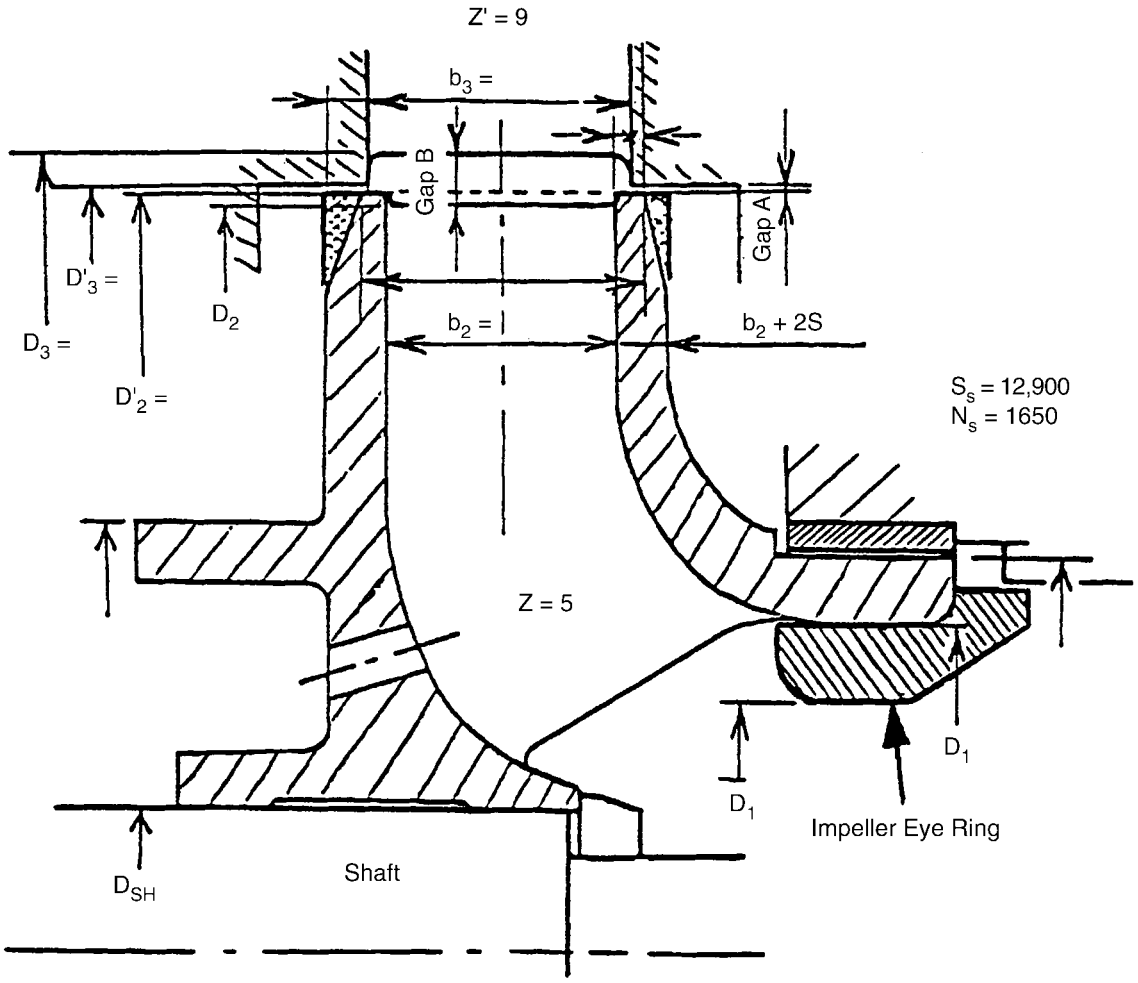

Figure 9-4
Impeller Eye Insert Ring Applied to the RJR Pumps During R&D Testing at Ingersoll-Rand to Find the Root Cause of the Low Flow Hydraulic Instability

10
PUMP HYDRAULIC INSTABILITY

The definition of hydraulic instability used here is not intended to satisfy the pure academic researcher. Instead, it gives a practical definition for those who must recognize it and cope with it, mainly pump designers, power plant engineers, maintenance people, and operators.

Once the flow becomes disturbed in the pump hydraulic channels to the point that the pump demonstrates higher-than-permitted rotor vibration levels, a phenomenon defined as pump-induced hydraulic instability occurs. This is characterized by high-pressure pulsations that cause damage to various components, feedwater piping vibration, feedwater or control system instabilities or complications, an unstable turbine drive governor, and excessive feedwater flow fluctuations. It is well defined in Reference 1, with several field examples given, and discussed further in Reference 11.

10.1 Minimum Recirculation Flow Requirements

The proper pump minimum flow requirement is a vital question in power stations. In particular, two separate pump types are discussed for the subject of minimum flow:

- Safe minimum recirculation flow for high-energy-input pumps such as boiler feed pumps (BFP), nuclear feed pumps (NFP), and reactor feed pumps (RFP). This is a realistic, practical question that affects plant reliability and availability.
- Minimum flow requirements for nuclear safety-related pumps, such as nuclear auxiliary feed pumps, RHR pumps, and HPSI pumps, as requested by the NRC Bulletin 88-04. These are usually lower level energy input pumps when compared to feed pumps; hence, it is somewhat more of a hypothetical question.

Hydraulic instability is probably the single most important criteria for establishing pump minimum flow requirements. There were no established design bases because competition among manufacturers dictated the requirement. Pump heatup during minimum flow operation and not hydraulic instability was the basic consideration by Worthington and others. The onset of hydraulic instability and, therefore, the recommended minimum flow depends on several parameters or factors such as:

- Geometry of pump hydraulic components
- Pump speed
- Pump size and type
- Constant or variable speed

- Horsepower input per stage
- Head per stage
- Specific speed (N_S) (see Figure 10-1)
- Suction specific speed (S_S) (see Figure 10-1)
- Quality of all machined and cast components (that is, application of quality controls)
- Quality and precision of rotor assembly

Anticipated useful operating ranges are shown in Figure 10-1 for pumps used in large nuclear and fossil power plants as functions of N_S and S_S. The inner line of the chart is for a properly designed impeller stage. The design margin is a function of the designer's ability, experience, and how up to date the designer is on current technology. Impellers with a larger-than-normal impeller eye, as indicated by high values for S_S, require higher minimum (recirculation) flows. Impellers with S_S higher than about 12,000 are not practical in power plant applications listed previously due to their high sensitivity to impeller eye (inlet) cavitation damage. Remedies to reduce such damages, such as the hook at the root of the vane inlet, vane elliptical shape, the anti-stall hump, or the backflow recirculator, are available and are often implemented to correct existing design mistakes. The last two are rarely used as design tools for new applications.

Figure 10-2 was published by Ingersoll-Rand for small pump applications in the petrochemical industry. It was quoted by several lecturers during the 1989 ASME/NRC Symposium as a guide for nuclear safety-related pump applications. Figure 10-2 in its present form does **not** apply to safety-related pumps, and especially it does not apply to boiler feed pumps. It was found that several institutions attempted to apply it incorrectly to auxiliary feed pumps in nuclear plants to establish minimum flow requirements as requested by the NRC Bulletin 88-04. Suction specific speed, the main variable in Figure 10-2, is only one of the many parameters that should be considered. For example, if hydraulic instability is already present (especially if it is well pronounced), the required minimum flow for that particular impeller and pump would be much higher than for another pump with stable characteristics in that same flow regime.

The useful operating range of a large single-stage, double-suction nuclear reactor feed pump is shown in Figure 10-3. Hydraulic instability islands were discovered during factory witness testing on both pumps at much higher flows than expected. Differences in the onset of instability locations, 76% of BEP for Pump No. 1 and 69% for Pump No. 2, are accredited to casing and impeller sand casting tolerances. Both pumps performed stably at 5200 RPM between 20% minimum (recirculation) and 130% run-out flow conditions after the introduction of proper gap; axial shuttling of the rotor was completely eliminated.

It was shown in Figure 8-13 that a Gap A modification by the pump OEM resulted in a 1.5% loss of efficiency due to excessive Gap A Overlap-Ratio (X=O/A=10) that caused high friction losses as shown in Figure 8-5. A high Gap A Overlap-Ratio resulted in excellent damping characteristics; however, in this case its effectiveness was lost due to the labyrinth seals put into the Gap A surface by the OEM. Pressure pulsation amplitudes were very low at vane passing frequency because Gap B was increased to 18.5% of the impeller diameter. When the same modifications were properly applied to similar pumps, an average of 2% increase in efficiency was measured, as reported in Reference 11 and as shown in Figures 8-12 and 10-12. Hydraulic

stability was achieved in the previously unstable flow range, including complete stabilization of axial thrust on the pump rotor.

The primary issue discussed in this chapter is determining the appropriate minimum flow for a particular design and application. A summary of figures is listed below to answer the question:

- Texas Utilities-Decordova (Figure 10-10), should minimum flow be 72% or 25% of BEP?
- Texas Utilities-Eagle Mt. (Figure 10-11), should minimum flow be 62% or 20% of BEP?
- Philadelphia Electric-Limerick (Figure 10-12), should it be 56% or 20%?
- Detroit Ed.-Enrico Fermi 2 (Figure 8-13 and 10-3), should the minimum flow be 76%, 69%, or 25% of BEP?
- PP&L-Montour No. 1 (Figure 10-8, described in more detail in Reference 25), should the minimum flow be 62% or 20% of BEP?
- Residual heat removal (RHR) pumps used in PWR applications (Figures 10-5 to 10-7), should the minimum flow be 68% or 12.5 % of BEP?

The answer is: Only if the geometry of the hydraulic passages, bearings, rotor components, etc., is all correct, can then the question, "How much minimum flow?" realistically be determined. Then, for large, high-energy-input feed pumps (roughly the inner line presented in Figure 10-1), would the issue apply. For low-energy-input pumps, such as nuclear auxiliary feed pumps, a somewhat lower value that has to be assessed on a pump-by-pump basis may be correct.

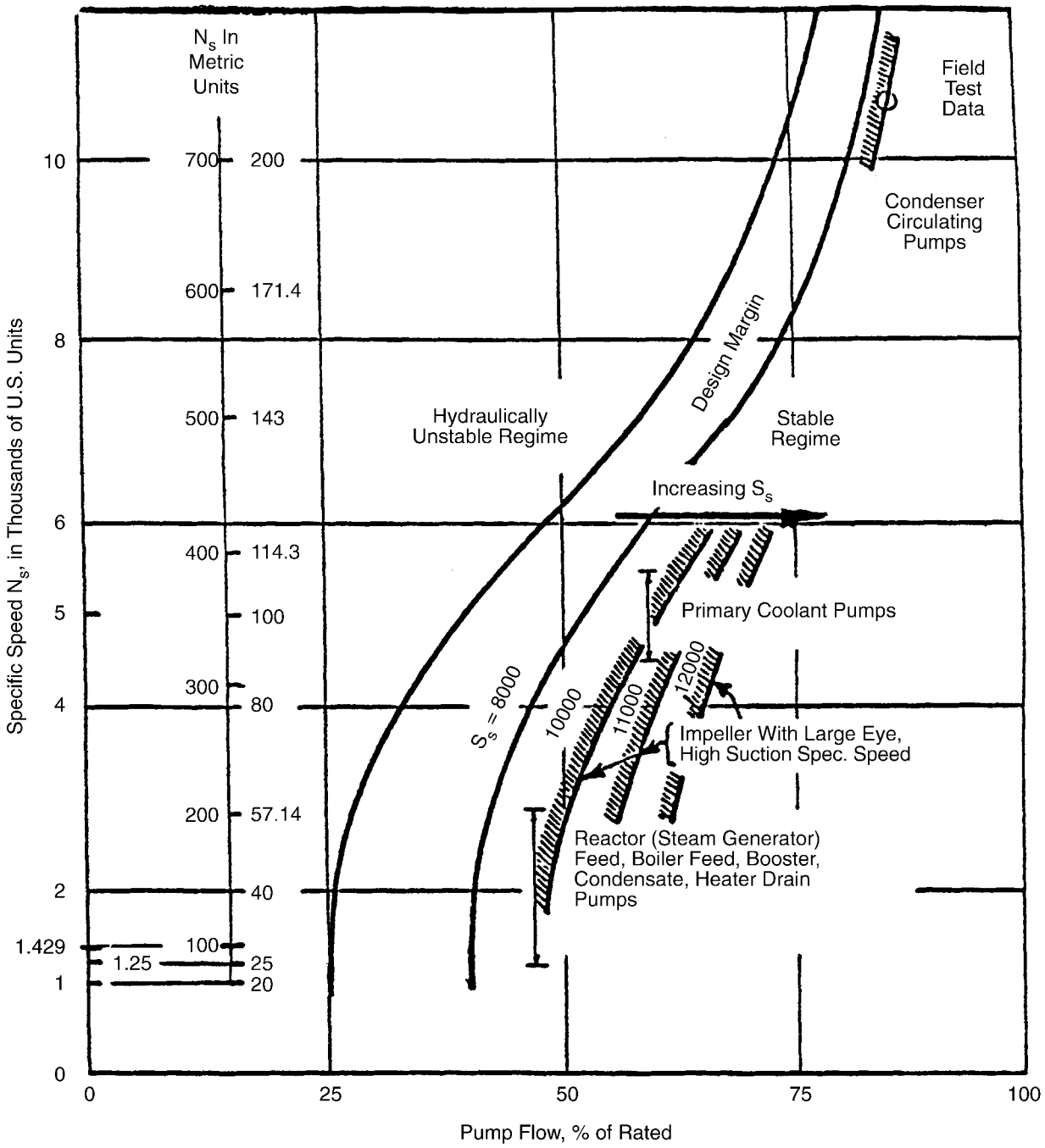

Anticipated useful operating ranges of centrifugal pumps used in large nuclear and fossil power generating units as a function of specific speed (N_s or impeller shape), and suction specific speed (S_s or NPSH).

Figure 10-1
Anticipated Useful Operating Ranges for Pumps Used in Large Nuclear and Fossil Plants

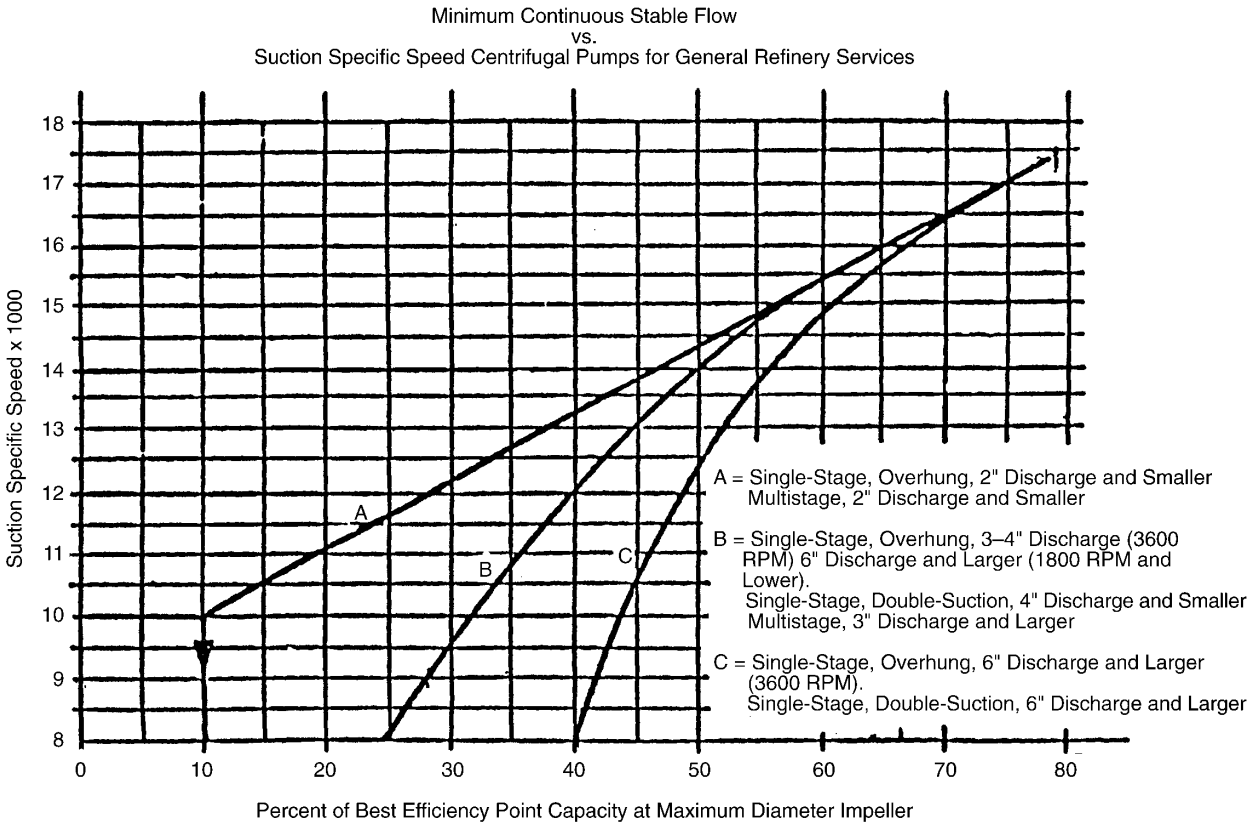

Figure 10-2
Minimum Flow Requirements – Do Not Apply to Nuclear Safety-Related Pumps (Source: Ingersoll-Rand, Charles E. Heald)

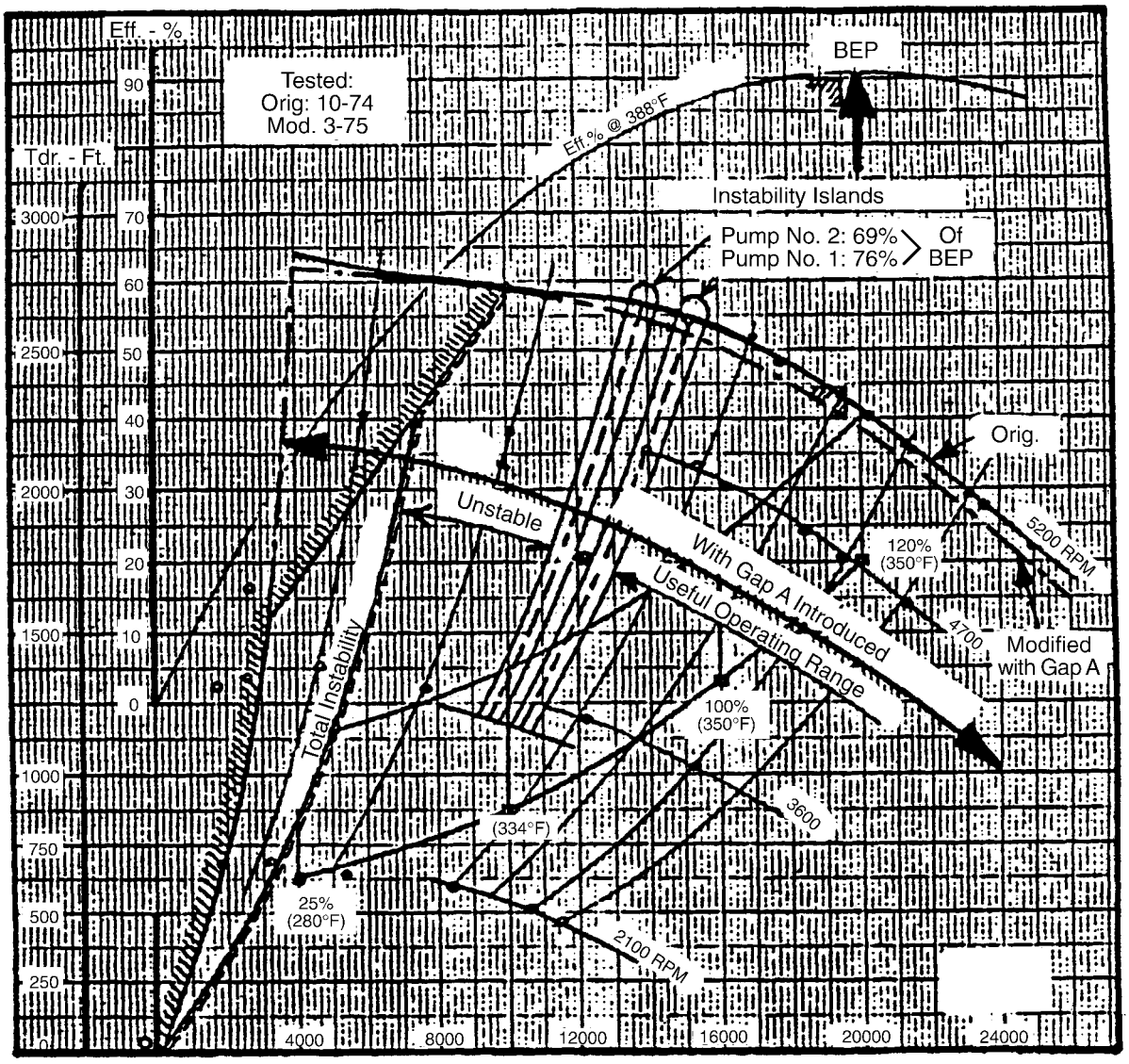

The useful operating range of a large single-stage, double-suction nuclear reactor feed pump is shown above. Hydraulic instability islands were discovered during factory witness testing on both pumps at much higher flows than expected. Differences in the onset of instability locations, 76% of BEP for Pump No. 1 and 69% for Pump No. 2, is accredited to casing and impeller sand casting tolerances. Both pumps performed "stable" at 5200 RPM between 20% minimum (recirc) and 130% run-out flow conditions after the introduction of proper Gap A geometry. Vibration levels and pressure pulsation amplitudes became normal, and axial shuttling of the rotor was completely eliminated.

Figure 10-3
Hydraulic Instability "Islands" in a Large Nuclear Feed Pump (Completely Eliminated with Gap A Modification)

10.2 Hydraulic Instability

Distinction should be made between hydraulic instability and other instability types. The most difficult to separate is hydraulic from rotor-dynamic instability because of the overlapping frequency range between the two phenomena. As discussed in Sections 4.3, 5.0, and 6.0, hydraulic instability problems are often incorrectly diagnosed as rotor dynamic problems.

10.2.1 Determination of Hydraulic Instability

The following ways are typically available to determine hydraulic instability with the limited amount of information available to the troubleshooting engineer:

- In the office with only a performance test curve available (a true test curve, not the French-curve type drawn up by a salesman).
- In the control room with a feedwater flow chart available (see Figure 10-4).
- By analyzing test data taken on the pump. Available measurements may be one or more of the following:
  - Pump discharge pressure pulsation (see Figure 10-5)
  - Shaft radial vibration displacement amplitudes and frequencies (see Figure 3-1)
  - Rotor axial vibration or axial thrust (see Figures 10-7 and 10-8)
- By analyzing test data taken on:
  - The feedwater piping
  - In the power house
  - At the BFP
  - At the turbine drive
  - In the vicinity of the BFP (but not on the BFP)
- In the repair shop during inspection of a failed rotor.

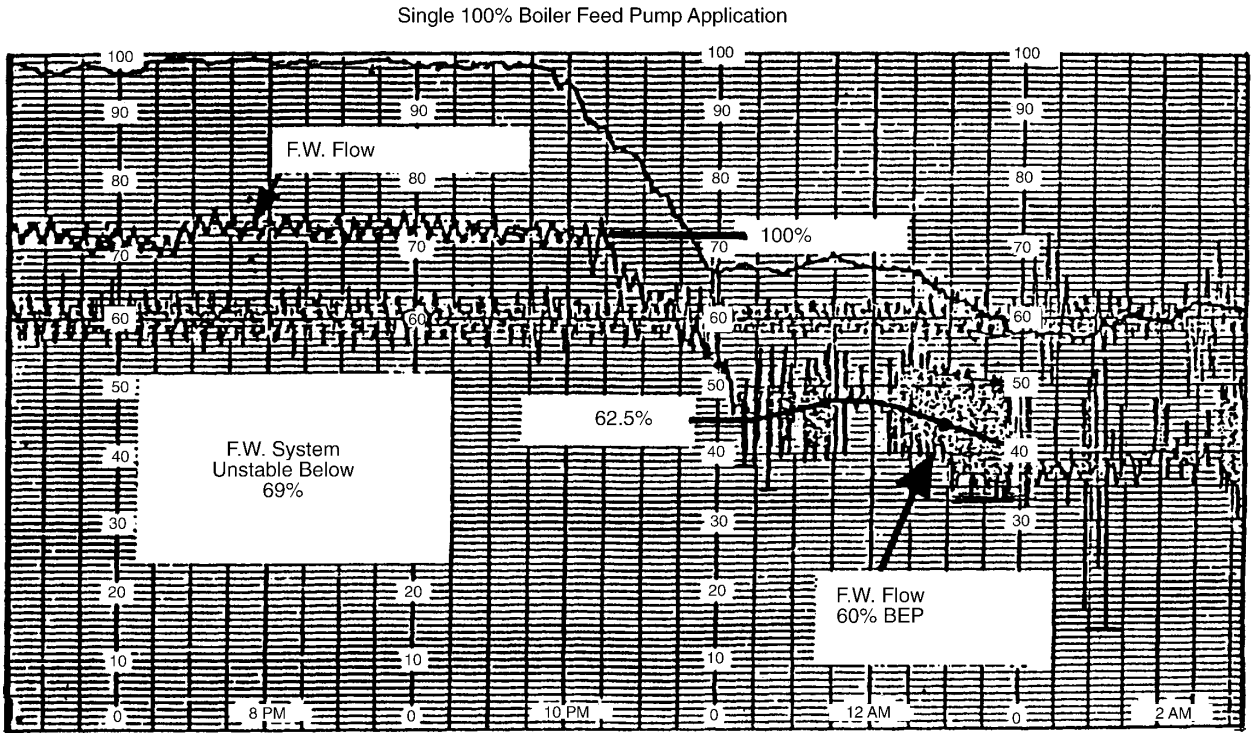

Figure 10-4
Feedwater Flow and System Instability at or Below 65% of Pump BEP

10.2.2 Symptoms of Hydraulic Instability

The following are the symptoms to look for to determine if the pump will develop, presently exhibits, or has experienced hydraulic instability:

- Head-flow (or performance) curve is flat or droopy. This usually occurs between 55% and 75% of BEP. The majority of designs develop this instability at about 65% flow.
- Feedwater flow instability may show strong flow fluctuation in the control room by observing the feedwater flow strip chart (see Figure 10-4).
- Overall pressure pulsation or vibration levels measured for the pump may go up in the unstable (65%) flow regime as shown in Figures 10-5 through 10-7 (RHR pump testing for Farley and Vogtle nuclear plants). Many times, this is accompanied by a 0.3 to 0.9 times RPM subsynchronous vibration component. This subsynchronous component, if it arises, is very distinct.
- Discharge pressure pulsations, at blade pass frequencies or its multiples, in the same flow area as described above.
- Suction pressure pulsation, same as described above. This instability can be very pronounced for impellers with high suction specific speeds (for example, large eye impeller, S_s above 12,000).

- If the pump design incorporates a balancing drum (not a disk), a change of rotor axial position may occur in the unstable flow regime due to a major change in axial thrust (see Figure 10-8).
- High thrust bearing temperature in the unstable flow regime due to a major change in axial thrust.
- Other minor component failures such as coupling damage, seal failure (if mechanical seal), or various broken internal bolts.
- Shaft breakage at Location No. 1 as illustrated in Figure 12-2.
- Feedwater piping vibration. Usually suction piping and at blade pass frequencies or its multiples in the unstable flow regime.
- Turbine drive governor instability in the unstable flow regime.
- Control system instability in the unstable flow regime.

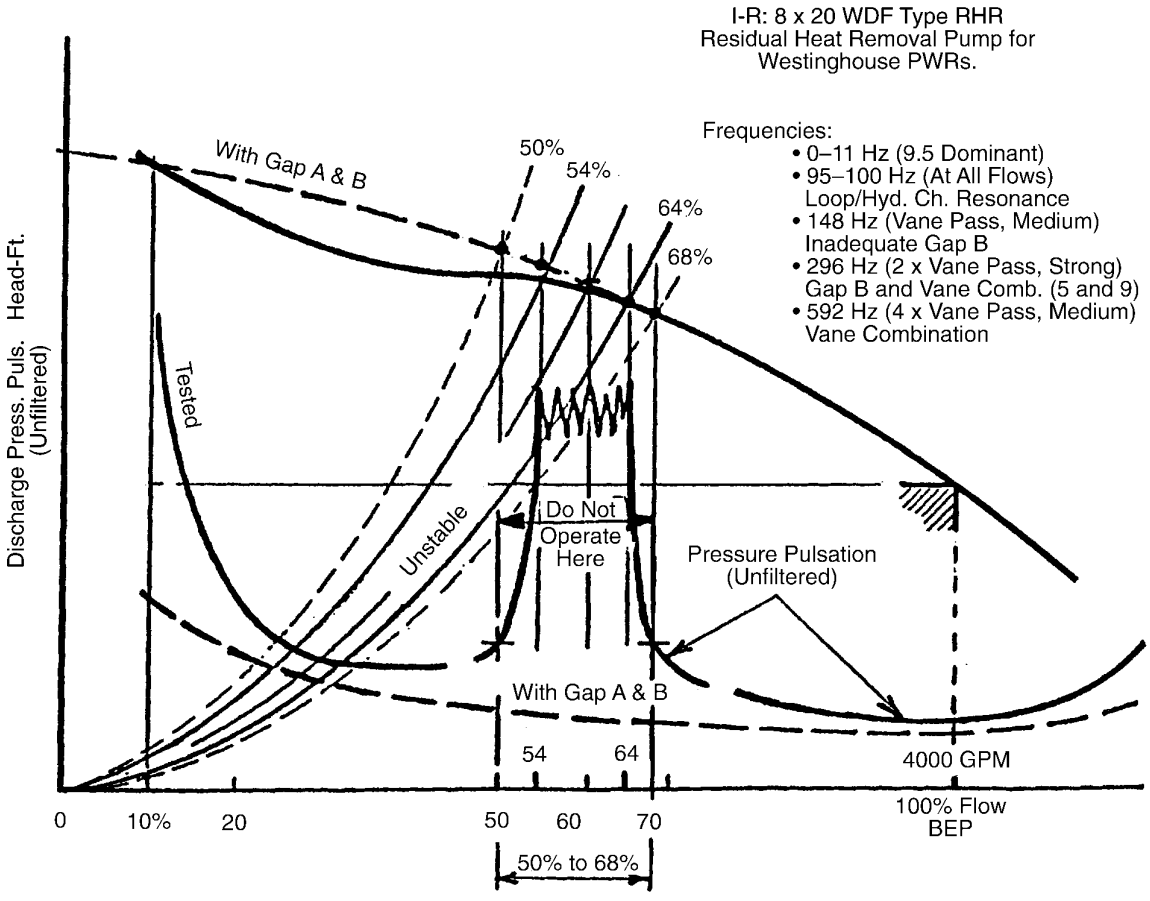

Hydraulic instability as determined by pressure pulsation measurements in the discharge piping. Location of the instability coincides with the midloop flow.

Figure 10-5
Hydraulic Instability of 8x20 WDF Type RHR Pumps as Determined by Pressure Pulsation Measurements at Various Flow Rates

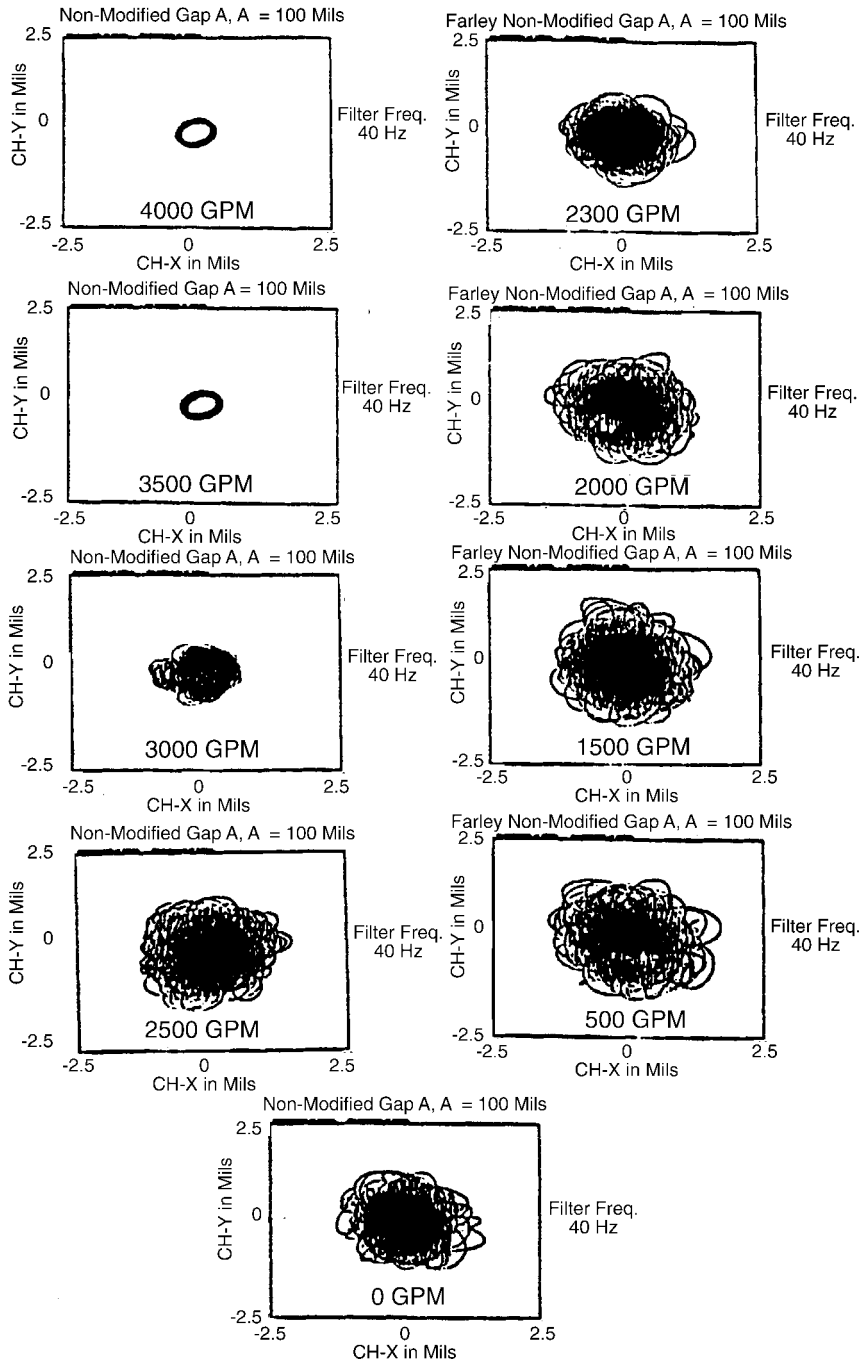

8 x 20 WDF RHR Shaft Orbit vs. Flow

Figure 10-6
Hydraulic Instability of 8x20 WDF-Type RHR Pumps as Determined by Shaft Vibration Measurements at Various Flow Rates

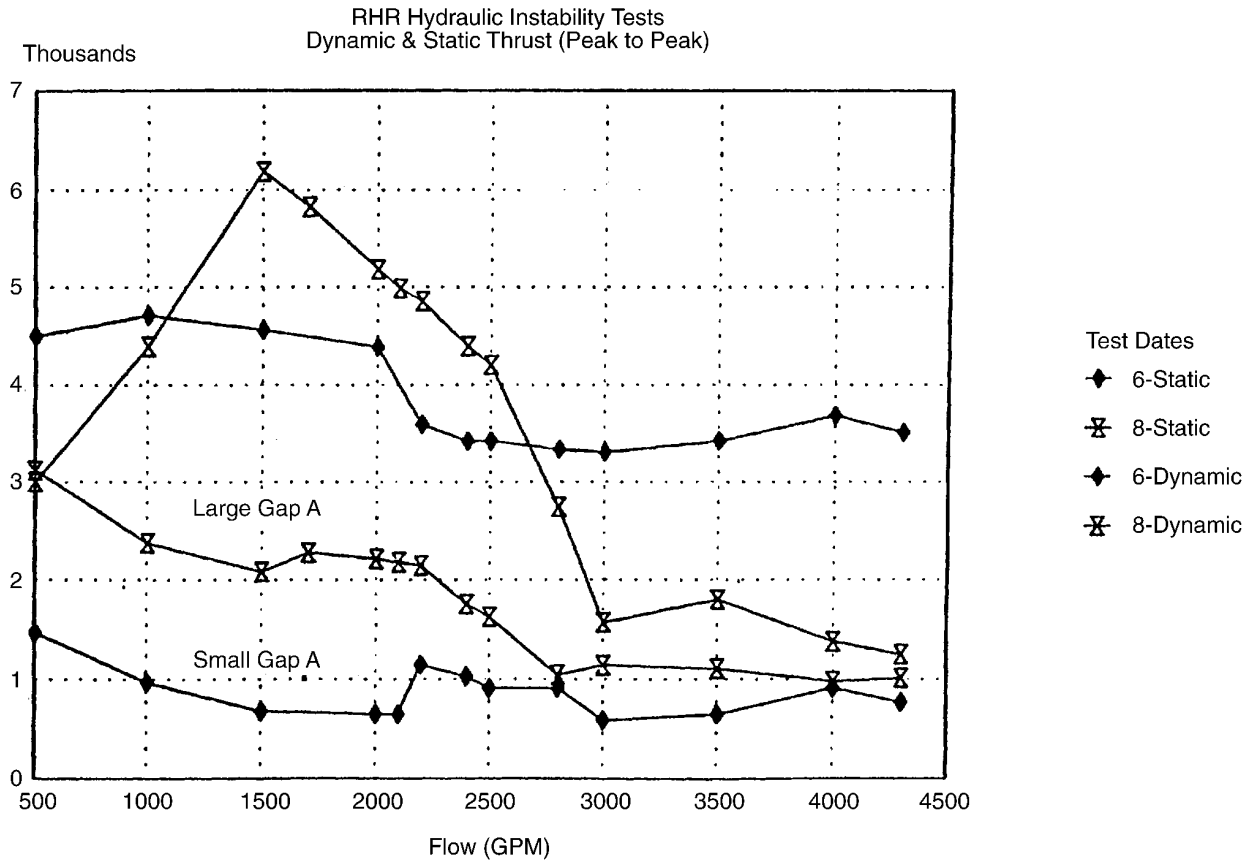

Figure 10-7
Hydraulic Instability of 8x20 WDF-Type RHR Pumps as Determined by Axial Thrust Measurements at Various Flow Rates

Determining hydraulic instability of the pump can be performed in the control room, especially if the operator has problems with controlling the feedwater flow, as shown in Figure 10-4 for a single, 100% boiler feed pump (BFP) application in a large (850 MW) fossil power plant. Feedwater flow began to fluctuate at about 69% of the boiler feed pump design point and got out of control at 62.5% of pump BEP.

Pressure pulsations at the pump discharge nozzle were used to determine hydraulic instability (see Figure 10-5), hence, the useful operating range for residual heat removal (RHR) applications in several large nuclear units. The window shown in Figure 10-5 between 50% and 70% of the BEP is the flow range to be avoided for continuous operation. It is probably safe to go through that island of instability, but a pump should not operate in that flow range for an extended period of time, unless the pump hydraulic components are modified for stability. Dominant frequencies of pressure pulsation measured were:

1 to 11 Hz (9.5 Hz strongest)
Vane passing (medium strong)
2 x vane passing (strong)
4 x vane passing (medium strong)

A major increase of axial thrust was also observed in that flow range, which was expected with the pressure pulsation behavior of the pump.

10.2.3 Field Test Data

The following example describes how hydraulic instability was detected when only field test data were available.

High vibration amplitude appeared at the onset of hydraulic instability at the PP&L-Montour station with an unusually high subsynchronous frequency (.92 x RPM). The instability for this 14WNC-type feed pump was 62% of BEP. It became clear during some well-organized testing that it was a function only of flow, not speed, as was shown before in Figure 5-4. The phenomenon was accompanied by rotor thrust reversal, detected by monitoring the shaft axial position as shown in Figure 10-8. The rotor moved outward (thrust reversed) and destroyed the outboard part of the thrust bearing, also frequently called the unloaded or inactive side, which is a misconception. Namely, a reversal in hydraulically induced axial thrust shows as positive loading on the outboard side of the thrust bearing. Regardless of the speed, thrust reversal occurred at 62% of BEP. This phenomenon, therefore, is concluded to be flow-related (hydraulic) and is not a rotor-dynamic or journal-bearing instability. After the introduction of Gap A and B modifications (no other changes), instability and thrust reversal were completely eliminated.

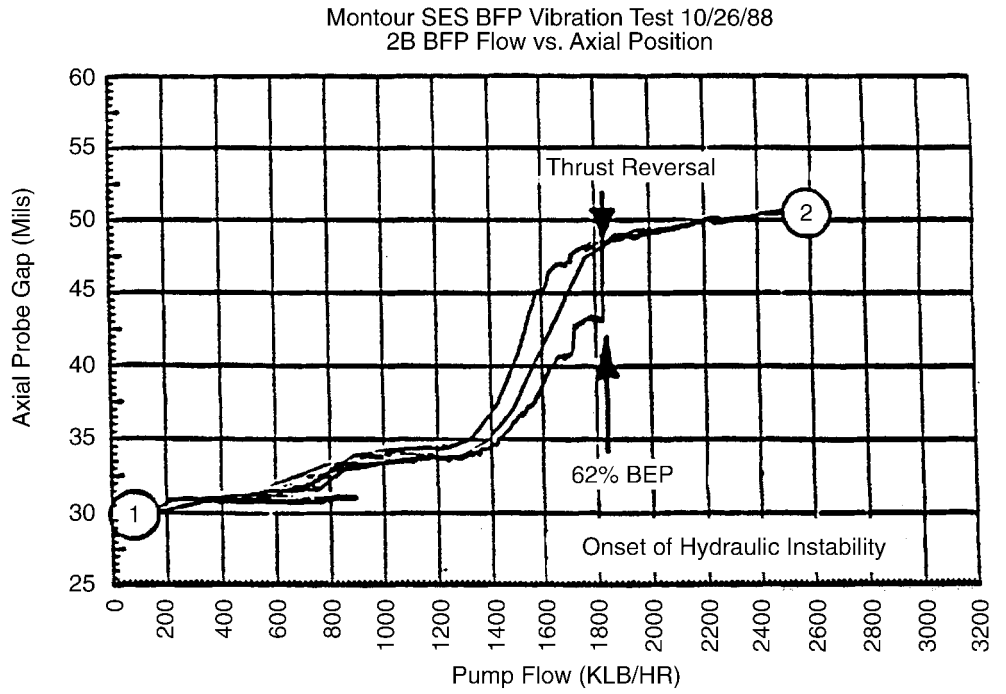

14 WNC-156 Type Boiler Feed Pump Axial Position Before Gap A and B Modification.
Shaft Moves Toward Outboard.

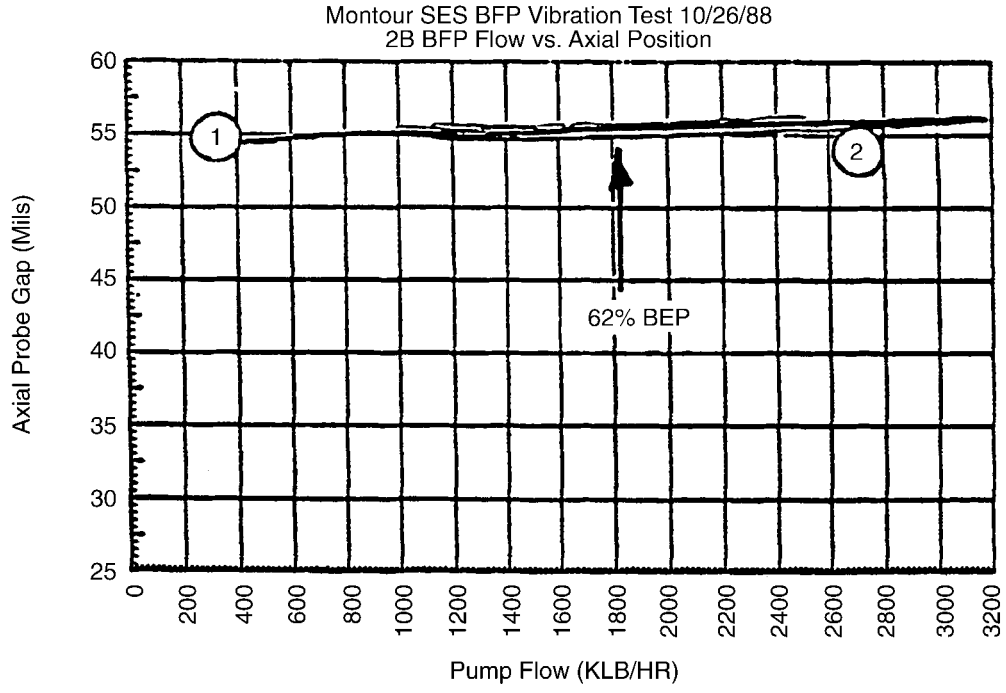

Axial Thrust Stabilized After Gap A and B Modification Introduced.

Figure 10-8
Change in Rotor Axial Position in an Unstable Flow Regime

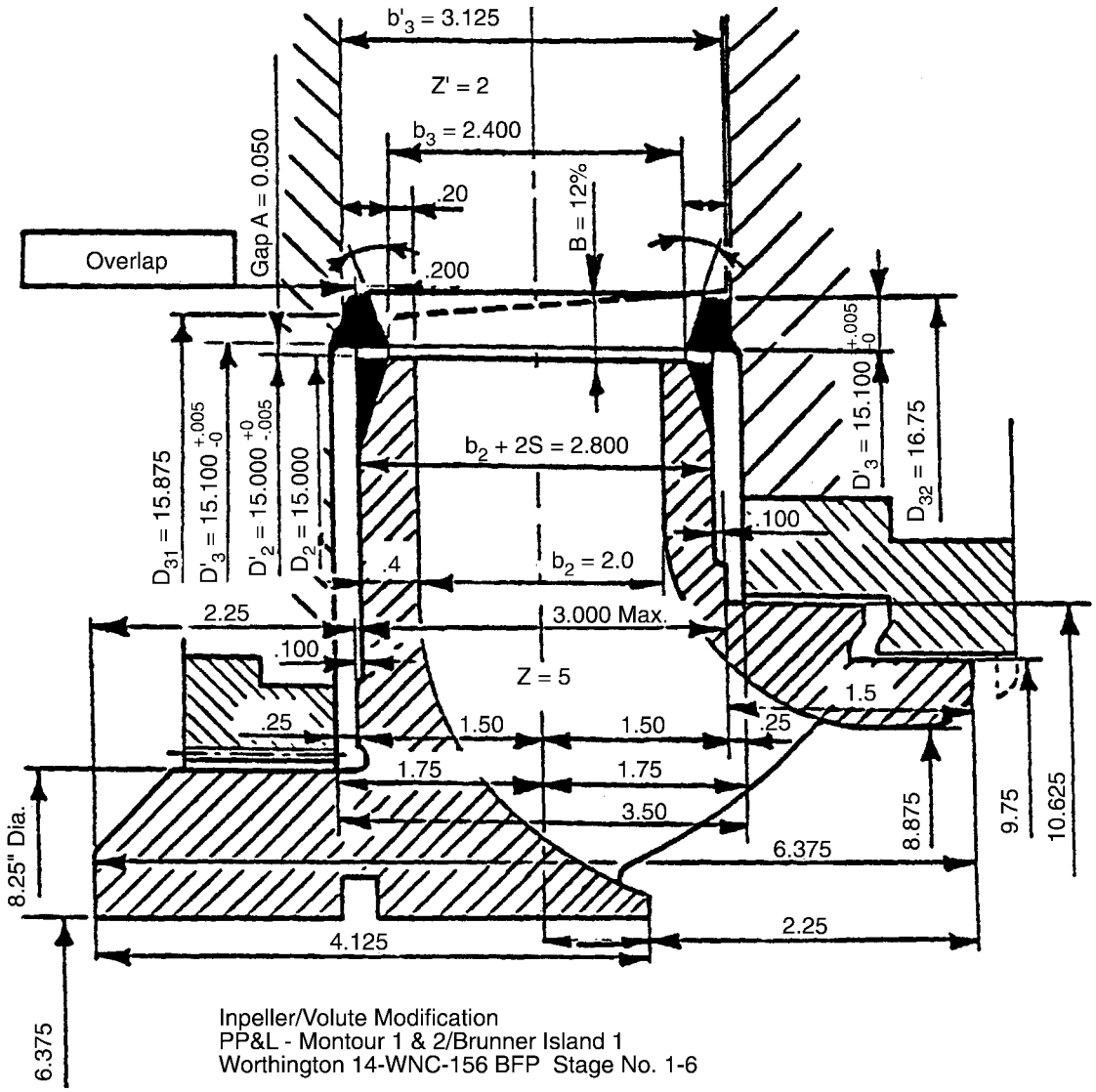

Inpeller/Volute Modification
PP&L - Montour 1 & 2/Brunner Island 1
Worthington 14-WNC-156 BFP Stage No. 1-6

Final Modification: For Gap A and its Overlap to be effective as a low-frequency filter, the impeller sideplates and the volute inlet should be welded up as shown above.

Note: When ordering new impellers from Worthington, give instruction on the P.O. not to chamfer the impeller sideplates.

Axial Float Per Design = [(0.250) + (0.250)] = 0.500
Measured = _____

Stage Spacing = 7-3/16"
Underfile All Impeller Vanes To: X = 1/4" Land
Journal Bearing Diameter = 5.500"

Figure 10-9
PP&L Montour #1, BFP- Modifications Required to Stabilize Head Curve

10.2.4 Factory Witness Test Data

Pump hydraulic instability with the aid of only a true H-Q curve obtained during factory witness testing should be determined considering the following:

- Sharp change in head rise at part load (60–70% of BEP)
- Droopy head curve toward low flows

Examples are given in Figures 10-10 through 10-12:

- Test results representing a 100% BFP for an 860 MW gas-fired plant are shown in Figure 10-10.
- An unusually droopy H-curve is shown in Figure 10-11. After unit startup, major system instability restricted power production at and below 65% of feedwater flow. All necessary details are fully described and explained in Reference 11.
- Test results of a nuclear reactor feed pump are shown in Figures 8-13 and 10-3. The pump was thoroughly instrumented upon the author's request because during the pretest trial run, strong axial shuttling of the rotor was experienced in the low flow regime. The tests in Figures 8-13 and 10-3 are self-explanatory.

In all four cases listed above, Gap A and B modifications completely eliminated the instability problem. The first two examples given above, as fossil units, could not justify performance testing. However, judging from the various design parameters (RPM, pressure, and flow) recorded during field testing, a slight increase in efficiency at full load was achieved after the incorporation of the proper Gaps A and B and the Overlap.

Controlled factory test (Figure 10-12) of the Limerick feed pump showed a distinct 2% increase in efficiency at BEP [11]. The test results for the Enrico Fermi 2 feed pump showed a 1.5% loss of efficiency as shown in Figure 8-13. The modifications for the Enrico Fermi 2 were performed by the OEM. There were strong indications that the modifications were not performed properly (X=O/A=10, instead of optimum). Therefore, friction forces were excessive.

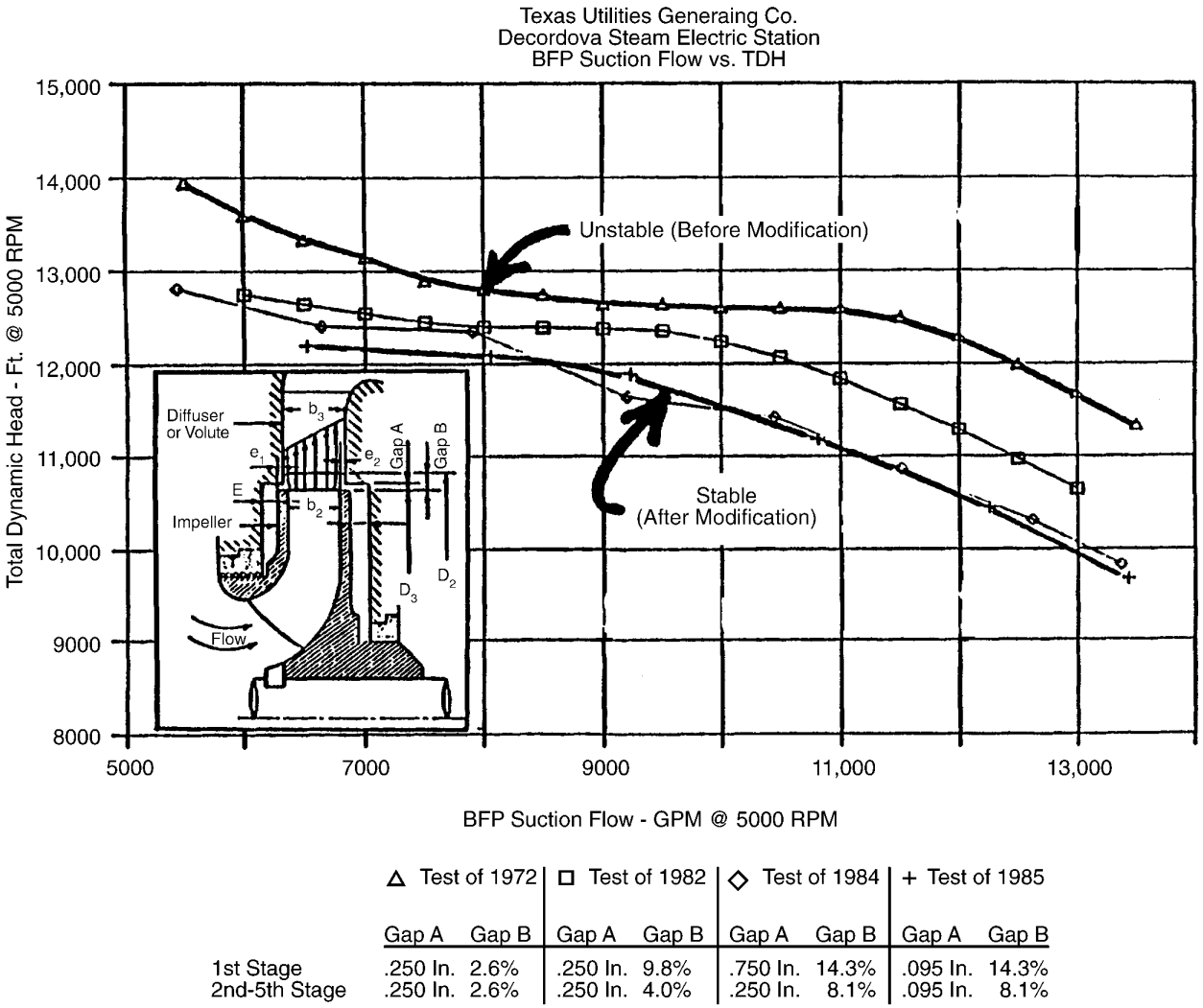

	△ Test of 1972		□ Test of 1982		◇ Test of 1984		+ Test of 1985	
	Gap A	Gap B	Gap A	Gap B	Gap A	Gap B	Gap A	Gap B
1st Stage	.250 In.	2.6%	.250 In.	9.8%	.750 In.	14.3%	.095 In.	14.3%
2nd-5th Stage	.250 In.	2.6%	.250 In.	4.0%	.250 In.	8.1%	.095 In.	8.1%

Figure 10-10
Hydraulic Instability at Decordova Station, BFP - Modifications Required to Stabilize Head-Flow Curve

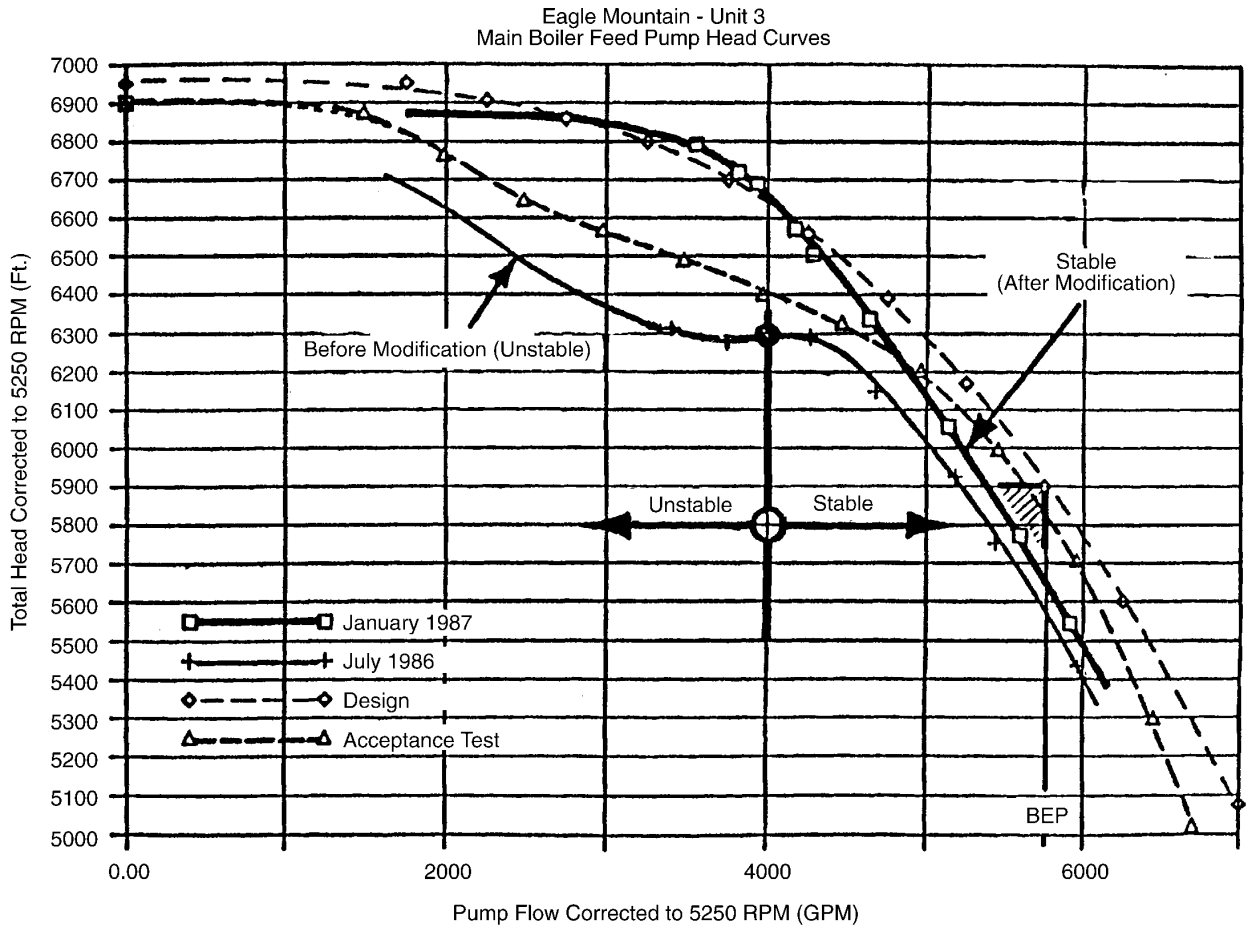

Figure 10-11
Eagle Mountain #3, BFP - Modifications Required to Stabilize Head Curve

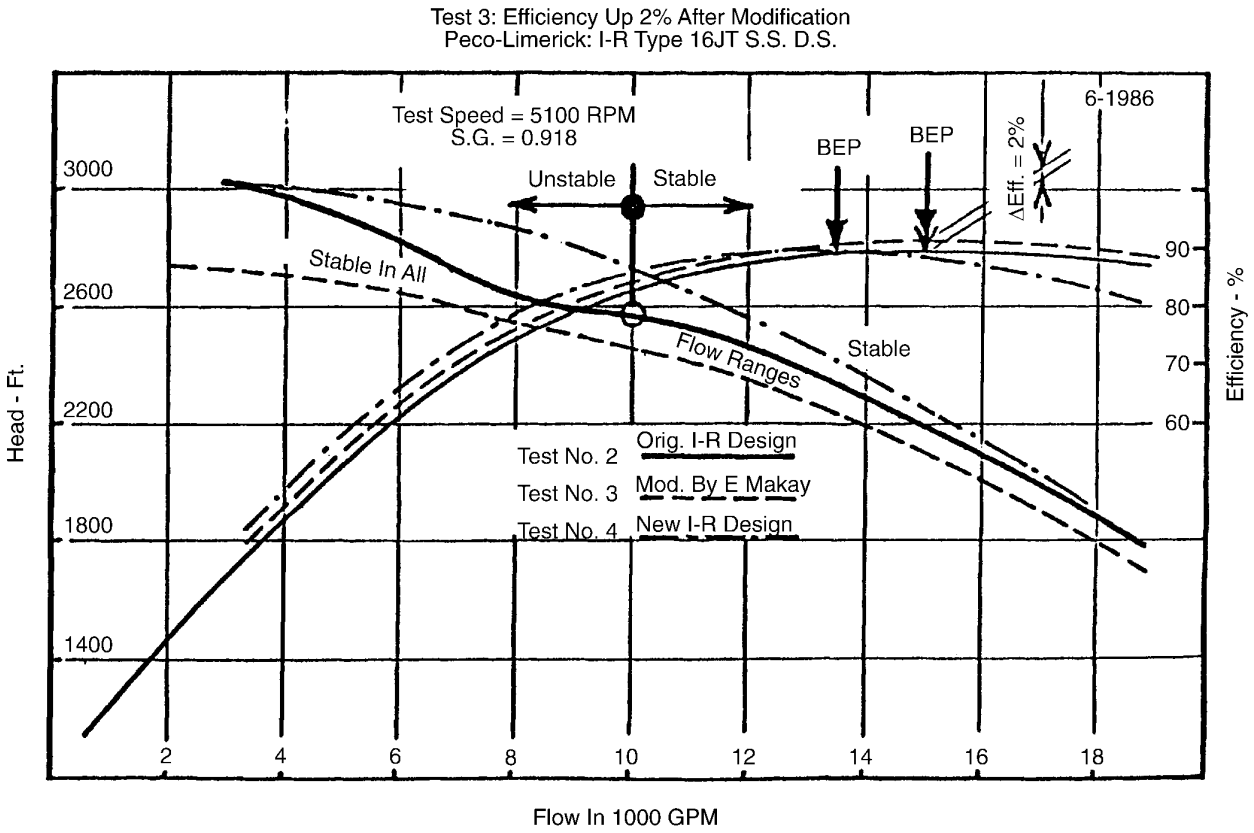

Figure 10-12
Limerick Nuclear Plant, Reactor Feed Pump - Modifications Required to Stabilize Head Curve

10.3 Swirl Break

The geometry of the swirl break and the description of its function as a hydraulic device strongly influencing rotor dynamic behavior of the pump rotor are explained in References 1, 12, 19, and 34. Its first application is mentioned in Reference 12 but without any description of the technology involved. A more detailed explanation is given particularly in Reference 34. The geometry of the swirl break at the impeller shroud is given in Figure 10-13, while Figure 10-14 shows the details at the impeller hub of the last stage to improve the rotor dynamic characteristics of the balancing device.

10.3.1 Swirl Break at the Impeller Eye

Swirl break at the impeller eye is shown in Figure 10-13 as an attempt to introduce more stability to the rotor and to equalize or stabilize axial thrust behind the impeller sideplate. It works, but at a substantial loss of efficiency. It should be applied only to given designs when there is no other way to eliminate dynamic instability. It should not be included in new designs because there are more efficient ways to ensure rotor stability.

10.3.2 Swirl Break at the Balancing Disk/Drum

Swirl break at the balancing disk/drum is shown in Figure 10-14. The first time this concept was introduced in open literature was by Massey [12]. This also introduces some loss of efficiency. The inlet swirl breaks are radial slots in the vertical face of the stationary disk/drum as shown both in Figure 10-13 and in Figure 10-14 from the side view. The purpose of the swirl break is to reduce the tangential velocity component of the fluid flow entering the cylindrical space of the balancing device. This reduction of the flow velocity will reduce the forward driving tangential force generated by a radial displacement of the cylinder. This force is a measure of the damping capability of the cylinder. The higher this force opposing the shaft rotation, the higher the damping capability of the cylinder.

10.3.3 Annular Swirl Break With Suppression Injection

Another way to achieve the same fluid dynamic action in the cylindrical portion of the balancing device is shown in Figure 10-15. The liquid injected with the proper angle creates the same tangential velocity component reduction, except the efficiency loss with this design method is substantially less than that with the design using radial slots as shown in Figure 10-14. Therefore, if additional rotor stability is needed, this is the preferred method to achieve it without substantial loss of the machine’s efficiency.

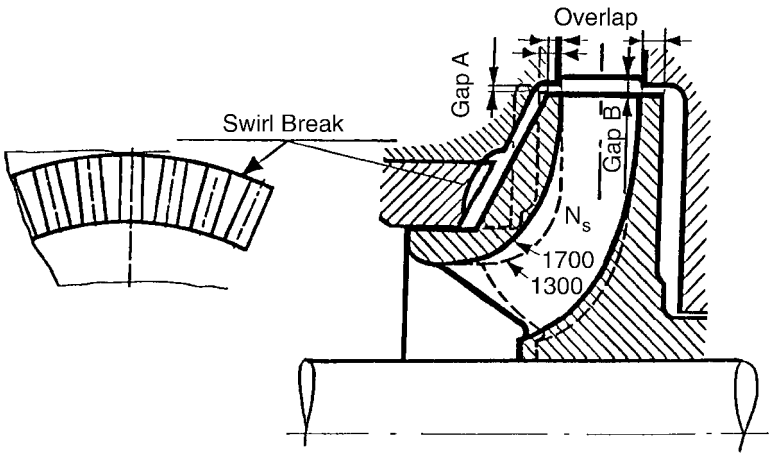

Figure 10-13
Swirl Break Applied at the Impeller Eye, Behind the Shroud Sideplate

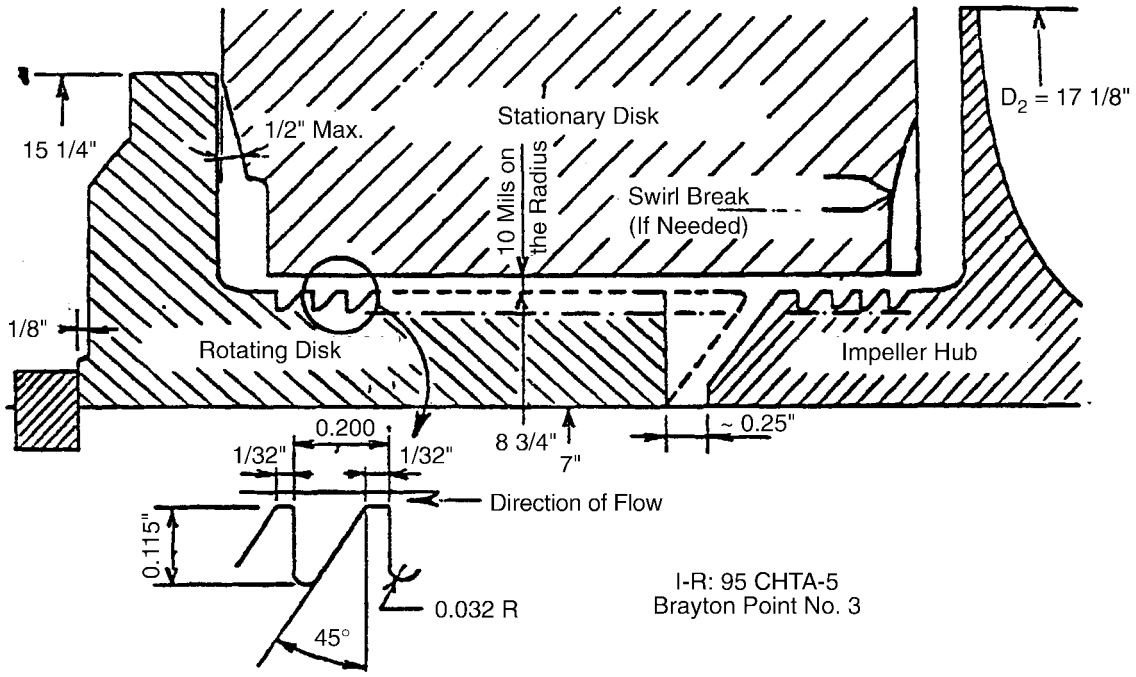

I-R BFP Axial Balancing Disk

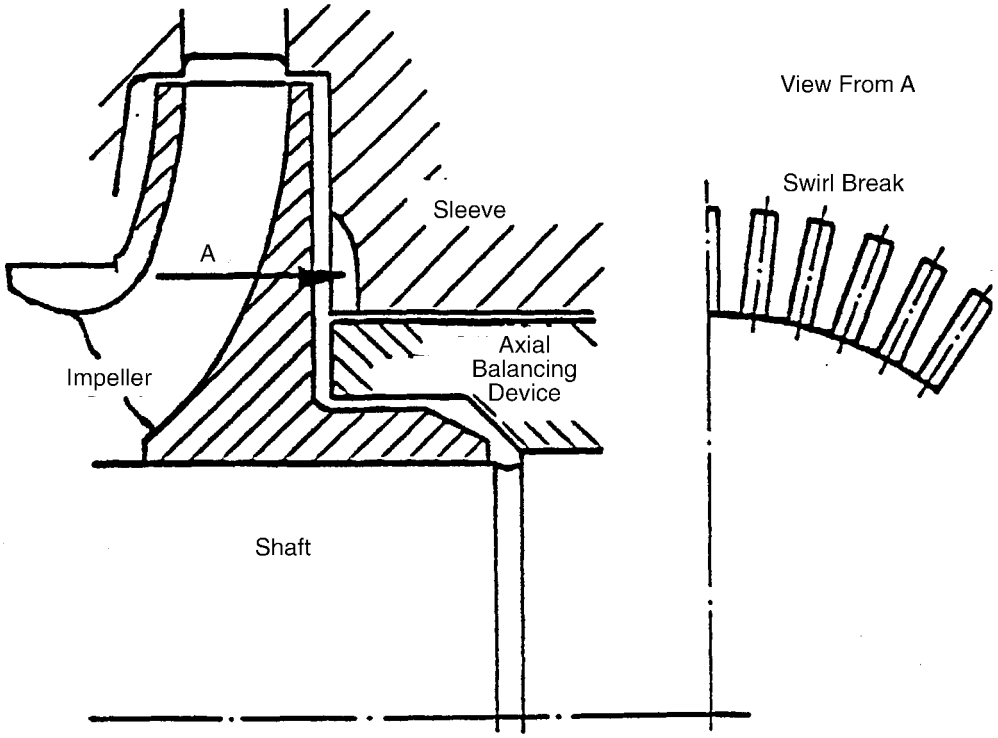

Figure 10-14
Swirl Break Applied at (A) Balance Disk and (B) Balance Drum (Piston)

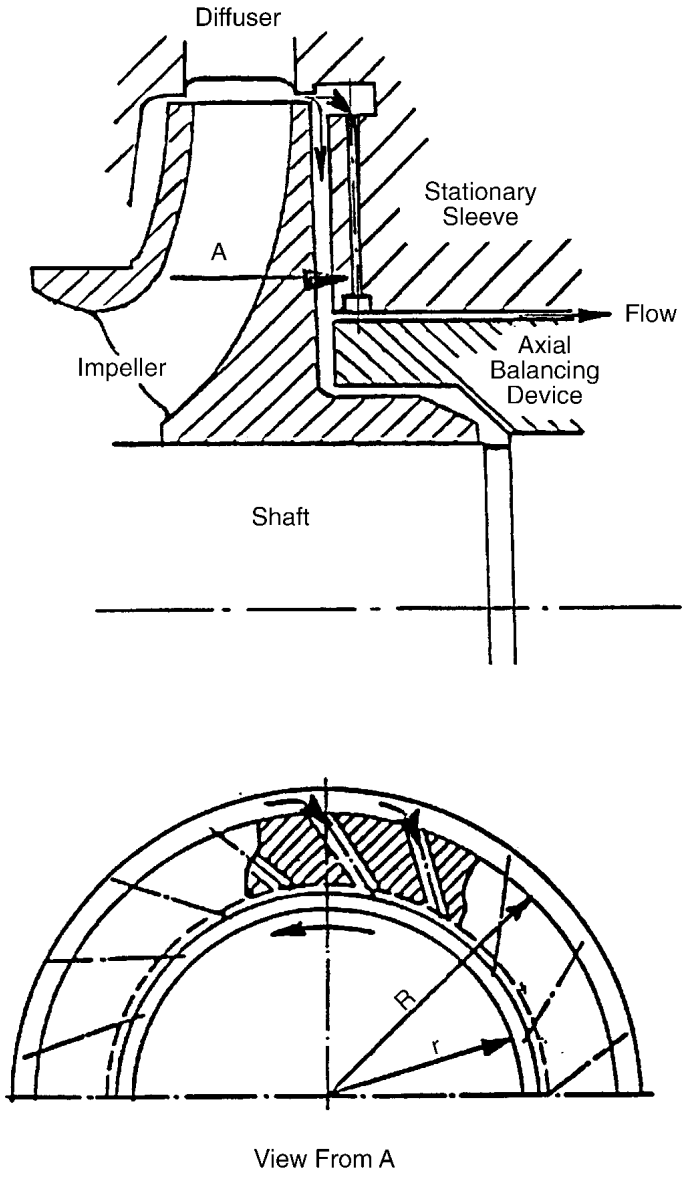

Figure 10-15
Annular Swirl Break Design With Suppression Flow Injection

10.4 Lomakin Effect

Additional rotor stiffness and damping can be achieved with the application of the ERCO improved Lomakin Effect break-down bushing labyrinth geometry, as shown in Figure 10-16 and explained in more detail in References 20 and 34. The effect of the Lomakin geometry on rotor critical speed is shown schematically in Figure 10-17. The force created by the geometry is shown and explained in Figure 10-18. Several rotors have received the improved geometry modification in high-speed BFP applications to improve rotor stability when subsynchronous rotor response had destructive effects. The depth of the grooves has been published as 5 to 10 mils; however, this is not very practical for large feed pumps. In all applications made by ERCO, the groove depth has been at least 15 mils. Examples are shown in Figures 5-7 and 6-9. The geometry is called the "shallow groove serration" in both figures.

Wear rings in the early BFP design days (the 50s and early 60s) were considered only from the point of view of sealing differential pressure between inlet and exit. The geometry requirements, therefore, were the tightest possible clearances with the longest flow path. This led to many costly BFP seizures, especially on turning gear operation. The load carrying and damping characteristics of close clearance surfaces were neglected or not known. These quantities are also referred to as hydro-static centering, or Lomakin Effects (after his publications in the mid-1950s, in particular Reference 44 published in 1958 in Russia). He realized that the load carrying capability is not based on the hydro-dynamic fluid film lubrication effect but on the differential pressure across the wear ring. The basic principles of hydro-static centering of a wear ring are shown in Figure 10-18. The velocity difference between the highest and lowest clearance sides will create a differential entrance loss resulting in a pressure difference between the two sides, giving rise to a shaft centering or stabilizing force. This force is particularly important if rotor critical speed is of concern or if subsynchronous vibration amplitudes are present.

Two schools of thought existed in the 60s and 70s about the geometry and the importance of its effects on reliable BFP operation, both at high speed and on turning gear. These two schools of thought are commonly referred to as the "Smoothies" and the "Groovies":

- The Groovies: This design concept promotes the use of deep groove geometries as shown in the upper three ring geometries of Figure 10-17. This design is mainly concerned about seizure, dirt, and particles (the less the contact area, the better). The goal is to maximize the antiseizure and dirt flushing characteristics at the expense of losing most of the Lomakin Effect, that is, the added radial damping and stiffness, which can be substantial for certain geometries of the wear ring cylindrical surfaces.
- The Smoothies: This design concept promotes geometries that take full advantage of the radial damping and stiffness (the lower two configurations shown in Figure 10-17), and are applied when rotor-dynamic stability and critical speed location come into question (the more the contact area, the better).

Wear-ring geometry and its material drew considerable attention in the 60s and 70s as feed pumps grew in size and speed increased. Its effect on rotor critical speed and rotor-bearing stability is discussed in Section 12.3 and shown in Figure 12-13. The following design considerations had to be studied, analyzed, and conclusions drawn for reliable BFP operation, reduction in failure rates, and easier maintenance:

- Wear ring design: Wear rings should not come loose during operation and should be easy to replace.
- Wear ring geometry: Wear rings should not seize and should aid rotor dynamics.
- Clearances: Clearances should be minimum for efficiency but reliable in operation.
- Material selection: Consider the best possible material selection (seizure proof and wear resistant) within economic restrictions.
- Material hardness: Hardness difference (10 HRC minimum), heat treatment.
- Operation: On turning gear, cyclic, hence frequently in the unstable regime.

Hydrostatic centering force for a smooth impeller wear-ring geometry is shown in Figure 10-18. The same applies to the shallow groove labyrinth configuration, often called improved Lomakin geometry, although it was developed by ERCO, independently from, but inspired by Lomakin. This geometry, combined with the material reported in Section 12, is presently the most reliable configuration for almost all centrifugal pump applications in large central stations, both nuclear and fossil

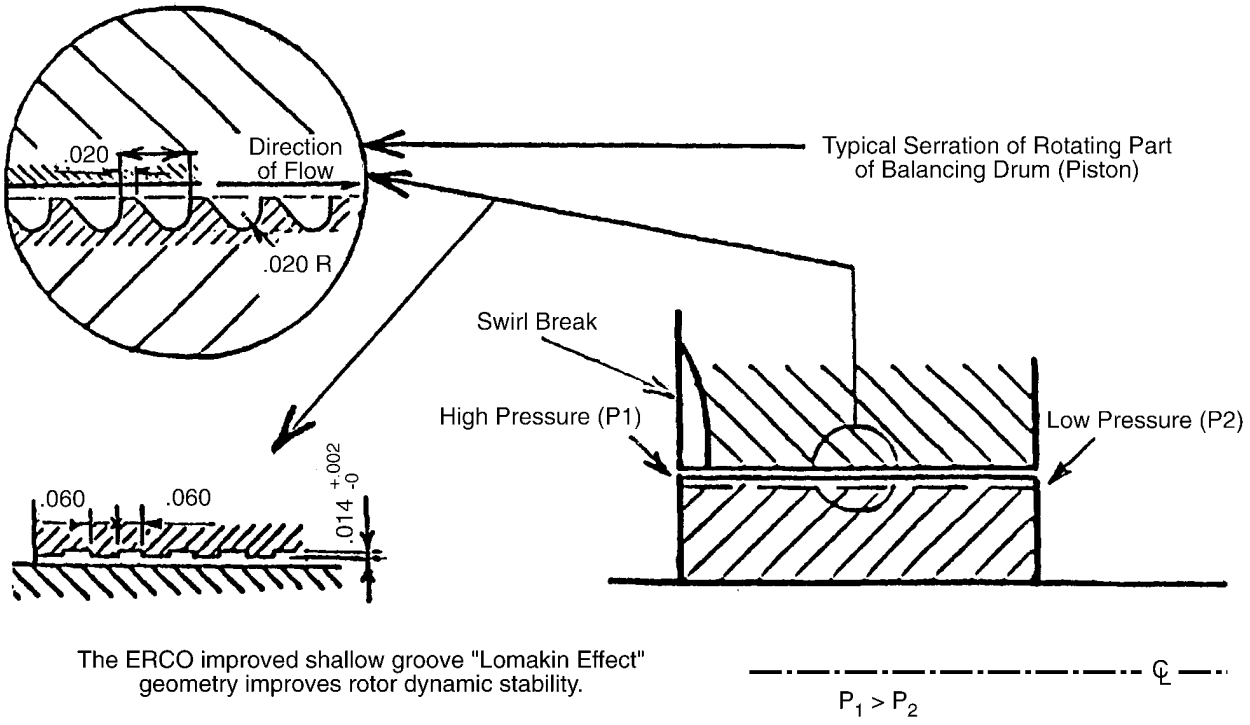

Figure 10-16
Lomakin Effect Geometry That Improves Rotor Dynamic Stability

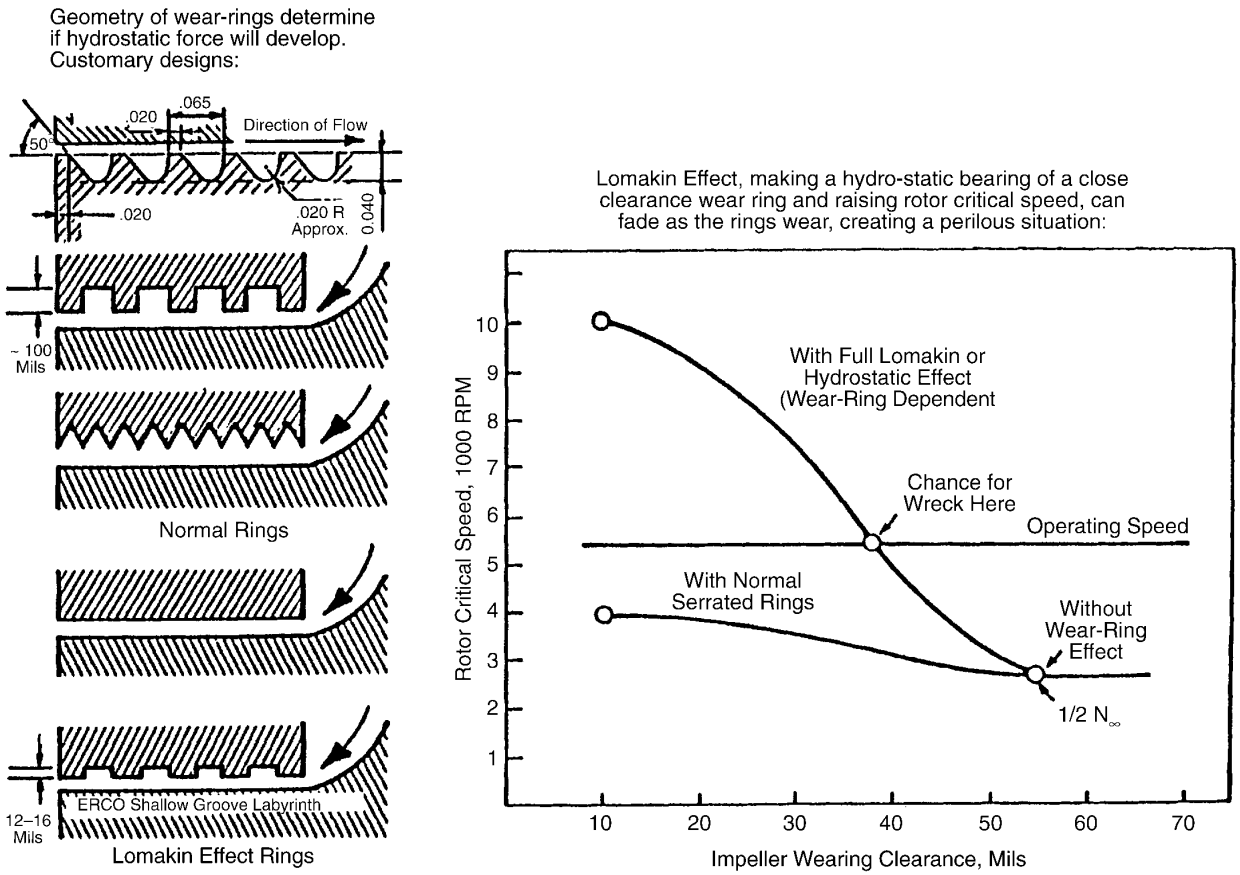

Figure 10-17
Lomakin Effect Makes a Hydrostatic Bearing of a Close Clearance Wear Ring and Raises Rotor Critical Speed

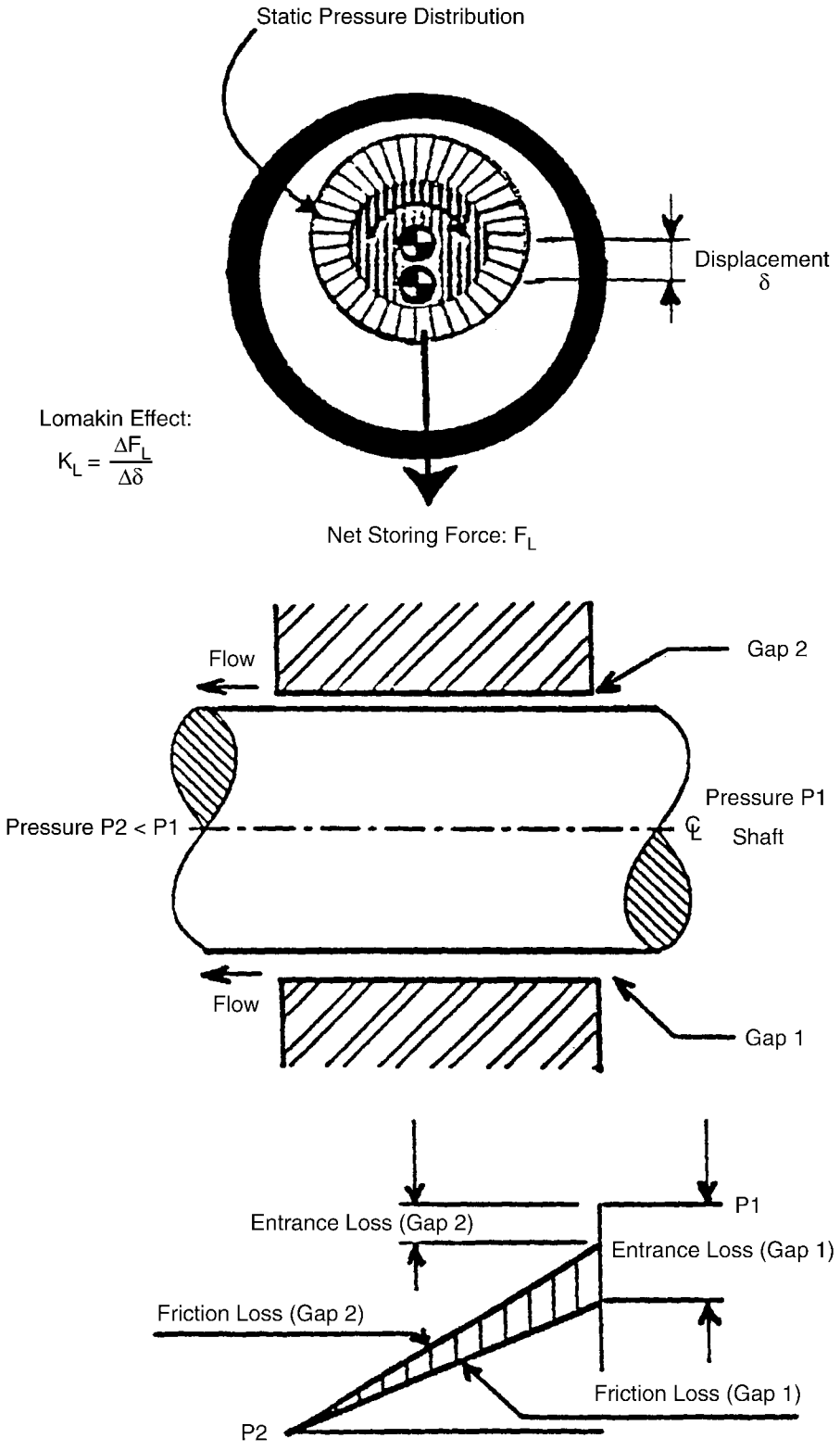

Figure 10-18
Hydrostatic Centering Forces in an Annulus Subjected to a Pressure Difference

11
AXIAL THRUST

The static axial thrust in a pump is created by the force differential acting on the impeller hub and shroud sideplates. The force is calculated from the surface area of the sideplate and the pressure acting on the sideplate, that is, A (in^2) times P (lb/in^2) = pounds force. As shown in Figure 11-1, for a single suction impeller, the area of the impeller hub sideplate, that is, opposite the impeller eye, is larger than the impeller shroud sideplate. Also, the pressure on the impeller hub sideplate is also greater than the pressure on the impeller shroud sideplate, that is, the discharge pressure on the hub sideplate, while the discharge pressure bleeds to suction pressure on the shroud sideplate. Therefore, the thrust of a single-suction impeller will be in the direction of the impeller suction. For a double-suction impeller, the thrust is technically balanced because the area and pressure on the sideplates are equal, resulting in equal opposing forces.

11.1 Controlling Axial Thrust Loads

A double-suction, single-stage pump incorporates a thrust bearing to control the thrust loads generated by the impeller during pump startups and shutdowns. These startup and shutdown thrust loads occur due to impeller casting inaccuracies and pressure differences that may occur at the pump discharge and suction. However, in a multistage, high-energy-input pump, (either single- or double-suction, with one or more single-suction impellers), the magnitude of the thrust generated is too great for a practical thrust bearing design to absorb. The pump designers typically have two devices for controlling the large thrust forces generated in a multistage pump: the balancing drum (piston) and the balancing disk. A third option is employing opposed impellers that theoretically have zero residual axial thrust acting on the rotor.

11.1.1 Balance Drum

A balance drum or piston (Figure 11-2) is basically a water-lubricated radial bearing. It influences the rotor dynamic behavior of the pump and, therefore, its design. The thrust-carrying capability of this design is equal to the pressure difference on each side of the balance drum and the radial area of the balance drum faces. A thrust bearing is then incorporated to handle the force difference at the balance drum and to handle the forces generated during startup or shutdown of the pump.

11.1.2 Balance Disk

The balance disk (Figure 11-2), on the other hand, is basically a water-lubricated radial bearing combined with a vertical water-lubricated thrust bearing. The small gap "e" between the stationary and vertical faces controls the pressure and, consequently, its thrust-carrying

capability. The balance disk is designed to carry all the thrust generated by the pump during normal operation. A thrust bearing is provided only to handle the forces generated during pump startup and shutdown; therefore, it is much smaller in size than the thrust bearing required for a balancing drum.

11.1.3 Opposed Impellers

All boiler feed pumps manufactured by Byron-Jackson (B-J) are of the opposed impeller designs with volutes and a cross-over channel. The residual axial thrust unbalance at the pump BEP is due only to the impeller and volute sand cast inaccuracies, which are well taken care of by the thrust bearing. At part-load operation, however, the axial thrust can exceed the thrust bearing thrust carrying-capacity due to the lack of Gap A geometry, resulting in rotor failure in the axial direction. This can manifest itself as thrust bearing failure, shaft breakage, or simply higher vibration levels.

A retrofit modification of introducing the proper Gap A geometry to correct for axial thrust instability is discussed in Section 8 and is shown in Figure 8-9. The retrofit modification requires precision work and is not inexpensive. The simplest way to overcome this initial design discrepancy is during the manufacturing of the pump. The additional work during that stage is minimal and very cost effective. In some cases, the cross-over channel introduces acoustic resonance, which appears as high vibration or pressure pulsation amplitude at impeller vane passing frequency or at its multiples, depending on the impeller-to-volute vane combination. This is discussed in Section 7, which includes an example of a large fossil station pump as shown in Figure 7-16.

Investigations have shown that the majority of failures incurred with high-energy-input pumps have been the result of axial thrust. However, it is usually not the static component that causes the failures, but the dynamic thrust developed due to operation in hydraulically unstable flow regimes of the pump. As discussed above, the static thrust component can be calculated with a reasonable degree of certainty (Figure 11-1) and a balancing disk or drum can be sized accordingly (note that this does not preclude an incorrectly designed balance drum or disk).

The dynamic thrust component generates force magnitudes that are not predictable by classical pump design calculations but that can be controlled by proper hydraulic geometries. The dynamic thrust is a function of the hydraulic geometry (that is, Gap A, Gap A Overlap, and Gap B) of the pump and the percent flow the pump is operated away from the BEP.

As discussed in Section 8, without the proper hydraulic geometry, typical high energy input pump designs become hydraulically unstable at approximately 65% of BEP. This instability has a margin and is dependent on several design parameters such as N_S and S_S, as can be seen in Figure 10-1. The proper geometry has shown that a pump can operate down to 20 to 25% of BEP without axial thrust instability (Figure 11-3), indicating that the dynamic thrust component has been brought under control.

The balance drum has a disadvantage in that the amount of thrust the device can carry is fixed when the radial diameter is chosen. Changes in the pump physical and/or operating conditions cause increased pump thrust loads and result in the axial thrust being transferred directly to the

pump thrust bearing. Also, a balancing drum allows the rotor to drift in the axial direction and offers no resistance to the axial thrust developed by hydraulic instabilities (that is, the rotor will shuttle axially, particularly at reduced flows).

In most high-energy-input pumps that incorporate a balance disk, the shaft is free to move axially within the limits of the thrust bearing float. This feature allows the balancing disk to be a self-compensating device, and as thrust loads increase, the rotating face of the balance disk moves closer to its corresponding stationary face. The smaller the clearance between the two faces, the more thrust the balance disk will carry, and the axial stiffness of the balancing disk will increase (Figure 11-4). The increased axial stiffness resists the axial thrust developed from hydraulic instabilities and, therefore, prevents axial shuttling.

An important design feature, developed by Energy Research and Consultants Inc. (ERCO), for the balancing disk is a taper (Figure 11-5) in the radial face of either the stationary or rotating component. The taper allows the balancing disk to continue carrying thrust loads up to and including contact of the radial faces. As shown in Figure 11-4, the thrust-carrying capability of a balance disk without the taper will collapse when the clearance closes to a very small dimension (about 0.5 mil) and will result in immediate destruction of the rotor. Therefore, the taper will prevent rotor destruction and can provide an increased safety margin against sudden changes of pump thrust. Even if the faces touch, the balance disk will not seize (due to minimum metal-to-metal contact) and will continue to operate as a proper balancing disk.

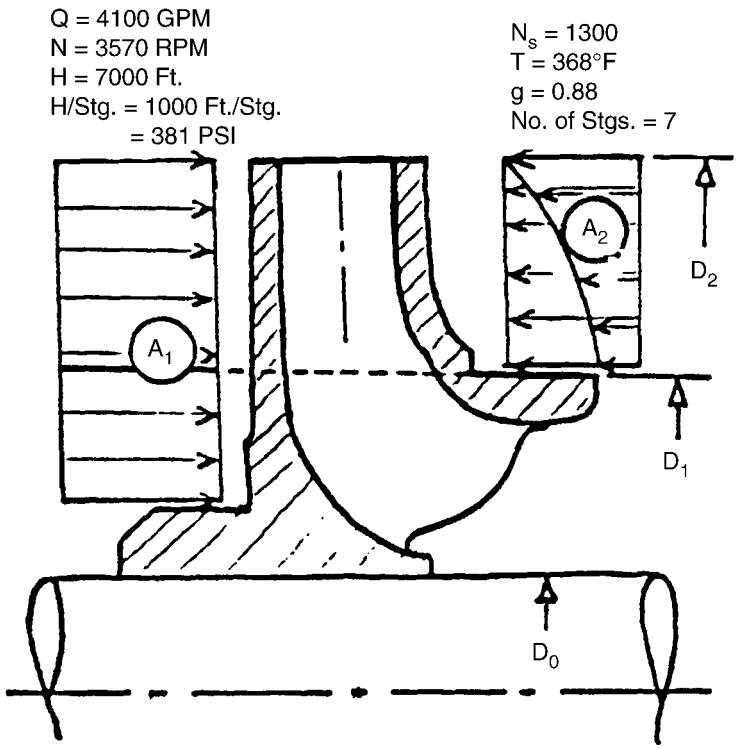

$A_1 = \pi/4\ (16.5^2 - 6.0^2) = 185.5\ In^2$
$A_2 = \pi/4\ (16.5^2 - 10^2) = 135.0\ In^2$
} $\Delta A = 50.5\ In^2$

Force (Static) Developed:
Normal: F = 19,240.5 x 7 = 134,683 Lb.
Worn: F_w = 27,542 x 7 = 192,794 Lb.
} At BEP

Force Increase: $\Delta F = F_w$ = 58,111 Lb.
Thrust Bearing Burned Out!

These are static forces only. See Dynamic Forces.
(Can be substantially larger than static forces,
especially if Gap A dimension is incorrect.)

Figure 11-1
Static Thrust Forces Developed by an Impeller

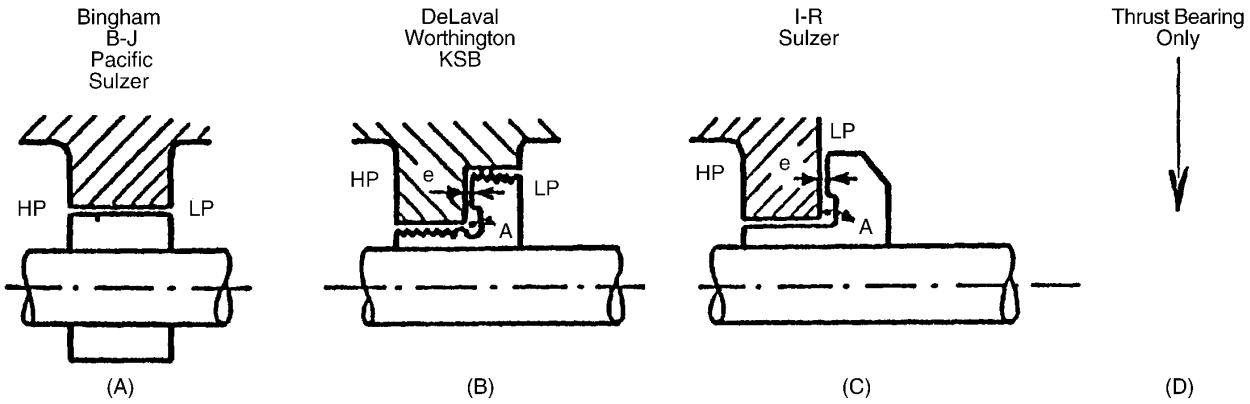

Customary axial thrust balancing device for high-pressure multistage boiler feed pumps: (A) balancing drum (piston), (B & C) and balancing disk. Another way to balance axial thrust is with imposed impellers. However, a much larger thrust bearing is then required (D).

Figure 11-2
Types of Axial Thrust Balance Devices: A. Balance Drum, B. and C. Balance Disks

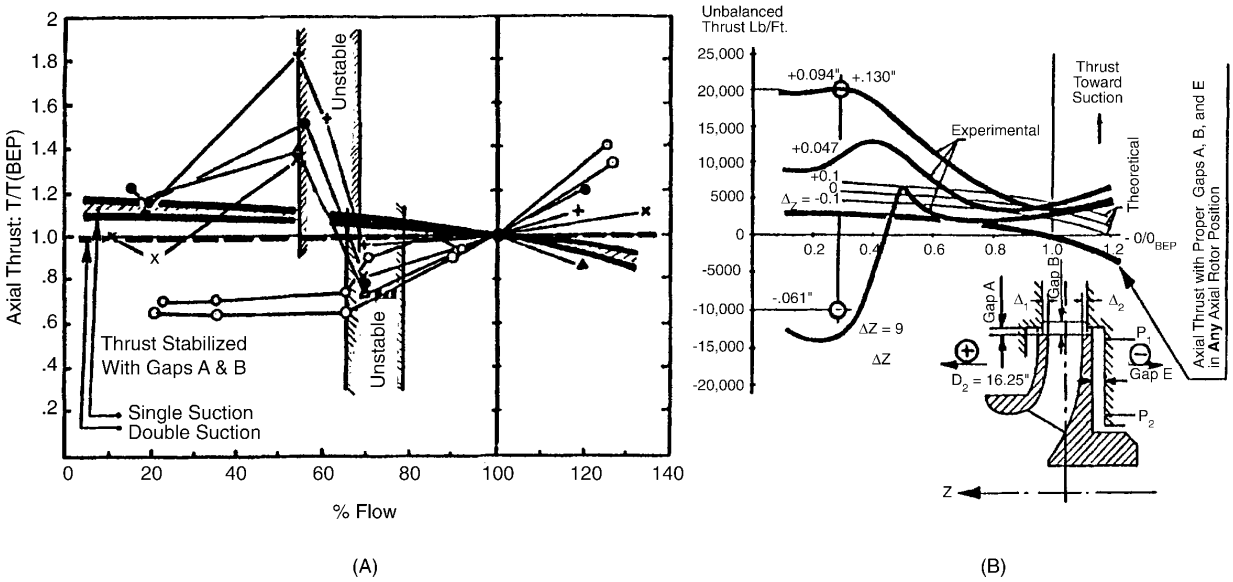

Figure 11-3
Axial Thrust Variation With and Without proper Hydraulic Geometry

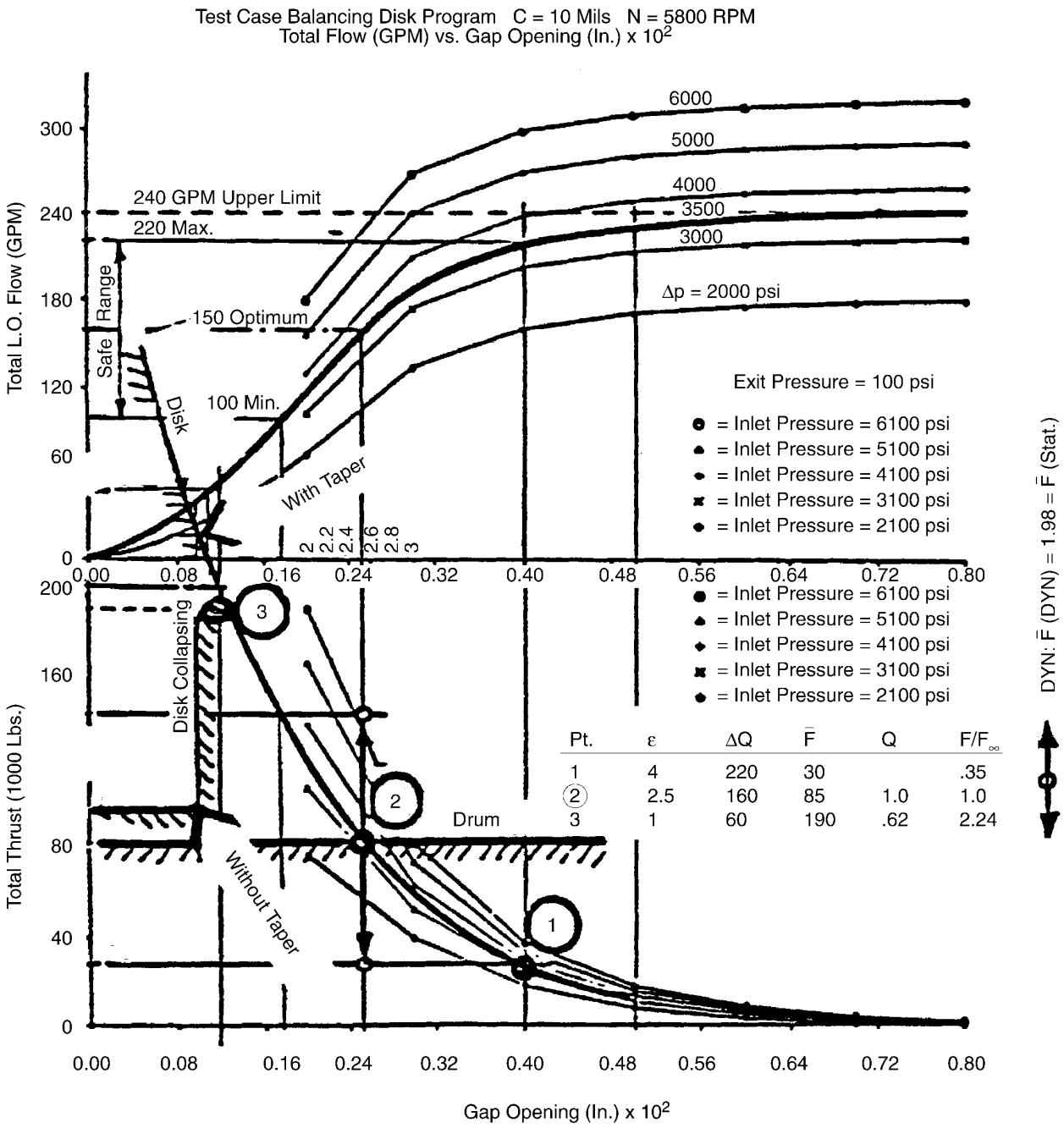

Figure 11-4
Thrust Carrying Capability of Balance Disk, With and Without Taper

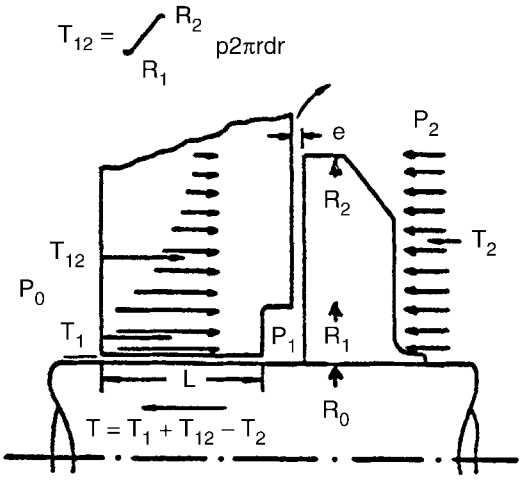

(a) Balance disk with parallel faces. Force equilibrium is shown when disk in normal open position.

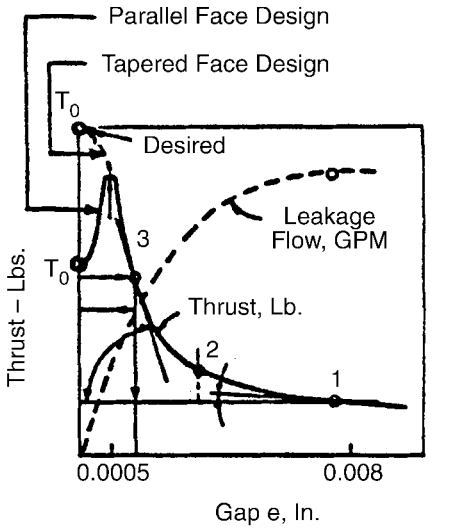

(c) Balance disk thrust carrying capability and leak-off flow.

Force Developed By Disk When Faces Just Closed. Faces Are:

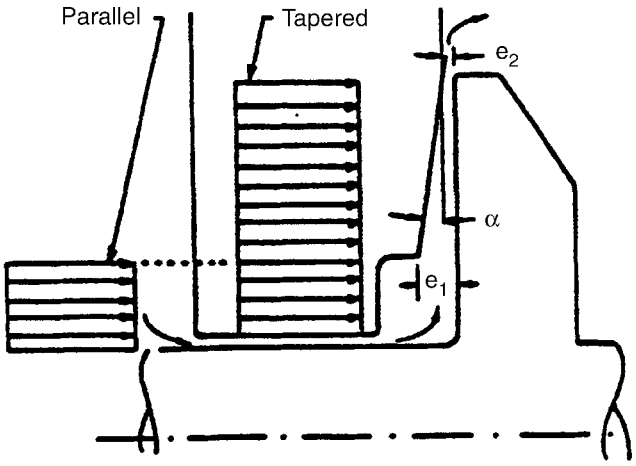

(b) Tapered face balance disk

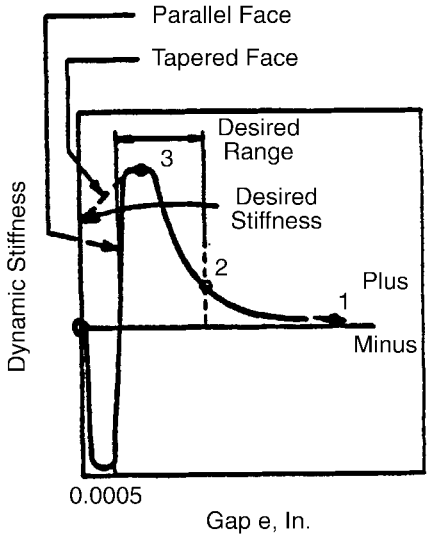

(d) Dynamic stiffness of balance disk

Figure 11-5
Balance Disk Taper, Very Important to Prevent Catastrophic Failures of Rotor

11.2 Rotor Axial Alignment

Proper axial alignment of the pump rotating components to their stationary counterparts is critical to satisfactory pump operation. Any hardware modifications (including Gap A and B) to improve efficiency, eliminate dynamic and hydraulic instabilities, or improve the vibration characteristics of a pump can be negated by improper alignment. Axial misalignment can:

- Cause hydraulic instability at all flows
- Excite vane passing (ZxN) or its multiples
- Affect synchronous (1xN) as well as subsynchronous vibration components equally
- Cause rotor axial shuttling and high thrust loads.

The impeller must be properly aligned within the diffusers or volutes (Figure 11-6), and the balance disk (if applicable) and thrust collar must be properly aligned to provide their intended function. Alignment should be tightly controlled both in the repair shop and during installation of the rotor in the field.

The relation of shroud and hub positions to the diffuser/volute and casing must be verified and determined (and documented to assist field installation) during assembly. Axially, the impeller discharge should be entirely within the axial width of the diffuser. If this is not the case, the flow from the impeller will discharge against the diffuser or casing walls. The rotor sensitivity to impeller and diffuser/volute alignment is dependent upon the ratio of the impeller exit vane width and diffuser vane width, and must be judged on a case-by-case basis. However, it will always be prudent to align the components as accurately as possible.

The first step or rule in a proper assembly is that the rotor should **always** be assembled in the vertical position. Vertical assembly will allow the forces of gravity to work with you in ensuring that the components stack against each other and align perpendicular to the shaft. The second step should be to measure the lift required to center each impeller. When the lift for a given stage is determined to be different from the previous stage, corrections must be made to make the lift the same. The third step should be to log the lift required in order to center the rotor and then provide this information to the field personnel for use during rotor installation.

Among the many field examples available on ERCO file, two typical examples are provided in Figure 11-6 from the following power plants:

Union Electric - Labadie: After many unexplained failures of a five-stage BFP, a failed rotor was examined in great detail at the HydroAir shop. The conditions found were as shown in Figure 11-6. The last stage impeller was axially misaligned by more than 200 mils. Proper corrections eliminated the basic problem.

Alberta - Sheerness Unit No. 1: In the OEM's repair shop, the final assembly of the rotor was performed with ERCO supervision. The last stage was found as shown in Figure 11-6-a (delta=0.205") and corrected as shown in Figure 11-6-b. The basic vibration problem was instantly eliminated.

These are two classic examples from the many seen by the authors, proving that a vibration problem does not have to come from a complex theoretical phenomenon such as rotor critical speed. Workmanship is as important as a differential equation.

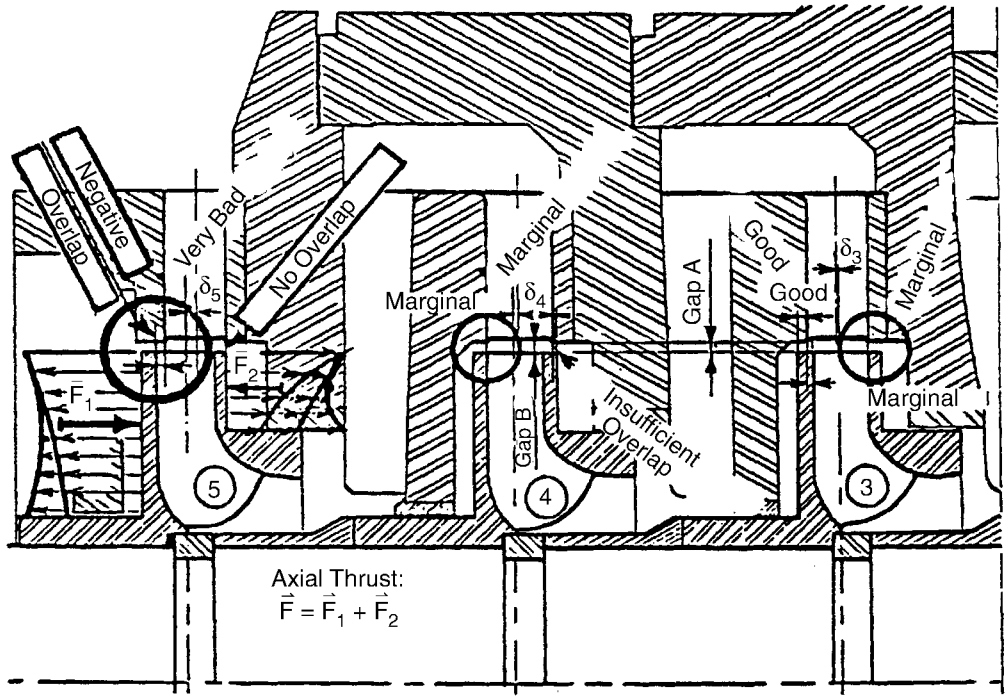

Five-Stage BFP

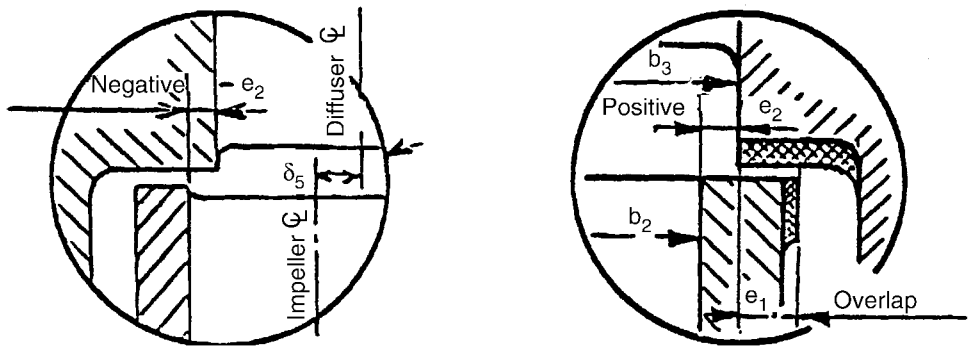

A – Incorrect B – Correct

Figure 11-6
Rotor Axial Misalignment. Also Shown: A-Incorrect, B-Correct Alignment

12
COMPONENT FAILURES

This section discusses pump components that have the highest probability of failures. In most cases, failure can be prevented with proper application, materials, machining practices, and installation. The component failures that are described in detail are:

- Shafts
- Impellers
- Wear rings
- Balancing disks
- Couplings

Bearings are not addressed in this chapter because a complete discussion of bearing failures is provided in Section 14.

12.1 Shaft Failures

The most common cause of shaft failure is metal fatigue. A typical high-cycle fatigue failure of a pump shaft is shown in Figure 12-1. Fatigue is a weakest link phenomenon; therefore, the failures occur at the most vulnerable point of the dynamically stressed shaft. The vulnerable points are referred to as "stress raisers" and can be mechanical, metallurgical, or a combination of the two. Mechanical stress raisers include such features as small fillets, sharp corners, grooves, splines, key ways, nicks, and press or shrink fits. Failures often occur at the edges of press-fitted or shrink-fitted members (that is, impellers, shaft sleeves, and couplings), where high degrees of stress concentration exist as a result of the inherent dynamic loading of a pump shaft. Such an increase in stress concentration effectively reduces the shaft fatigue resistance, especially when coupled with fretting. Metallurgical stress raisers may be quench cracks, corrosion pits, gross non-metallic inclusions, brittle second-phase particles, weld defects, or arc strikes.

Figure 12-1
High Cycle Fatigue Failure of a Pump Shaft

Fractures of pump shafts originate at points of stress concentration that are inherent in the design or are introduced during fabrication, repairs, installation, and operation. Design features that concentrate stress include key ways, impeller edges, shaft sleeve or coupling press fits, fillets at shoulders, and thread roots (Figure 12-2). Stress concentrators caused during manufacture or repair include grinding marks, machining marks or nicks, improper heat treatment, improper machining, and excessive heat used to straighten a shaft. Failures due to installation can result from misalignment, mismatch of mating parts, or careless handling during which the shaft is nicked, gouged, or scratched. During operation, stress concentrators occur at cavitation areas and damaged areas caused by broken pump components other than the shaft.

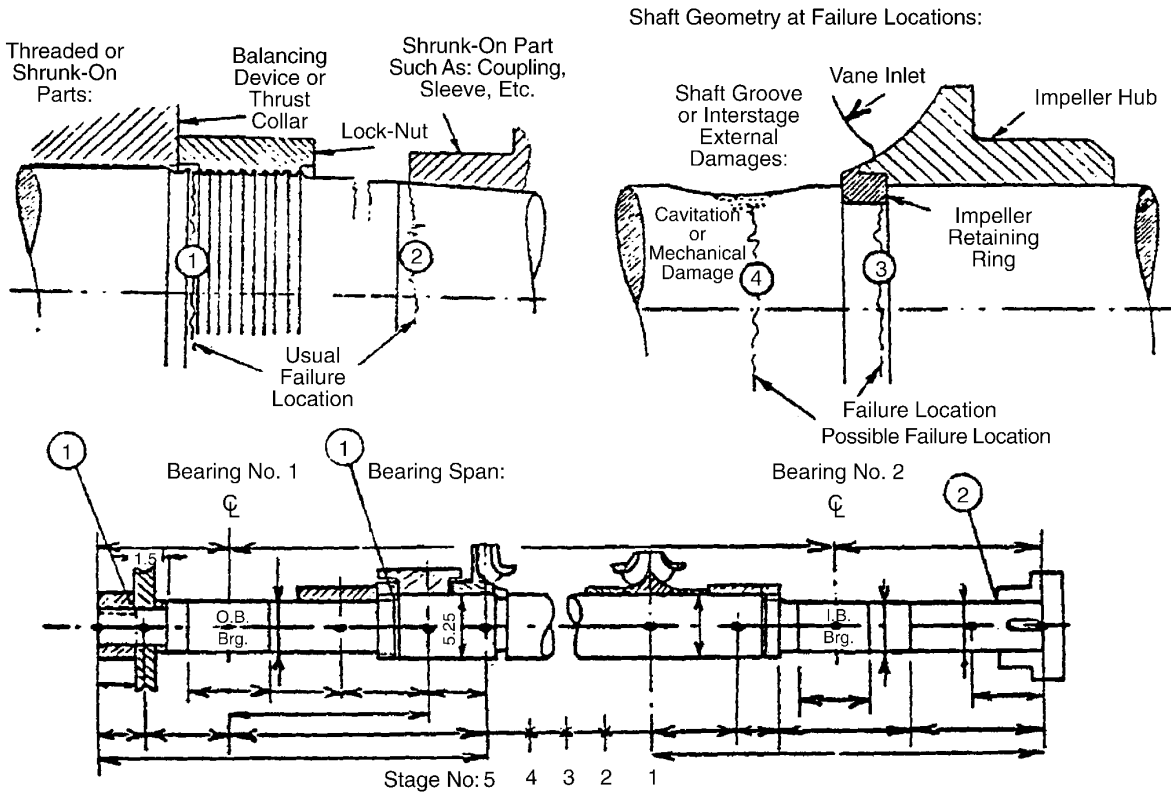

Figure 12-2
Typical Multistage Centrifugal Pump Shaft Failure Locations, Numbered in Order of Failure Frequencies

Although a failed shaft may not always be identified as broken, other symptoms as listed here may also be placed in the failed shaft category:

- Cracked or bent shaft
- Bearing failure or damage
- Shaft seal failure

The above three symptoms are often viewed as indicators that a shaft failure (as shown in Figure 12-1) would have occurred due to design, manufacturing or repair, installation, or operation of the shaft.

12.1.1 Boiler Feed Pumps

A recent survey of several hundred boiler feed pump shaft failures resulted in the following discrepancies that were reported as directly or indirectly causing shaft failure [33]:

- Incorrect shaft geometry, size, sharp corner at undercut or key way.
- Incorrect material, heat treatment, or shafts being straightened with bows greater than 6 mils total indicated runout (TIR).

- Thrust collar or balancing device vertical faces not truly perpendicular to the shaft axis or not sitting up right against the shaft shoulder, resulting in cyclic stress reversal The thrust collar is particularly important for cyclic units (that is, load following plants). The shaft life is determined by the number of starts or the length of operation on recirculating flow or low loads because, during normal operation, the thrust bearing is normally unloaded.
- Lock nut mating surface not true and/or over-torqued. The result is the same as above. The lock nut may also become loose. Therefore, the method of securing the nut is critical. However, radial set screws are not considered an acceptable design for large boiler feed pumps.
- Thrust shoes or leveling plates uneven, or misapplication of a Kingsbury-type thrust bearing without leveling plates. Tolerances on thrust bearing parts, including collar or lock nut, were not tight enough to prevent slop in the thrust collar. Bearing housing where the thrust bearing assembly sits (fits) up is not true.
- Impeller core shift due to casting inaccuracies resulting in an apparent dynamic unbalance. This is actually hydraulic unbalance and cannot be corrected by balancing, even in air or in a vacuum. It is known as the "shaft breaker."
- Bow in the shaft, initial crack during manufacturing (heat treatment), or other manufacturing errors in the shaft.
- First critical speed of the rotor coincides with warm-up speed (only if variable speed drive), or second critical speed is approached at full speed, resulting in high lateral rotor vibration and sensitivity to misalignment and foundation type.
- Unstable journal bearing and/or heavy rubbing at close clearance rotor locations permitting subsynchronous rotor whirl to develop, resulting in seizure at wear rings or other close clearance cylindrical surfaces.
- Incorrect impeller-to-diffuser/volute geometry resulting in hydraulic instability especially at low flows or at recirculation These can be Gaps A and B, incorrect impeller-to-diffuser axial alignment, b_3 to b_2 ratio, or unfavorable impeller-to-diffuser vane combination. Any of these can introduce large hydrodynamic forces resulting in substantial cyclic stress reversal.
- Minimum flow (recirculating) is lower than desired. Both axial and radial dynamic load components may approach levels sufficient to break the shaft.
- Inadequate dynamic balance quality of rotor or added balance weight in an incorrect plane (for example, coupling or thrust collar are common), resulting in an excessive bending moment of the shaft, hence excessive cyclic stress reversal.

Any combination of the above items can be responsible for shaft failures. It is clear that proper design of the shaft, correct shrink fits, elimination of sharp corners, documented manufacturing procedures, proper heat treatment, conscientious quality assurance, proper torquing of all retaining nuts, and correct alignment of pump hydraulic components (as well as the rotor itself) are all very important actions necessary to prevent shaft failures. Shaft sleeves should be locked to the shaft properly and sealed to prevent leakage between the shaft and the sleeve. Snap rings should not be used to position shaft sleeves or impellers. If sleeves are keyed to the shaft, sharp corners must be avoided.

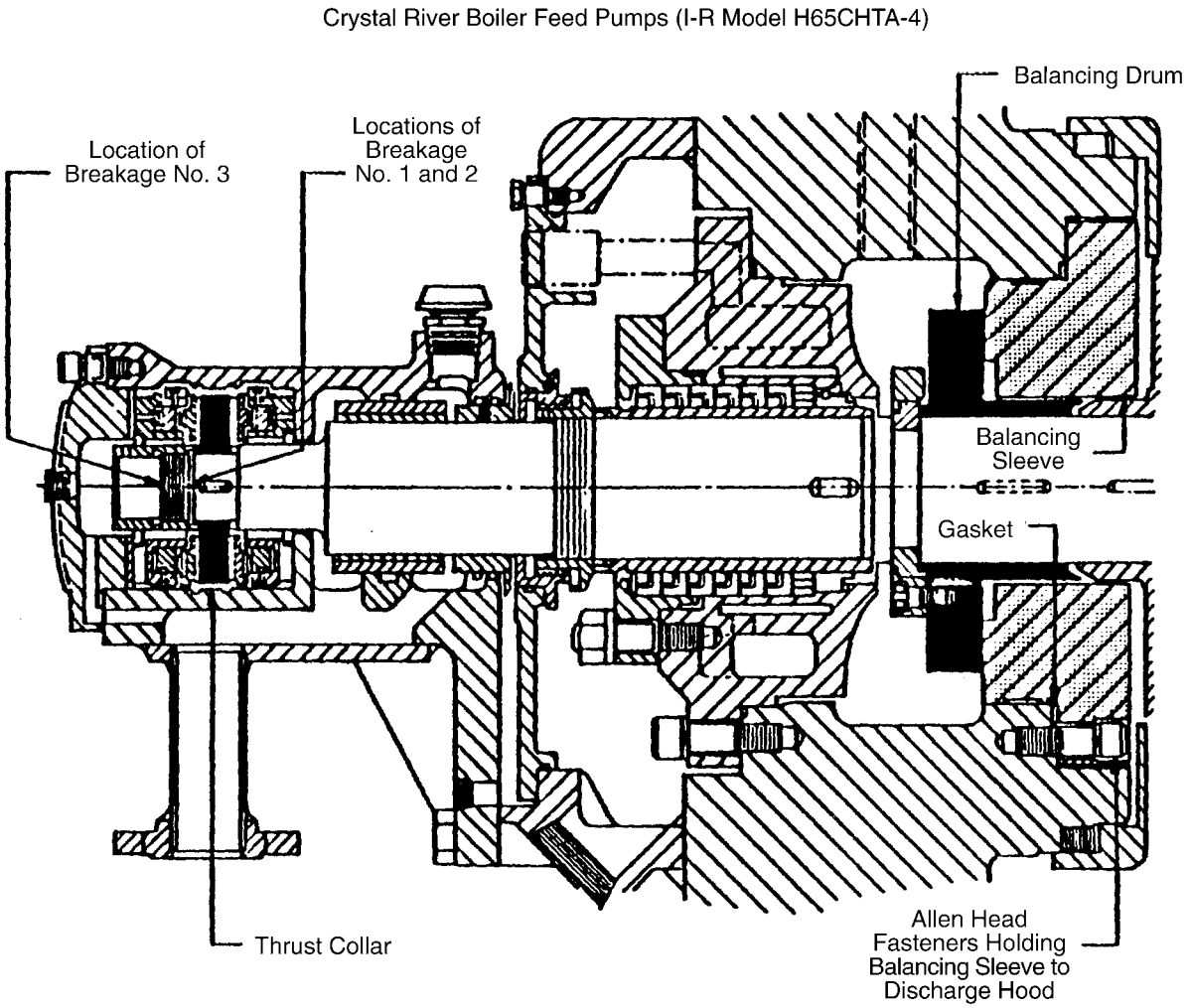

Figure 12-3
Recurring BFP Shaft Breakage of 65-CHTA-4 (Crystal River Unit 2)

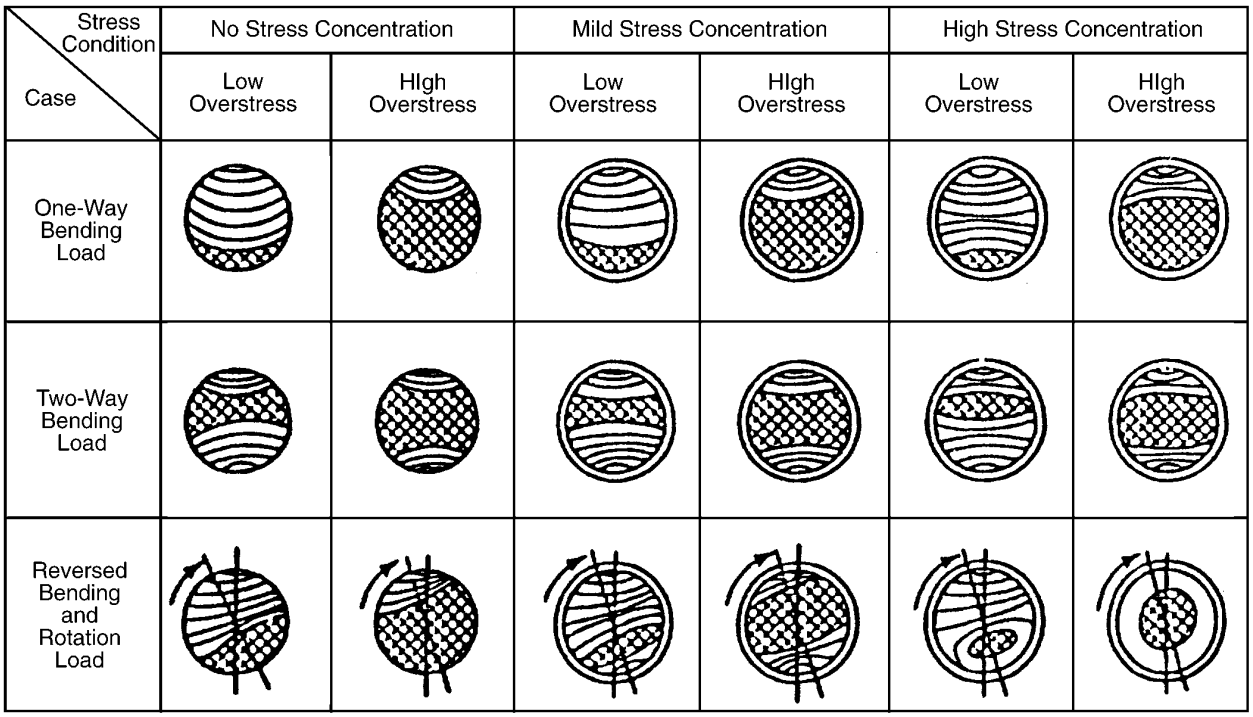

Figure 12-4
Fracture Appearances of Bending-Fatigue Failures (Final Fracture Zones Are Shown as Crosshatched Areas)

12.1.2 Nuclear Reactor Coolant Pumps (RCP, PCP, RRP, MCP)

During the 1991 EPRI International Pump Symposium for Reactor Coolant Pumps [28 to 31], the frequency of shaft breakage or damage at the vicinity of the thermal barrier was emphasized, regardless of the manufacturer or pump type. The nuclear plant owners from Japan, China, and Europe also reported similar experiences. A typical shaft breakage location is shown in Figure 12-5 for the Crystal River-3 nuclear plant [29].

The industry work performed to date has concentrated largely on the detection of PCP shaft cracks, as opposed to determining the root cause of the problem. Upon examining a large number of PCP shaft failures, an early summary of possible root causes is presented.

12.1.2.1 Effects and Types of Hydraulic, Thermal, and Stress Concentration Defficiencies

- Large hydraulic forces are generated due to incorrect component geometry, such as Gaps A and B, Overlap, etc., and as a result high-cycle fatigue failures occur. These hydraulic forces are frequently the primary cause for shaft failures and are also known as the "shaft breaker" for high-energy-input boiler/reactor/SG feed pumps.
- Impeller core shift due to casting inaccuracies results in a dynamic unbalance, but most important, a hydraulic unbalance is created. At the factory, the rotor and impeller are typically balanced to ISO G-6.0, instead of ISO G-1.0. The hydraulic unbalance cannot be corrected by dynamic balancing, even in air or in a vacuum; therefore, the magnitude of the hydraulic unbalance forces are not encountered until the pump is installed at the station. The combination of an unacceptably high dynamic balance criterion and the hydraulic unbalance caused by the core shift frequently results in a large unbalance magnitude at the station. Usually in the field, the counterbalance for the dynamic and hydraulic forces is added in the coupling (for example, at St. Lucie: U=12.5 lbs.). If corrected by adding weight at the coupling, a large residual unbalance moment is created, as illustrated in Figure 12-6. This compensation method is well known as a shaft breaker.
- Excessive static radial forces due to flow interaction between the impeller and diffuser/volute casing can also exist. These forces are a minimum at BEP, are significant at off-design flows, and are a function of casting quality.
- Thermal mixing in the flow field between the seal and pump bearing (both low- and high-cycle thermal fatigue mechanisms) causes thermal shocks to the shaft and high thermal stresses.
- A large number of starts/stops results in hydraulic and/or thermal stress mechanisms during each heat-up and cool-down cycle.
- Zero rotational speed during startup with injection flow on results in high thermal transients, especially for the last pump to start.
- The shrink-fit between the journal bearing and shaft causes stress raisers or hydraulically induced thermal shocks (the first being high-cycle and the second low-cycle fatigue).
- Loss of (or transient) component cooling water flow and loss of seal injection flow introduce low-cycle thermal fatigue mechanisms.

- Extreme operating conditions, such as low pressure or one pump operating mode, result in high-cycle, large amplitude hydraulic forces, especially the vane passing and subsynchronous components.
- Improper vane combination between the impeller and diffuser results in multiples of vane passing frequency excitations.

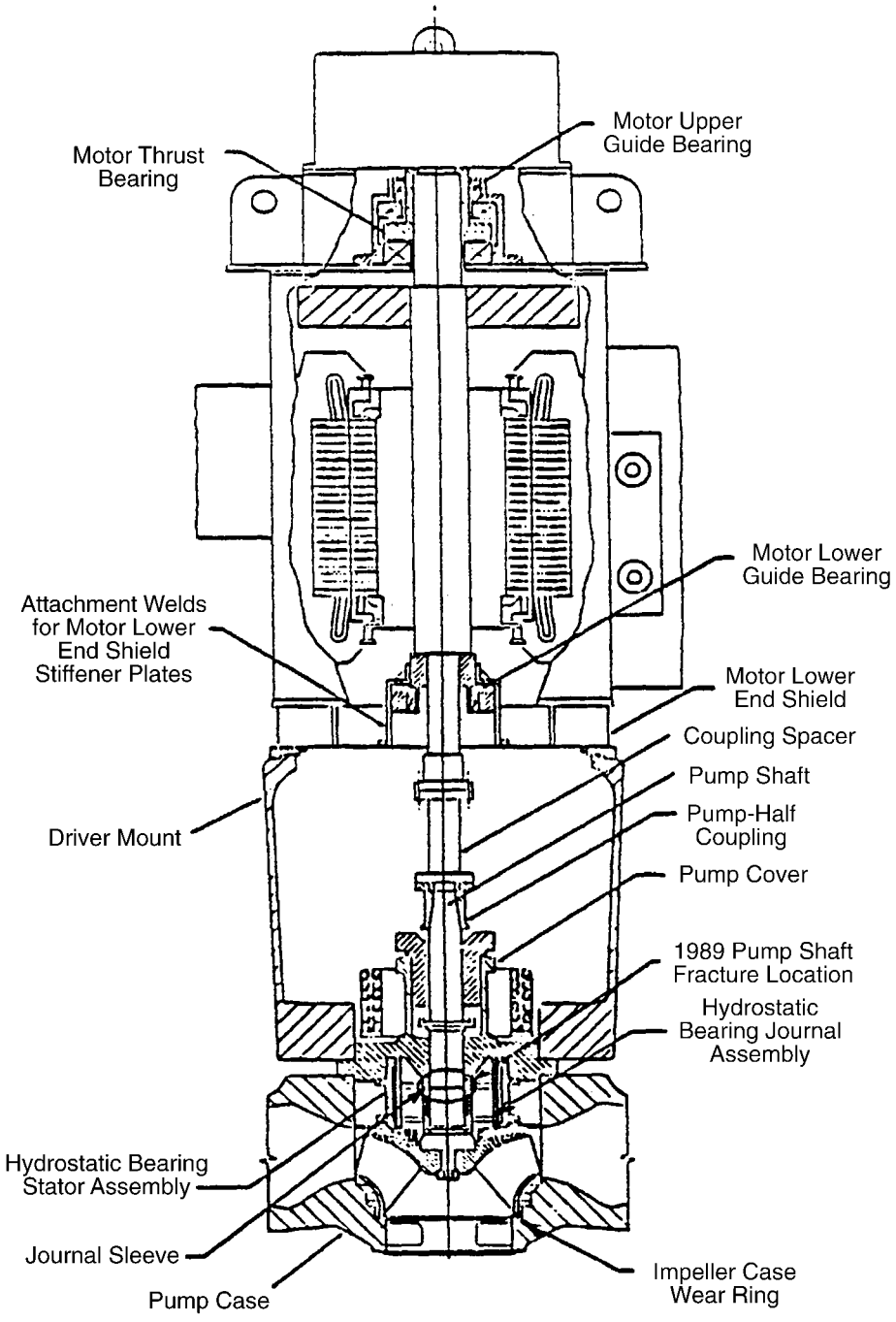

Figure 12-5
Crystal River Unit 3, Reactor Coolant Pump A, Simplified Sketch Showing 1988 Pump Shaft Fracture Location

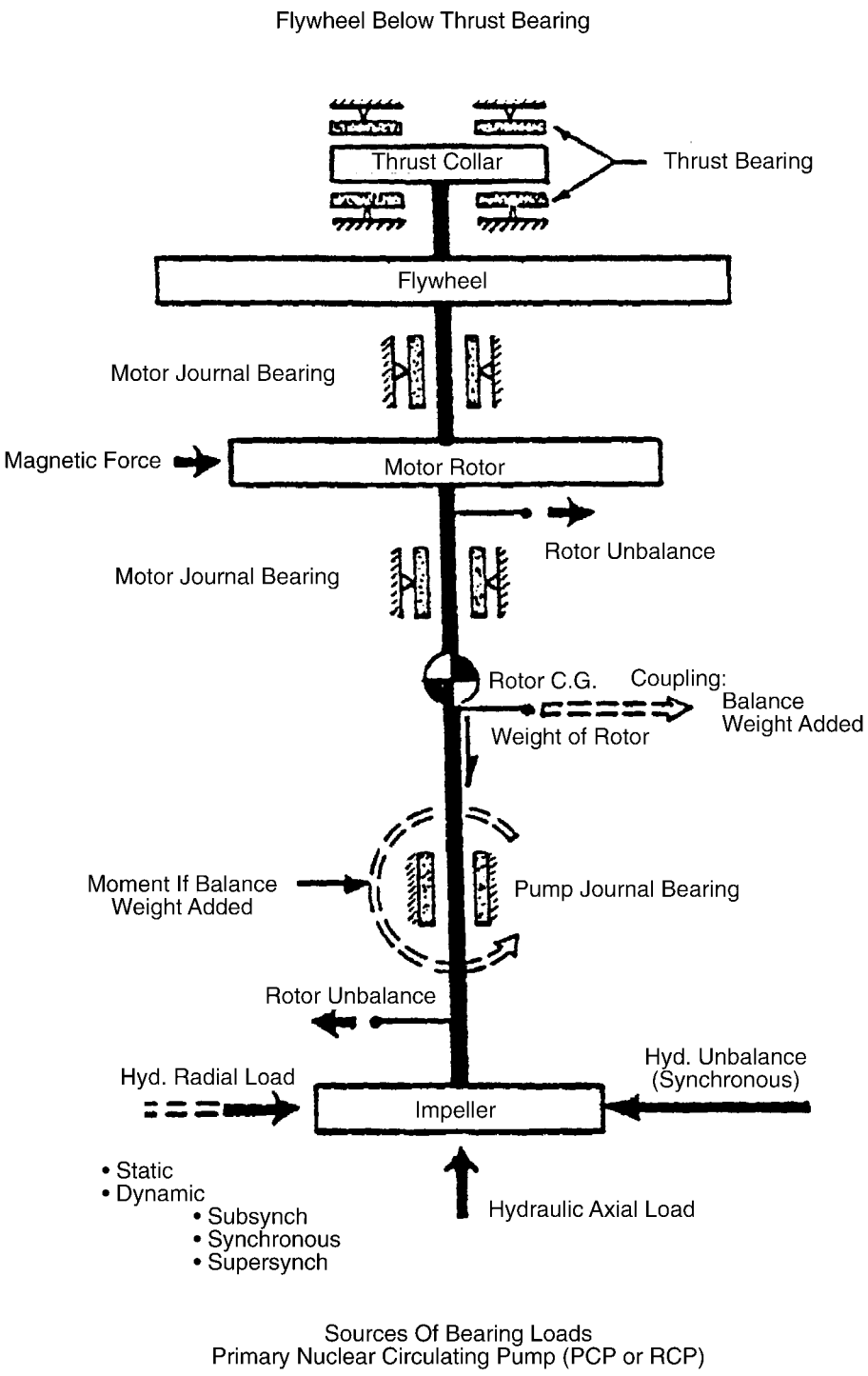

Figure 12-6
Sources of Bearing Loads and Shaft Stresses in Primary Coolant Pumps

12.1.2.2 Effects and Types of Journal Bearing Rotor Dynamics, Critical Speeds, and Dynamic Balancing Deficiencies

- Excessive vibration amplitudes (always evaluate frequencies)
- Bowed/bent shaft (synchronous vibration, also other frequencies if rubbing occurs)
- Excessive unbalance in the pump/motor rotor (very frequent)
- Large amount of weight correction in the coupling (very frequent, for example, St. Lucie)
- Excessive bearing/impeller wear-ring clearance resulting in reduced rotor damping, improper location of critical speed and development of subsynchronous vibration amplitudes/oil-whip [31]
- Correct bearing type in electric motor with improper geometry (for example, no preload in tilt-pads (fitted type), therefore, no damping)
- Rotor critical speed at or close to operating speed or to higher harmonics
- Incorrect bearing type in electric motor (sleeve type) resulting in decentering the shaft at that bearing
- Torsional critical speed at or close to operating speed or to higher harmonics (could excite it especially by rubbing at pump bearing/impeller wear-ring)

12.1.2.3 Types of Shaft Material and Geometry Deficiencies.

- Incorrect or defective shaft material, incorrect heat treatment of shaft or other manufacturing errors (may be quality assurance non-conformances) [28 and 31]
- Foreign material damaging shaft, introducing stress risers, crack initiation

12.1.2.4 Types of Quality Control: Assembly, Alignment Deficiencies

- Incorrect quality control, such as welding the journal bearing sleeve to the shaft by mistake as found at CR-3 and improperly machining many shafts just above the journal bearing as found by the authors
- Misalignment between pump and rotor (frequent), shift in alignment during operation, loose components, heavy balance weight in coupling, loose impeller retaining bolts, and/or drive pins as found at Crystal River-3 [29]

12.1.3 Case History – Model APKD Shaft Failure

Pump Service: Condensate

Pump Model: 34APKD, 7 Stage

Motor: 3000 HP, 1180 rpm

Shaft Material: 410 stainless steel

Subcritical annealing temperature – 1450°F

Temperature > 1500°F results in material hardening

On May 31, 1992, a domestic nuclear plant experienced a main feed pump suction pressure drop of approximately 100 psi. The A condensate pump was removed from service and disassembled. The pump shaft was broken between the third and fourth stages.

Investigation:

The shaft fracture surface was typical of a high-cycle, low-stress fatigue failure. Visual examination of the shaft surface revealed localized heat spots. A heat-affected area on one of the heat spots was determined to be the initiation point of the fatigue crack. Figures 12-7 and 12-8 shows the shaft heat spots and the crack found in the heat-affected area. The microstructure in the area of the heat spot consisted of untempered martensite with a hardness of 43 to 48.5 Rockwell C. The microstructure outside the heat-affected area showed a normal microstructure for 410 stainless steel of tempered martensite, with hardness ranging from 21.1 to 22 Rockwell C. The shaft had failed due to the hard and brittle martensitic structure present in the heat-affected area on the shaft.

Figure 12-7
Heat Spots From Straightening 34APKD Shaft

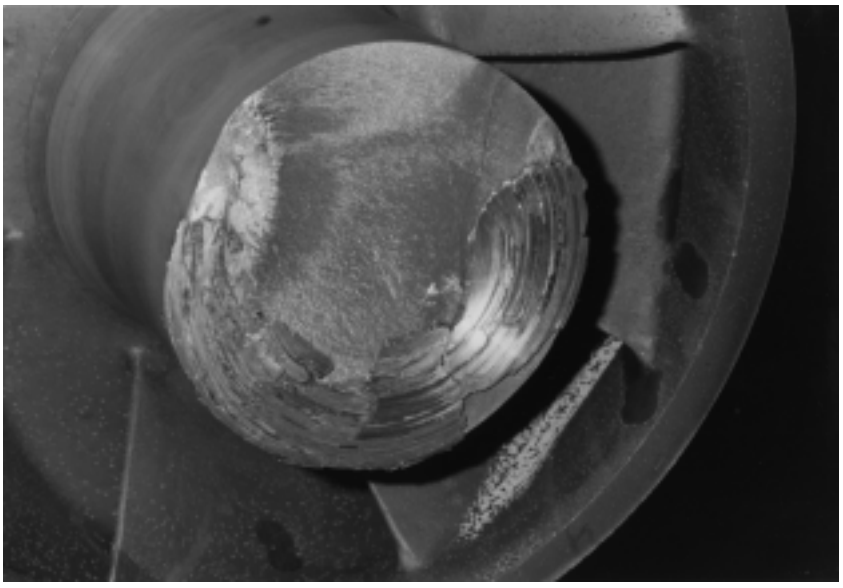

Figure 12-8
Fatigue Failure Initiates in Heat-Affected Zone

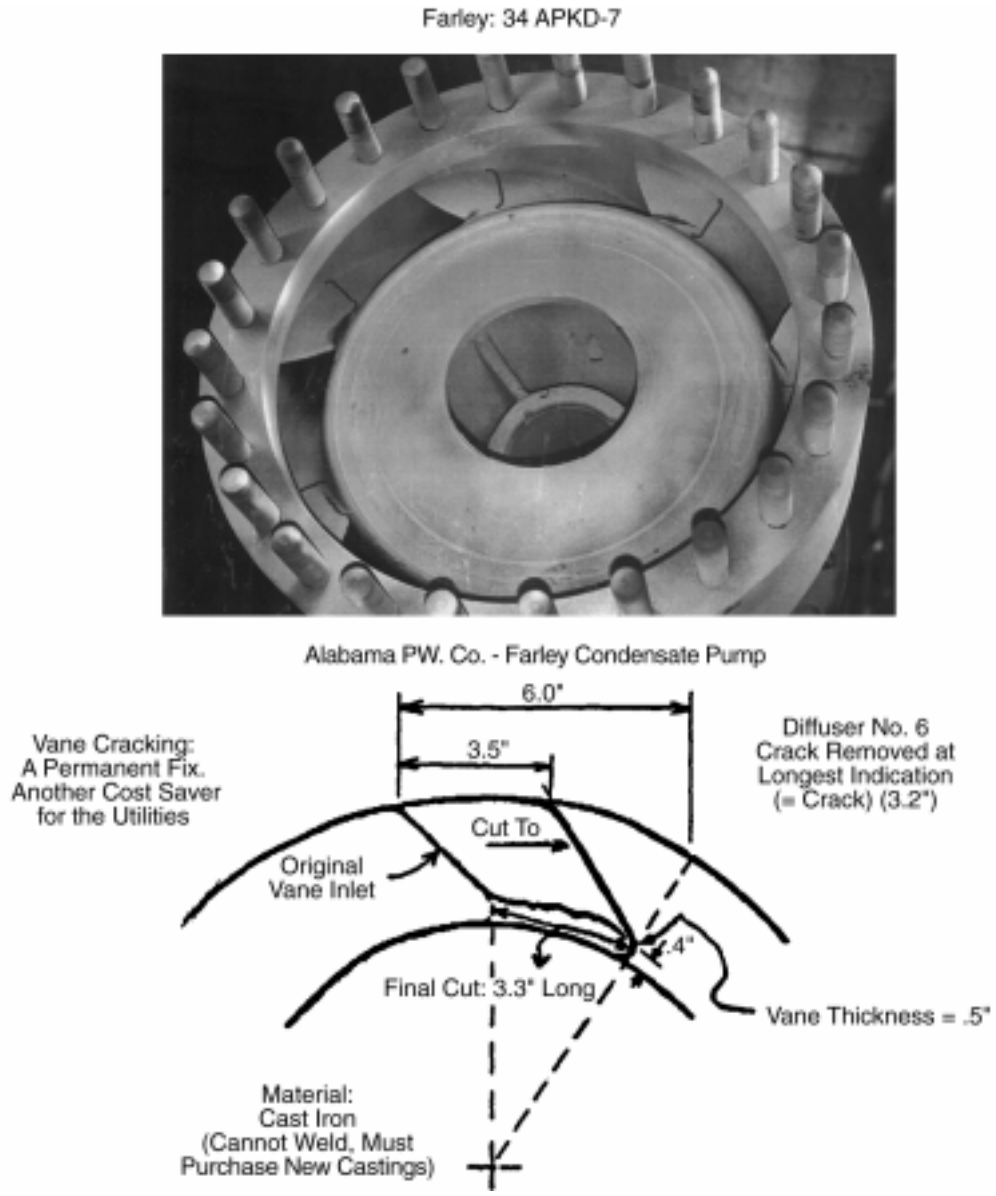

Figure 12-9
Correcting Broken Diffuser Vanes

Root Cause:

The OEM had not properly controlled the heat applied to the shaft during shaft straightening procedures. The evidence clearly showed that the temperature had exceeded 1500°F, resulting in localized hardening of the shaft. When heat is used to straighten a shaft of 410 stainless steel, the temperature must be tightly controlled between 1100–1200°F. However, it is preferred that heat not be used to straighten a shaft.

12.2 Causes of Typical Impeller Sideplate Breakage

- Impeller structure is not strong enough (thin sideplate or vanes with high-energy input).
- Faulty casting (poor quality, core shift, porosity, inclusions, and intergranular corrosion.
- Sharp corners between vanes and sideplates (incorrect vane under-filing) or other locations (incorrect machining).
- Improper welding or incorrect welding rod is used.
- Incorrect hardness (above Rc 30), improper heat treatment/stress relieving.
- Mechanical damage (stamp marks, lifting with C-clamps, and machine tool marks).
- Inadequate Gap B combined with high head per stage.
- Impeller/diffuser vane combination is unfavorable causing hydraulic interaction (combinations such as 6-8, 7-8, 6-11, and 7-13).
- One of the impeller natural frequencies is at or near major vibration frequencies (usually vane passing). Acoustic resonance is amplified (usually vane passing or harmonic).

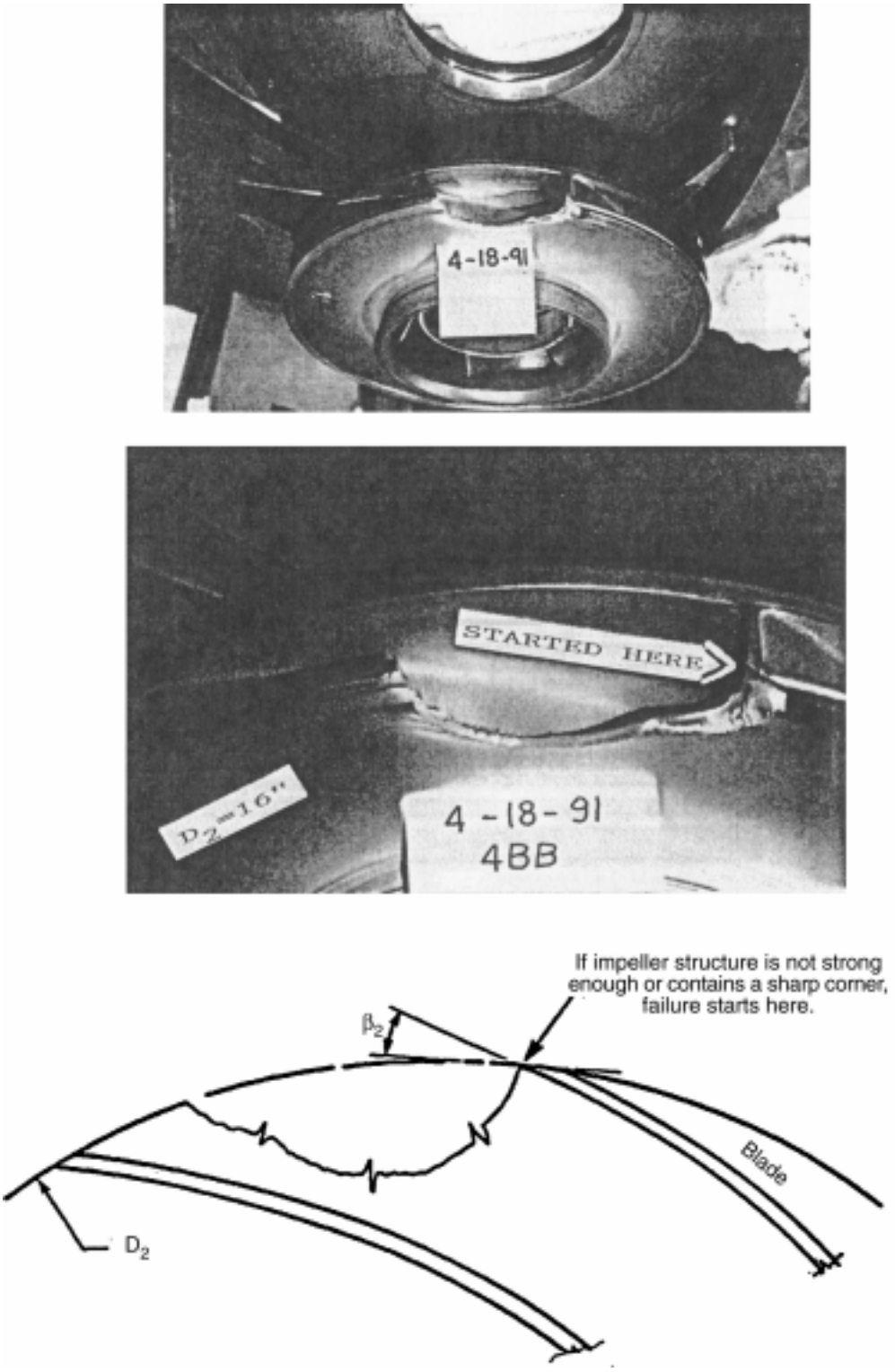

Figure 12-10
Typical Impeller Sideplate Breakage If Material Is Stainless Steel

Figure 12-11
Typical Impeller Damage at the Exit If Material Is Bronze (Booster Pump)

12.2.1 Case History: 95-CHTA-5 Impeller Breakage

Figure 12-13 illustrates a failure of a fifth-stage impeller. In this case, a metallurgist could not explain how the impeller structure gradually changed from Rc 28 to Rc 48 during heat treatment.

12.2.2 Repair or Replacement Criteria

Today it is quite possible to weld repair broken vanes at the impeller inlets, exits, or the impeller sideplates if the broken-out pieces are not extensive. The appropriate technology has been perfected recently in this type of weld repair mainly because the necessity of weld addition when the Gap A design modification was introduced. Where applicable, this can be combined with the repair of cavitation erosion damage.

The weld repair should be done with weld rods matching the metallurgy of the base metal, and proper pre- and post-weld heat treatments must be used. Most boiler feed pump impellers are made of a 13 chrome stainless. Typical materials are CA15, CA6NM, and 17-4 PH. Be certain of the exact material specification before weld repairing.

Hardness of the impeller is critical. In the case of 17-4 PH (also for 15-5 PH), the hardness range of Rockwell 27–31 Rc or 265–300 Brinell measured on the hub and shroud (sideplates), at the outer diameter at four locations 90° apart is recommended if possible. Measurements should be taken where the vanes support the sideplate, not between the vanes. Also, the impeller structure should be supported solidly; otherwise, the readings will be inaccurate and often meaningless. The impeller shown in Figure 12-12 has six vanes; therefore, good readings may be taken only at three locations 120° apart (at locations 1-A, 2-A, and 3-A). If the values are outside the specified range, full mapping as shown in Figure 12-12 is required (at locations A, B, and C on all three vanes, both on the hub and shroud side). In this case, repeating the heat treatment of the impeller as well as remachining all critical dimensions would also be recommended.

The same principle applies to all other materials, but in different, well-specified hardness ranges. A hardness difference of 10 Rc (100 Brinell) for interfacing stationary parts is considered best engineering practice. With the exception of some special cases, the stationary component should be harder.

Because of the heat treatment, the close tolerance fits on the impeller (particularly the bore, wear-ring areas, OD dimensions, and Gap A dimensions) may be lost, requiring weld up of these areas so they can be machined back to required or specified dimensions.

It is essential that the weld repair areas be carefully restored to the original vane profile both at the inlet and the exit by hand grinding, paying particular attention to proper fillet radii between the vane and sideplates.

Impellers should be dynamically balanced after repair and before rotor assembly to the specified balancing standards (1W/N [oz-in] is expected normal in the U.S. industry (see the balancing criteria in References 1, 3, and 33). MILSPEC 167 [39] permits a maximum of 4 x W/N, which is not quite adequate for high-speed boiler feed pump rotors, especially in cases of high technology troubleshooting.

ERCO Standard
Impeller Hardness Test

Scale - HRC

1-A = 37.9	5-A = 38.1
1-B = 39.4	5-B = 37.1
1-C = 37.6	5-C = 35.5
Average: 38.30	Average: 36.90
2-A = 38.9	6-A = 40.6
2-B = 39.0	6-B = 39.6
2-C = 38.5	6-C = 38.9
Average: 38.80	Average: 39.70
3-A = 37.9	7-A = 39.4
3-B = 36.5	7-B = 39.2
3-C = 37.8	7-C = 38.2
Average: 37.40	Average: 38.93
4-A = 39.6	8-A = 41.7
4-B = 37.8	8-B = 42.4
4-C = 38.0	8-C = 41.0
Average: 38.46	Average: 41.70

Impeller No.: 1-B
Inspector: Gene
Date: 10/12/91

Above data was taken on the hub side (Points: 1-A/B/C To 4-A/B/C) and on the eye side (Points 5-A/B/C To 8-A/B/C). Total of 245 points with questionable results. Above figures show a six-vaned impeller with the correct point locations. Picture varies with the number of vanes.

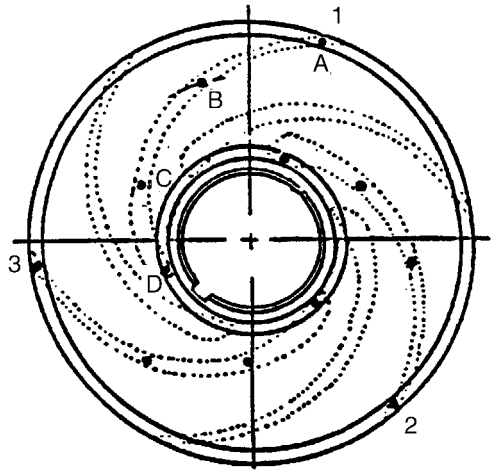

Hub Side

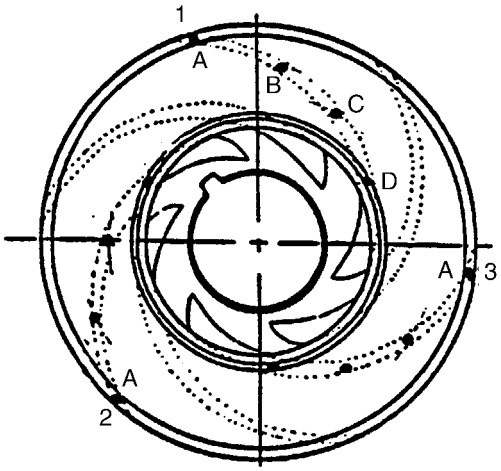

Shroud/Eye Side

Figure 12-12
ERCO Standard for Hardness Mapping of BFP Impellers

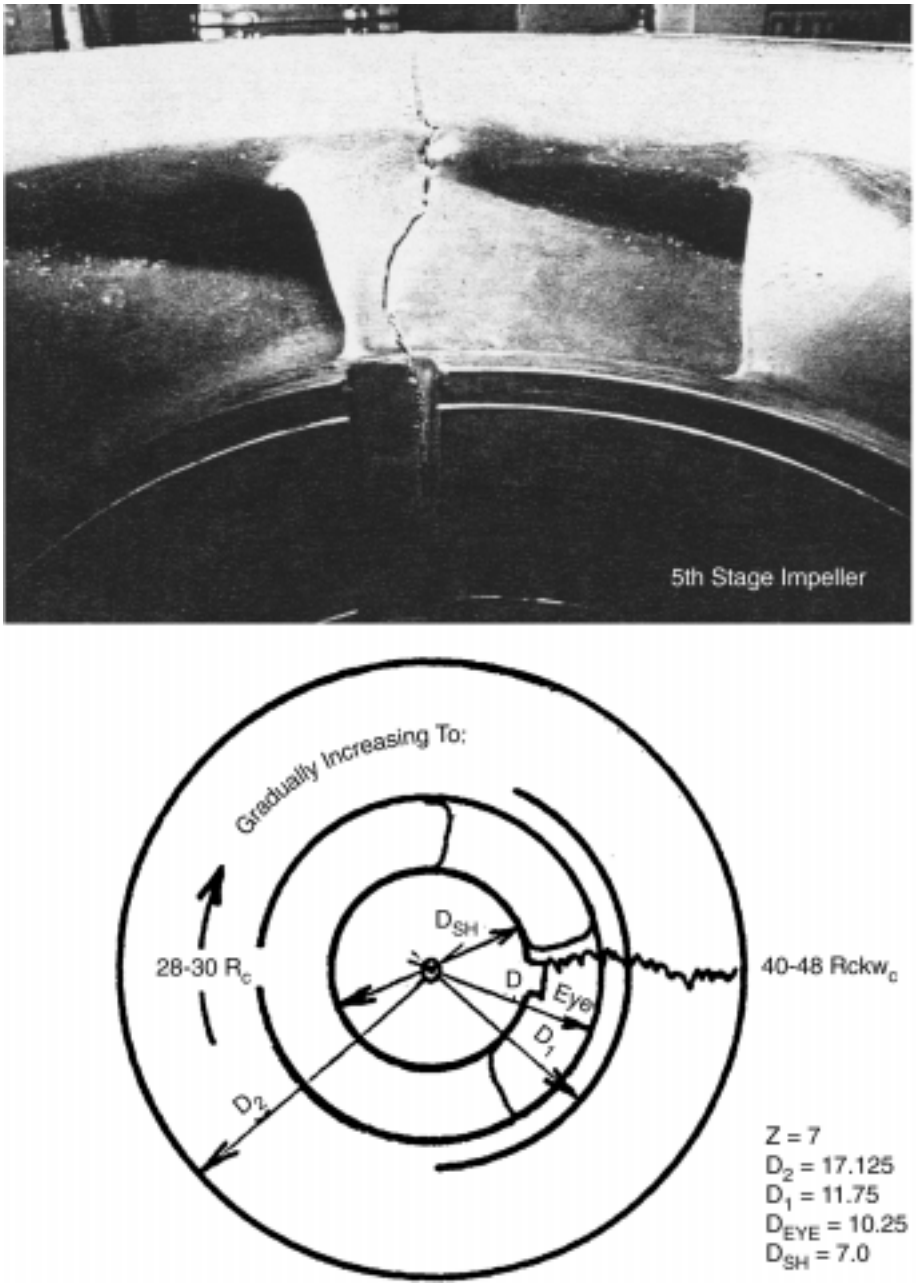

Figure 12-13
Location of Fifth-Stage Impeller Breakage (95-CHTA-5) at Brayton Point Unit 3

12.3 Impeller Wear-Ring Failure

The purpose of wear rings in a pump is to provide a renewable surface that is the stationary boundary of the annulus space between the front and back hubs of the impellers. The wearing surface of the wear ring and the impeller hubs typically have configurations such as both flat, one flat and the other grooved, or both grooved. Older pumps have flat surfaces. This was followed by a period when it was thought that grooved rings would yield less leakage and higher efficiency and be more wear- and gall-resistant, thus less likely to seize. Some grooves were even machined in a spiral to reduce the amount of leakage through the annulus. The grooves can be V grooved or grooved with a flat land between, sometimes with a single or multiple spiral. The grooving can also be shaped as a labyrinth tooth to reduce leakage rates. Or, when added rotor-dynamic stability is needed, the Lomakin Effect geometry has frequently been used. Various customary geometries are shown in Figure 12-14. The land portion of the grooved area is sometimes chrome plated. However, the plating often rubs off or peels off rapidly, resulting in accelerated maintenance. Now that the rotor-dynamic characteristics of feed pumps can be modeled much more easily with present computer codes, the flat rings and hubs are more often used because of their higher damping coefficients.

Pump components such as shaft seals (if labyrinth type), impeller and case wear rings, and axial balancing devices (disk, drum or piston, and break-down bushings) cause many pump failures and often result in unanticipated maintenance repairs and an unexpected reduction of unit availability [2]. Wear rates of the wear rings, galling, and the tendency to cause rotor seizure (especially on turning gear operation, for example) have caused much additional maintenance time and expense.

12.3.1 Wear Ring Development in the United States

Significant developments and corrective actions for high-energy-input centrifugal pumps (such as boiler feed pumps) in the United States have occurred since 1970 [2]. Most of the reported developments were performed or at least directed by ERCO, as the only practical R&D center left in the U.S. for utility pump applications. The most significant items reported are:

- Eliminating seizure and reducing wear in BFP close clearance components (wear rings, labyrinth seals, and balancing disk/drum) through research, testing, and experimentation in materials, hardness, and wear surface geometries.
- Changing materials to seizure-proof, free-machining material with proper hardness, combined with proper geometry and optimum radial clearances, may increase pump capacity at BEP as well as pump efficiency.

Extensive experimentation showed that a minimum difference of 100 Brinell hardness should be maintained between stationary and rotating components regardless of the OEM's practice. This converts to a difference of 10 Rockwell C hardness. Most BFP impellers have a hardness of 25 to 30 Rc. Some impellers are flame hardened to an Rc 50, and some impellers in older designs also have wear rings on the impeller eye (shroud side). The basic rule is for one material to be the free-machining SS 416, 420F, or CA40F running against 410; 420; 440 A, B, C; 17-4 pH; CA15; or CA6NM, which provides an excellent condition to prevent galling or seizure. Therefore, the critical wear-ring features are:

- Material (420F/CA40F for at least one of the mating surfaces)
- Hardness (a minimum of 10 Rc difference between mating surfaces)
- Geometry (see Figure 12-14; choose an appropriate configuration for each application from a rotor-dynamics point of view)

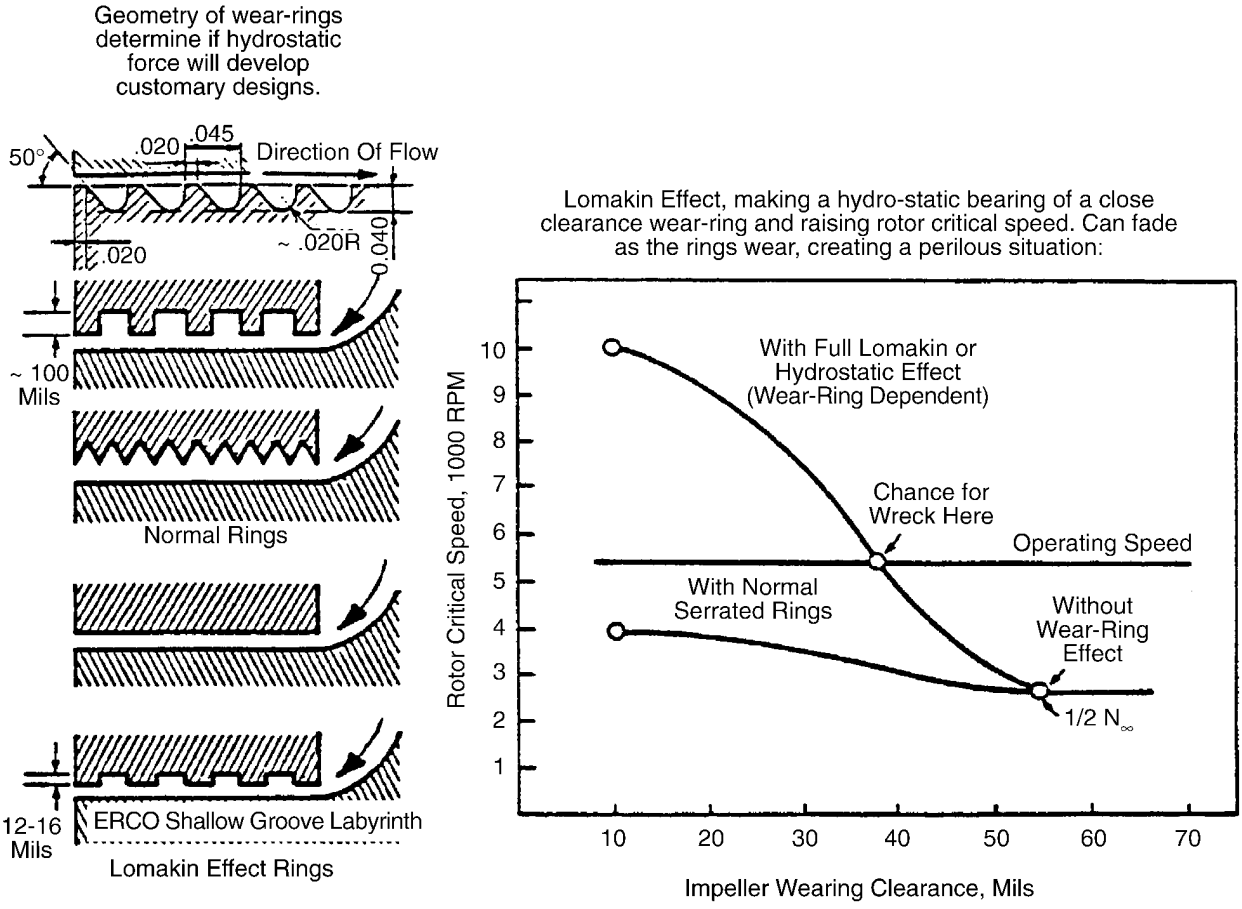

Figure 12-14
Various Wear Ring Geometries and the Effect of Wear on the Lateral Critical Speed of the Rotor

12.3.2 Probable Root Causes

The use of the proper wear-ring geometry and materials reduces the susceptibility of the rings to galling and/or seizure when metal-to-metal contact occurs. However, it does nothing to prevent the metal-to-metal contact. Therefore, the most probable root causes of wear, galling, and/or seizure, occasionally resulting in shaft failures, are:

- Incorrect wear ring material (420F/CA40F is the only practical, seizure-proof and free-machining material).
- Incorrect hardness of the mating surfaces (A minimum of 10 Rc hardness difference is required between the stationary and rotating rings, regardless of the material used and with the stationary ring being the harder material.)
- Excessive vibration caused by one of the following symptoms:
  - Rotor unbalance due to a bent or bowed shaft, loose rotor parts (most frequently a case ring), and improper or lack of precision rotor balance.
  - Also, frequently missing or incorrectly sized keys are found, and grease lubricated couplings can be overgreased, causing a major unbalance when the grease collects on one side of the coupling.
  - Misalignment between pump and driver.
  - Poor rotor-dynamic characteristics in the pump, including rotor resonance in the operating range.
  - Excessive hydraulic forces on the rotor caused by impeller-to-diffuser/volute interaction (Gaps A and B, Overlap, b_3/b_2, vane combination Z_2 and Z_3).
  - Inadequate journal bearing design (such as plain cylindrical sleeve bearings, incorrect pocket dimensions for the pressure-pad-type bearing, and negative preload for the tilting-pad-type bearing).
  - Thermal bowing of the barrel and/or rotor, caused by improper warm-up procedures.
  - Inadequate minimum flow systems (for example, insufficient capacity).
  - Excessive piping loads (forces and moments) on the pump causing either distortion or movement.
  - Heavy rubbing inside the rotor caused by one or more of the above items resulting in subsynchronous rotor vibration leading to heavy damage or destruction of the rotor, occasionally with a broken shaft at locations shown and explained in Section 12.1.

12.3.3 Corrective Actions

Depending on the verified root cause, one or more of the following corrective actions may be necessary to either prevent or reduce the frequency of wear-ring replacements. Wear rings are never repaired; they are almost always replaced.

- Change to 420F or CA40F stainless steel, which is less prone to seizure, galling, or wear than most other 400 series materials, with proper hardness (a minimum of 100 BHN or 10 Rc

hardness difference is required between rubbing surfaces). This may also prevent rotor seizure, particularly on turning gear operation.

- Revise overhaul procedures, specifying balancing tolerances and close oversight of the rotor balancing.
- Check for proper shaft key sizes. The largest key is always in the coupling, if not the shrunk-on type (becoming more popular). An improper key results in high vibration and/or rubbing, hence accelerated wear or seizure.
- If the coupling is grease lubricated, install the proper amount of grease during maintenance. Excessive amounts of grease will collect on the periphery in batches, resulting in unbalance. A symptom of this fault is random change in vibration amplitude after each startup due to the fact that the grease collects at a different location after a shutdown, resulting in a different unbalance.
- Revise the alignment techniques or system evaluation to determine if there is pump and/or driver movement due to external loads.
- Analyze vibration data to determine the causes and implement the necessary changes.
- Redesign the journal bearings to either pressure dam, tri- or four-lobe, or tilting-pad type. (Consider the type most appropriate for that application or the type that could be adapted to the given bearing housing geometry. Tilting pad is usually the best but requires more radial space than would be available for a given pump).
- Redesign the warm-up system or revise the warm-up procedures.
- Modify the minimum flow (recirculation) system if the recirculation flow is less than permissible for that pump.
- If there are other major problems in addition to excessive wear-ring wear, consider a redesign of the element rotor-dynamic and/or hydraulic problems.

12.3.4 Conclusions

AISI 416 and 420F or CA40F materials were demonstrated as excellent wear-ring materials that eliminate or at least reduce impeller hub/shroud and wear-ring seizure, galling, and wear. They have high sulfur or phosphorus content (two versions are available), which reduces galling and wear and, therefore, extends operating life. The AISI 416, because of its low carbon content, is subject to surface cracking when heat treated to or above 40 Rc; hence, it has limited application as wear-ring material. Therefore, AISI 420F or CA40F material should be specified when replacement parts are ordered. They typically do not cost more than presently used materials. The above approach has given satisfactory results without pump lock-ups, with good efficiency and extended wear life, and also has resulted in good turning gear operation for the customary low RPM operation range in the United States (5 to 10 RPM, while outside the United States, it is 100 RPM or higher).

12.3.5 Research Results

The long lasting research project concluded in our 1979 report on the subject. The report marked the end of our material testing in search of a seizure-proof wear ring material for high-energy-input, high-temperature centrifugal pumps. The research project had been conducted due to a very large number of pump seizures, mainly in fossil BFP applications, regardless of the OEM, the size or speed of the pump, and subsequent loss of plant generation. Most frequent seizures occurred during startup thermal shock and low-speed turning gear operations. The several basic materials originally selected were reduced to three final choices by elimination, based upon test results.

Rapid thermal shock and large amounts of foreign materials were applied in the test rig. Of the several selected materials, only the 420F material gave satisfactory results. As a result of the extensive testing, this material was adopted as the solution when impeller/wear-ring seizure occurred. However, it should be pointed out that we were able to make even the 420F material gall and seize if there was no hardness difference between the mating surfaces.

12.3.6 Wear Ring Material Specification

The specification of the final approved seizure-proof material is as follows:

ASTM A296 Grade CA40 (free matching material, hence, the names 420F or CA40F were recognized and adopted)

Aluminum, %	0.06% maximum

The material must contain combinations of selenium, phosphorus, and molybdenum or sulfur and molybdenum as follows:

Selenium, %	0.20–0.35
Phosphorus, %	0.17 maximum
Molybdenum, %	1.5 maximum

or

Sulfur, %	0.20–0.40
Molybdenum, %	0.40–0.80

The ASTM A296 designation was officially changed to A743 in June 1979. Also, the CA40 special material was accepted as A743 Grade CA40F or with the AISI code as 420F.

12.4 Balancing Disk Failures

The number of axial-balancing-disk-caused failures mushroomed to many hundreds as the multistage feed pump sizes increased. Hydraulically induced axial forces can have static components in excess of 400,000 lbs. in a large BFP. The dynamic components can easily have magnitudes over +/- 100,000 lbs. Users started to demand the drum design, which on the surface was responsible for fewer failures and less maintenance. Pump companies quickly switched to the drum design when the users (especially oil companies: ARAMCO, ARCO, and SOHIO) demanded this design as opposed to putting their efforts into research and proving the significant advantages of the disk design.

For a proper disk design, the magnitude of the force and its variation between maximum and minimum flows, as well as the mechanisms creating it, must be known accurately (within the thrust-carrying capability of the applied thrust bearing). These factors were not known or well understood by many. The easy way out was to switch to the drum design.

A typical failure is shown in Figure 12-15, which occurred due to poor ductility of the material. In this case, the fracture surface was brittle in nature. For rotating components, forged material should be used with proper hardness (not to exceed 30 Rc). Other failure modes are discussed in Section 11 and References 1, 2, 4, 9, 19, and 33.

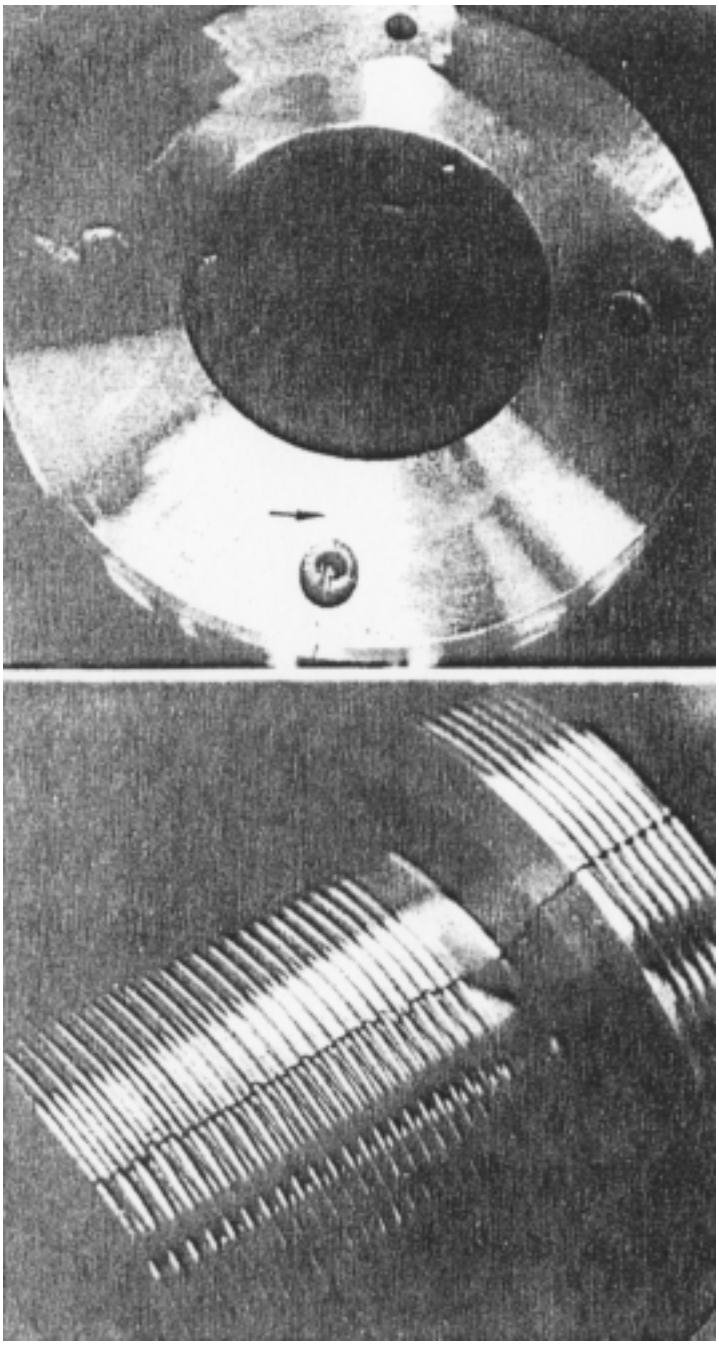

Figure 12-15
Failed Balancing Disk Due to Poor Material Ductility (Spin Cast Instead of Forging)

12.5 Coupling Failures

The purpose of the coupling is to transmit torque from the pump driver to the pump shaft. There are basically two categories of couplings: rigid and flexible. Rigid couplings are used primarily in low-energy, process-type pumps or where thermal growth causing misalignment between the pump and driver is not anticipated. Flexible couplings are used in most BFP, boiler feed booster, and nuclear pump applications.

The two styles of flexible couplings on the market today are geared style and diaphragm disk pack style.

The flexible geared coupling design preceded the diaphragm disk pack and was the coupling of choice through the 1970s and early 1980s. However, the diaphragm disk pack designs offer significant advantages over the geared couplings and are being used for upgrades or modifications to improve pump reliability, maintainability, and troubleshooting. Advantages of the diaphragm disk pack coupling are that it:

- Does not require lubrication
- Completely isolates the pump and driver, even in the axial direction
- Provides greater protection against misalignment

12.5.1 Geared Coupling Failures

The geared couplings (Figure 12-16) are subject to failure due to:

- Gear tooth wear
- Lockup due to loss of lubrication or friction
- Excessive or improper lubrication application

The driven torque is transferred to the pump shaft through the gear teeth of the geared coupling and, inevitably, friction wear and/or fretting wear will occur. However, with proper alignment, installation, and lubrication, and in the absence of pump hydraulic or rotor-dynamic instabilities, the wear can be minimal and the geared coupling will provide reliable service. There are no known acceptable methods to repair the coupling gear teeth; thus, coupling replacement will be required when wear or pitting of the gear teeth is observed.

The gear teeth wear, failure to lubricate the coupling, leakage of lubrication, or axial shuttling of the pump shaft will cause excessive friction and heat at the coupling gear teeth. The excessive heat can cause lubrication breakdown and result in lockup between the gear teeth. When lockup of the coupling occurs, a major failure of the rotating machinery can be expected.

There have been cases documented where excessive or improper lubrication has resulted in a major unbalance force in the coupling. The grease collects in one area of the coupling and causes the unbalance (for example, one case had a 5 lb. unbalance). It is also a confusing problem to diagnose because when the unit has been started up after inspection or during testing, the unbalancing force can change location and magnitude because the lubrication will settle to a different area in the coupling and create a different unbalance force.

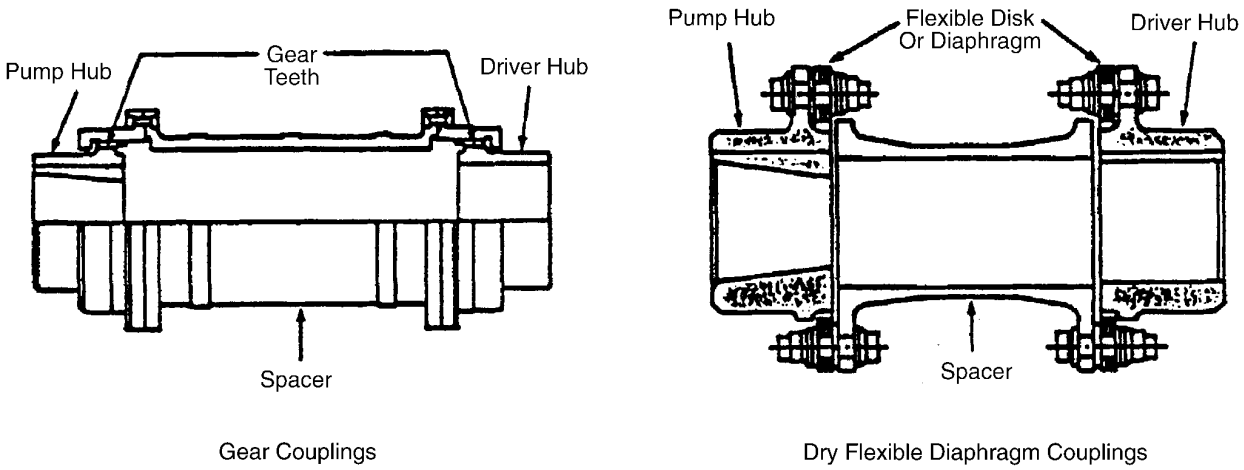

Figure 12-16
Typical Gear and Diaphragm Type Couplings for High-Speed BFP Applications

12.5.2 Diaphragm Disk Pack Failures

The heart of the diaphragm disk pack coupling is the stainless steel diaphragm pack as shown in Figure 12-17. The pack consists of several thin diaphragms or disks, separated by inside diameter filler rings and segmented outside diameter fillers. The disks are sandwiched between thick end plates to give rigidity to the pack but still provide coupling flexibility and dynamic isolation between the pump and driver. There have been cases of disk failures in the coupling disk packs. The root cause of the problem has been improper installation of the coupling. The coupling is designed so that the disks are not to be axially loaded during operation. Therefore, the coupling must be set up for pump shaft movement (usually due to balance disk closure), so that the coupling is in a neutral position when in operation.

In cases where diaphragm disk failure has occurred, a major failure of the rotating machinery has not occurred. The failed disks were discovered during outage or maintenance inspections. A total failure of the coupling requires approximately 50% failure of the total number of disks on a side of the coupling, and can be prevented by inspection of the coupling (at normal maintenance periods) for cracks or distress areas in the outer diaphragm of the pack.

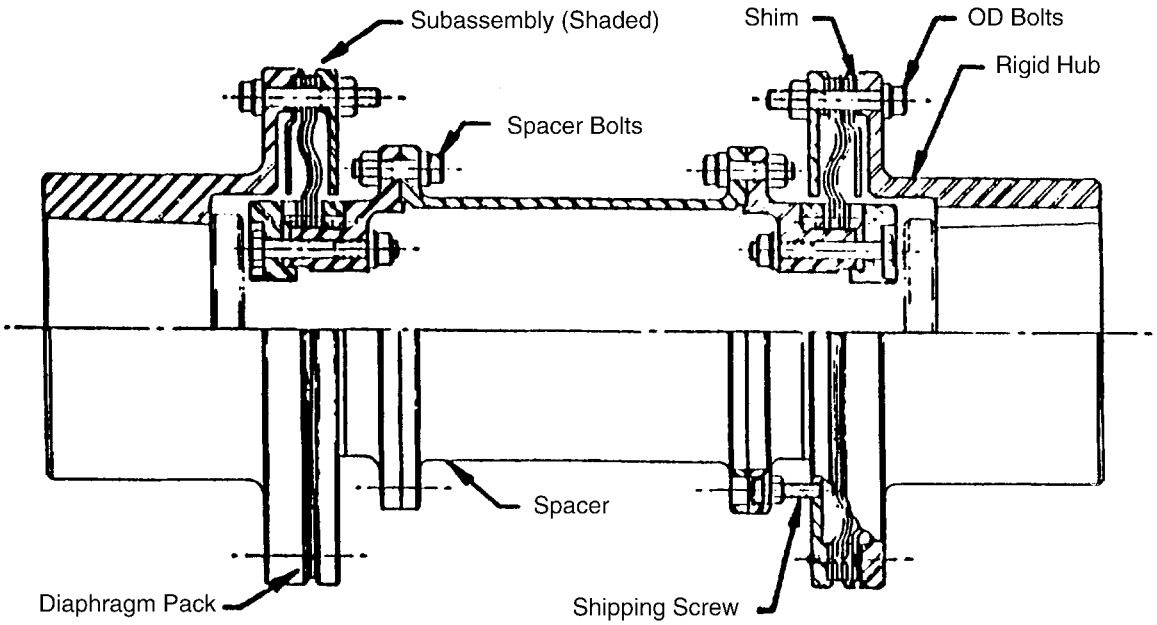

Figure 12-17
High-Performance (HP) Series Zurn-Ameriflex Dry, Flexible Diaphragm Coupling (The diaphragm profile permits large axial and angular deflection with low stiffness. The diaphragm pack is tightly clamped at the ID, causing it to act as a solid unit in the transmission of torque.)

13
ELIMINATION OF IMPELLER INLET CAVITATION DAMAGE: THE ANTI-STALL HUMP

One of the problems that has arisen as pump energy levels have increased is cavitation damage or erosion in the suction stage impellers. This occurs because the higher head of a reasonably-efficient centrifugal impeller is accompanied by a correspondingly greater peripheral speed of the impeller blades. This in turn requires more NPSH with the consequent increase in erosive pitting of the surfaces, as always-present bubbles collapse nearby. Progress has been made in extending the life of these suction stage impellers against cavitation erosion, but the problem has become complicated by the unsteady two-phase flow behavior that has arisen from the lower-than-design flow rates through the pump [3].

Studies of cavitation at both design and lower pump flow rates have led to a new understanding of the role that the two-phase flow phenomenon plays in pump hydraulic instabilities. This has been possible with the help of laboratory test pumps in which cavitating impeller flow is observed through transparent casing walls, and appropriate hydraulic design changes were made [5]. Such changes have produced longer impeller life through the reduction of both cavity size and bubble formation on the impeller inlet vane [6].

But the flow visualization research has also revealed the oscillation of the unsteady two-phase flow behavior in which cavities on the suction, or visible, side of the blades are seen to oscillate rather violently as the pump flow rate is reduced below that of the BEP [7]. This oscillating cavitation is beginning to be recognized as a major source of fluid/structure interactions that are characterized by pressure pulsations and the associated forces. If oscillating cavitation occurs in a high-energy pump, excessive stresses in the pump and system structures can result [8].

The goal then becomes one of reducing the total volume of vapor or cavity volume that can exist within the impeller through the introduction of new design features and practices [8]. This not only increases pump resistance to cavitation erosion but also increases reliability through the elimination of the oscillating cavitation occurring in the suction stage of the pump. The primary zone of cavitation within an impeller to look for cavitation is the suction (visible) surfaces of the blades. This is where most of the total cavity volume exists, and it is conveniently observable in flow visualization tests, as 1 microsecond photographic exposures attest [5, 8]. Quantitative efforts to predict pump life under cavitating conditions have evolved from empirical correlation of field data on well-designed conventional impellers [14,15] to formulas that involve the length of well-defined cavities along the blade surfaces and emanate from the leading edges [9].

For flow rates at or below the BEP, these cavities occur on the suction (visible) or trailing faces of the blades. But at flow rates sufficiently below that of the BEP, recirculation breaks up these cavities, creating an unsteady two-phase flow in which bubbles are scattered within random

vortices generated by the shearing action of the emerging backflow [5]. Some of these bubbles collapse on both the pressure (nonvisible) and suction (visible) sides of the blades and some within the main flow stream. This chaotic flow configuration no longer approximates a cavity, and the understanding of this configuration could yield a reliable life prediction.

Observations indicate that the operating range over which a cavity length along blades can be determined is probably that for flow rates above which recirculation occurs [16, 17]. Generally, feed pumps do not operate for significant periods above BEP flow rates. Thus, measurable suction side cavities exist most of the time in typical pump installations. In the late 1970s, research began to develop modifications to impeller inlet vanes to prevent suction and pressure side cavitation.

13.1 Anti-Stall Hump Development

Almost simultaneously, the following three hydraulic research scientists were independently working on modifications to prevent impeller inlet vane cavitation:

- Dr. E. Makay, Energy Research and Consultants Corp., Morrisville, PA
- P. Hergt, KSB, Frankenthal, West Germany
- Dr. P. Cooper, Ingersoll-Rand Pump Co., Phillipsburg, NJ

Interestingly enough, all three researchers developed similar modifications designed to prevent flow stall along the vane inlet surface. Six basic cavitation damage types at the impeller eye (inlet) are shown in Figure 13-8 with the appropriate summary of causes and solutions. Various combinations of the six basic types can make the damage appear more complicated, and more difficult to classify, and more difficult to find the right geometry modification.

- Dr. Makay developed the anti-stall hump shown in Figure 13-1. The first experimental modifications were being performed in 1976, and the first practical applications were being performed on a series of circulating water pumps in 1983 with 218 applications implemented by 1993 as shown in Figure 9-1. The majority of the modifications were made on large circulating pumps including some RCP (PCP) applications in PWRs, and a smaller number applied to high-energy-input large feed pumps.
- P. Hergt patented his concept (Figure 13-2) in 1983, but the geometry was very restrictive. The patent specifies the shape of the hump line (that is, straight), limits the length of the hump line, limits the vane inlet angles (such as, 0° to 5° to hump line), specifies the inlet vane radius, and limits the design to radial and mixed flow impellers. The limitations thus restrict the application so much, that any logical modifications fall outside the patent, and, therefore, there are no known modifications in service in the United States that meet the requirements of the patent.
- Dr. Cooper's version of the anti-stall hump was called the bias wedge, as shown in Figure 13-3 [42], and it is understood to have a patent pending at the time of the original publication of this report. The first field application of the bias wedge did not occur until the late 1980s and only at a handful of power stations with various reports of success. Also, the bias wedge has not been implemented as a modification to existing impellers; instead, it has been applied only in the design of new impellers.

The anti-stall hump developed by Dr. Makay was not patented because it was believed to be too theoretical and not capable of receiving a patent. Due to the different impeller inlet vane geometries, inlet flow conditions, inlet cavitation damage, pump applications, and pump service requirements, a single design was not feasible to address all situations. Each case is special on its own, and probably no two cases are identical. Also the designs of P. Hergt and Dr. P. Cooper addressed cavitation only on the suction side, while the anti-stall hump has been applied on both the suction side and pressure side of impeller inlet vanes by Dr. Makay with equal success. The anti-stall hump has been applied to large circulating water pumps (for example, condenser and cooling tower applications) and to the first-stage impellers of large high-speed BFP, when cavitation was severe enough to warrant impeller replacement or a new impeller design.

The advantages of applying the anti-stall hump, if diligently applied, are:

- Starting out with a known impeller behavior or condition can be easier to correct and is more practical than designing a new impeller.
- The cost of modification is at least one order of magnitude less than the design of a new impeller, particularly considering costs associated with engineering, making a new pattern, casting, and the risk of design or manufacturing errors.

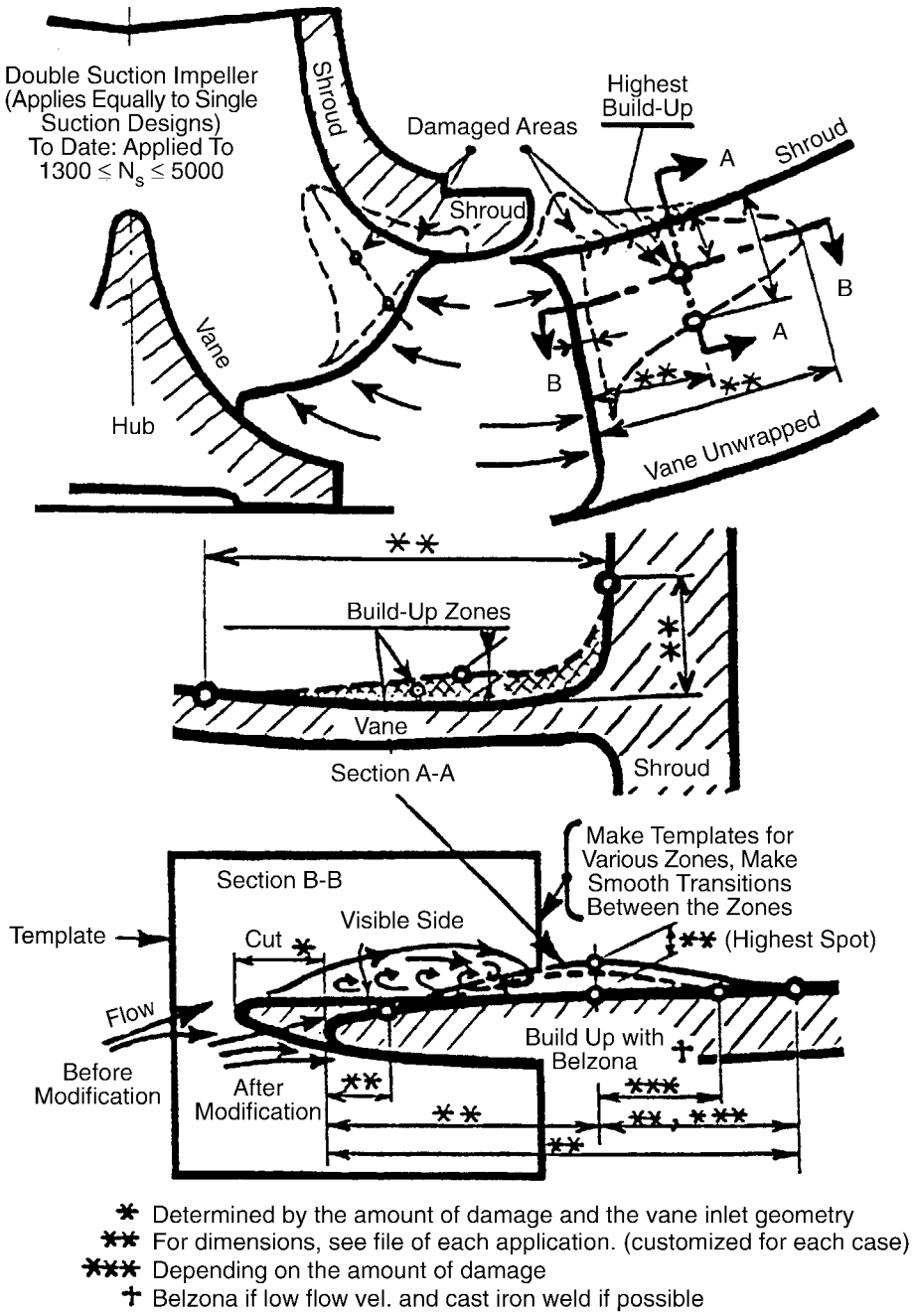

Figure 13-1
Example of Anti-Stall Hump Applied by Dr. E. Makay in 1983

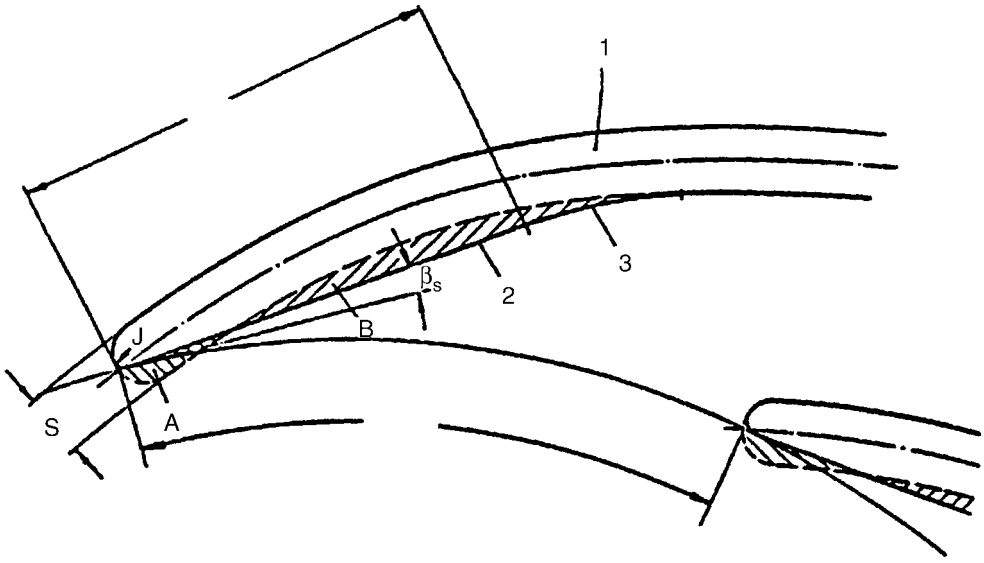

Figure 13-2
Design of Hump as Patented by Peter Hergt of KSB (Germany)

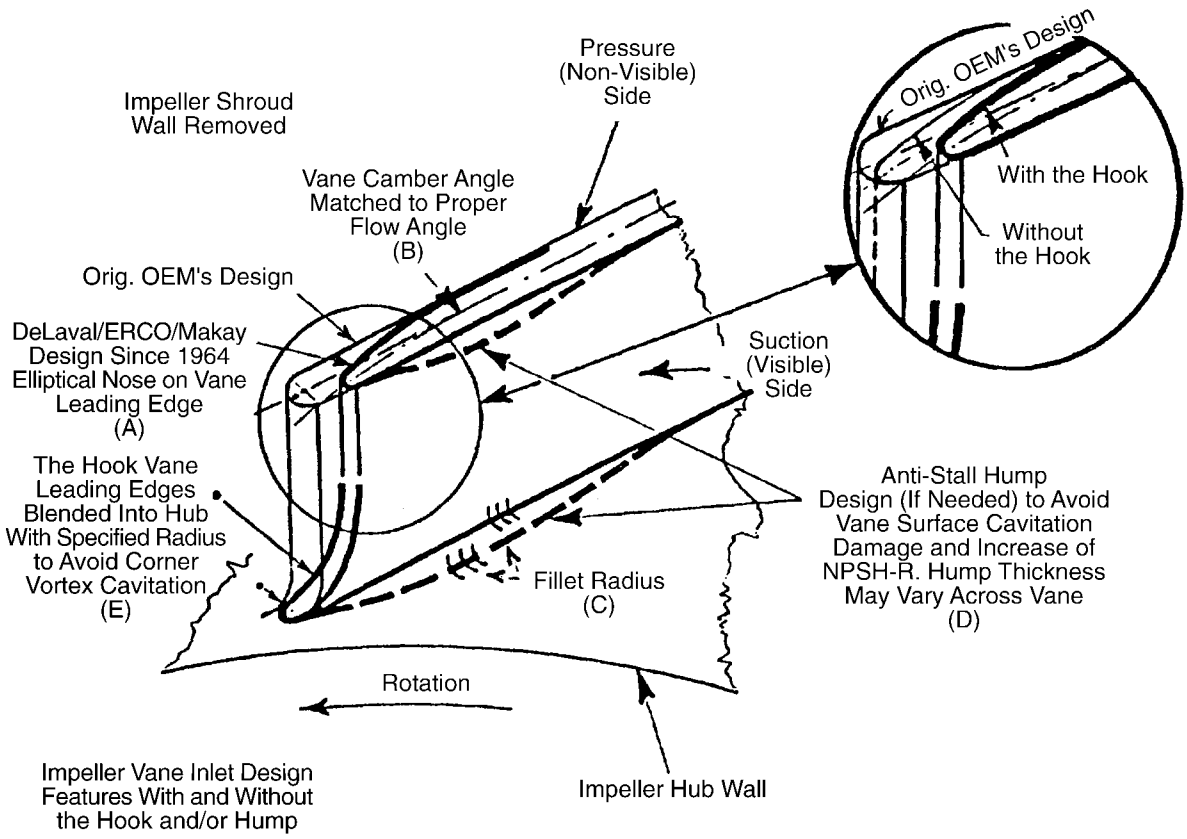

Design Features of Proper Impeller Vane Inlet (Eye): The features shown on this representative vane correspond to the features listed above as (A) to (E). Each feature is integrated into the total design to ensure reduced cavitation activity with no adverse impact on overall performance levels (Patent applied by Ingersoll-Rand Co.). However, (A) & (B) used by DeLaval and ERCO (Makay) since 1964, (C) by more or less everybody, and (D) & (E) by ERCO (Makay) since 1976. NOTE: If the hump (D) is applied during troubleshooting, remember that each application is different; one solution may not apply to another (if the impeller is sand-cast, solution may be different from vane to vane). Thickness of the hump may vary across the vane, depending on the amount of the cavitation damage.

Figure 13-3
Proper Impeller Inlet Vane (Eye) Design Features, including ERCO's Anti-Stall Hump, or as called by Dr. P. Cooper, the Bias Wedge

13.2 The Anti-Stall Hump Case Histories by ERCO

Typical cavitation on the suction side of the impeller inlet vane can be seen in Figure 13-4. There are at least three ways to correct a problem causing this type of damage:

- Replace the impeller with a new impeller that has the same inlet vane design or repair (if possible) to the original design configuration.
- Redesign the impeller, which can be a risky proposition because the people who developed the original design would probably be asked to develop the new design.
- Install the anti-stall hump. This would alter the vane contour to complement the flow pattern of the fluid. This option has proven to be the most cost effective and practical approach in at least 203 cases.

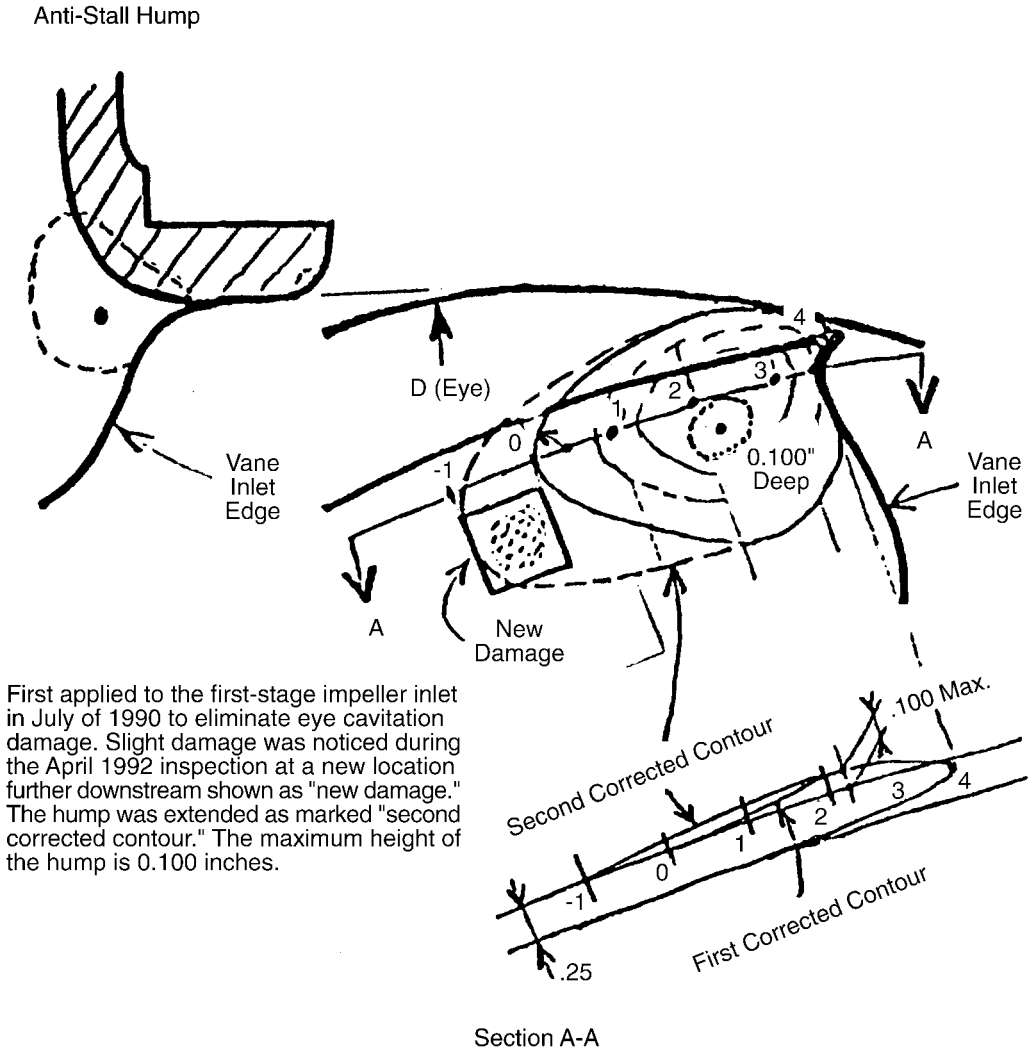

Figure 13-4
The Anti-Stall Hump on the Main BFP of Unit 5

13.2.1 Circulating Pump Impeller Eye Cavitation: The Anti-Stall Hump

The mechanism of eye recirculation is discussed in prior sections and also in Reference 11. Cavitation damage, mainly in large condenser circulating pumps, is addressed from the following two points of view:

- Eliminate cavitation damage at the impeller inlet (the impeller eye).
- Increase capacity of the pumps when load is restricted during the summer because cooling water temperature increases and limits the heat removal capacity of the condenser at a constant cooling water flow. (In many cases, a 5–10% increase in circulating pump capacity removes this limit.)

These reports and measurements were revealed after the modification had rectified the problems with flow, NPSH, and cavitation. Previously, assumptions were made that the pumps operated at over 120% of BEP and that the available NPSH was inadequate (shown as point 3 in Figure 13-7). As a result of these incorrect assumptions, the modifications were also incorrect. They created even more rapid cavitation damage and, thus, greater power reduction during summer. The area damaged by cavitation is shown in Figure 13-1. The normal repair time due to the severe damage was six months.

To rectify this condition, the vane inlets were reshaped by filing, as shown in Section B-B of Figure 13-1 (Cut * = 0 case in Section B-B). For the first fossil fuel unit application, no effort was made to build up the area that might be damaged by the stall that would form after the modification. An inspection 18 months after the vane modifications revealed only minor erosion damage at the new stalled area that had shifted downstream from the original area of damage as expected.

Early in 1983, the circulating pumps in the nuclear units were also altered without filing the vane inlets. The stainless steel impeller vanes were thick with unusually large areas damaged. A decision was made to estimate the stall shape, as shown in Figure 13-1, and build up the vanes with Belzona, an epoxy material. This material adhered very well to the rough surface damaged by cavitation erosion. Inlet velocities were found to be low enough to believe that the Belzona would adhere and not peel off. Several inspections have shown that the epoxy remained on the steel surface and that cavitation damage was eliminated.

The most significant change, however, came from the modification of the impeller inlet due to its beneficial effect on cavitation damage. Previously, cavitation damage to the pump caused forced outages of the unit resulting in a premature refueling (performed earlier than scheduled during the plant operating cycle). Due to the inlet modification, the cavitation damage did not recur. This avoided a repetition of the early shutdown and premature refueling, which would have had significant cost penalties.

Since that time, several other circulating pumps were successfully modified with various combinations of the modifications shown in Figure 13-1. The modifications/alterations discussed cannot be applied uniformly to every case. Each case must be judged by its characteristics:

- The nature, location, and amount of damage
- Inlet angles
- Vane thickness
- Vane shape
- Flow velocities
- Compositions and temperature of the pumped fluid
- The effect of build-up on inlet flow area
- Changes in flow velocities
- Impeller material and size

It should be kept in mind that the appearance of cavitation damage can be misleading, and may result in an incorrect judgement. The appearance of the damage at two entirely different flow conditions shows why the cause of cavitation is misjudged in many cases. Damage can occur if modifications are based on incorrect interpretations.

13.2.2 Selected Cases of Field Applications

The BFP at Crystal River Unit 4 had experienced strong first-stage cavitation damage on the visible side of the impeller inlet vane (typical of Figure 13-4). The pump also experienced severe feedwater flow instability at about 65% of pump BEP. The first step in modifying the pump was to perform Gap A, Gap A Overlap, and Gap B modifications in an effort to correct the flow instability at 65% BEP. In performing the modifications, the author predicted that the inlet cavitation would be greatly reduced because the discharge instability had a strong influence on the stability of the suction flow. When the pump was inspected 2 1/2 years later, only mild inlet vane cavitation damage was found in the upper corner (near the hub), about the size of a penny with a maximum depth of 60 mils. The anti-stall hump was installed on all six impeller vanes with a maximum height of about 80 mils and approximately 1 inch downstream of the vane leading edge, as shown in Figure 13-4. This work showed that indiscriminately installing the hump could have led to disastrous results, if the discharge conditions had not been corrected first.

Modifications of the anti-stall hump at PS Oklahoma on the 45x47S type circulating water pumps are shown in Figure 13-5. At the time of this report's original publication, it was too early to provide comment on the success of the modification.

Modifications of the single-stage, single-suction, vertical circulating water pumps at the Farley Nuclear station took place in 1983. The impeller material was carbon steel and the impeller eye diameter was 108 inches. The anti-stall hump was added using Belzona. The impeller vane geometry at the exit was also modified. The goal was to prevent impeller eye cavitation and to gain flow when the main turbine was derated during the hot summer days. The cavitation was completely eliminated and 12% flow was gained, which was very much welcomed during the hot summer months.

Modifications to the horizontal, double-suction cooling tower circulating water pumps at the Harrison Fossil Station (Allegheny Power Company) were performed in April 1983. The impeller material was bronze and the impeller OD = 48 inches. The OEM had the first chance to make corrections. The hydraulic designer used their proprietary computer program to calculate new vane inlet angles. Modifications were made in their repair shop. Cavitation damage became considerably worse. The author had a second chance (as described in Figure 13-1). The hump was added by welding in a local shop near the station with ERCO supervision. Cavitation was completely eliminated and a 14% gain was measured in flow, which was needed during the hot summer months (impeller vane geometry at the exit was again modified for that purpose). Based on the high success, later stainless steel castings were ordered from an engineering company by copying a modified impeller. Casting dimensions were considerably in error, which resulted in a loss of 15% flow, and cavitation reappeared. All four SS castings had to be discarded.

The hump was also incorporated in the first stage of the BFP at KCG&E's La Cygne Station Unit 2 in 1989. The BFP was the largest feed pump made by Pacific Pumps (18-inch RSLB-4). There were a total number of five pumps manufactured. All five received various major modifications by ERCO, in particular Gaps A and B, and impeller hub geometry modifications to receive ERCO's heavier shrink fit.

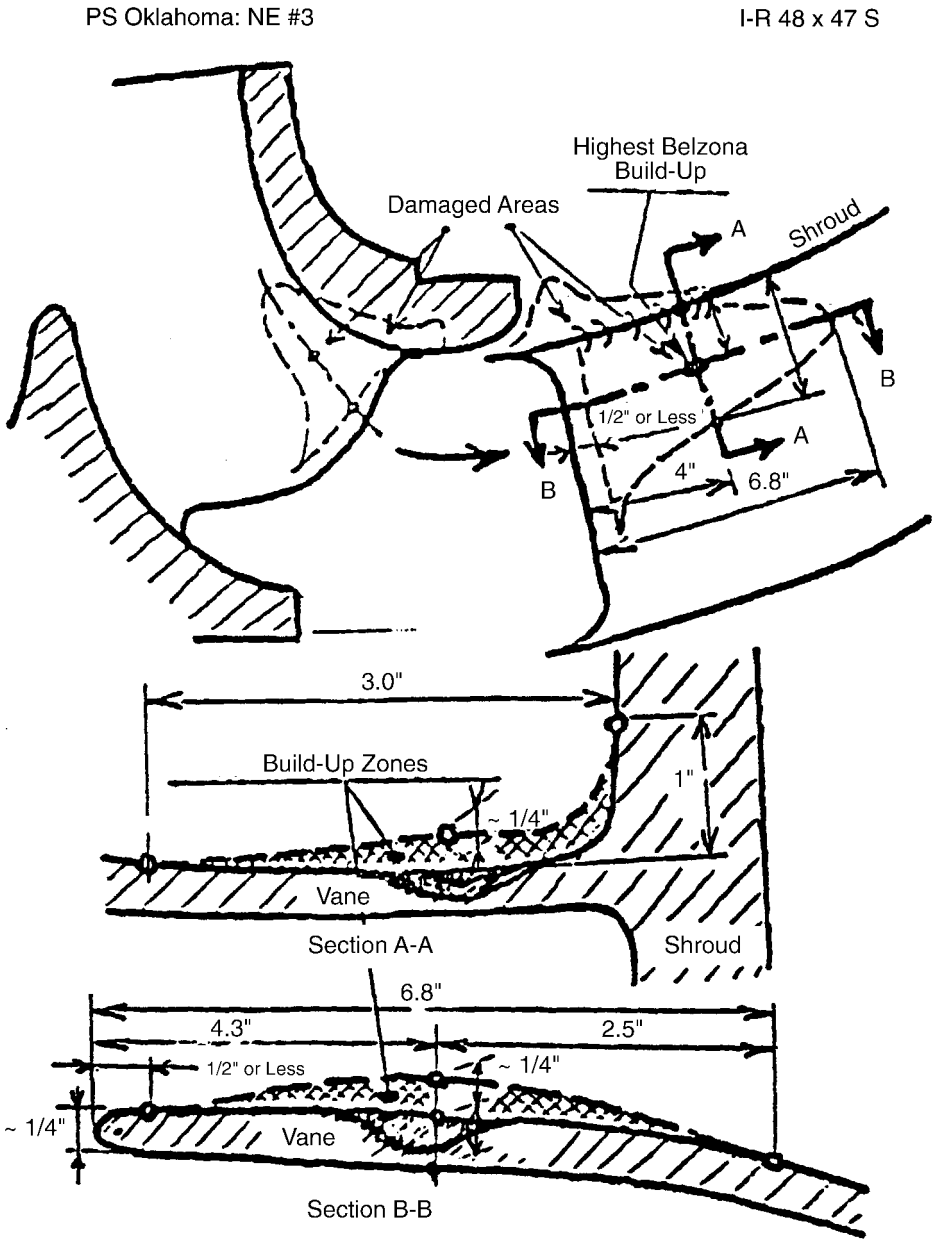

Figure 13-5
The Anti-Stall Hump Applied to a 48x47S Type Large Circulating Pump at PSO's NE Unit 3 in 1990

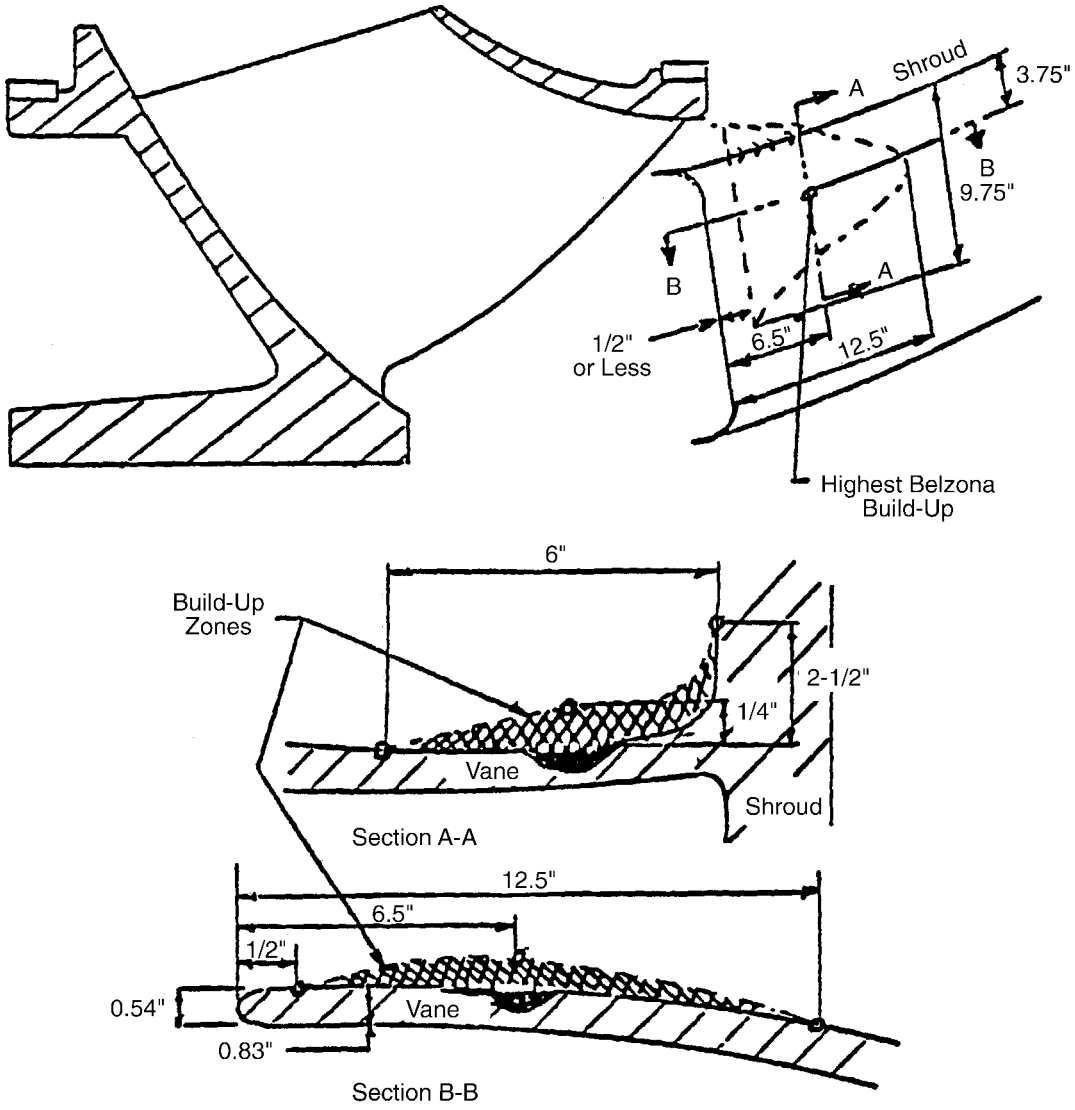

Figure 13-6
Application of the Anti-Stall Hump to an Al-Ch Type 114x78 WMCC Circulating Pump in a Large BWR Nuclear Plant in 1992. Belzona was used to build up the hump.

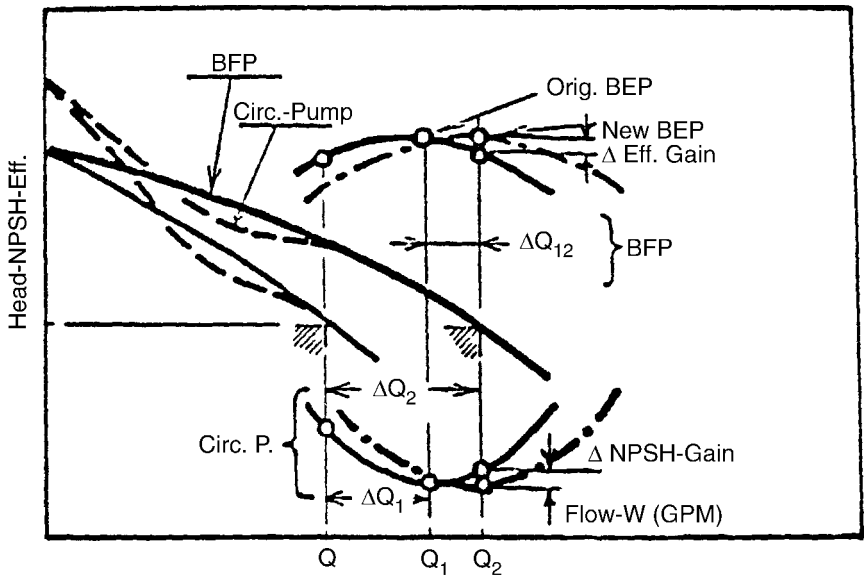

Extension of condenser (cooling tower) circulating pump capacity by modification of both impeller inlet and exit. All modifications were performed by manual filing. Examples are: Allegh-Harrison (Gained 14%), Alabama-Farley Nuclear (Gained 12.5%). Total of 203 pumps modified between 1978 and 1993 with ERCO supervision.

Figure 13-7
Extension of Condenser Circulating Pump Capacity

13.3 Causes of Cavitation

Cavitation damage is caused by the production of very low local pressure adjacent to fluid flow boundaries. This causes vapor-filled pockets to form and then collapse violently when they are transported into higher pressure regions. Damage is most likely to occur in the inlet of the pump impeller if caused by lack of NPSH but may be carried through the impeller, causing erosion of the impeller exit or the diffuser/volute inlet. Possible failure locations can be:

- Impeller eye (inlet) at various places, as described in Figure 13-8
- Impeller exit, as illustrated with an example in Figure 12-11
- Diffuser or volute inlet, as illustrated with an example in Figure 7-4

Six locations of cavitation damage at the impeller eye are shown in Figure 13-8, which is organized to show (left to right) the following:

- Type of cavitation damage
- Flow mechanisms to induce the damage
- Possible root causes
- Possible solutions to eliminate the damage

Some of the most common cavitation damage may be caused by the following:

- Insufficient available NPSH or the impeller is not performing in accordance with its design. The damage nearly always shows on the impeller inlet and on its downstream portion. Sometimes, in addition to the impeller, insufficient available NPSH also damages the inlet portion of the diffuser or volute as shown in Figure 7-4. System NPSH available vs. NPSH required with 3% head breakdown is shown in Figure 13-9 and is supported by actual factory test results as shown in Figure 13-10.
- Flow recirculation in the impeller eye. Most likely occurs if the pump is operated at off-design flow conditions. The damage is always on the impeller eye.
- Incorrect impeller vane inlet angles at design flow or operating at off-design flows for extended periods of time. These two are the same because they both involve mismatched flow angles. The damage always shows on the vane with mismatched angles. Cavitation, if strong enough, may get carried downstream and damage additional downstream surfaces.
- Incorrect diffuser or volute vane inlet angle, or operating at off-design flows. Damage appearance will be the same as described above for the impeller.
- Incorrect hydraulic channel geometry (impeller or diffuser) allowing flow separation (curved diffuser or guide vane channel). Most damage occurs on that channel; some may occur downstream.
- High localized velocities caused by sharp corners and other flow disturbances, such as a misplaced inlet guide vane. Damage always starts from the point of origin of high velocities and carries downstream.
- Vortex formation due to obstacles in the flow path, sharp elbows in the suction piping, incorrect pump inlet geometry, and blunt trailing edges of guide vanes. The damage is special in its appearance and occurs where the vortex touches a solid surface.

Cavitation Damage Mechanisms and Remedies: 1. Impeller Eye

	Type of Cavitation/Damage	Flow Mechanisms to Induce Damage	Possible Causes	Possible Solutions
1	Visible (suction) side of vane starting close to leading edge of vane. 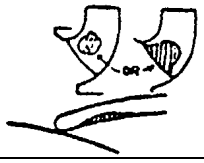	Sheet cavitation on suction of vane at Q < BEP • Damage hub to shroud • Damage near shroud • Damage near hub 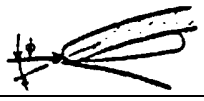	• High incidence angle • Improper leading edge profile • Incorrect vane design • Shroud inlet angle (β) too large • Hub inlet angle (β) too large	•Introduce anti-stall hump (least expensive) •Increase flow rate (if practical) •Reduce vane inlet angles, improve inlet edge profile •Introduce eye ring (35) •Reduce eye diameter (35) •Increase prerotation
2	Visible (suction) side of vane, within channel. Erosion may also be observed on the shroud and/or non-visible (pressure) side of vane. 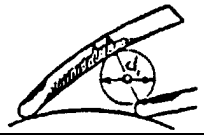	Vortex cavitation on suction side of vane at low flow and low σ_{U1} σ_{U1} = NPSH / (U_1^2 / 2g) 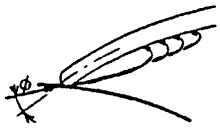	• High incidence angle and low σ_{U1} ($\leq$ 0.3) σ_{U2}= NPSH / (U_1^2 / 2g) NPSH based on 3% head breakdown	•Introduce anti-stall hump •Reduce vane inlet angle •Increase $NPSH_A$ •Reduce eye diameter (35) •Increase cavitation resistance of impeller material (means new casting needed, expensive)
3	Non-visible (pressure) side of vane, any location, forming close to leading edge of vane. 	Sheet cavitation due to flows above BEP (high incidence angle). 	• Incorrect flow angle at operating point • Incorrect vane design • Improper vane profile • Q > BEP	•Reduce flow rate (if practical) •Introduce ANTI-STALL-HUMP •Modify vane geometry/ profile
			Standard design feature at De Laval and at ERCO (has the least cavitation damage among all BFP applications). Used by ERCO to troubleshoot other OEM's designs.	
4	Non-visible (pressure) side of vane, damage occurs middle of vane to outer diameter. 	Part-load recirculation resulting in cavitation bubble impingement on the vane. 	• Impeller eye too large • Impeller throat area too large • Incorrect flow inlet angle	•Introduce anti-stall hump •Increase flow rate (if practical) •Insert inlet ring to reduce eye and throat area [35] •Modify vane geometry/profile
5	Non-visible (pressure) side of vane, damage near hub. Difficult to distinguish from 3 unless known if pump operated below or above BEP.	Part-load recirculation creating high incidence angle near hub. 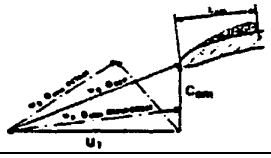	• Incorrect flow angle near hub causing recirculation at partload	•Introduce Anti-Stall Hump •Increase flow rate (if practical) •Modify vane geometry/ profile (if possible) •Reduce prerotation at the impeller eye (if possible)
6	Hub, or shroud, or corner (Fillet) Radii damage 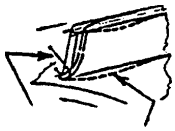 The hook and the anti-stall hump	Vortex cavitation at the corner, may be combined with high incidence angle. 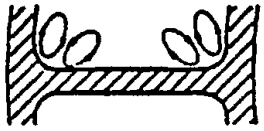	• Increase flow angle • Fillet radii too large • Operating at low flow (if on visible side)	•Try anti-stall hump •Modify fillet radii •Add proper hook •Mod. vane profile as in 3 •Impeller redesign (modify vane angles: most expensive, least practical)

Figure 13-8
Cavitation Damage Mechanisms and Remedies at the Impeller Eye

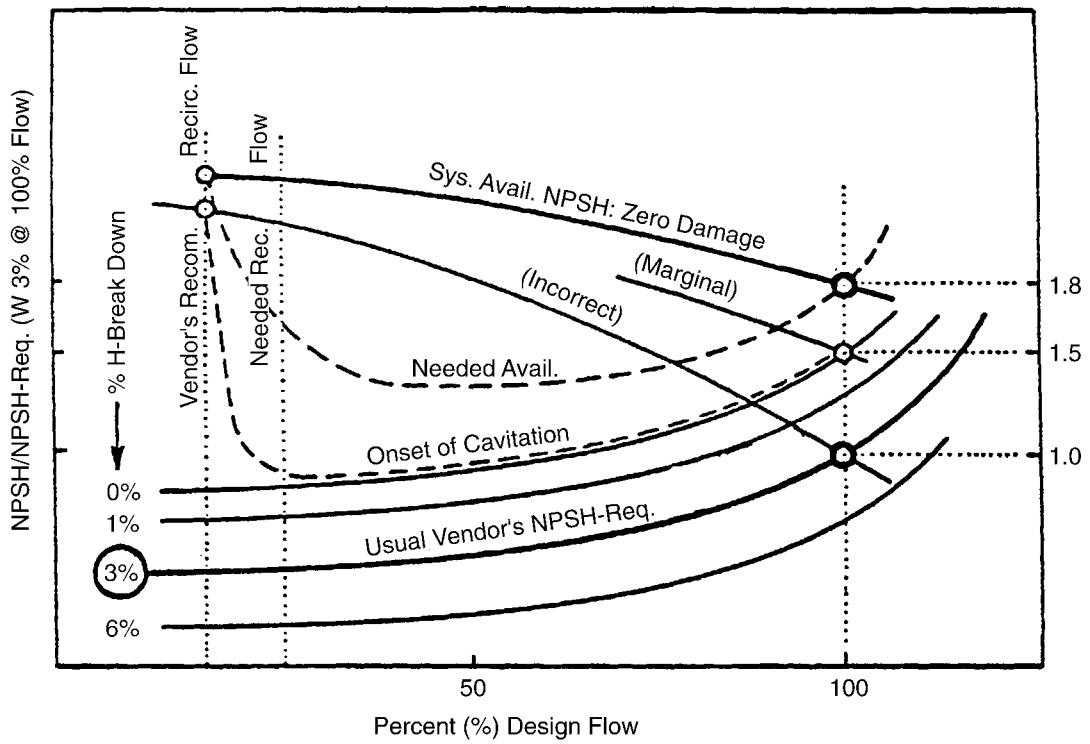

Figure 13-9
System Available NPSH vs. NPSH-Required with 3% Head Breakdown [4 and 5]

NPSH-required, as quoted by all OEMs, was misunderstood by many utilities and A/Es for decades. Its definition at the OEMs was NPSH with 3% head breakdown, which meant the pump was in a fully developed cavitating stage. Figure 13-9 shows what really is needed for cavitation-free operation in boiler feed pumps. An actual factory test is shown in Figure 13-10 where the difference in "guaranteed" and actual-measured NPSH is very dramatic. The A/E believed the OEMs quoted NPSH at minimum flow and designed the nuclear plant accordingly. The pump never operated as designed. Details of the associated problems and attempts to correct it are reported partially in Reference 61. The final solution to the problem was never known because the nuclear plant was subsequently cancelled. Changing the minimum flow for these service water pumps might have been the final solution, but one that could have been economically unfeasible.

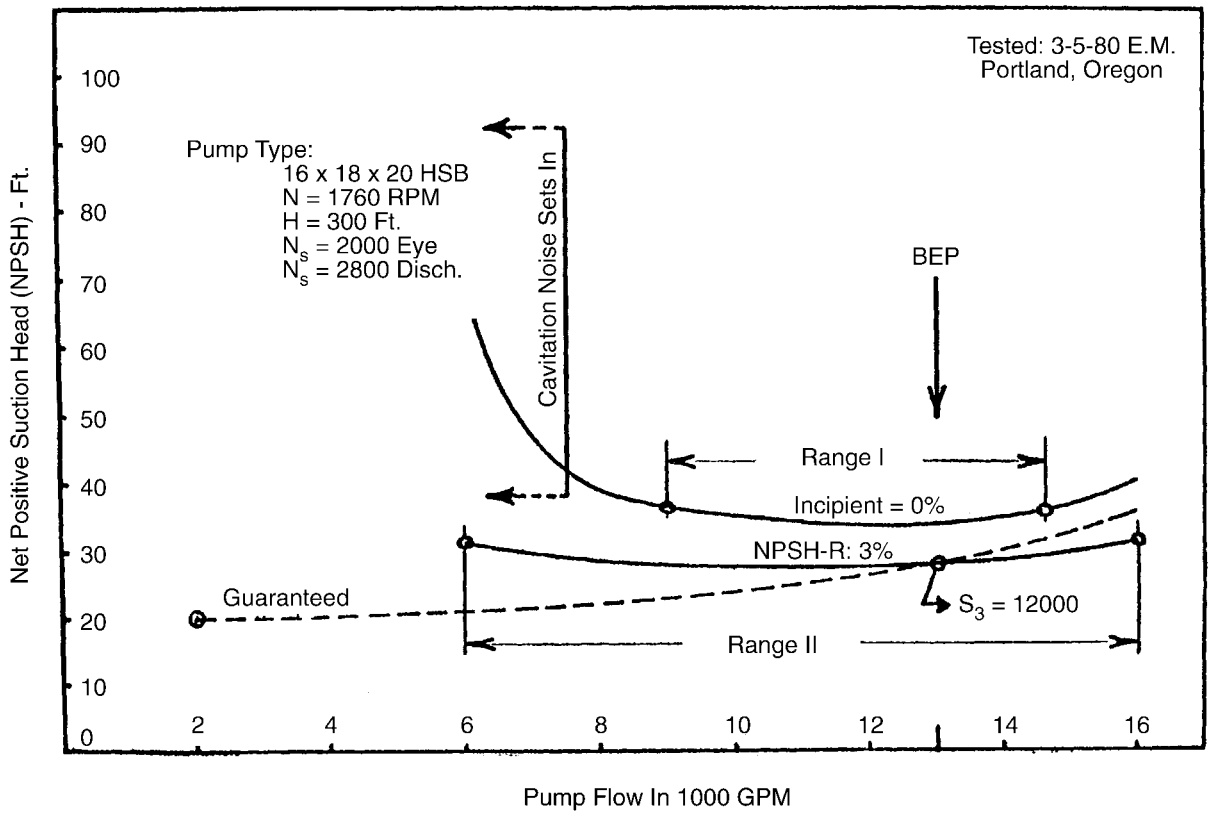

NPSH capability of the Zimmer Nuclear Service water pump with redesigned impeller tested at Bingham Pump. Co., Portland, Oregon, on March 5, 1980. Curve shows results at incipient (0% head breakdown) and at the usual 3% head breakdown conditions.

Figure 13-10
NPSH Predicted (Guaranteed) vs. NPSH Tested, for a Single-Stage, Double-Suction Service Water Pump for a Large Nuclear Station

14
JOURNAL BEARINGS

Practically all boiler feed pumps (BFPs) apply flexible shafts. This means that the pump operates above the first lateral critical speed. The BFPs have a relatively light rotor weight and, consequently, the journal bearings are lightly loaded. This makes them susceptible to oil whip or half-frequency whirl. Single-stage nuclear feed pumps in general operate below the first critical speed, but the rotor weight is even lighter than the BFP rotors. The problem with lightly loaded bearings is that the speed at which rotor-dynamic instability occurs, or threshold speed, is lower than expected.

Above the threshold speed, the bearing fluid film loses its ability to dampen rotor excitation forces at frequencies below pump running speed, resulting in a self-excited subsynchronous rotor whirl instability, sometimes called oil whip. The loss of or the marginal ability of a lightly loaded bearing to provide the necessary low-frequency bearing damping is particularly harmful in feed pump applications because of the potentially large hydraulic forces produced by hydraulic instabilities, particularly at part loads (see Sections 6 and 7). Self-excited bearing instability can be a deadly occurrence, often resulting in catastrophic failures, particularly in large turbine rotors. Therefore, it is extremely important to determine the nature or source of subsynchronous vibration components.

Subsynchronous vibration can be induced by large dynamic unbalance, oil whip, rubbing, hydraulic instabilities, or subharmonic resonance. Journal bearings with only marginal subsynchronous vibration damping capacity, such as lightly loaded bearings, can become self-excited due to the motion generated by the subsynchronous vibration components. This results in uncontrollable vibration amplitudes and rotor destruction.

14.1 Radial Journal Bearing Types

In power plant pump applications, the following basic radial bearing types are applied, as shown in Figure 14-1:

- Plain cylindrical sleeve
- Axial groove
- Elliptical (Figure 14-2)
- Pressure-dam (Figure 14-3)
- Tri-lobe (actually tri-dam) (Figure 14-4)
- Hydrostatic (Figure 14-5)
- Tilting pad (Figs. 14-6 to 14-8)
- Rolling element

The most widely used bearing designs are the sleeve bearings. The plain sleeve and axial grooved bearings (Figure 14-1) are the least expensive and simplest bearing types a manufacturer can supply, but they are not considered suitable for high-speed feed pump applications. These bearings have high static load carrying capacity but offer no resistance to subsynchronous excitations. It is also the type of bearing that can cost the user the most in repair costs and pump availability. Over the years, several variations of the sleeve bearing (such as elliptical, pressure-dam, and tri-lobe or tri-land) have been used by the pump vendors in an effort to eliminate subsynchronous rotor-dynamic instabilities. These efforts have been successful in stabilizing the rotor during normal operation, but they still do not offer significant stability margins to protect against large hydraulic forces, heavy internal rubbing, bearing misalignment, or large unbalance. Thus, if a rotating piece of equipment has a history of wiping journal bearings or damaging rotating assemblies, the application and design of the journal bearing should be examined carefully.

The elliptical journal bearing, shown in Figure 14-2, is widely used in Europe. The bearings have been incorporated in the United States in many cases as a “quick and cheap” method of providing rotor stability. As shown in Figure 14-2, the vertical diameter of the bearing is less than the horizontal diameter (usually by only a few mils), resulting in the name elliptical or lemon bearing. The elliptical geometry provides good bearing stiffness and damping in the vertical direction only. No bearing stiffness and damping are provided in the horizontal direction. As a result, if the excitation forces are in the horizontal direction, the bearing could become unstable. Also, as wear occurs in the vertical direction, the bearing will take on the geometry of a plain sleeve or axially grooved bearing with large clearances and subsequently become dynamically unstable.

The pressure-dam bearing (see Figure 14-3) provides the greatest stability margin of all the sleeve-type bearing designs. The pressure-dam in the upper half of the bearing provides a downward stabilizing force on the shaft to protect against subsynchronous excitation forces. It is important that the pressure dam not be open to the axial groove of the bearing. This would prevent pressure from building and the downward stabilizing force from developing. However, since the geometry of the bearing is fixed, the amount of downward stabilizing force is also fixed. This limits the ability of the bearing to protect against extreme hydraulic forces, heavy internal rubbing, and/or large rotor unbalance.

The tri-lobe or tri-land bearing (Figure 14-4) is basically a pressure-dam bearing with three pressure-building pockets. The depth of the lobes, however, is only 5 mils, which makes it susceptible to losing its function due to wear. Also, because of the shallow depths, the tri-lobe bearing is inferior to a properly designed pressure-dam bearing. The tri-lobe bearing has been used in vertical pump applications where subsynchronous vibration has developed, but it was only marginally successful. It has been able to increase the mean time between failures but not to the extent to justify the increased bearing costs and modifications.

Tilting-pad bearings incorporate a series of circumferentially oriented pads, which are self-compensating when changes in rotor position, unbalance, increased vibration, or speed occur. This self-compensating feature makes the tilting-pad bearing the most dynamically stable bearing design available, particularly for lightly loaded, high-speed bearing conditions. These bearings are initially more expensive than the other bearing designs, but more and more utilities are switching to tilting-pad bearings to solve rotor-dynamic stability problems. The results have

been greatly improved rotating equipment reliability and ultimately less maintenance and capital costs. These bearings are discussed further in Section 14.2.

Hydrostatic bearings (see Figure 14-5) are water-lubricated bearings, where lubricating water is injected into the bearing. The injected water establishes the rotor-dynamic characteristics of the bearing. This type of bearing has been used exclusively by Byron-Jackson in their reactor primary coolant pumps.

Rolling element bearings are used in very small boiler feed pumps, nuclear auxiliary feed pumps, and other small (primarily process-type) pumps in a power station. The main problems with rolling element bearings are:

- Their RPM is limited; they typically are not used above 4000 RPM.
- Rotor-dynamic damping is not provided, while infinite stiffness is produced (both very poor characteristics for a centrifugal pump application).

The reasons rolling element bearings are used in centrifugal pump applications are the very low price and the great convenience during design and especially during maintenance.

A. Plain Cylindrical Bearing: Liquid Lubricated - Laminar and Turbulent Film Gas Lubricated

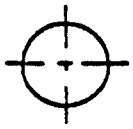

Not for Boiler Feed Pumps

B. Two Axial Groove Bearing:
(Four Axial Groove Bearing) Liquid Lubricated - Laminar Film

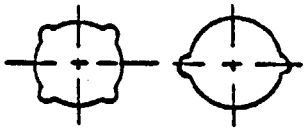

For Low Speed BFP.
(Unstable at High Speed)

C. Elliptical Bearing: Liquid Lubricated - Laminar Film

Used Occasionally to Regain Stability. Widely Used in Europe.

D. Pressure-Dam Bearing: Liquid Lubricated - Laminar and Turbulent

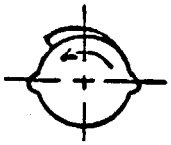

Used by B-J and Pacific Only

D-1: Trilobe of I-R (Actually a Three-Dam Bearing)

E. Tilting-Pad Bearing: Liquid Lubricated - Laminar and Turbulent Film

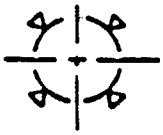

Std. By DeLaval Only. Others upon Request. (Stable at all Flows and Speeds.)

F. Hydrostatic Bearing: Water Lubricated

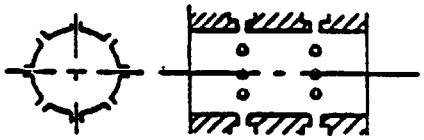

B-J: Exclusively in Nuclear Primary
Reactor Circ. (Coolant) Pumps (RCP).

G. Ball Bearing:

Only in Very Small BFP. Many Nuclear Aux. Feed P.
Many Small Pumps in Nuclear Applications.

Figure 14-1
Various Types of Radial Bearings in Power Plant Applications

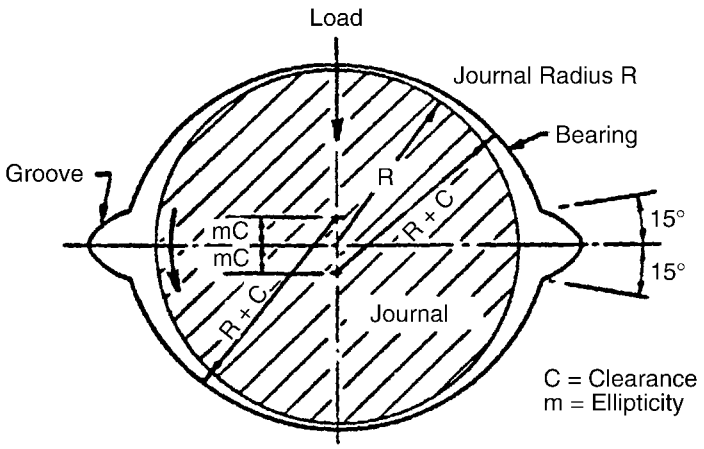

Elliptical Bearing
Stiffness/Damping in the Horizontal Direction Is Limited

Figure 14-2
Elliptical Bearing (Widely Used in Europe)

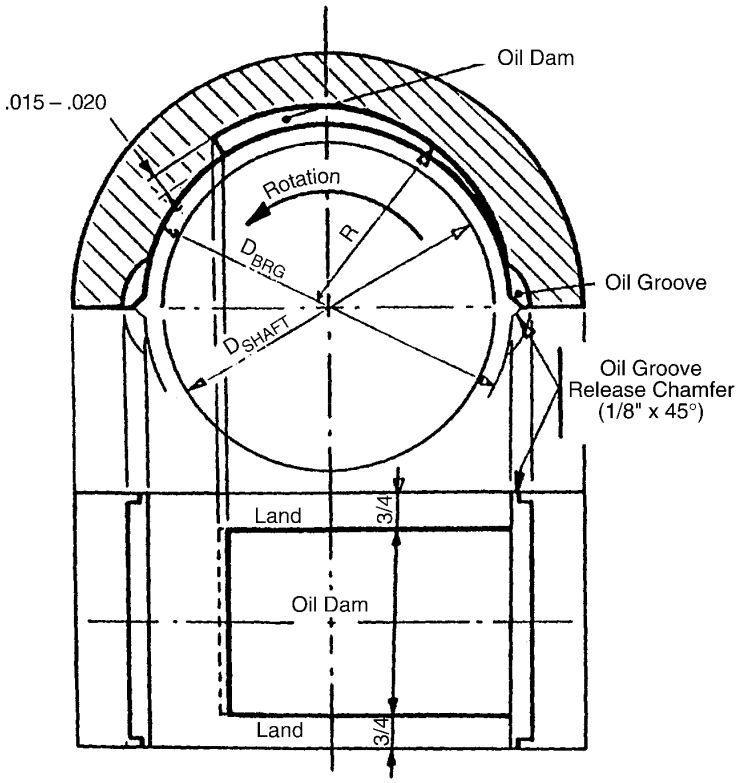

Upper half of oil-dam (pressure-dam) journal bearing
for high-speed Pacific and B-J boiler feed pumps

Figure 14-3
Pressure-Dam Bearing, Used Only by Byron Jackson and Pacific

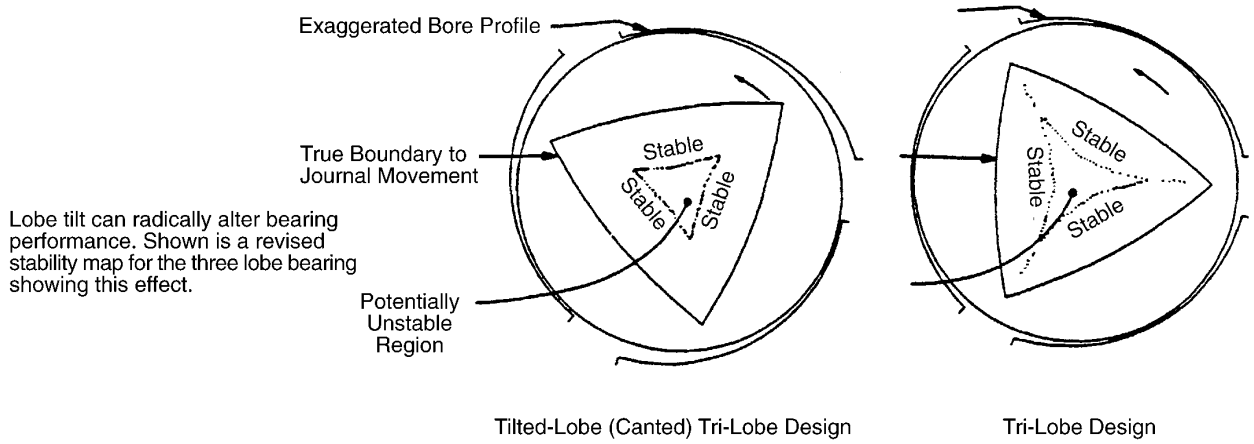

Figure 14-4
Tri-Lobe or Tri-Land Bearing Used Only by Ingersoll-Rand Only

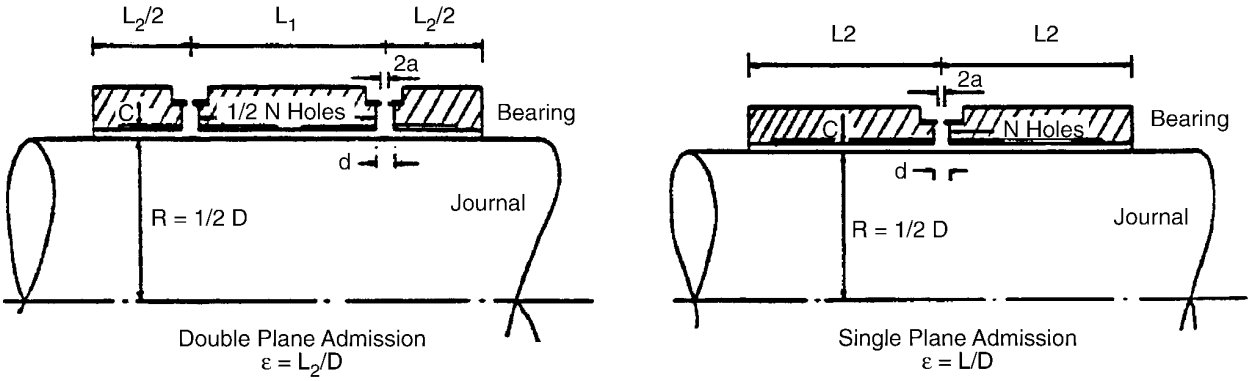

Figure 14-5
Hydrostatic Bearing, Used Exclusively by Byron Jackson in Reactor Coolant Pumps

14.2 Tilting-Pad Bearings

The tilting-pad bearing design, (Figure 14-6) offers excellent performance for all bearing loads. They have whirl-free characteristics, making them prime candidates for use in high-speed, lightly loaded rotating machines (for example, boiler feed pumps, nuclear feed pumps, and vertical pumps or motors). Specifically, tilting-pad bearings provide the following advantages:

- They have the best ability to suppress subsynchronous vibration components caused by oil whip (even when lightly loaded), hydraulic instabilities, and heavy axial rubbing.
- They minimize high-vibration amplitudes in emergency operating situations more effectively than any other bearing type (except perhaps for magnetic bearings, a technology which has not been fully tested). For example, in cases where large turbine rotors have lost a blade, tilting-pad bearings have allowed the turbine rotor to coast to a stop with minimal vibration amplitudes. In contrast, cylindrical bearings have become extremely rough in the critical speed range and, in several cases, have resulted in rotor destruction.
- They can accommodate more misalignment than other bearing types because a properly designed pad can tilt in two directions.
- They can be preloaded to improve bearing oil film stiffness and damping properties for conditions of lightly loaded bearings.

Tilting-pad bearings are like an insurance policy against catastrophic failures and are the best solution to rotor-dynamic instabilities problems. Tilting-pad bearings do cost more than other radial journal bearings. They can also run higher lube oil temperatures due to tighter bearing clearances, but if one major failure can be avoided or an instability problem resolved, the benefits typically far exceed the costs.

A very important design parameter for a tilting-pad bearing is the pad preload. The oil film developed by a positively preloaded tilting-pad bearing provides the stiffness required to suppress extraneous vibration and permit a rotating machine to operate smoothly during any operating condition. A tilting pad bearing with a positive preload causes the oil wedge between the shaft and the bearing pad to become a converging/diverging nozzle. This creates a hydrodynamic force (load) on the journal in addition to the rotor weight. Also, with the individual pads equally spaced within the bearing, the converging/diverging oil wedge will always be present. This provides rotor stability, regardless of the direction and magnitude of the excitation force.

Preload is defined as the ratio of the clearances C' / C, where C is the machined radial clearance between the shaft and bearing, and C' is the pivot circle radial clearance. In machining or designing tilting-pad bearings, three types of preload are possible, as shown in Figure 14-7:

- Positive preload
- No preload
- Negative preload

If C' / C is greater than 1, a negative preload exists. Typically, this occurs when the bearing shoes are machined to the same radius as the shaft (also called a fitted bearing), and the shoes are

pulled away from the shaft to provide bearing clearance (C'). This is not conducive to good lubrication practice and can cause the shoes to lock up, restricting their ability to pivot and provide proper bearing support. Therefore, negative preload should be avoided, especially in machines with vertical shafts, such as primary coolant pumps.

When C' / C = 1, the machined radius of the shoe is equal to the radius of the shaft, plus the clearance (C') at the pivot point, and is considered has having no preload. No preload is not as bad a condition as negative preload, but it should be avoided due to fretting damage that has been observed along the outer circumferences of the pads. This effect is mainly due to fluttering of the shoes. A remedy for that is the Spragg relief as shown in Figure 14-10 [62]. This remedy can sometimes suppress self-excited unloaded pad vibration. Westinghouse adopted this modification to their main turbine as well as to the RCP electric motor tilting-pad bearing designs to eliminate pad flutter. It should be understood that the Spragg relief is just a remedy when the preload is incorrect. In conclusion, the Spragg relief can provide the following results when problems occur with tilting-pad bearings:

- Shoes will behave properly if the preload is zero or negative; however, it will not improve spring and damping characteristics of the bearing.
- Eliminates shoe flutter, which is self-excited, unloaded pad vibration.
- Eliminates babbit fatigue at the leading edge of the shoes.
- Prevents lockup of the shoes when preload is absent.

When C' / C is less than 1, a positive preload exists. This means that the radius of the shoe is greater than the radius of the pad's pivot circle or > R + C'. Recommended preloads for power plant rotating equipment range from 0.5 to 1.0. An example of preload calculations from an actual field case has been provided in Figure 14-8. The calculations for an RCP electric motor application where the pad geometry, preload geometry, and preload were optimized by ERCO are shown in Figures 14-11, 14-12, and 14-13. It should be strongly emphasized that in the case shown in Figure 14-13, the Spragg relief is not only unnecessary, but it will shorten the pad length. This can be disadvantageous depending on the basic pad design. Bearing configurations for three electric motor OEMs are shown in Table 14-1.

Do not confuse hydraulic and rotor-dynamic instabilities. Installing tilting-pad bearings will not eliminate hydraulic instability. Be aware of the frequency overlap around 0.5 or 0.6 X as shown in Figure 3-1 as frequency components 3 and 4. This is discussed in detail in Section 3.

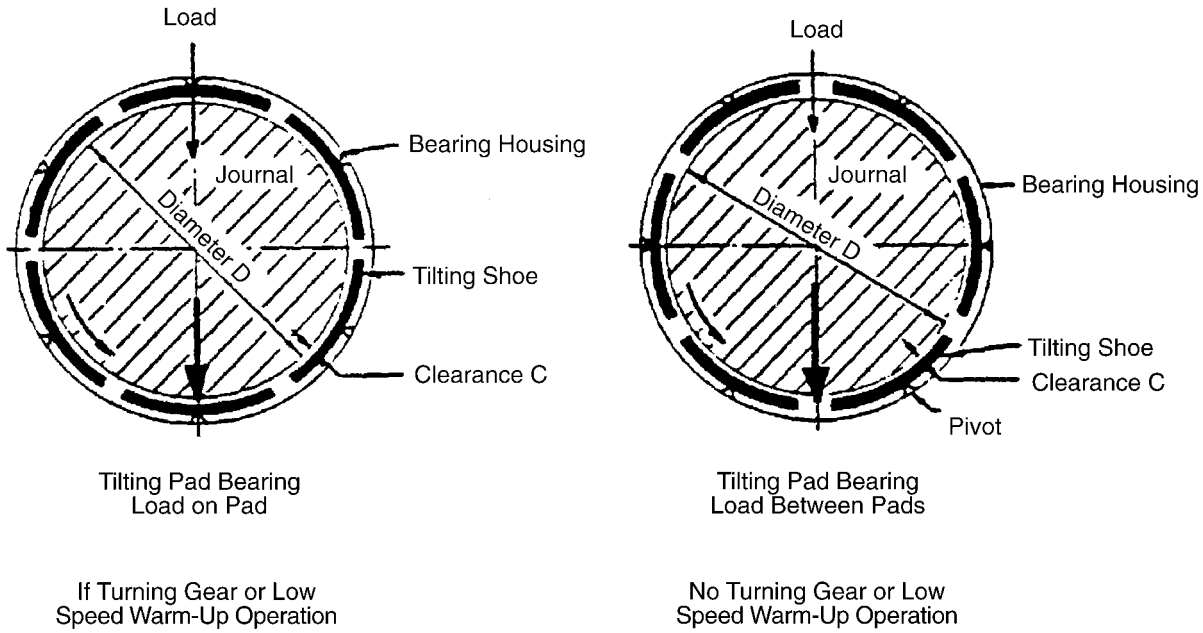

Figure 14-6
Typical Tilting-Pad Bearing Design

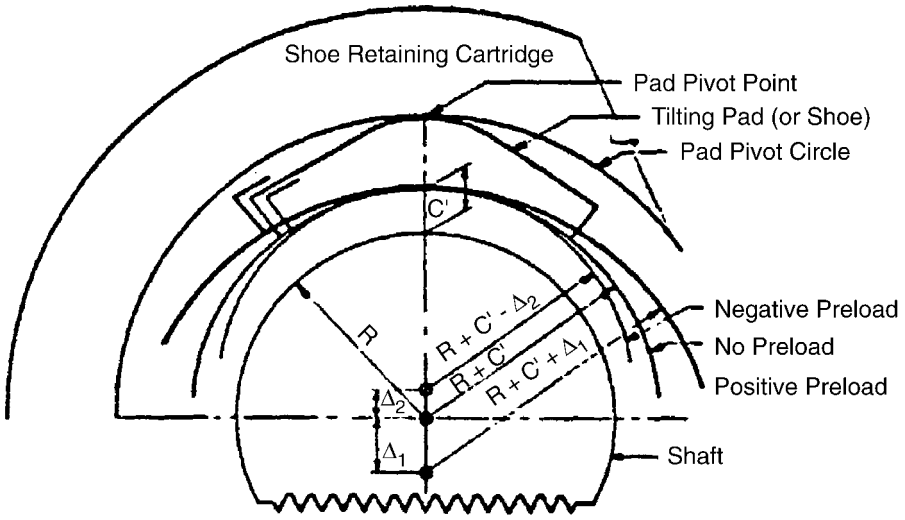

Preload (P) does not exist in case 1, where C = C', C'/C = 1, and P = 1 - C'/C, or zero. Preload is negative in case 2, where C = C' - Δ_2, C'/C is greater than 1, and P = 1 - C'/C is a negative value. Note that if Δ_2 = C', the radius of the bearing shoe is the same as that of the shaft, and the bearing is referred to as a fitted bearing. Preload is positive in case 3, where C = C' + Δ_1, C'/C is less than 1, and P = 1 - C'/C is a value greater than zero.

Figure 14-7
Determination of Tilting-Pad Bearing Preload

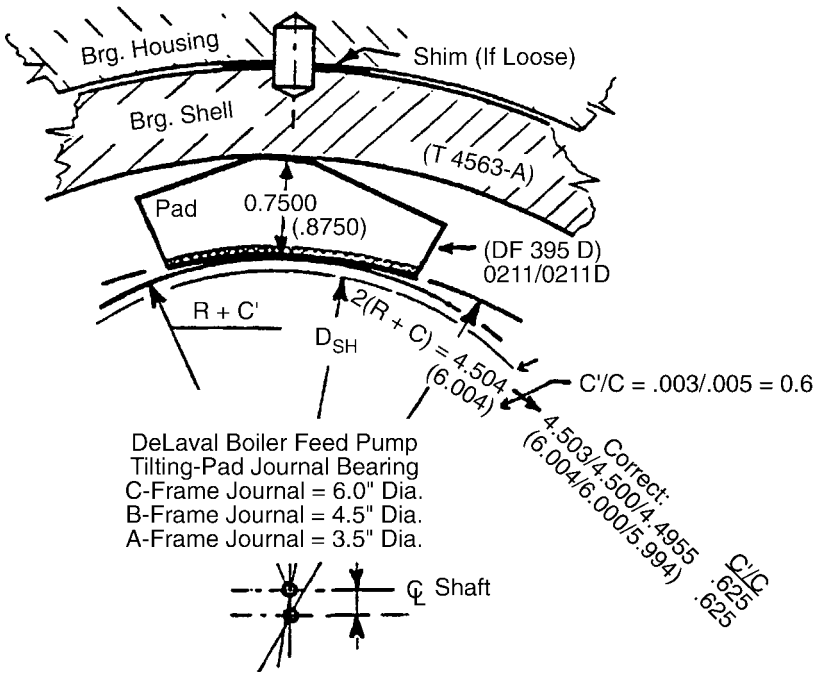

Figure 14-8
Example of Bearing Preload Calculation, From Actual Field Case

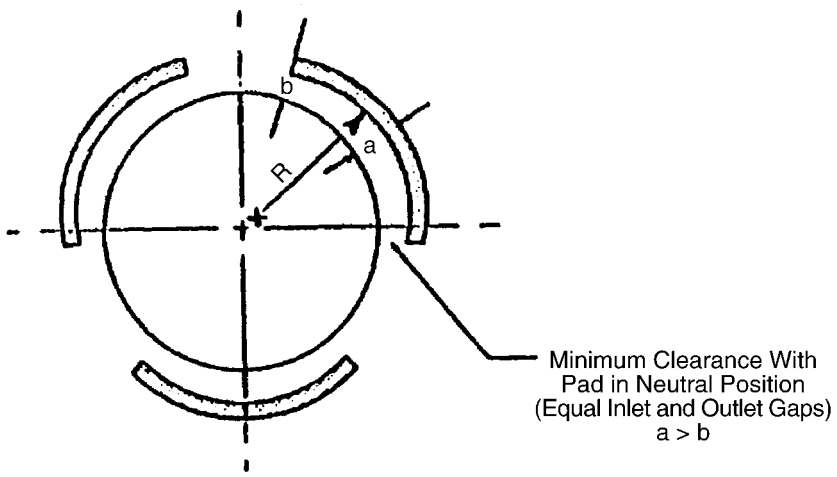

Fitted Pad Bearing

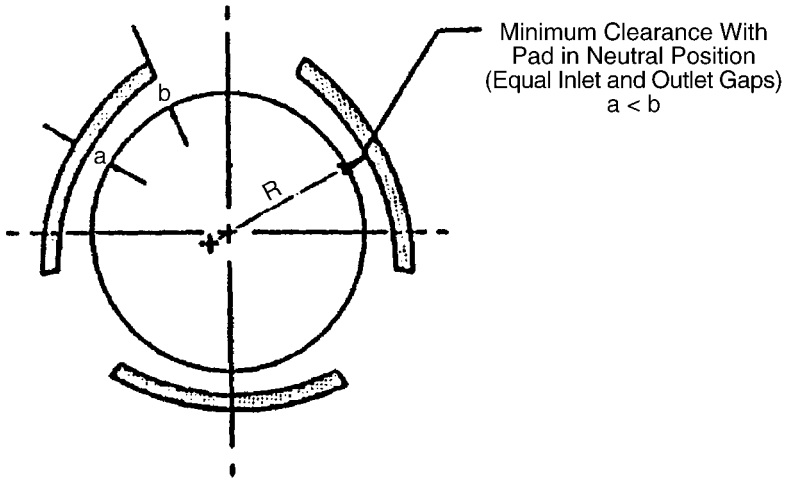

Preloaded Bearing

Schematic of Fitted Pad and
Preloaded Bearing Geometry

Figure 14-9
Illustration of Fitted (Negative Preload) and Preloaded (Positive Preload) Tilting-Pad Journal Bearing Geometry (Fitted Bearing Is Not Recommended for All Applications.)

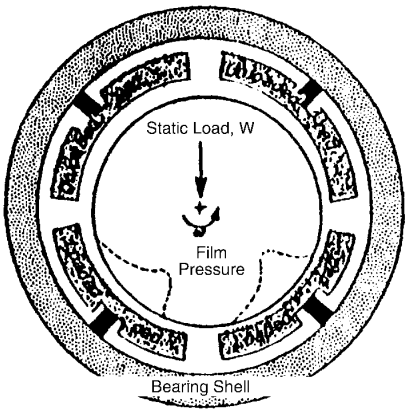

1. Typical Four-Pad Design Has Dead-Weight Load Between Bottom Pads.

2. Fatigue Crack Damage Can Result to Top Pads That Are Statically Unloaded.

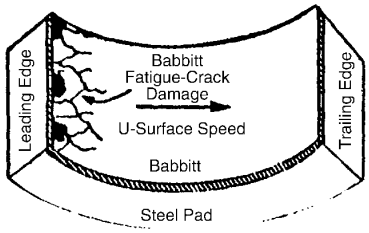

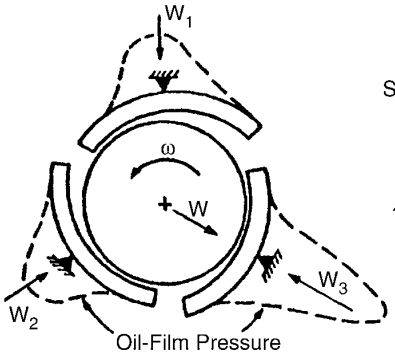

3. Sufficient Static Preloading Can Eliminate Pad Flutter.

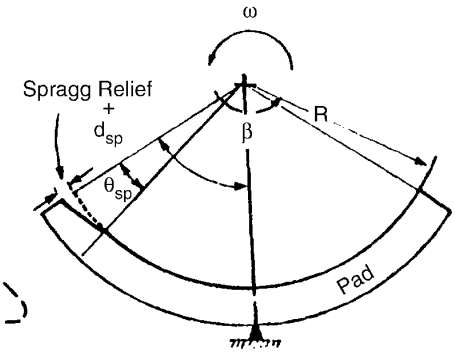

4. Spragg Relief Can Sometimes Suppress Self-Excited Unloaded-Pad Vibrations.

Reprinted From Power, May 1983

Table 1: Results of Parametric Study to Eliminate Pad Flutter in Tilting-Pad Journal Bearings

Value	Response*	Touches Pivot?	Frequency Ratio
Operating Pivot Clearance, C_s/C			
2.1	NU	No	0.45
1.6	NU	No	0.45
1.0	S	Yes	–
Pad Arc (β), Deg			
65	S	Yes	–
80	NU	No	0.45
100	U	No	0.49
Spragg-Relief Angle (θ_{sp}), Deg			
5	NU	No	0.45
10	S	Yes	–
15	S	Yes	–
Spragg-Relief Depth (d_{sp}/C)			
0.1	U	No	0.49
1	NU	No	0.45
10	U	Yes	0.43
Pivot Location (α/β)			
0.44	U	No	0.44
0.50	NU	No	0.45
0.56	U	Yes	0.45
0.63	U	No	0.43
0.70	S	Yes	–

*U-Unstable NU-Nearly Unstable S-Stable

Figure 14-10
Elimination of Tilting-Pad Flutter and Babbit Damage with Proper Preload or Spragg Relief

Explanation/Nomenclature:

$C = C' + \Delta 1$ $C'/C = C' / (C' + \Delta 1)$

$D_{SH} = 2 \bullet R_{SH}$

$16.498 \leq D_{SH} \leq 16.500$

$D_{SH} = 16.500 + 0/-.002$

$0.0040 \leq C' \leq 0.0060$

Machined in Circle Radius:

$R = R_{SH} + C'$

$D = 2(R_{SH} + C')$

$16.500 \leq D \leq 16.502$

$D_{PAD} = 2(R_{SH} + C)$

Preload: C'/C

$0.5 \leq C'/C \leq 0.8$

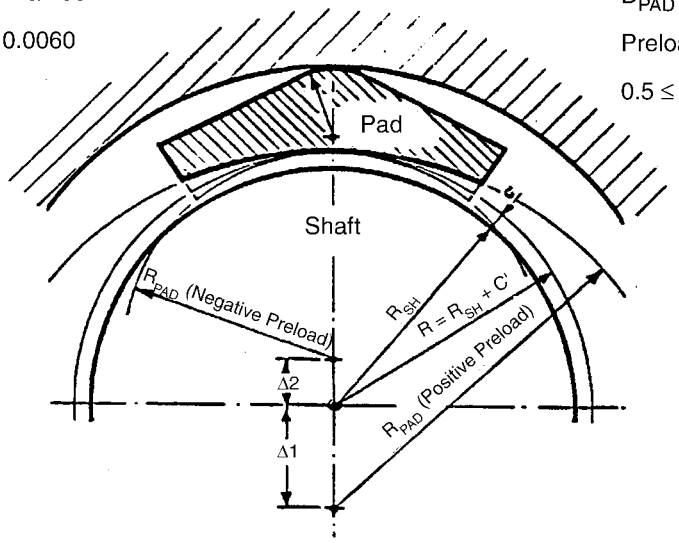

The present bearing tolerances as designed and made by Westinghouse are: (1) shaft dia (D_{SH}) + 0/-.002, (2) tilting shoes (D_{PAD}) +.002/-0. This, with a combination of "no preload" (Westinghouse design condition) can push a bearing into the "negative preload" area which results in no stiffness. The ERCO recommended preload dimensions and tolerances will always leave the motor journal bearings in the "positive preload" range.

Present and ERCO recommended dimensions and tolerances of the Westinghouse electric motor tilting-pad bearings for "PCP" applications (7 pads) (Vogtle Nuclear Plant)

Figure 14-11
Present and ERCO-Recommended Dimensions and Tolerances of the Westinghouse Electric Motor Tilting-Pad Bearings for PCP Applications (Seven Pads)

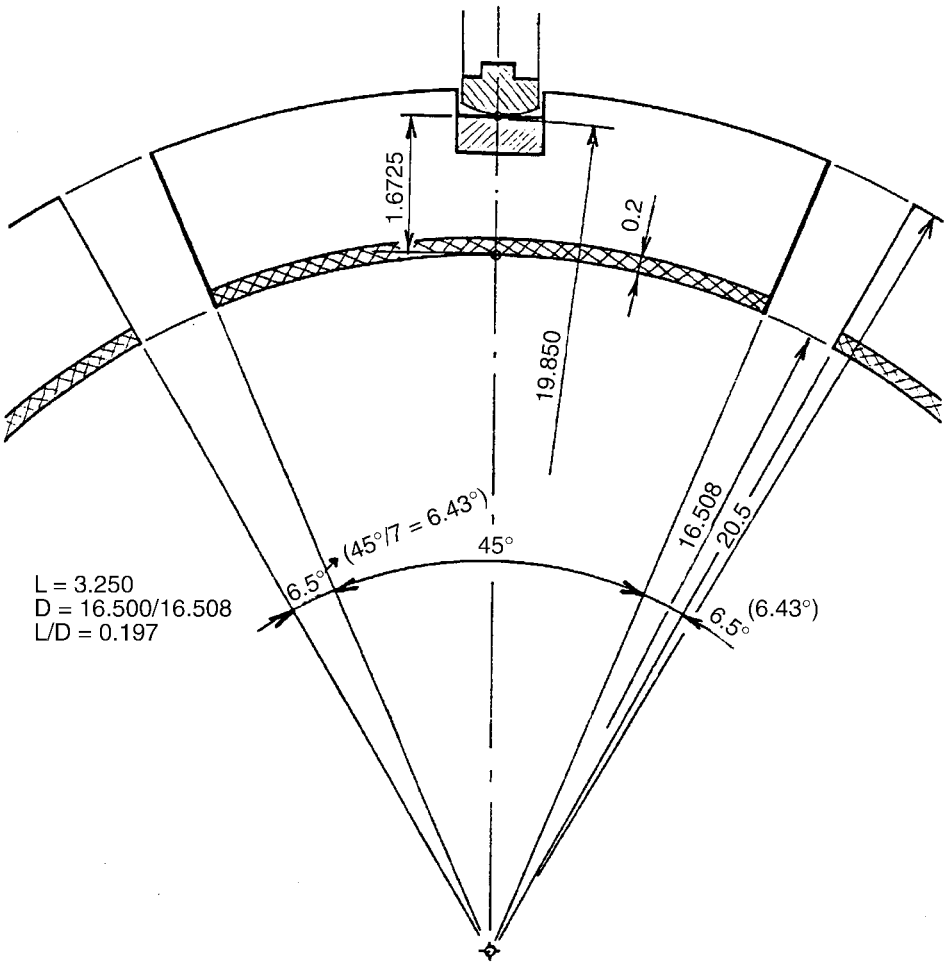

Figure 14-12
Dimensions of Tilting Pad for Westinghouse RCP Lower Motor Bearing

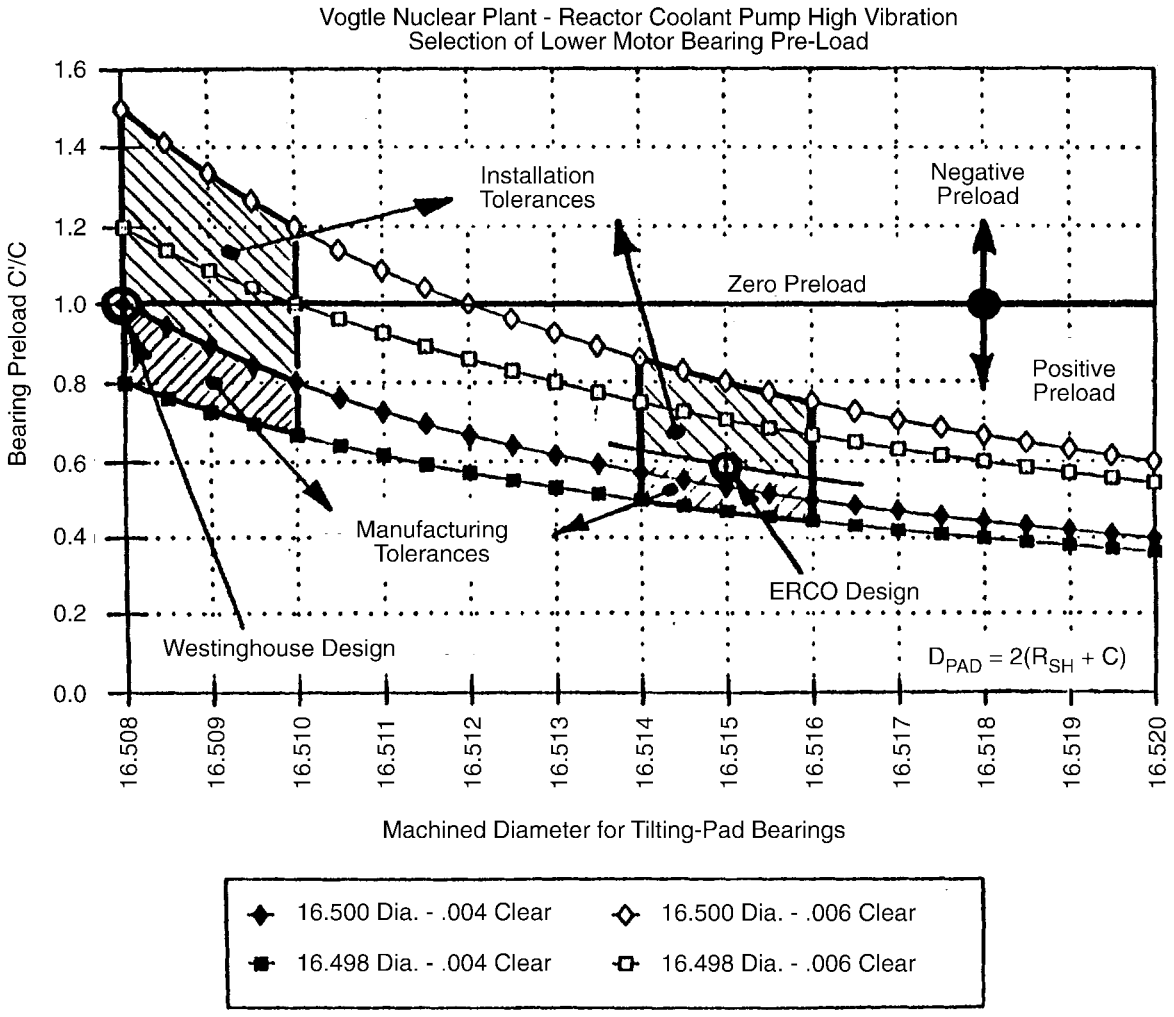

Figure 14-13
Vogtle Nuclear Plant - Reactor Coolant Pump High Vibration

Table 14-1
Bearing Configurations for Electric Motor Drives of Nuclear Reactor Primary Coolant Pumps

	Allis-Chalmers	**Westinghouse**	**AEG**
Upper Bearing:			
No. of Pads	6.0	7.0 (or 9.0)	8.0
Clea. C	0.007	0.004–0.006	.004
Preload C'/C	1.2 (Fitted)	1.0 (None)	0.2 (Heavy)
D	17.0	16.5	17.7
L	5.0	3.5	5.0
L/D	0.3	0.21	0.28
K_{ii} (@ 1200 rpm)	50 – 100 x 10^3	200 – 500 x 10^3	3.5 x 10^6
Lower Bearing:			
No. of Pads	5.0	7.0	10.0
Clea. C	0.0055	0.004–0.006	0.004
Preload C'/C	1.2	1.0	0.2
D	13.0	16.5	20.855
L	4.2	3.5	5.0
L/D	0.323	0.21	0.24
K_{ii}	100 – 400 x 10^3	200 – 500 x 10^3	3 – 4 x 10^6

14.3 Journal Bearing Stability Calculations

As stated elsewhere in Section 14, lightly loaded journal bearings have a threshold speed or stability threshold located above the area where rotor-dynamic instability occurs. Rotor stability depends upon the design of the support foundation, as well as the rotor/bearing system. Therefore, accurate calculation of the threshold speed requires a rigorous analysis that is difficult to simplify in the form of design curves. However, a reasonable approximation of whether oil whip will be a problem can be achieved by assuming that the rotor mass acts at the bearing center, that is, the bearing is analyzed for a point-mass load. For this simplified system, design charts like the one used in Example 1 of this section (Figure 14-14) can be used to predict stability.

When using the approaches described here, if the calculations indicate that a machine will be operating near or outside the stability region, reexamination of the unit is warranted. Modifications to improve marginal designs can be made and should be considered. The most effective way to eliminate the stability concerns is to change the bearing design to tilting pads, even though other modifications (for example, increasing bearing loads, pressure dam, or elliptical designs) may be acceptable. However, it cannot be stressed enough that you should ensure that the hydraulic stability has also been considered prior to making any bearing modifications.

Example 1: Determine the probability of oil whip in a pump designed for 3600 rpm operation with three-groove axial journal bearings.

Required Data:	Sample Data:	
Total rotor weight (W_T)	224	pounds
Distance of the center of gravity from the center of the journal at the thrust end of the shaft, (A)	31	inches
Bearing span (B)	56	inches
Journal diameter (D)	3	inches
Bearing length (L)	1.5	inches
Length/diameter ratio (L/D)	0.5	
Bearing clearance (C)	0.003	inch
Lubricant viscosity (ì), at 145°F	3×10^{-6} lb.-sec / in^2	

First Step: Compute the fraction of the rotor mass (M) supported by bearings 1 and 2:

$W_1 = [1 - (A/B)] \times W_T = [1 - (31 / 56)] \times 224 = 100$ lb. $\quad W_2 = W_T - W_1 = 224 - 100 = 124$ lb.

Compute the mass moment of inertia (M) at each bearing:

$M_1 = W_1/g = 100 / 386 = 0.259$ lb-sec^2/in

where, g = 32.17 ft./sec^2 = 386 in/sec^2

$M_2 = W_2/g = 124 / 386 = 0.321$ lb-sec^2/in

To evaluate the stability of a rotor system, further calculations need to be performed only on the lightest loaded bearing, which in this case is bearing number 1. The stability calculations will be performed at various speeds (3600 rpm, 5000 rpm, and 6600 rpm) to show the importance of calculating all operating points for a variable speed machine.

Second Step: Determine the stability of the bearing:

Speed (N) = 3600 rpm = 60 rps Note: R = D/2

Sommerfield Number (S) = $[(\mu\ N\ D\ L)/W]\ (R/C)^2$

$= (3 \times 10^{-6} \times 60 \times 3 \times 1.5 \times 1/100)\ (1.5 / 0.003)^2 =$ **2.025**

Critical mass parameter (M_{CR}) = $(C\ W\ M)^{0.5} / (\mu\ D\ L\ (R / C)^2$

$= (0.003 \times 100 \times 0.259)^{0.5} / (3 \times 10\text{-}6 \times 3\ 1.5 \times (1.5 / 0.003)^2 =$ **0.0825**

Figure 14-14 can now be used to evaluate the bearing stability by plotting S versus M_{CR}.

The critical mass parameter remains constant at all speeds; therefore, only the Sommerfield Number has to be calculated for the other speeds.

For N = 5000, S = **2.81**

And for N = 6600, S = **3.71**

It can be seen by plotting the points in Figure 14-14 that operation at 3600 rpm is acceptable but that stability problems can be expected at 5000 and 6600 rpm.

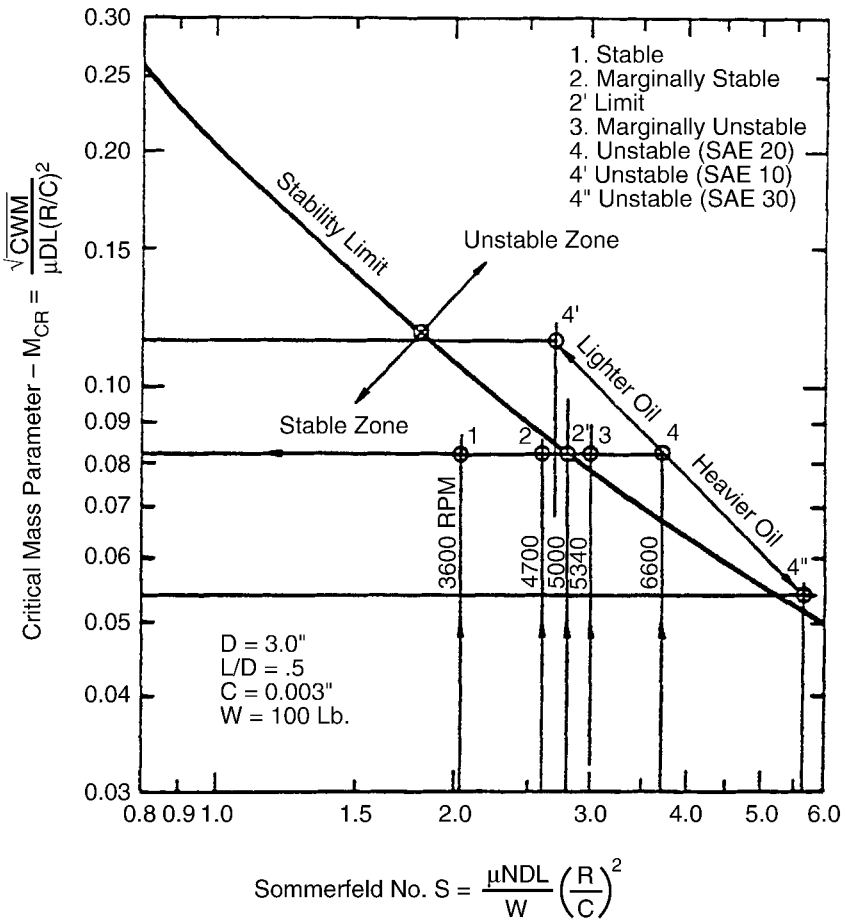

Figure 14-14
Bearing Stability Chart for Three-Grooved Journal Bearings

EXAMPLE 2: This example deals with an OEM's request to increase journal bearing design clearances during manufacture of an 82 MW, 3600 rpm combustion turbine rotor. The journals had been damaged during shipment and required machining to clean the bearing surfaces. The utility was requested to approve plating to restore clearances, accept clearances as is, or accept a non-standard bearing in the unit. The utility would not consider plating or nonstandard bearings; therefore, the issue was the bearing stability given the increased bearing clearances.

Figure 14-15 was used to evaluate the bearing stability. Figure 14-15 provides the relationship between bearing characteristic number (A), bearing eccentricity ratio (ε), bearing length to journal diameter ratio (L / D), and bearing stability. The bearing stability was evaluated as described below:

The OEM provided the following information:

Note: Variables are described in Figure 14-15. Subscripts T and C refer to the turbine end and compressor end bearings, respectively.

e_T = .0043 inch e_C = .0048 inch c_d = D - d

D_T = 9.8575 inches D_C = 11.0425 inches $\varepsilon = 2e / c_d$

d_T(design) = 9.8414 inches d_C(design) = 11.0224 inches

d_T(actual) = 9.8366 inches d_C(actual) = 11.0203 inches

L_T = 8.31 inches L_C = 8.19 inches

Therefore,

design: $c_{dT} = D_T - d_T(\text{design}) = 9.8575 - 9.8414 = .0161$ inch or 16 mils
$c_{dC} = D_C - d_c(\text{design}) = 11.0425 - 11.0224 = .0201$ inch or 20 mils

$\varepsilon_T = 2e_T / c_{dT} = 2(.0043) / .016 = .54$ $L_T / D_T = 8.31 / 9.8575 = .84$
$\varepsilon_C = 2e_C / c_{dC} = 2(.0048) / .020 = .48$ $L_C / D_C = 8.19 / 11.0425 = .74$

actual: $c_{dT} = 9.8575 - 9.8366 = .0209$ inch or 21 mils
$c_{dC} = 11.0425 - 11.0203 = .0222$ inch or 22 mils

$\varepsilon_T = 2(.0043) / .021 = .041$
$\varepsilon_C = 2(.0048) / .022 = .044$

The eccentricity ratios (both design and actual) were plotted on Figure 14-15 for the corresponding L / D ratio. It can be seen that the bearings remain in the stable region of the chart, but their stability margin has been reduced by approximately one-third. The question in this case became: Did the utility wish to accept a newly manufactured component with a reduced stability margin due to an error by the OEM? The utility's response was, "No."

While not used in this case, the bearing characteristic equation has been provided for completeness:

$A = (6 \mu \omega / P_a)(R / C)^2$ where: μ = absolute viscosity of fluid (lb. - sec^2 / in^2)

ω = angular velocity (rpm x 2 π)

P_a = bearing load (lb. / in^2)

R = journal radius (inches)

C = bearing clearance on the radius (inch)

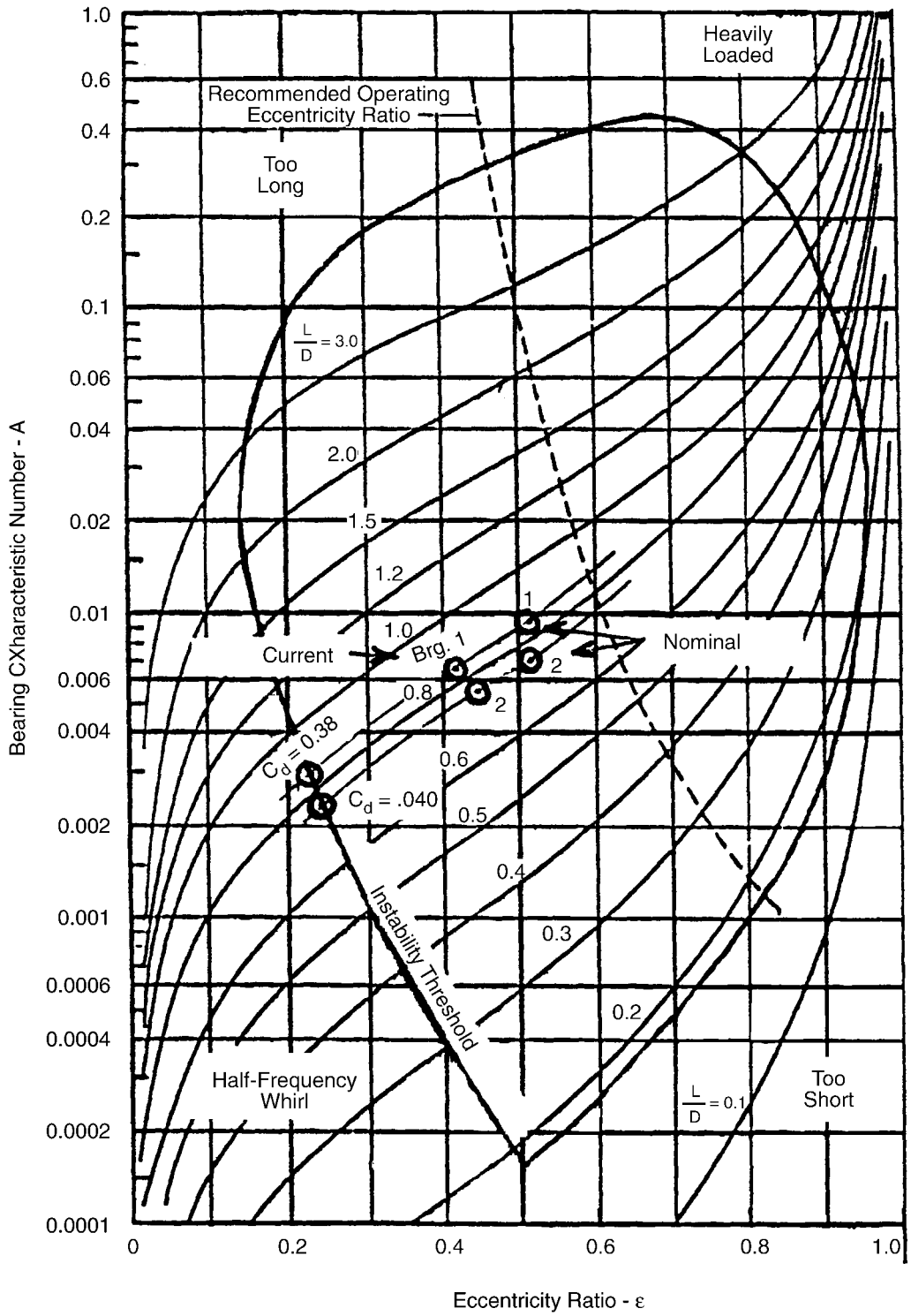

Figure 14-15
Bearing Stability Chart

	Bearing Type	Resistance to Half Speed Whirl	Load Capacity	Stiffness	Damping	Acceptance of Rotating Load	Typical Range of Bore Size mm	Relative Cost (s)	Advantages	Disadvantages	Applications	Usage in BFP
1	 Plain Bore Two Axial Groove	•	•••	••	••	••	20–600	0	Simple to install and line up machine.	Prone to half speed whirl with light load and may require very low length/diameter ratio.	All rotating machines, gearboxes and screw compressors.	Decreasing
2	 Plain Bore Circumferential Single Groove	•	••	••	••	••••	20–250	0	Best for rotating load. Simple to install and line up machine.	Requires high oil supply pressure. Prone to half speed whirl with light load.	Blowers. Quill shaft steady bearings, stome gearbox bearings	None
3	 Lemon Bore	••	•••	••	••	••	50–600	00	Simple to install and line up machine.	Low stiffness in horizontal direction.	Large turbines, electrical machines, pumps.	Moderate
4	 Offset Halves	•••	•••	••••	••••	••	30–400	00	Maximum stiffness with split at 45° after load line.	Not suitable for reverse rotation.	Turbines, pumps, electric machines, compressors.	Occasional
5	 Tilting Pad	••••	•••	•••	•••	•	20–600	000	Inherently most stable of all bearings. Adapts to changing load conditions (d).	Pivots liable to fretting with rotating load.	All rotating machines, horizontal or vertical.	Increasing
6	 Three Lobe	••	••	•••	••	••	20–100	00	Slightly higher load capacity than four-lobe.	Difficult to machine and check. Not suitable for making in halves.	Small turbines, compressors, blowers.	Decreasing
7	 Multipocket	•	•	•	•	•	50–200	00	Suitable for use between contra-rotating shafts if pockets very shallow (taper land 0.001 mm/mm)	Low load capacity due to four grooves and large lobe clearances.	Dynamometers, fluid couplings, turboblowers, contra-rotating shafts.	Decreasing
8	 Dammed Groove	•	•••	•	•	•	100–500	00	—	Poor load capacity in top half, often leads to fatigue damage. Types 3, 4, & 5 preferred.	Turbines, compressors, generators.	Decreasing

Performance Rating
- •••• Very High
- ••• High
- •• Moderate
- • Poor

Relative Cost (a)
- 0 Low
- 00 Moderate
- 000 High

Figure 14-16
Relative Journal Bearing Performance Characteristics for High-Speed Feed Pumps (Nuclear and Fossil Applications)

15
INCREASED POWER PLANT OUTPUT WITH EXTENDED PUMP CAPACITY

15.1 Increased Power Plant Output With Extended Pump Capacity

The subject of increasing power output comes up frequently, especially for older and smaller units; but very large units are not exempt from this problem. In several cases, investigation revealed that the feedwater pumps, or sometimes the circulating water pumps, were found to be the limiting restriction in the system. When pumps run out to the maximum desired capacity, inlet cavitation and vibration may become severe enough to cause concern for increased maintenance. It, therefore, becomes a question of BFP hydraulic component design.

Modification requires an investigation of the feed pump, component by component and section by section, to determine the limitations. The question is to determine which components can be modified that would lead to a trouble-free extension of feed pump capacity. The following areas were investigated first:

- Impeller inlet area, the impeller eye, suction area (inlet of pump casing), and suction nozzle.
- Impeller exit area, back-filing of the vanes at the discharge, correctness of exit area ratio, and vane exit angle.
- Diffuser inlet area, vane inlet angle, radial gap (Gap B) between the impeller exit and diffuser inlet, depth (b_3) of diffuser channels.
- The NPSH available vs. required NPSH conditions. In some cases, a limited amount of improvement can be achieved by minor component modifications, such as improving the impeller eye.
- Casting quality (especially the diffuser), machining errors (for example, an error in the impeller eye as shown in Figure 15-1).
- Close clearance surfaces should be examined to determine whether materials and their respective hardness are up to date with the latest standards that would permit reducing the original clearances (only for a BFP).
- Balancing device geometry and clearance (if balancing leak-off flow can be reduced from 100 gpm to 80 gpm, the gain in efficiency and capacity is 1% for a small 200 gpm BFP).
- Other variables and/or imperfections as shown in Figure 15-1.

Based on the items listed above, two major pieces of equipment will be discussed: boiler feed pumps and condenser (cooling tower) circulating pumps.

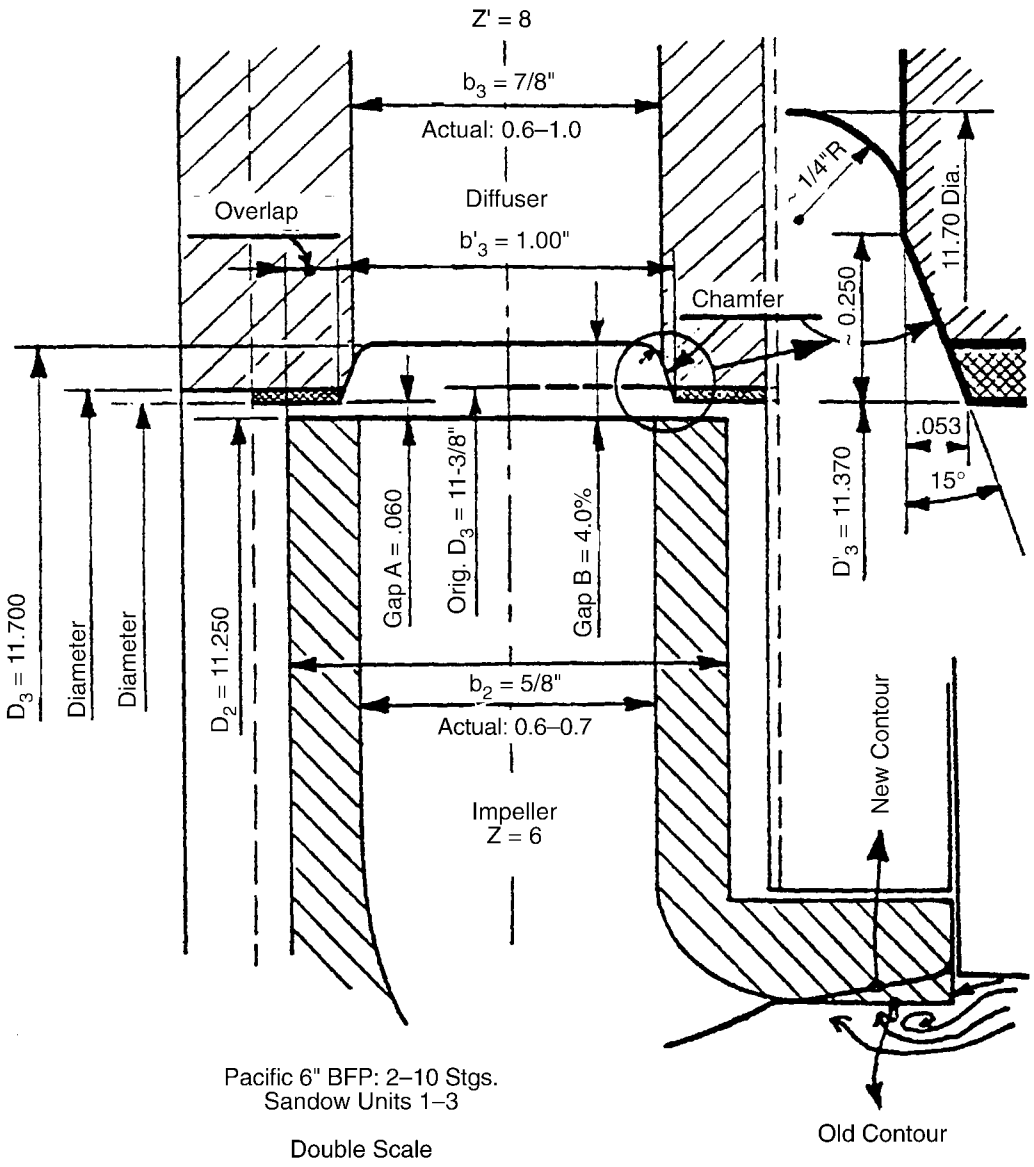

Figure 15-1
Stage Dimensions at the Sandow Power Station (TU Electric) Following Modifications as Shown

15.1.1 Increased Power Plant Generating Capacity (Boiler Feed Pumps)

The following is a list of several possibilities for modifying a boiler feed pump that can increase its capacity with only minor alterations and expense:

1. Underfile the impeller vanes at the impeller outside diameter. This modification is shown in Figure 15-4. The result depends on vane exit angle (β_2), number of impeller vanes (Z), vane thickness at the exit, and specific speed (N_S). The amount of flow increase comes from two resulting effects: an increase of flow exit area and increase of the exit absolute velocity, tangential component (Figure 15-2). These changes can increase flow by up to 10% (at BEP)

for low specific speed impellers such as those used in BFPs. For pumps with higher specific speed such as circulating pumps, this gain can be substantially greater.

2. Cut back the diffuser inlet vane tips. By cutting back the diffuser vane tips, as shown in Figures 1-6, 7-4, 8-11, 15-1, and 15-5, the diffuser throat area increases, which will increase the BEP. Depending on the diffuser design, the expected increase in flow may be 2 to 4 %. If, however, the diffuser channels are too long, the vanes are curved, and the casting quality is poor, the improvement may be much more substantial than these typical values. A good example is provided in Figure 15-1.

3. Mill the diffuser channels to a uniform or larger geometry. Achieving uniformity in diffuser channels can increase flow by up to 1%. Also, optimum area ratio A_2/A_3, as shown in Figure 2-9, can be achieved, which not only permits control of BEP but can also increase the efficiency substantially.

4. Chamfer the diffuser inlet. Chamfering the diffuser inlet as shown in Figure 15-1 does not alone increase capacity, but the pump will become less sensitive to axial alignment because of the improved flow pattern, which in turn could increase the efficiency.

5. Optimize Gap A geometry. As discussed in Sections 7 and 8, optimizing Gap A improves both flow and efficiency.

6. Introduce proper serration on the balancing disk or drum. Introducing proper serration and optimizing this geometry may increase flow by 1 or 2%. If a balancing disk is used, the taper on the vertical face should be included. An explanation of the taper is given in Section 11, and the geometry of the taper is illustrated in Figure 11-5 (a).

7. Introduce proper serration to the impeller wear-ring surfaces. Proper serration geometry of impeller wear ring surfaces (normally on the stationary part) may increase flow by ½ to 1%.

8. Change the wear-ring material. Changing the wear-ring material to the seizure-proof, free-machining-type material with the proper hardness, combined with proper serration geometry and optimum radial clearances, may increase the flow by up to 1%. Development history and material specifications are given in Section 12.3.

9. Increase the impeller exit dimension b_2. Increasing the impeller exit dimension is highly dependent upon the casting quality. The poorer the casting, the more can be gained. Smaller gains can be expected on precision quality impellers. For sand cast impellers, in general, an 8 to 10% gain can be expected since more ineffective material can be removed from sand castings.

In summary, the foregoing corrections or modifications can yield the following percent increases in pump capacity, as shown in Table 15-1:

Table 15-1
Compilation of Percent Increases in Pump Capacity for Various Modifications

Modification Item Number	Minimum % Increase Expected	Maximum % Increase Expected
1	2.0	10
2	2.0	4
3	0	1
4	0	0
5	0	0
6	0.5	1
7	0.5	1
8	1.0	1
9	0	10
Totals:	6%	28%

These alterations or modifications were performed by ERCO on many pumps. A few examples are listed in Table 15-2 and are described in more detail below.

Table 15-2
Increased Power Plant Generating Output by Increasing Pump Capacity in Terms of Percent BEP Flow

Station & Pump Type	MW	Z	Z'	Percent Flow Increase Achieved	N_s
10-Stage BFP	4x200	7	8	8	1400
Single Stage, Double-Suction Circulating (Horizontal)	2x800	6	2	14	3670
Single-Stage, Single-Suction Circulating (Vertical)	2x900	5	11	12.5	4905
Sandow 1–3: BFP	3x200	6	8	6	1100
Lake Hubbard 2: BFP	530	7	9	3	1635
Warrick: BFP	160	7	9	5	1100
River Crest 1: BFP	115	4	2	8.6	903
Eagle Mountain 3: BFP	400	6	8	12	1345
Graham 1: BFP	240	7	8	8.4	1238
THC-2 + DEC: BFP	2x800	7	8	4.5	1550

Variations of dimension from rotor to rotor make it very difficult to make one set of drawings for the repair shops. It was necessary to modify each rotor element individually. Hydraulic passages in impellers and diffusers were individually modified and other similar detailed changes were made. For example, the rotors from pumps in three different stations were supposedly interchangeable. At one station, the impeller width b_2 was 1.00 in. for the first rotor that was modified. On the second rotor, although "interchangeable" on paper, the impeller width b_2 was substantially different, varying from 0.90 to 0.93 in.

Ten BFP rotors were modified in three different units. Although all rotors were allegedly interchangeable, cast components varied not only from rotor to rotor but from stage to stage within the same rotor. Each component had to be individually hand corrected. The result is that they are now all uniform.

All BFP rotors were modified for the three units at the Sandow Station. Similar to the foregoing cases, it was necessary to mill all diffuser channels to the correct dimensions. According to the drawing, diffuser channel depth b_3 was 7/8 inch. In actuality, b_3 varied from 0.67 to 1.00 in. Impeller castings at the eye were originally left unmachined on all impellers, forming a disturbance in the flow path. Recontouring was necessary, as shown in Figure 15-1, to remove the flow irregularity in the eye of the impellers.

The Warrick Plant had similar but somewhat larger BFPs than Sandow. Very high maintenance costs were caused mainly by continuous damage to the diffuser vanes and adjacent components and from very high vibration levels. The principal purpose of modifying the BFPs was to increase capacity. The power plant wanted to have an output of 105% of plant design capacity for their units. Although every component was sized for power generation at 105% capacity, the plant was able to produce only 100% of rated output, especially when pump internal components were worn.

The motor-driven BFPs were the only limitations to achieving the desired performance. Inspection revealed that the diffusers were very poor quality sand castings and the radial Gap B was less than 1%. Modifications to the stages were very similar to those shown in Figure 15-1. The diffuser tip modification was similar to that shown in Figure 1-6. The diffuser vane geometry permitted an increase of Gap B to 6%. Combined with other minor modifications, this increased plant output to the desired 105% capacity. In addition there was a significant reduction in pump-emitted noise, again proving that BFPs need not be noisy. The increased plant output clearly indicated a significant increase in pump efficiency, but more important, it gave each unit additional capacity to 105%.

Graham Unit 1 was capacity-limited because of feedwater flow. In addition, the boiler feed pumps screamed at high loads, and all handrails and surrounding piping vibrated. Gap A and B modifications were made to the 50% capacity, 10-stage boiler feed pumps along with under-filing the exit vanes of the seven-vaned impellers. The improvements were remarkable. All vibration of surrounding piping and handrails ceased, pump vibration dropped dramatically, and the screaming high-pitched noise was reduced considerably. The pumps gained 8.4% feedwater flow capacity. This flow capacity gain allowed the unit to produce maximum megawatt output with the turbine valves wide open.

Lake Hubbard Unit 2 was also capacity-limited because of feedwater flow limitation, especially during emergency fuel-oil-burning conditions. The pump is a three-stage, turbine-driven variable-speed machine. Proper modifications and under-filing of the impeller vanes again increased feedwater flow and plant capacity by 3% in this case.

Rivercrest Unit 1 was capacity-limited when operating with two 50% design-capacity boiler feed pumps. This unit has a third 50% pump for stand-by. However, to obtain full load on the unit, the third pump was required to deliver adequate feedwater flow. This mode of operation increased the unit auxiliary load. The double-volute six-stage pumps were modified, and the four-vaned impellers were under-filed. The feedwater flow increased by 8.6% on each pump. This increased flow now allows a two-pump operation to obtain full power output with the turbine valves wide open and without operating one set of feedwater pump train auxiliaries.

15.1.2 Increased Power Plant Generating Capacity (Circulating Pumps)

Cooling water circulating pumps control the heat exchange rate in the main turbine condenser and, therefore, the back pressure of the LP turbine. Some large units lose capacity during the summer months when the temperature of the cooling water increases, which in turn increases turbine back pressure. The fixed capacity of the circulating pumps was inadequate in these cases to maintain adequate condenser vacuum. Increasing the flow through the system would restore the rated output of the generating unit.

The first cases to overcome such conditions were for two 800 MW fossil and two 900 MW nuclear generating stations. The investigations were initiated to address heavy cavitation damage to the impeller eye. An attempt was made to solve both the cavitation problem and the pump capacity problem at the same time.

Based on design calculations and supporting factory tests, it was concluded that the pumps were operating at flows below BEP capacity as shown in Figure 13-7 at point 0. Elevating the head curve and perhaps increasing the BEP from point 1 to point 2 in Figure 13-7 could move the operating capacity from point 0 to point 1 and finally to point 2. This could solve both problems at once.

The impeller eye had to be modified without reducing the pump capacity and without decreasing the eye inlet area. Preliminary calculations indicated that the casing area downstream from the impeller exit would not choke the flow. Excess flow passing through those discharge channels, including discharge nozzles, also would not retard the flow.

With these facts in mind, work began to make two major fluid-mechanical changes with only minor hardware changes. All alterations involved hand "art" work and were required to be performed in place. The alterations were as follows:

- **Impeller inlet**: The flow pattern was changed to eliminate stall, preventing cavitation at the inlet. This was done without decreasing the impeller eye area, as discussed in Section 13. The change moved the operating point in Figure 13-7 from point 0 to point 1.
- **Impeller exit**: The exit flow area and vane exit angle were both increased. This is discussed in more detail in Section 15.1.3. This moved the operating point in Figure 13-7 from point 1 to point 2.

Large circulating pumps are excellent candidates for vane under-filing if pump capacity needs to be increased. Most impellers have very thick vanes at the impeller exit. The specific speed for mixed-flow impellers is in a very favorable range ($3500 \leq N_s \leq 5000$). If the vane exit angle is in the correct range, more head can be gained by under-filing than on low specific speed impellers such as BFPs. The vane exit angles were between 20° and 21° in the modified pumps, which were major reasons for achieving the end results.

The gain for the two nuclear units was 14%, while for the higher specific speed pumps of the fossil units, the modifications resulted in a flow increase of more than 12%. The pumps in the fossil fuel units were tested after modifications and found to have increased efficiency by 2.7%.

Shock losses, due to instability or incidence angle at low flow conditions for high-energy-input, low specific speed feed pumps, are relatively low at the impeller inlet but are quite high at the impeller exit. The reverse appears to be true for circulating pumps. Therefore, alterations to the impeller eye could result in a more significant change in performance than changes at the exit. The vane shape at the inlet, therefore, must be designed more carefully. Standard vane-shape formations at the inlet are applied by pump designers. For troubleshooting considerations, each case must be treated individually, based upon the nature of cavitation damage and the nature of flow changes desired for that particular application.

15.1.3 Under-Filing the Impeller Vanes at the Exit

Filing the trailing edge of impeller vanes is used by pump manufacturers if extra head is required from an impeller. The velocity triangle in Figure 15-2 shows that by filing, the exit angle β_2 also changes, resulting in a higher C_{U2} component. This yields a higher head at design flow without changing shut-off conditions. The influence of Z and β_2 on slip shows an upper limit of β_2 for every Z where the useful head-producing velocity component C_{U2} ceases to increase. This angle $\beta_{2(max)}$ is higher for a lower number of vanes.

A systematic study showed a very definite logical trend in the magnitude of possible gain that can be achieved by under-filing. The percentage of head gain is a function of the number of vanes, the exit angle, and the specific speed N_S. Figure 15-3 shows the nature of the family of curves. As the N_S and Z grow, the possible head rise also grows.

The head produced by an impeller is proportional to:

$$H = C'_{U2}*U_2 - C_{U1}*U_1$$

For simplicity, assume that: $C_{U1} = 0$ then,

$$H = C'_{U2}*U_2$$

After under-filing, the increased head is:

$$H(F) = H + \Delta H = C'_{U2}(F)* U_2 = (C'_{U2} + \Delta C'_{U2}*U_2)* U_2$$

Therefore, the net gain of head is: $\Delta H = H*\Delta C'_{U2}/ C'_{U2}$

This change in trailing edge geometry reduces shock losses by reducing the magnitude of the wake. As a result, efficiency may increase slightly. With the same radial Gap B, under-filing also reduces noise level for high-speed, high-energy-input pumps. But, noise is not reduced by under-filing for low-head applications. The boundary layer remains the same, but the exit area increases; therefore, efficiency improves for low N_S applications, such as a BFP. The smaller the size, the greater this effect can be.

The technique of under-filing is critical to maintaining material integrity. The impeller must not be filed to sharp corners where the vane joins the sideplates. A sharp corner may initiate cracks and cause failure of the impeller structure. The radius between the vane exit and sideplates for BFP impellers should not be less than 5 mm, as shown in Figure 15-4. This applies only to BFPs. For other pumps, such as circulating pumps, the radius dimension should be determined individually.

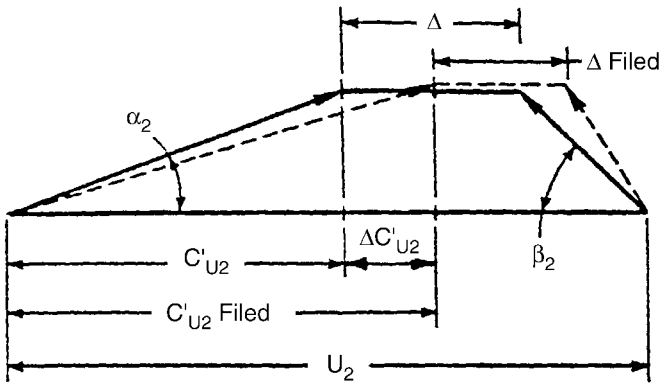

Figure 15-2
Impeller Exit Velocity Triangle Before and After Filing Vanes

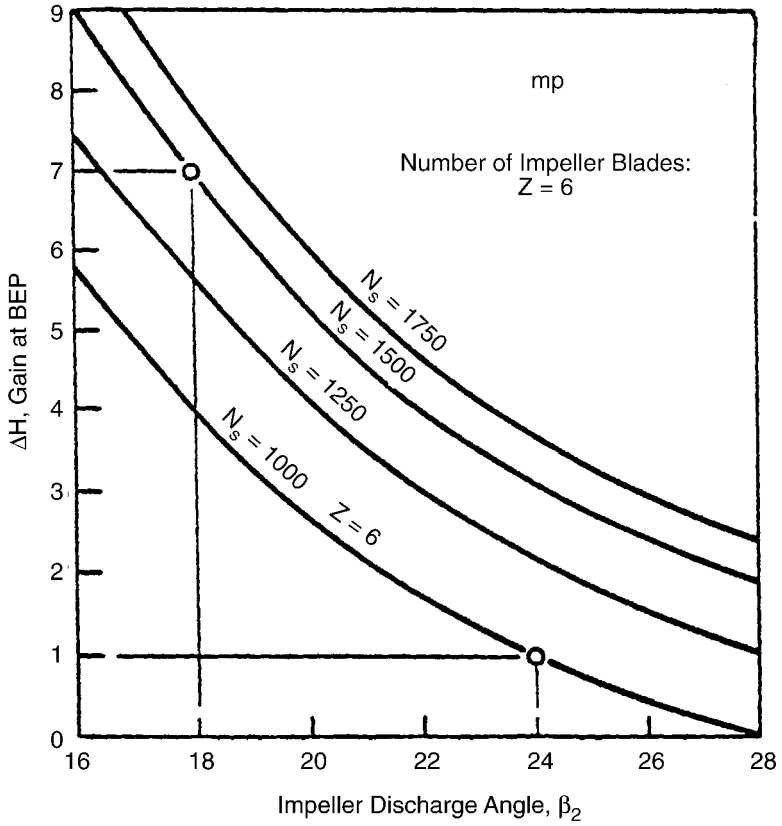

Figure 15-3
Possible Head Gain of a Centrifugal Pump Impeller by Changing Only the Exit Angle

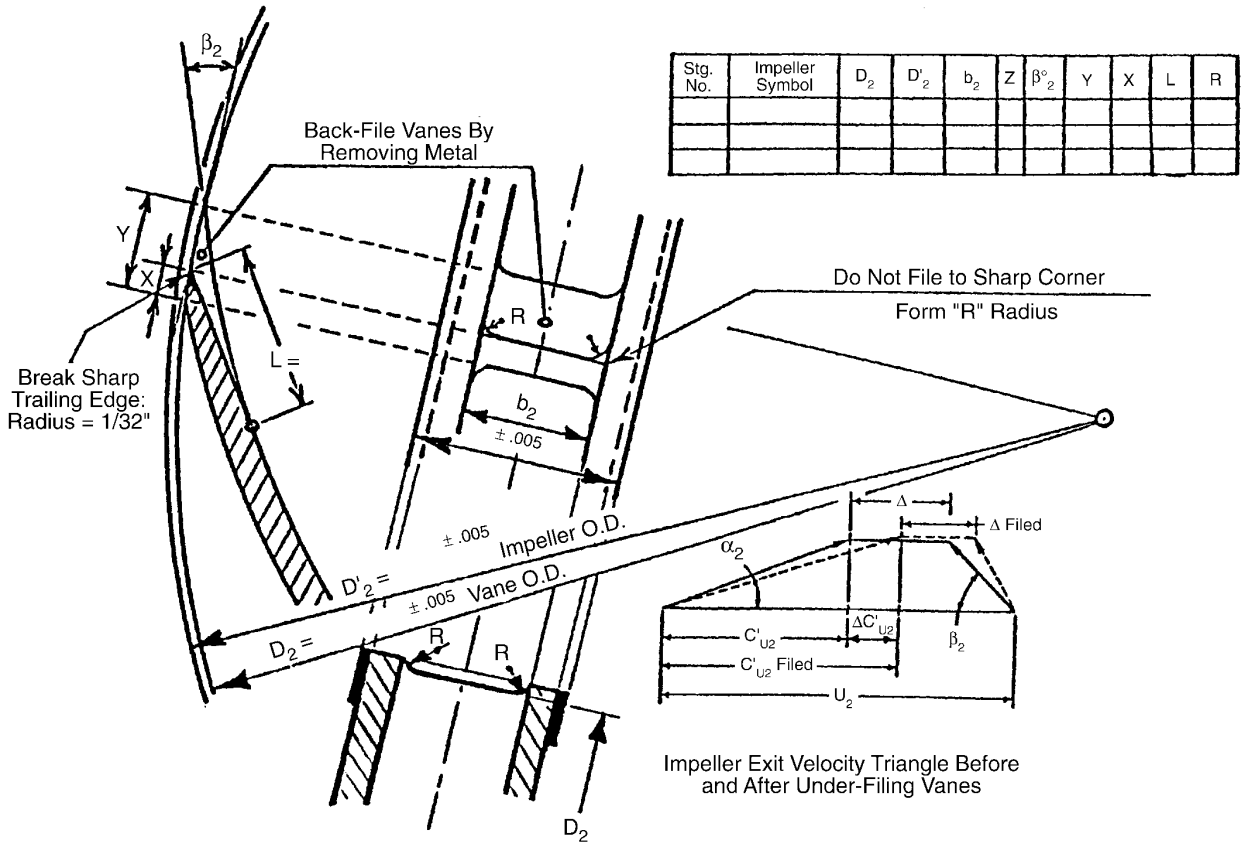

Stg. No.	Impeller Symbol	D_2	D'_2	b_2	Z	$\beta°_2$	Y	X	L	R

Under-Filing Vanes at the Impeller Exit to Gain Head and BEP Location.
Head at Shut-Off Flow Remains Unchanged.

Figure 15-4
Under-Filing Vanes at the Impeller Exit to Gain Head and BEP Location

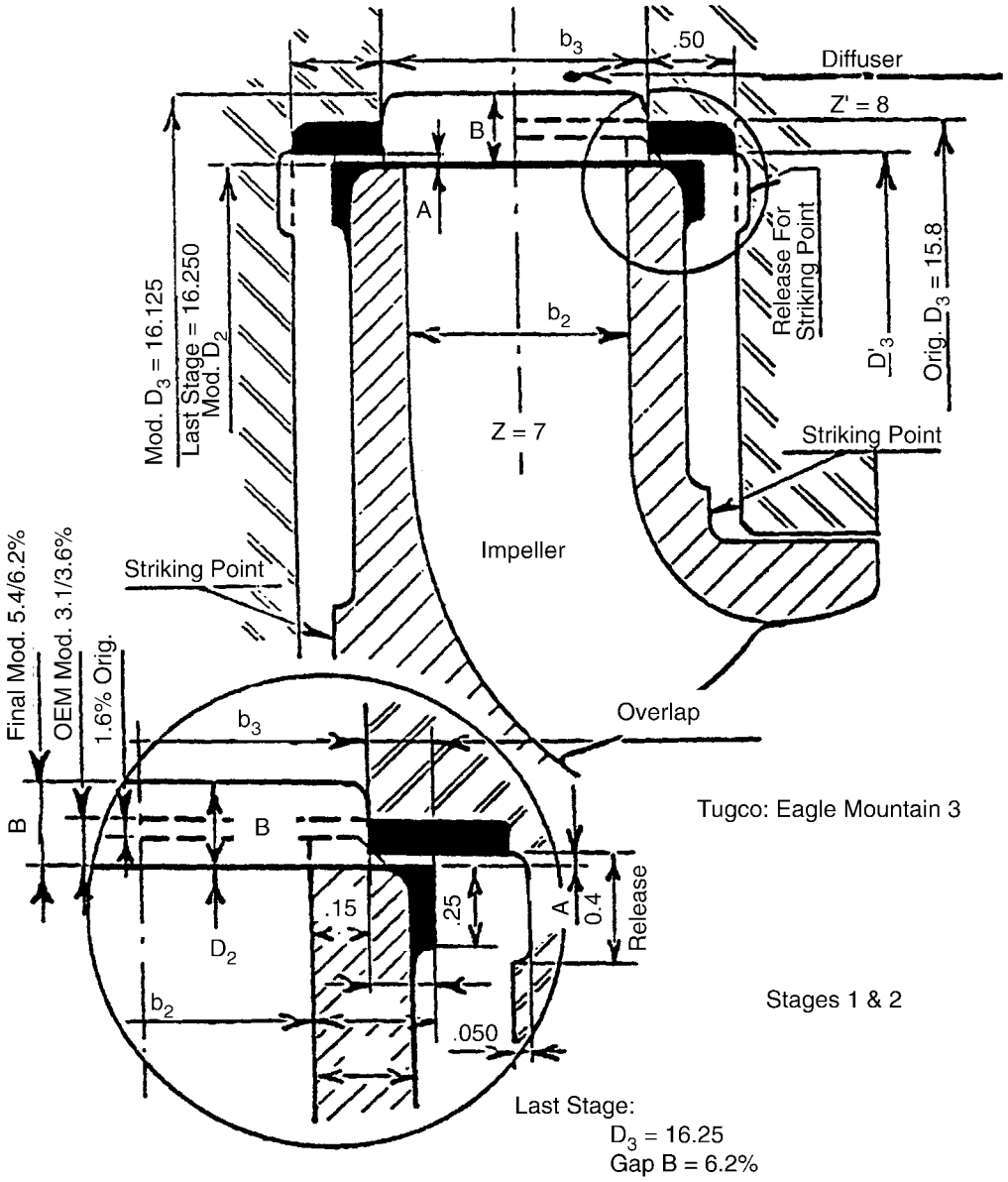

Figure 15-5
Impeller-Diffuser Stage Basic Dimensions and ERCO Modifications [1]

16
REFERENCES

1. E. Makay and J. A. Barrett, “Successful Field Fixes on Power Plant Pumps: Case Histories,” EPRI Symposium: Power Plant Pumps, New Orleans, LA (March 1987). *EPRI Symposium Proceedings* (June 1988). CS-5857.

2. E. Makay and J. A. Barrett, “Changes in Hydraulic Component Geometries Greatly Increased Power Plant Availability and Reduced Maintenance Cost: Case Histories,” First International Pump Symposium, Texas A & M University (May 1984).

3. E. Makay, “Eliminating Pump-Stability Problems,” *POWER.* Vol. 114, No. 7, pp. 62–63, (1970).

4. *Survey of Feed Pump Outages.* EPRI, Palo Alto, CA: April 1978. FP-754.

5. *Recommended Design Guidelines for Feedwater Pumps in Large Power Generating Units*. EPRI, Palo Alto, CA: September 1980. CS-1512.

6. *Centrifugal Pump Hydraulic Instability.* EPRI, Palo Alto, CA: June 1980. CS-1445.

7. E. Makay and J. Donnersberger, “Analyzing and Correcting Vibration Problems in Rotating Equipment: Case History,” *POWER.* Vol. 119, No. 10, pp. 72–74 (1975).

8. M. L. Adams, T. McCloskey, and E. Makay, “Bearing Protects Against Unbalance.” *POWER*. Vol. 128, No. 9, pp. 111–112 (1984).

9. E. Makay and J. Saez, “High Pressure Boiler Feed Pump Troubles Clear Up After Balancing-Disk Changes,” *POWER.* Vol. 118, No. 6, pp. 80–82 (1974).

10. E. Makay and J. A. Barrett, “Field Experience Brings Help to Embattled Pump Users,” *POWER.* Vol. 131, No. 7, pp. 27–30 (1987).

11. P. Cooper, T. Wotring, E. Makay, and L. Corsi, “Minimum Continuous Stable Flow in Feed Pumps.” EPRI Symposium: Power Plant Pumps, New Orleans, LA (March 1987). *EPRI Symposium Proceedings* (June 1988). CS-5857.

12. I. Massey, “Subsynchronous Vibration Problems in High Speed Multistage Centrifugal Pumps,” 14th Turbomachinery Symposium, Texas A & M University (1985).

13. E. Makay and J. A. Barrett, “Ten Ways to Improve High-Energy Pump Performance," *POWER*. Vol. 132, No. 1, pp. 37–40 (1988).

14. “Liquid Rocket Engine Turbopump Inducer, The Backflow Deflector,” NASA SP-8052, (May 1971). E. Makay, Project Reviewer for the *NASA Project Manager*, (Oct. 1970).

15. P. Cooper, Roto-Dynamic Pump with a Backflow Recirculator, U.S. Patent No. 4,375,937, assigned to Ingersoll-Rand (Issued March 8, 1983).

16. N. Jones, E. Makay, and W. Saxton, “Modify Problem Boiler-Feed Pumps to Perform Better, Run Cheaper,” *POWER.* Vol. 134, No. 3, pp. 17–18 (1990).

17. E. Makay, "Trouble-Shooting Large Pump Vibrations: Case Studies for Sub-Synchronous Vibrations," EPRI Symposium: Power Plant Rotating Machinery Vibrations, Case Western University, Cleveland, OH (August 1990).

18. H. Maxwell, Personal Communication. An Analysis of a Palo Verde Nuclear Primary Circulating Pump and the Havasu Project Two Times Vane Passing Frequency Problems (May 1990).

19. E. Makay, "Significant Developments in Utility Pump Technology and Applications," EPRI Symposium: Power Plant Pumps, New Orleans, LA (March 1987). *EPRI Symposium Proceedings* (June 1988). CS-5857.

20. E. Makay, “How Close Are Your Feed Pumps to Instability-Caused Disaster?” *POWER*. Vol. 124, No. 12, pp. 69–71 (1980).

21. E. Makay, “Enlarged Radial Gap in Feed Pumps: A Remedy with Positive Side Effects,” *POWER.* Vol. 125, No. 3 (1981).

22. E. Makay and D. Nass, “Gap-Narrowing Rings Make Booster Pumps Quiet at Low Flow,” *POWER.* Vol. 126, No. 9 (1982).

23. F. F. Ehrich, *Identification and Avoidance of Instabilities and Self-Excited Vibrations in Rotating Machinery.* ASME (1972). 72-DE-21.

24. E. Makay, "Corrective Measures for Utility Pump Low Flow Hydraulic Instability," ASME/NRC Symposium on Inservice Testing of Pumps and Valves, Washington, D.C. (August 1989) pp. 165–198.

25. C. W. Huguenard, “Boiler Feed Pump Testing and Repair,” Presented to the Southeastern Electric Exchange, Ft. Myers, FL (Oct. 1990).

26. D. A. Fuge, “Experience with Upgrade Modifications on Boiler Feed Pumps,” EPRI Symposium: Power Plant Pumps, Tampa, FL (June 1991).

27. O. L. Newell, "Retrofit and Modification Cases," EPRI Symposium: Power Plant Pumps, Tampa, FL (June 1991).

28. C. W. Huguenard and E. Makay, "Repair Practices and Modifications to increase Feed Pump Performances, Reliability and Service Life,” EPRI Symposium: Power Plant Pumps, Tampa, FL (June 1991).

29. EPRI Symposium: Fourth International Workshop on Main Coolant Pumps, Phoenix, AZ (April 1991).

30. M. D. Clary, “Crystal River Unit-3 Reactor Coolant Pump Shaft Failures,” EPRI Main Coolant Pump Diagnostic Workshop, San Francisco, CA (March 1989). *EPRI Symposium Proceedings.* NP-6885.

31. G. O. Hayner and M. D. Clary, "Summary of Failed Reactor Coolant Pump Rotating Assembly Experience at Crystal River Unit-3," EPRI Symposium: Fourth International Workshop on Main Coolant Pumps, Phoenix, AZ (April 1991).

32. “Main Coolant Pump Shaft Failures,” *EPRI Symposium Proceedings* (March 1989). NP-6885.

33. E. Makay, M. L. Adams, and W. Shapiro, "Design and Procurement Guide for Primary Coolant Pumps Used in Light-Water-Cooled Nuclear Reactors," published by the Atomic Energy Commission (November 1972). ORNL-TM-3956.

34. E. Makay, "Pump Trouble-Shooting: Diagnosis Methods and Case Studies," Short Course Lecture Notes. EPRI Symposium: Power Plant Pumps, Tampa, FL (June 1991).

35. E. Makay, "Keynote Address: A Summary of Power Plant Problems and Solutions Over the Last 25 Years 1965–1990,” EPRI Symposium: Power Plant Pumps, Tampa, FL (June 1991).

36. E. Makay and G. E. Drechsler, "Troubleshooting Large Pumps for Nuclear and Fossil Central Stations," *POWER.* Vol. 117, No. 12, pp. 40–41 (1973).

37. J. P. Den Hartog, "Mechanical Vibrations in Penstocks of Hydroelectric Installations," *Trans. ASME,* Vol. 51, pp. 101–110 (1929).

38. E. Makay, W. Gates, and J. P. Hogan, “Be Aware of Acoustic Resonances in Pump Vane Impeller Problems," *POWER.* Vol. 137, No. 2, pp. 55–58 (1993).

39. E. Makay, P. Cooper, D. P. Sloteman, and R. Gibson, "System Pulsation Associated with a 60,000 HP Vertical Water Pump,” AECL-CANDU Conference on Acoustic Vibration, Canada (March 1993).

40. Navy Balancing Limits for Types I and II Rotating Machines, (May 1974). MIL-STD (MILSPEC)-167-1 (SHIPS).

41. P. Hergt et al., German Patent (KSB, Inlet Vane Conditions to Suppress Cavitation on the Visible Side of Vanes), No. DE 27 08 368 C 2, 3-24-83.

42. D. P. Sloteman, P. Cooper and E. Graf, "Design of High-Energy Pump Impellers to Avoid Cavitation Instabilities and Damage," EPRI Symposium: Power Plant Pumps, Tampa, FL (June 1991).

43. E. Makay, “Design of Fluid Movers,” *Machine Design,* pp. 140–144 (May 1971).

44. A. A. Lomakin, "Calculation of Critical Speed and Conditions of Dynamic Stability of Hydraulic High-Pressure Pumps Considering the Forces Arising in the Gap Seals," *Energomashinostroenie,* Vol. 4, No. 4, pp. 1–5 (1958).

45. V. Martzinkowsky and J. B. Karincev, "Influence of Gap Seals on Critical Speeds of Boiler Feed Pump Rotors," *Energomashinostroenie,* Vol. 6, p. 33 (1960).

46. J. E. Corley, Vibration Analysis of Pumps, Tutorial Lecture Notes, ARAMCO, 87.

47. E. Makay, "Failure Analysis of Rotating Machinery," *POWER*. p. 56 (1971).

48. R. T. Knapp, "Centrifugal Pump Performance as Affected by Design Features," *Trans. ASME*, Vol. 63, pp. 251–160 (1941).

49. Carl Blom, "Development of the Hydraulic Design for the Grand Coulee Pumps," *Trans. ASME*, Vol. 72, pp. 53–70 (1950).

50. John Parmakian, "Vibration of the Grand Coulee Pump Discharge Lines," *Trans. ASME,* Vol. 76, pp. 783–790 (1954).

51. E. Lindros, "Grand Coulee Model-Pump Investigation of Transient Pressures and Methods for Their Reduction," *Trans. ASME,* Vol. 76, pp. 775–781 (1954).

52. U. Domm and R. Dernedde, "Uber eine Auswahlregel fur die Lauf- und leit-schaufelzahl von Kreiselpumpen," *KSB Tech. Report*, 9, Frankenthal (1964).

53. B. N. Zotor, "Selection of the Number of Rotating and Guide Vanes for Centrifugal Pumps," *Russian Engineering Journal*, Vol. L11, No. 11, p. 19.

54. Tim J. Moore, "Diffuser Type Pump Vibration Resulting from Impeller/Diffuser Vane Force Interaction," Presented at the Vibration Institute Annual Meeting (April 1983) pp. 13–21.

55. Y. Kubota, T. Suzuki, H. Tomita, T. Nagafugi, and C. Okamuta, "Vibration of Rotating Bladed Disk Excited by Stationary Distributed Forces," *Bulletin of the ASME*. Vol. 26, No. 221 (1983). 56. M. Dubas, "Uber die Erregung infolge der Periodizitat von Turbomaschinen," *Ing. - Arch.* 54, pp. 413–426 (1984).

56. U. Bolleter, "Blade Passing Tones of Centrifugal Pumps," *Vibrations.* Vol. 4, No. 3 (1988).

57. H. Maxwell, "MATHCAD," Computer Program for Vane Interaction Based on References 12 and 18 (1988).

58. F. O. Ruud, "Vibration of Penstocks in Hydroelectric Installations," *Waterpower*. p. 2215 (1991).

59. M. Murakami and N. Heya, "Improvement of Pump Performance by Eye Throttling," ASME Paper 69-FE-26, 1969.

60. T. R. Morton and G. L. Olin, “Realistic Design Specifications Increase Pump Reliability,” 10th Annual Turbomachinery Symposium, Texas A & M University (December 1981). *Proceedings*, pp. 101–109.

61. M. L. Adams and E. Makay, “How to Avoid Damage to Unloaded Journal Bearing Pads,” *POWER*. May 1983.

Targets:
Nuclear Power

About EPRI

EPRI creates science and technology solutions for the global energy and energy services industry. U.S. electric utilities established the Electric Power Research Institute in 1973 as a nonprofit research consortium for the benefit of utility members, their customers, and society. Now known simply as EPRI, the company provides a wide range of innovative products and services to more than 1000 energy-related organizations in 40 countries. EPRI's multidisciplinary team of scientists and engineers draws on a worldwide network of technical and business expertise to help solve today's toughest energy and environmental problems.

EPRI. Powering Progress

TR-114612-V1

EPRI • 3412 Hillview Avenue, Palo Alto, California 94304 • PO Box 10412, Palo Alto, California 94303 • USA
800.313.3774 • 650.855.2121 • askepri@epri.com • www.epri.com